THE UNIVERSITY OF MICHIGAN

INDUSTRY PROGRAM OF THE COLLEGE OF ENGINEERING

MASS TRANSFER WITH CHEMICAL REACTION IN VIEW OF VARIOUS MODELS

Lalitkumar H. Udani

A dissertation submitted in partial fulfillment
of the requirements for the degree of
Doctor of Science in The
University of Michigan
Department of Chemical Engineering
1961

October, 1961

IP-536

Doctoral Committee:

Associate Professor Kenneth F. Gordon, Chairman
Professor Lloyd L. Kempe
Professor Joseph J. Martin
Associate Professor Donald R. Mason
Associate Professor Milton Tamres

ACKNOWLEDGMENTS

I extend my sincere thanks to:

Professor Kenneth F. Gordon, whose interest and continued encouragement were a tremendous and indispensable source of inspiration in my work and who has been to me a 'friend, philosopher and guide' in every sense. Dr. Gordon's philosophy and example will have continued influence in my future life.

Professors J. J. Martin, L. L. Kempe, D. R. Mason and M. Tamres for their generous help and guidance during the course of this study and for their criticism and valuable suggestions during the preparation of this dissertation.

The members of my family, whose many sacrifices, ceaseless support and abundant affection thousands of miles away from home made my education in this country possible. I hope I will have opportunities to repay the great debt I owe them in years to come.

Dr. M. R. B. Klinger, Dean John Bingley, Dr. R. L. Hess, Mr. R. W. Hodges, Mr. E. O. Johnson and many friends in Ann Arbor for their sustained interest in my well-being and education.

Mr. F. R. Harrell of the Engineering Library and his staff and the staff of the Chemical and Metallurgical Engineering Department office and shop for fine cooperation.

The Industry Program of the College of Engineering for assistance and cooperation in preparing this dissertation.

TABLE OF CONTENTS

TABLE OF CONTENTS (Continued)

TABLE OF CONTENTS (Continued)

LIST OF TABLES

LIST OF TABLES (Continued)

LIST OF TABLES (Continued)

LIST OF FIGURES

LIST OF FIGURES (Continued)

ABSTRACT

Liquid phase mass transfer coefficients with and without reaction for a gas-liquid system were obtained to interpret the effect of chemical reaction kinetic coefficients on the rate of absorption of the gas.

The effect of chemical reaction on the rate of absorption for a fluid-fluid system is expressed in terms of the factor $\gamma = (k_L/k_L^o) - 1$ where k_L and k_L^o are the liquid phase mass transfer coefficients with and without reaction respectively. Various models describing this factor have been developed, the Hatta, the Sherwood-Wei, and the Sherwood-Ryan models based on the classical two film theory, the Higbie and the Danckwerts models based on penetration theories and the Kishinevskii model based on surface renewal theory.

The liquid phase mass transfer coefficients with reaction were determined in a stirred pot reactor where both the gas and the liquid phases are stirred, the interface between the two fluids smooth and the interfacial area known. The system used was the absorption of oxygen by solutions of sodium sulfite alone or with $CuSO_4$ and $CoCl_2$ as the positive catalysts, and mannitol, $CH_2OH\,(CHOH)_4\,CH_2OH$, benzyl alcohol, $C_6H_5CH_2OH$, and catechol, $C_6H_4(OH)_2$ as the negative catalysts. Runs with positive catalysts show increased rates and those with negative catalysts decreased rates. Increase in stirrer speed, at constant catalyst concentration, increased the absorption rate. Use of 99.5 per cent oxygen gas in place

of air gave slightly lower coefficients except at catalyst concentrations less than 10^{-9} gm mol $CoCl_2$/l . Varying the sulfite concentration showed that the absorption rate was first order in sulfite concentration up to 0.14 gm equiv/ℓ and as the concentration was increased further the rate increased and then declined.

The liquid phase mass transfer coefficient for absorption without reaction, k_L^o , was determined by the absorption of oxygen in pure water. The factor $\gamma = (k_L/k_L^o) - 1$ for various models was compared with the data. Measured absorption rates 4-50 times those without reaction showed the increase as expected from the various models for infinitely fast reaction, namely those of Hatta, Sherwood and Wei, Higbie, Danckwerts and Kishinevskii. The data cross the various theoretical lines as the rate increases.

In order to determine the chemical kinetic coefficients for Cu^{++} and Co^{++} catalysed reaction air was sparged through sodium sulfite solution in the rapidly stirred baffled reactor. Previously reported coefficients obtained by conventional techniques were found not to be true chemical kinetic coefficients since the mass transfer resistance was found to be important, as established by lower stirrer speed and air rate giving lower transfer rates. The chemical kinetic coefficient for reaction without catalyst determined by taking into consideration the mass transfer resistance was found to be 11 x 10^2 liters/gm equiv min .

Using a recently published computer solution of the diffusion equation for the case of absorption with reaction in view of the penetration model the chemical kinetic coefficients for reaction catalysed by Cu^{++} , Co^{++} , mannitol and benzyl alcohol as well as for reaction without a catalyst

were determined. The chemical kinetic coefficient for reaction without a catalyst was found to be 12 x 10^2 liters/gm equiv min which compares favorably with that determined by the technique where air was sparged in a rapidly stirred solution.

STATEMENT OF THE PROBLEM

Present theory on mass transfer with chemical reaction is based on the assumption that the fluid dynamics of the system, gas-liquid or liquid-liquid, remains unchanged by the reaction. Various models have been proposed based on classical two film theory, the penetration theories and the surface renewal theory for mass transfer with chemical reaction. Inadequate experimental evidence indicates that these models are far from satisfactory when each phase is turbulent.

The purpose of this research is to obtain mass transfer coefficients with and without chemical reaction for a gas-liquid system and to interpret the effect of chemical reaction kinetic coefficients on the absorption of the gas in view of various models. In order to incorporate the effect of reaction on the absorption rate a knowledge of chemical kinetic coefficients is necessary The chemical kinetic coefficients should be determined for the reaction.

I. MASS TRANSFER WITH CHEMICAL REACTION

1. HISTORY AND OBJECTIVES

A. INTRODUCTION

Chemical reaction accompanies mass transfer into a fluid for a large number of biological, chemical, metallurgical and geological processes of either engineering or purely scientific interest. Examples include corrosion, fermentation, combustion, digestion, electrolysis, oxygenation of haemoglobin, smelting and a host of industrial chemical processes such as the manufacture of nitric acid and sodium bicarbonate and refining of petroleum.

In order to study the kinetics of mass transfer into fluids with simultaneous chemical reaction models have been developed by various workers. These models are based on the classical two film theory and the recent penetration and surface renewal theories. The film theory assumes the existence of physical films of finite resistance. The penetration theories assume unsteady state molecular diffusion of the solute into the surface elements

of the fluid which are continually being replaced. The theory of surface renewal without penetration precludes the molecular diffusion of the solute into the surface element.

The effect of chemical reaction on absorption is measured by the factor $\gamma = (k_L/k_L^o - 1)$ where k_L and k_L^o are the liquid phase mass transfer coefficients, with and without chemical reaction respectively defined by Equations 1 and 2.

$$N_A' = k_L(C_{Ai} - 0) \tag{1}$$

$$N_A' = k_L^o(C_{Ai} - C_{Ao}) \tag{2}$$

Expressions for γ , for each model will be derived.

a. Models based on film theory

The film theory assumes the presence of a stagnant layer of each fluid at the interface. The 'thickness' of the fictitious film is calculated by assuming that the flux through the film is due to molecular diffusion only. The thickness is usually small enough for the transfer to be treated as steady state diffusion through the stagnant layer. Whitman[50] imagined that the turbulence in the liquid is damped out near the surface. The scale of turbulence and

the eddy diffusivity get progressively smaller as the surface is approached until the transport by the eddy diffusion becomes of negligible importance. Although it is realized that both molecular and eddy diffusion may be present the total resistance is supposed to be caused by the stagnant film through which transfer is solely by molecular diffusion.

There are three models based on film theory; the Hatta model, the Sherwood-Wei ion diffusion model and the Sherwood-Ryan boundary layer model. Hatta[18] modified the two film model for the case of absorption with chemical reaction by assuming that the chemical reaction takes place in the liquid film. He derived an expression for the liquid phase mass transfer coefficient, k_L, for a rapid irreversible reaction as a function of the molecular diffusivities, the concentrations of the reactants and the film thickness.

Sherwood and Wei[43] modified the Hatta model correcting the diffusivities of the ions for the presence of other ions. Using the treatment of Vinograd and McBain[48] for diffusion in mixed electrolytes, Sherwood and Wei derive diffusion equations for each ion imposing the condition of electrical neutrality for the ion mixture. From these equations an expression for the liquid phase transfer coefficients as a function of diffusivities of individual ions

and their concentrations was derived. Their test of this model in a diffusion cell showed excellent results. The model has not been tested in a stirred pot or a flow system where eddy diffusion is also important.

Sherwood and Ryan[41] propose the turbulent boundary layer model for a flow system. Following the film theory they assume that one mole of component A reacts rapidly and irreversibly with b moles of component B at a plane a distance y_R^+ from the interface. The mass transfer coefficient is then expressed as a function of the Schmidt number and the dimensionless distance from the interface, y^+. This leads to results similar to those of Hatta with the important difference that the resistance per unit length varies with the distance from the interface.

Friedlander and Litt[12] present a solution for the case of rapid chemical reaction in the laminar boundary layer on a flat plate. Their theory also leads to results similar to Hatta's. Potter[30] has reported theoretical work on instantaneous and irreversible reaction in the laminar boundary layer. Chambré and Young[5] made a similar study from a physicist's viewpoint.

b. Models based on penetration theories

Higbie[19] proposed the penetration theory, later greatly modified by Danckwerts[6] in his 'random surface renewal theory' which postulates that turbulence extends to the liquid interface so that the eddies are constantly bringing elements of fluid from the interior to the surface where they are exposed for a finite time before being replaced. Unlike in the film theory the surface is being constantly renewed.

Higbie examined a wetted wall column assuming each element of the fluid surface to be exposed for the same length of time with transfer taking place at the same decreasing rate as into an infinite stagnant layer. Danckwerts modified the Higbie model so that the surface does not have an element of fluid exposed only once as in the wetted wall column, but the surface is repeatedly renewed by elements coming from the interior for various lengths of time. Thus, the difference between these two models is in the concept of the surface age distribution. The average rate of absorption per unit area is obtained by integrating the rate of all surface elements of various ages.

c. Model based on Kishinevskii theory

Kishinevskii[22] proposed a theory which can be described as surface renewal without penetration. Eddy diffusion is taken to exist up to the interface with molecular diffusion into the surface element not playing a role. Danckwerts, on the other hand, considered that during the period of exposure of the surface element the absorbed gas molecules move from the interface into the element by molecular diffusion. Kishinevskii derived expressions for absorption with chemical reaction for two limiting cases, the complete and a negligible degree of unsaturation or neutralisation of the interface.

In Kishinevskii's expression the ratio of diffusivities of reactants in the Hatta equation is replaced by a stoichiometric factor. If the concentrations are expressed as equivalents per unit volume this factor becomes unity.

d. Models based on film-penetration theory

Following the observations made by Danckwerts[7] and Hanratty[16] regarding the limitations of the film and the penetration models in their application to specific cases, Toor and Marchello[45] show that for purely physical ab-

sorption the two models are not separate unrelated concepts but rather are limiting cases of a more general model and that the two theories are complementary rather than being mutually exclusive.

Toor and Marchello considered the transfer between a gas and stirred liquid which has its surface randomly replaced by eddies from the bulk of the liquid. If the eddies remain at the surface a short time, each may be assumed to absorb matter at the interface by unsteady state transfer. As the life of the element increases the penetration into the element increases and again after a long time a steady gradient will be set up in the element of film thickness, no more accumulation will take place, and material will be transferred through the element. Thus, the young elements follow the penetration theory and the old elements the film theory. The middle aged ones have the characteristics of both theories. In this intermediate case the penetration has reached the edge of the element but the steady gradient has not been established. If elements of all ages are present all three types of transfer take place simultaneously. This model is described as the film-penetration model. However, as shown in Appendix I in the case of absorption with

reaction this model gives an expression for k_L similar to Danckwerts' equation which covers all ages of surface elements.

The effect of a chemical reaction on the rate of absorption can be measured by the factor $\gamma = (k_L/k_L^o - 1)$, the fractional increase due to chemical reaction. Table 1 gives this factor for various models as derived in Appendix I for the limiting case of infinitely fast reaction.

B. PREVIOUS EXPERIMENTAL WORK

Stephens and Morris[44] recognized the effect of diffusivity of the reactants and their concentrations in the bulk and at the interface obtaining a good correlation for the $Cl_{2(gas)}$-$FeCl_{2(aq)}$ system, empirically based on the Hatta model,

$$\left[\frac{k_L}{k_L^o} - 1\right] = 0.75 \left[\frac{C_{Bo}}{C_{Ai}}\right]^{0.83} \qquad (3)$$

Roper[34] used a Stephens-Morris column for the absorption of chlorine (Component A) from air into solutions of 2-ethyl-hexene-1 (Component B) in carbon tetrachloride with iodine as a catalyst. His correlation is

$$\frac{k_L}{k_L^o} - 1 = 39.2 \left[\frac{(C_{I_2} + 0.0005) \cdot C_{Bo}}{C_{Ai}}\right]^{0.5} \qquad (4)$$

or

TABLE 1

Factor γ for various models for infinitely fast reaction

Model	$\gamma = k_L/k_L^o - 1$
A. Film models:	
i. Hatta model	$D_B/D_A \cdot C_{Bo}/C_{Ai}$
ii. Sherwood and Wei model	$\frac{9.16 \times 10^{-4}\, q}{D_A \times C_{Ai}} \left[\frac{6000n + 9600m}{7800(n+m) - 1356\, q}\right]^*$
	* For oxidation of sodium sulfite, the reaction used in this thesis, based on the equation for diffusion of ion:
	$N_{\pm} = -\frac{RT}{F}\frac{u_{\pm}}{n_{\pm}}\left[G_{\pm} \pm n_{\pm}C_{\pm}\frac{\sum u_+G_+/n_+ - \sum u_-G_-/n_-}{\sum u_+C_+ - \sum u_-C_-}\right]$
iii. Sherwood and Ryan Boundary layer model	Cannot be applied to present work
B. Penetration models:	
i. Higbie model	$\frac{1}{\mathrm{erf}(\beta/\sqrt{D_A})} - 1$
ii. Danckwerts model	$\frac{1}{\mathrm{erf}(\beta/\sqrt{D_A})} - 1$
C. Kishinevskii model:	C_{Bo}/C_{Ai}
D. Film-penetration model:	Expression same as that for the Danckwerts model.

$$\gamma \propto \left[\frac{k' \cdot C_{Bo}}{C_{Ai}}\right]^{0.5} \qquad (5)$$

In Equation 3 the increase in the coefficient is proportional to 0.83 power of C_{Bo}/C_{Ai} unlike Hatta's equation, Table 1, which has the exponent of one. According to Sherwood and Pigford[39] this is "just what would be expected if the reaction should become slow and effectively first order." However, the increase in the reaction rate due to catalytic action does not alter the index as seen in Equation 4. Roper concludes that this might be due to the index being a function of diffusivities. The correlation in Equation 4 was not satisfactory. Comparable results have been reported for the Cl_2-H_2O system by Peaceman.[28] To both Roper and Peaceman the most significant aspect of the failure was that while the film or penetration theory predicts that the liquid film coefficient should decrease with increasing concentration of chlorine it was found experimentally that k_L remains constant for low concentrations and then increases sharply at higher concentration.

Danckwerts and Kennedy[11] concluded that the two penetration models lead to closely similar predictions about the effect of chemical reaction on absorption rates. Attempts to verify the penetration model have not been highly successful.

Higbie[19] found poor correlation between the experimental and theoretical values. He found that the data agreed with theory if he assumed the gas to undergo a 'first order process' i.e. a process whose rate is proportional to the degree of unsaturation instead of being at equilibrium at the surface. Ripples at the interface and unknown end effects make the verification all the more difficult. Lynn, Straatemeier and Kramers[26] studied absorption in long and short wetted-wall columns in the light of the penetration theory. Their data has a remarkably low scatter, while the total uncertainty due to a systematic error was ±5 per cent mainly due to the film surface temperature. Danckwerts[10] has shown how to calculate the surface film temperature rise. Lynn, et al. could not eliminate the end effect when working with short columns.

Pozin[31] concluded that the liquid film coefficient should be proportional to the 1/6th power of the density divided by the 5/6th power of the liquid viscosity. In their work on Cl_2-air or SO_2-air and $NaOH_{(aq)}$ system Pozin and Opykhtina[32] confirm this observation. Van Krevelen and Hoftijzer[47] give an empirical correlation for k_L in terms of dimensionless groups.

C. OBJECTIVES

Present theory on mass transfer with chemical reaction is based on the assumption that the fluid dynamics of the situation is unchanged by the reaction. Thus for a fluid-fluid two phase system, liquid-liquid or gas-liquid, the resistance of one phase to mass transfer is assumed to be unaltered by the presence of chemical reaction in the other phase. The resistance of the other phase, where the reaction takes place, can be calculated from the various models described above. However, the present theories are suspect as the inadequate experimental evidence available indicates that they are far from being satisfactory. This may be due to a change in the fine structure of the fluid dynamics in the region close to the interface. Sherwood and Wei[42] in their study of liquid-liquid extraction observed differences in gross fluid behavior but this change usually cannot be detected.

The purpose of this research is to obtain accurate values of k_L for a gas-liquid system and to interpret the effect of chemical reaction on the absorption of the gas in terms of the various models. The chemical kinetic coefficients will be determined for the reaction using non-classical techniques.

2. DETERMINATION OF LIQUID PHASE MASS TRANSFER COEFFICIENTS

A. SELECTION OF A SYSTEM AND APPARATUS

a. Selection of a system

In order to obtain accurate values of k_L and k_L^o the system used must have a known interfacial area. Such is the case in a stirred pot reactor where both phases are stirred and turbulent, yet the interface between the two fluids is smooth. Searle and Gordon[36] and Sherwood and Wei[42] used such a reactor for their liquid-liquid studies. A gas-liquid system with negligible gas phase resistance offers a better opportunity for the study of various models as the larger interfacial tension may minimize the spontaneous interfacial activities.[42] The oxidation of sodium sulfite is such a system. Fuller and Crist[13] studied the kinetics of this reaction using $CuSO_4$ as a positive and mannitol as a negative catalyst. They reported a thousandfold variation in the values of reaction rate constants obtained by varying the concentration of the positive and the negative catalysts. The system selected for the present study was the oxidation of aqueous sodium sulfite by air or oxygen.

b. Apparatus

The apparatus, Figure 1, includes a metered supply of air or oxygen, gas heating and scrubbing equipment and a stirred pot reactor in a constant temperature bath. Air from a 30-psi main or cylinder oxygen is passed through a pressure regulator to a Drierite-glass wool air filter, a florator and a tubular heater. A mercury manometer gives the pressure drop. The heated gas is saturated with water before entering the reactor, Figure 2. The pyrex jar is 23 cm tall with a cross sectional area of 167 cm^2. It is held tight between a platform and a gasketed stainless steel cover. Thermometers yielded the liquid phase, wet bulb and dry bulb gas temperatures. The gas inlet and outlet ports, as well as the sampling port with a tube extending below the liquid surface, are located at the periphery of the cover. A Swagelok male connector welded at the center of the cover holds a teflon stirrer which has two blades, each 1 in. x 1/2 in., located 2 in. above the liquid surface and at the lower end a 1/8 in. rod 2 in. long kept 1 in. below the liquid surface. An electric motor and gear reducer runs the stirrer at 70 rpm. The reactor is maintained at 25±1°C by a constant temperature bath. All thermometers were calibrated against N.B.S. thermometers.

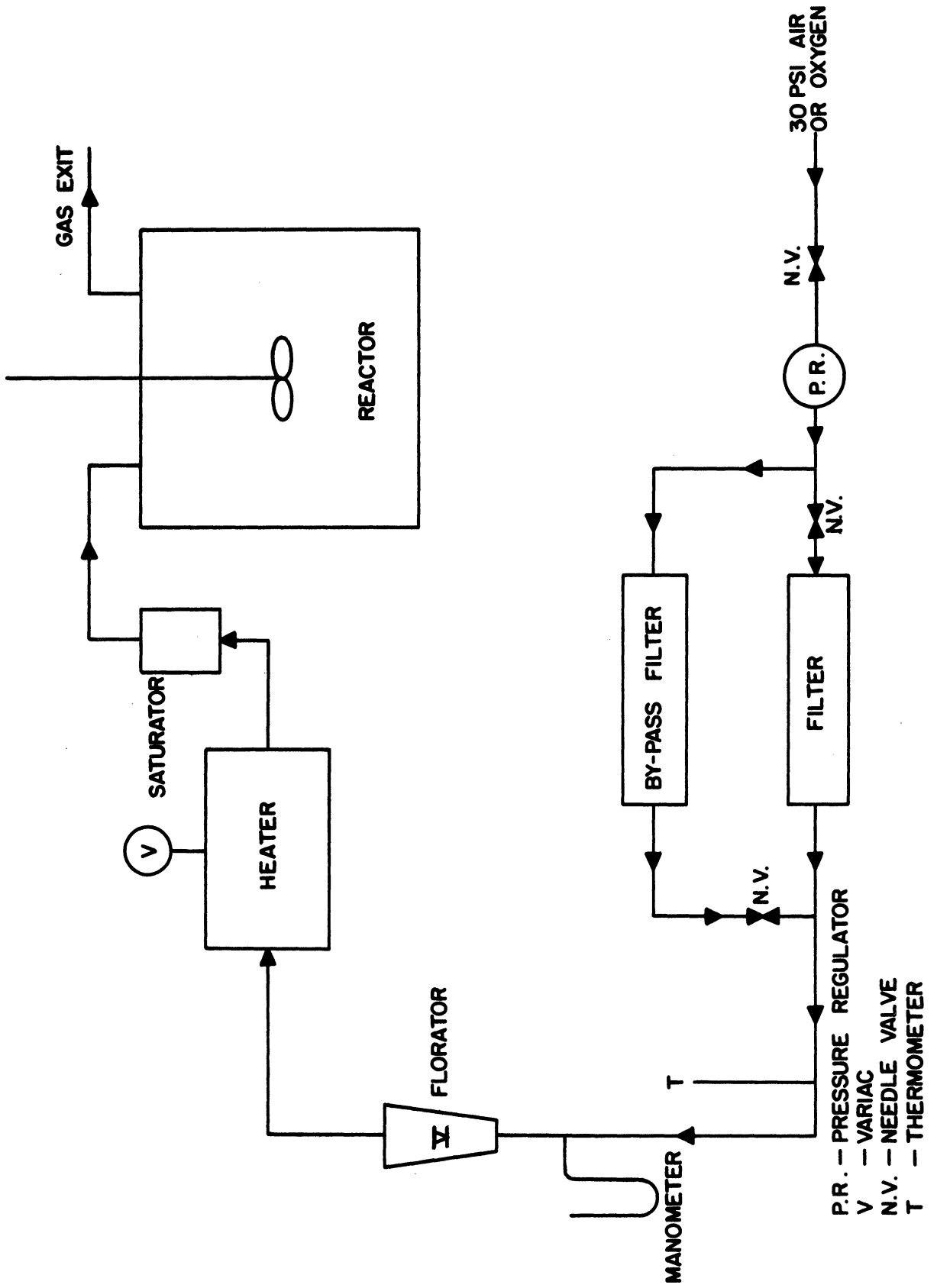

Figure 1. Flow Sheet.

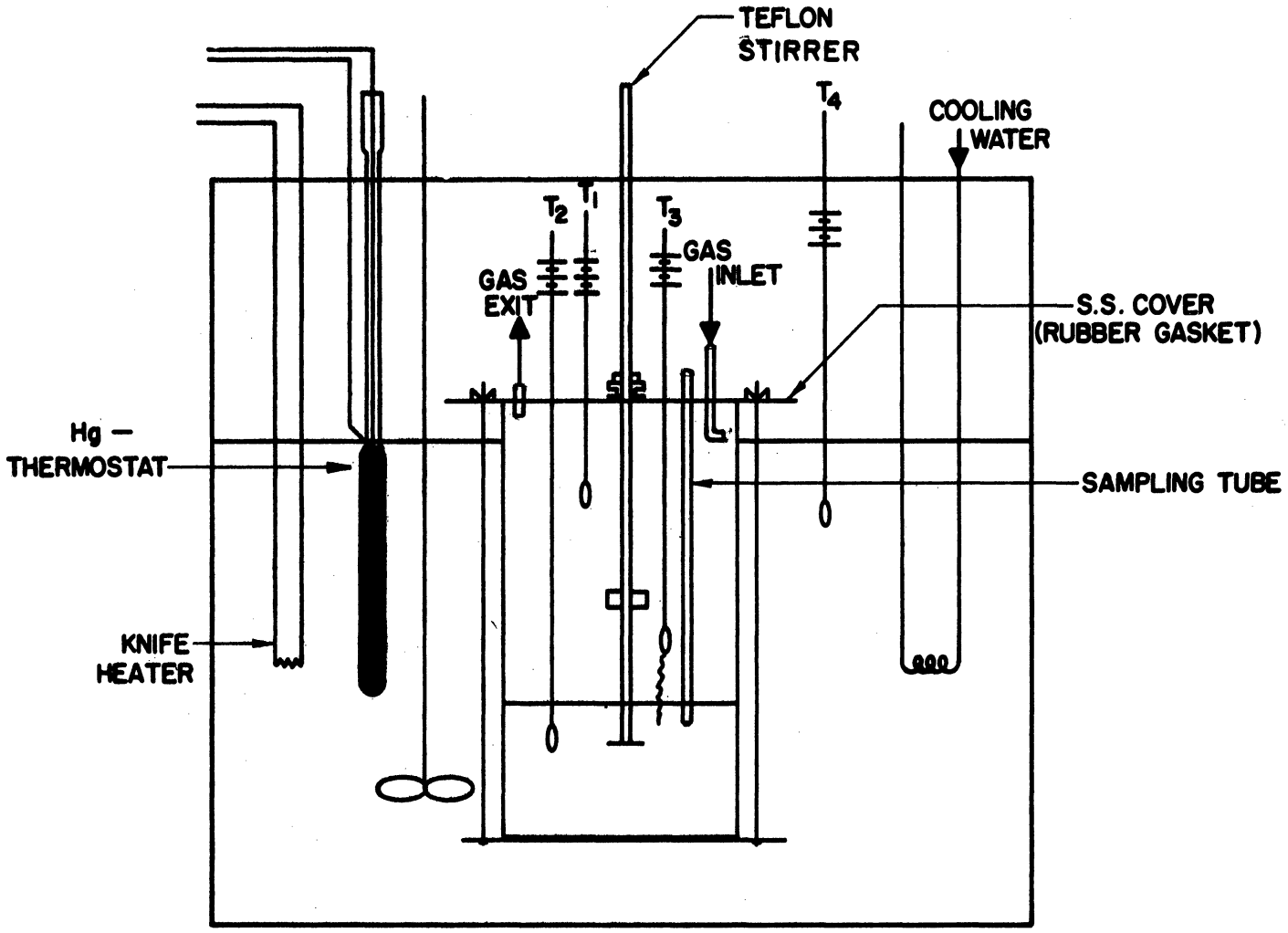

Figure 2. Reactor.

B. PROCEDURE

a. Determination of k_L

One liter of sodium sulfite solution freshly prepared with analytical reagent grade sodium sulfite in double distilled water was placed in the reactor. Every precaution was taken to avoid contamination of the solution by metallic ion to which the reaction is very sensitive. A predetermined amount of the catalyst solution was added to the sulfite solution. The reactor was then covered, placed in the constant temperature bath and gas line and stirrer connected. The saturated gas flow passed at 0.5 SCFM with a line pressure drop of 32 cm Hg. The small pressure built up in the jar, about 1/2 cm of water, was neglected. When a thermal equilibrium was established in the system, i.e. when the wet bulb, the gas and the liquid temperatures reached 25 ± 1°C, sampling started. A 10 ml sample of the solution was withdrawn each time by a pipette through the sampling tube and replaced by an equal amount of double distilled water, maintaining a constant liquid level. Since the gas was saturated with water only the oxygen transfer was important. All temperatures, pressures and the florator were kept constant. Samples, taken every 15 min, were analysed for

sulfite by the standard technique. Runs were usually made for 3 hr. Positive catalysts were $CuSO_4$ and $CoCl_2$ and the negative catalysts were mannitol, $CH_2OH(CHOH)_4CH_2OH$, benzyl alcohol, $C_6H_5CH_2OH$, and catechol, $C_6H_4(OH)_2$.

b. Determination of k_L^o

Values of k_L^o for oxygen in pure water (without reaction) were measured. The oxygen concentration in water was measured by Winkler's method.[15] Sherwood and Holloway[38] claim 1 per cent accuracy for their results with this method.

A stream of nitrogen gas was passed over one liter of freshly boiled double distilled water in the reactor to provide an oxygen free atmosphere while thermal equilibrium was being established. As soon as it was reached nitrogen was turned off and air turned on for the remainder of the run. The runs lasted for 0, 20, 60, 120 and 240 min. At the end of each run air was turned off and nitrogen turned on simultaneously and the entire content of the jar was fixed for its oxygen content by injecting 4 ml of Winkler's manganous sulfate solution immediately followed by 4 ml of alkaline potassium iodide solution through calibrated hypodermics with extended needles reaching below the liquid surface. The

precipitate, $Mn(OH)_2$, was allowed to settle with nitrogen gas still on. Finally, 12 ml of conc. HCl were introduced and the solution mixed thoroughly. The precipitate dissolved completely while a brown coloration appeared due to liberated iodine equivalent to the amount of oxygen absorbed. A 100 ml sample of solution was analysed for its iodine content, yielding the oxygen concentration and the rate of absorption. k_L^o was then obtained from Equation 2.

C. RESULTS

a. Calculations of k_L^o

The rate of absorption of oxygen in pure water is given by

$$N_A' = k_L^o(C_{Ai} - C_{Ao}) \tag{2}$$

or

$$N_A = k_L^o \cdot a \cdot (C_{Ai} - C_{Ao}) \tag{6}$$

Again,

$$N_A = - \frac{V\, dC_A}{dt} \tag{7}$$

Therefore,

$$- V \frac{dC_A}{dt} = k_L^o \cdot a \cdot (C_{Ai} - C_{Ao}) \tag{8}$$

Hence,

$$k_L^o \, dt = - \frac{V \, dC_A}{a \, . \, (C_{Ai} - C_{Ao})} \tag{9}$$

On integrating,

$$k_L^o \, . \, \Delta t = - \frac{V}{a} \, . \, \Delta \, \ell n (C_{Ai} - C_{Ao}) \tag{10}$$

With $V = 1000 \text{ cm}^3$ and $a = 167 \text{ cm}^2$ for a given run

$$k_L^o = - \frac{2.303 \, . \, 1000}{167} \, . \, \frac{\Delta \log (C_{Ai} - C_{Ao})}{\Delta t} \tag{11}$$

For a series of values of C_{Ao} from either a number of samples or a series of runs

$$k_L^o = - 13.75 \, [\text{slope of } \log (C_{Ai} - C_{Ao}) \text{ vs } t] \tag{12}$$

To determine the amount of oxygen in the modified Winkler's method 100 ml of the sample was titrated against N/40 thiosulfate solution. For iodimetric estimation we have the following stiochiometric relation:

$$1000 \text{ ml of N/10 thiosulfate} = 0.8 \text{ gm of } O_2 \tag{13}$$

Therefore,

$$1 \text{ ml of N/40 thiosulfate} = 2 \text{ ppm of } O_2 \tag{14}$$

and

$$C_{Ao} = \frac{(\text{ppm}) \, . \, 10^{-3}}{8} \tag{15}$$

The data and results are given in Appendix III. The average value of k_L^o for nine runs is 0.057 cm/min or 0.118 ft/hr.

A check of the consistency of the results is given in Figure 3 where Equation 12 is plotted. The line in Figure 13 has a slope corresponding to the mean value of $k_L^o = 0.057$ cm/min. The slope appears to be higher than that which might be obtained by drawing a line through the data 'by the eye'.

b. Calculations of k_L

The data for each run were recorded on a data sheet, Figure 22, Appendix IV. The O_2 absorbed during the period between samples equivalent to the sulfite consumed was calculated after making a suitable allowance for dilution by make-up water. Figure 23, Appendix IV is a typical calculation sheet. In the rate equation

$$N_A' = k_L(C_{Ai} - 0) \qquad (1)$$

N_A' was determined for each run from a plot of gm equiv. of oxygen absorbed vs time as in Figure 4. The interfacial area was taken as the cross section of the jar, 167 cm^2. The interfacial concentration of O_2, C_{Ai}, was obtained from the equation

$$N_A' = k_g(p_A - p_{Ai}) \qquad (16)$$

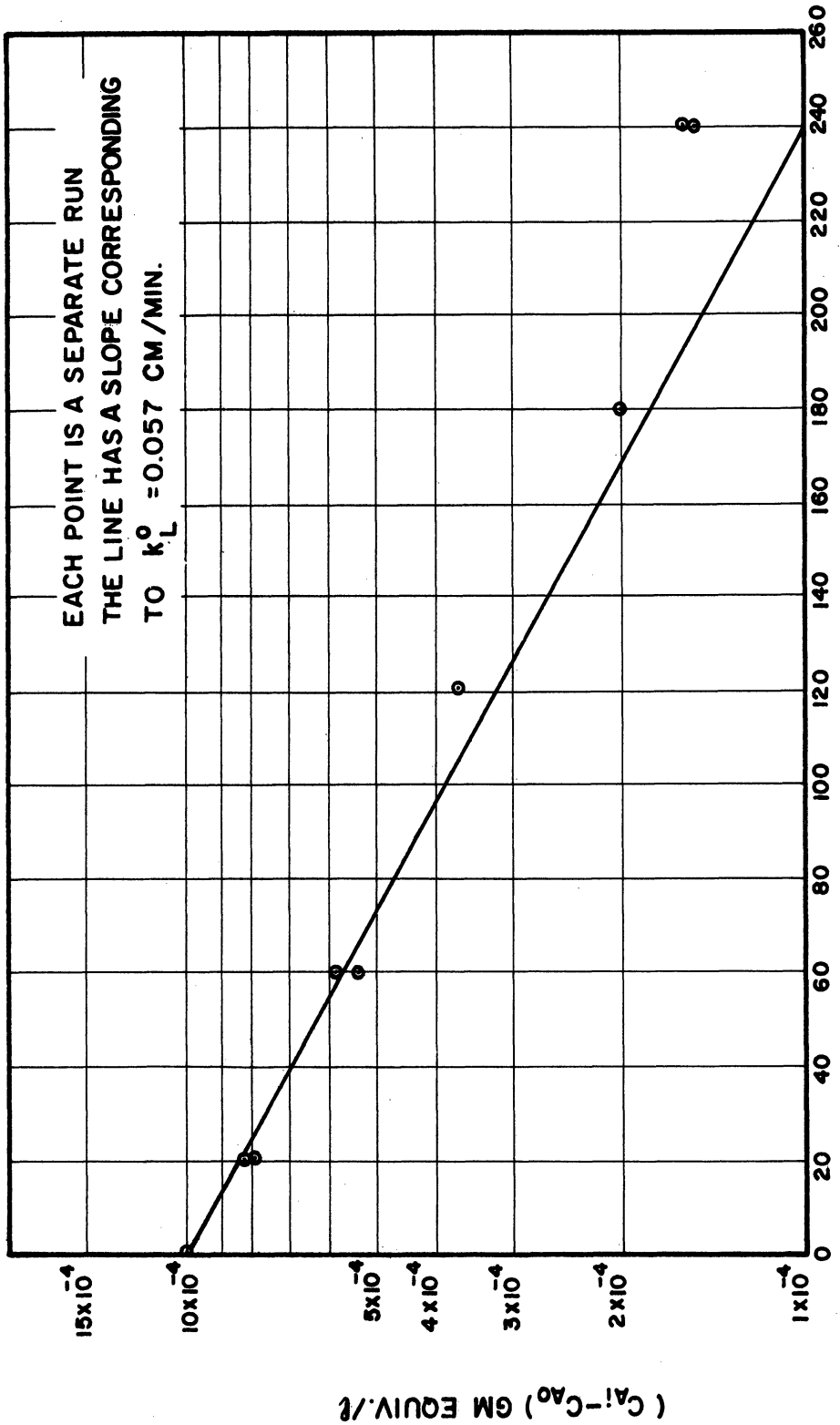

Figure 3. $(C_{Ai} - C_{Ao})$ versus Time.

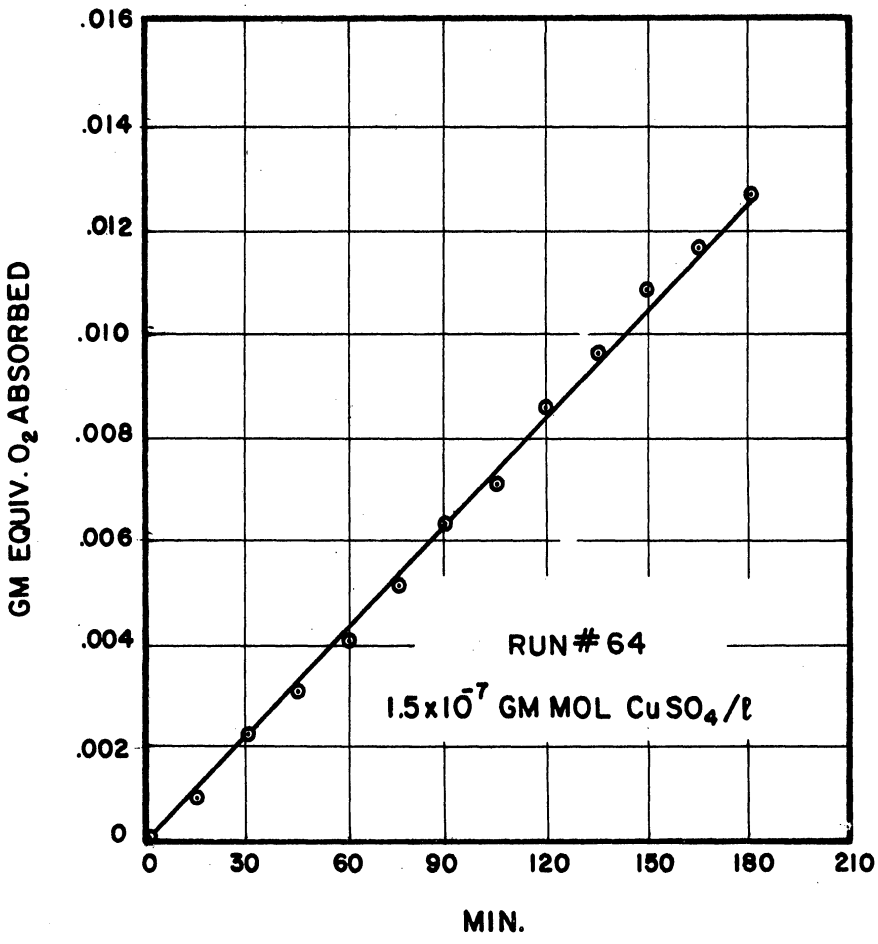

Figure 4. Oxygen Absorbed versus Time.

assuming that Henry's law applies to this system. The value of k_g the gas phase mass transfer coefficient for oxygen was estimated from that for water in air-water system obtained by Udani and Gordon[46] for a similar apparatus. The gas resistance was about 0.06 per cent of the total resistance, Table 8, Appendix IV. A sample calculation of C_{Ai} and k_L is shown in Table 8, Appendix IV.

i. Effect of catalyst concentration on k_L :

The catalysts were $CuSO_4$, 4×10^{-9} to 2×10^{-5} gm mol/l , $CoCl_2$, 1×10^{-11} to 2×10^{-5} gm mol/l , and the negative catalysts were mannitol, 5×10^{-6} to 1×10^{-2} , benzyl alcohol, 5×10^{-7} to 1×10^{-4} gm mol/l , and catechol, 1×10^{-4} to 1×10^{-3} gm mol/l . In the case of positive catalysts greater concentrations resulted in visible black precipitates presumably of copper or cobalt hydroxide. Figure 5-a is the plot of k_L against the amount of catalyst added from the data in Table 9, Appendix IV.

The data plotted in Figure 5-a were obtained for sulfite concentration range of 0.048 - 0.17 gm equiv/l . This was done during the earlier period of experimental work having relied on the statement by Fuller and Crist[13] that

the catalysed rate was independent of sulfite concentration above 0.03 gm equiv/l . Later in this study the reaction was found to be first order in sulfite concentration below 0.1 gm equiv/l . The data for k_L within a narrow range of sulfite concentration, 0.07 - 0.12 gm equiv/l taken from Figure 5-a and plotted in Figure 5-b indicates better the effect of the catalysts without confounding the results with change in sulfite concentrations. The effect of sulfite concentration on the rate for reaction without catalyst is indicated by the band between the dashed lines in Figure 5-a and Figure 5-b.

While the rates obtained with mannitol and benzyl alcohol fall between the limits of k_L without catalyst and k_L^o as would be expected the rates with catechol fall below k_L^o presumably because of the plugging of the interface by the alcohol as reported by Udani and Gordon.[46]

ii. Effect of stirrer speed on k_L : Gaden and Schultz[14] found the stirrer speed had no effect on k_L up to 100 rpm and above that speed k_L decreased. They added a relatively high concentration of catalyst, 10^{-4} gm mol $CuSO_4$/l which is above the solubility limit. Possibly at

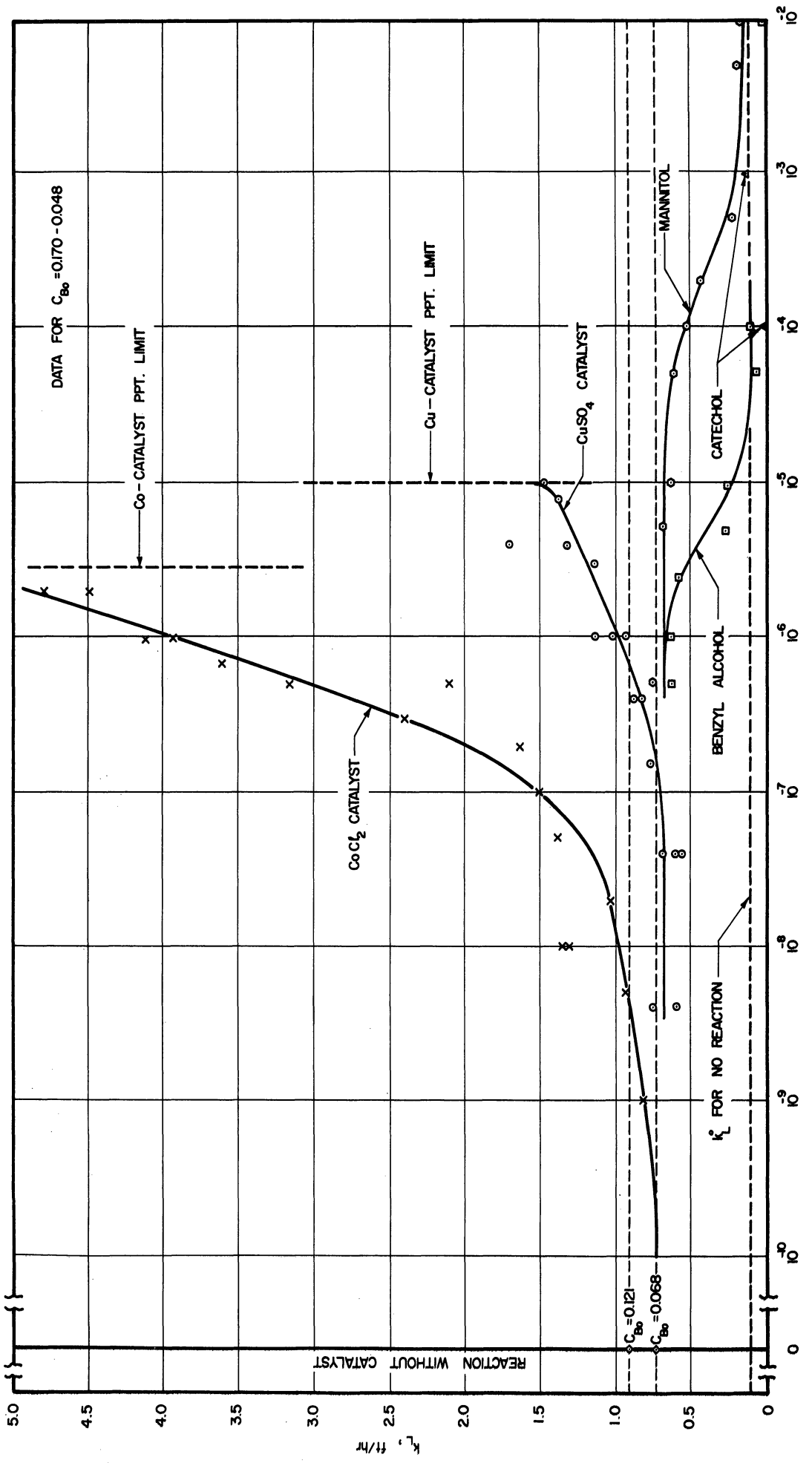

Figure 5. a. k_L versus Catalyst Concentration for C_{Bo} = 0.048 - 0.17 gm equiv/l.

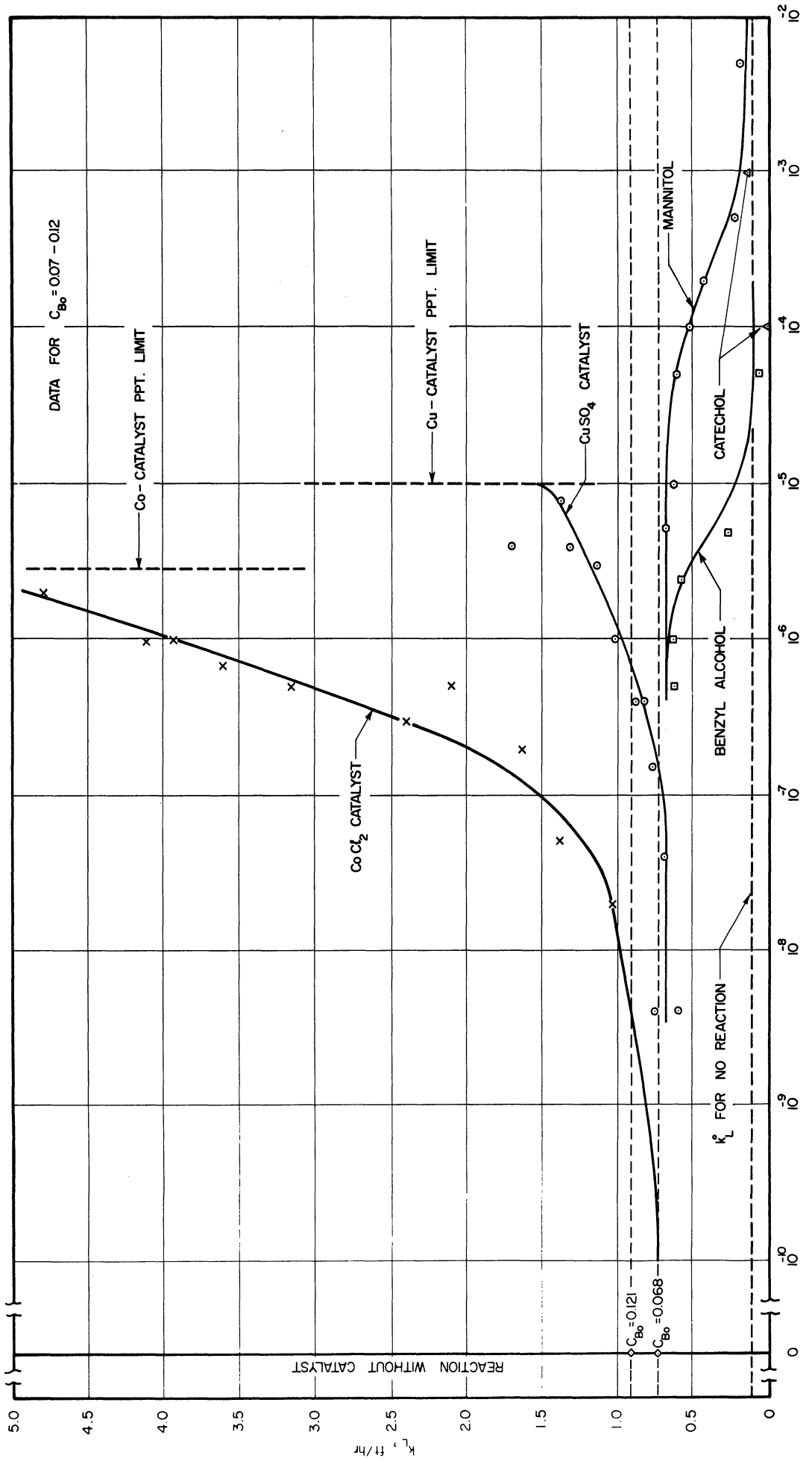

Figure 5. b. k_L versus Catalyst Concentration for C_{Bo} = 0.07 - 0.12 gm equiv/l

high stirrer speeds the catalyst precipitates out as $Cu(OH)_2$, reducing the effective catalyst concentration and lower values of k_L were obtained. Phillips and Johnson[29] added 1×10^{-5} gm mol $CuSO_4$/l as catalyst to their baffled reactor. With pure oxygen their data showed k_L to be proportional to the 0.66th power of the stirrer speed up to 250 rpm. At higher speeds they observed a sharp increase in k_L. Yoshida et al.[51] find similar results for Na_2SO_3-air and Na_2SO_3-O_2 systems. They have not specified the catalyst concentration used. Hyman and Van Den Bogaerde[20] have published a summary of similar work done by various workers on gas-liquid contactors using Na_2SO_3-air system. All used sparged reactors showing k_L proportional to 1.6 to 3.0 power of the stirrer speed. Voznesewskii and Klucharev[49] observed the rate of absorption of oxygen in aqueous sodium sulfite to be unaffected by stirring. They explain this by assuming that the diffusion takes place during reaction between oxygen and sodium sulfite and additional stirring adds little to it.

In view of the conflicting reports the effect of stirrer speed on k_L was examined from 35 to 210 rpm using the best catalyst concentration, 2×10^{-6} gm mol $CoCl_2$/l. At and above 210 rpm a vortex was formed increasing the

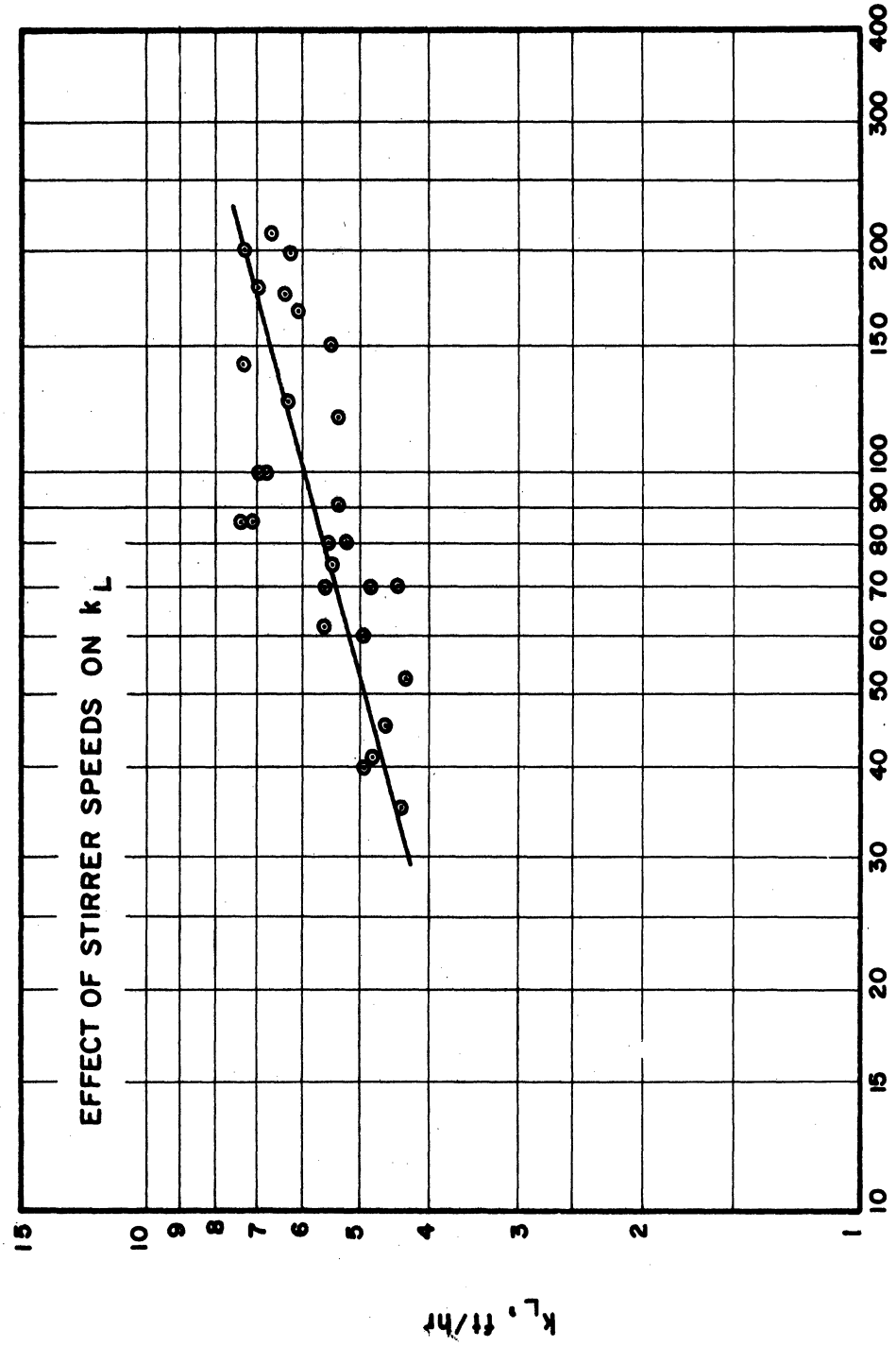

Figure 6. Effect of Stirrer Speeds on k_L.

interfacial area. Below 35 rpm a lack of turbulence was noted as indicated by suspended balsa shavings in the liquid. At low stirrer speeds a ±2 per cent fluctuation in speed was observed due to reduced voltage employed which resulted in loss of torque. At high speeds the rpm varied less than ±1/2 per cent Figure 6, k_L versus stirrer speed from data in Table 10, Appendix V, shows k_L increasing continuously with stirrer speed.

The stirrer speed of 70 rpm used in the determination of k_L in the absorption studies is well within the turbulent region and is adequate as no ripples are formed at the surface at this speed.

iii. Effect of 99.5 per cent O_2 on k_L : 99.5 per cent oxygen gas was used instead of air. In order to economize on oxygen each run was started with air until thermal equilibrium was reached. Air was then turned off and oxygen turned on for 20 min before starting to take samples. Figure 7 is a plot of k_L as a function of $CoCl_2$ concentration for both Na_2SO_3-air from Figure 5-a and Na_2SO_3 from data in Table 11, Appendix VI. For the Na_2SO_3-O_2 system k_L is slightly lower than for the Na_2SO_3-air system except at low catalyst concentrations (below 10^{-9} gm mol/l).

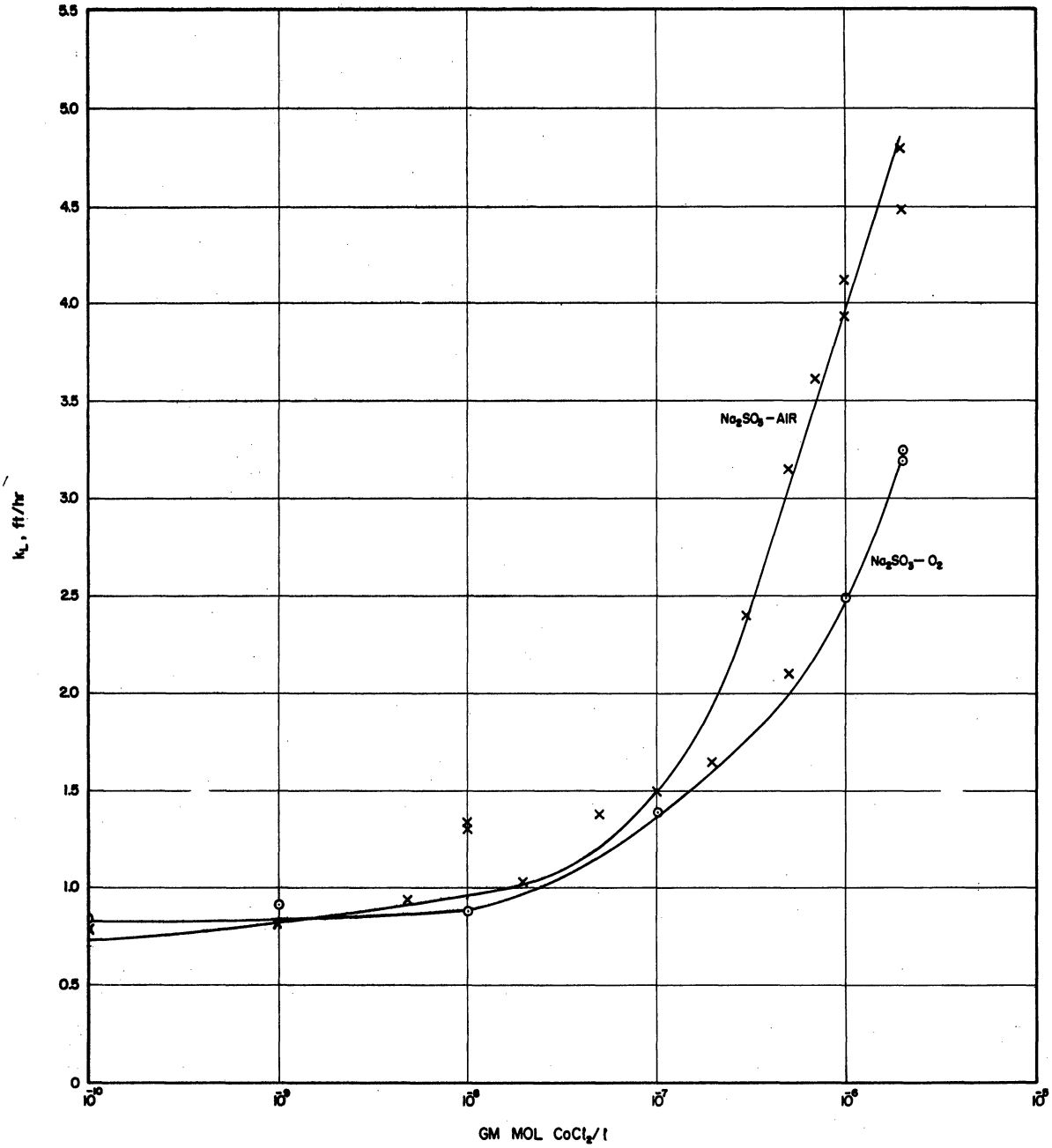

Figure 7. Comparison of Results for Air and Oxygen.

When pure oxygen is used in place of air the interfacial concentration of oxygen increases, resulting in a higher driving force than that with air. But at high catalyst concentrations the reaction rate, which is high already, does not change commensurately indicating a higher 'resistance due to chemical reaction'.

iv. Effect of sodium sulfite concentration on k_L : According to Fuller and Crist[13] the oxidation of sodium sulfite in aqueous solution is of first order with respect to sulfite ion concentration when the concentration of the Cu^{++} catalyst was no more than 10^{-9} gm mol/l. Phillips and Johnson[29] report that the oxygen uptake rate was dependent on sulfite concentration only up to 0.2 gm mol/l. Gaden and Schultz[14] report that the rate is independent of sulfite concentration between 0.015 and 1.0 gm mol/l.

In the present study k_L was determined for the Na_2SO_3-air system with highest catalyst concentration, 2×10^{-6} gm mol $CoCl_2$/l , with 0.00135 - 0.894 gm mol Na_2SO_3/l. The solubility of oxygen in the sulfite solutions decreases with Na_2SO_3 and Na_2SO_4 concentrations thus decreasing the interfacial concentration of oxygen. In the absence, naturally, of the solubility data for oxygen in sulfite solutions the data for sodium sulfate solution as

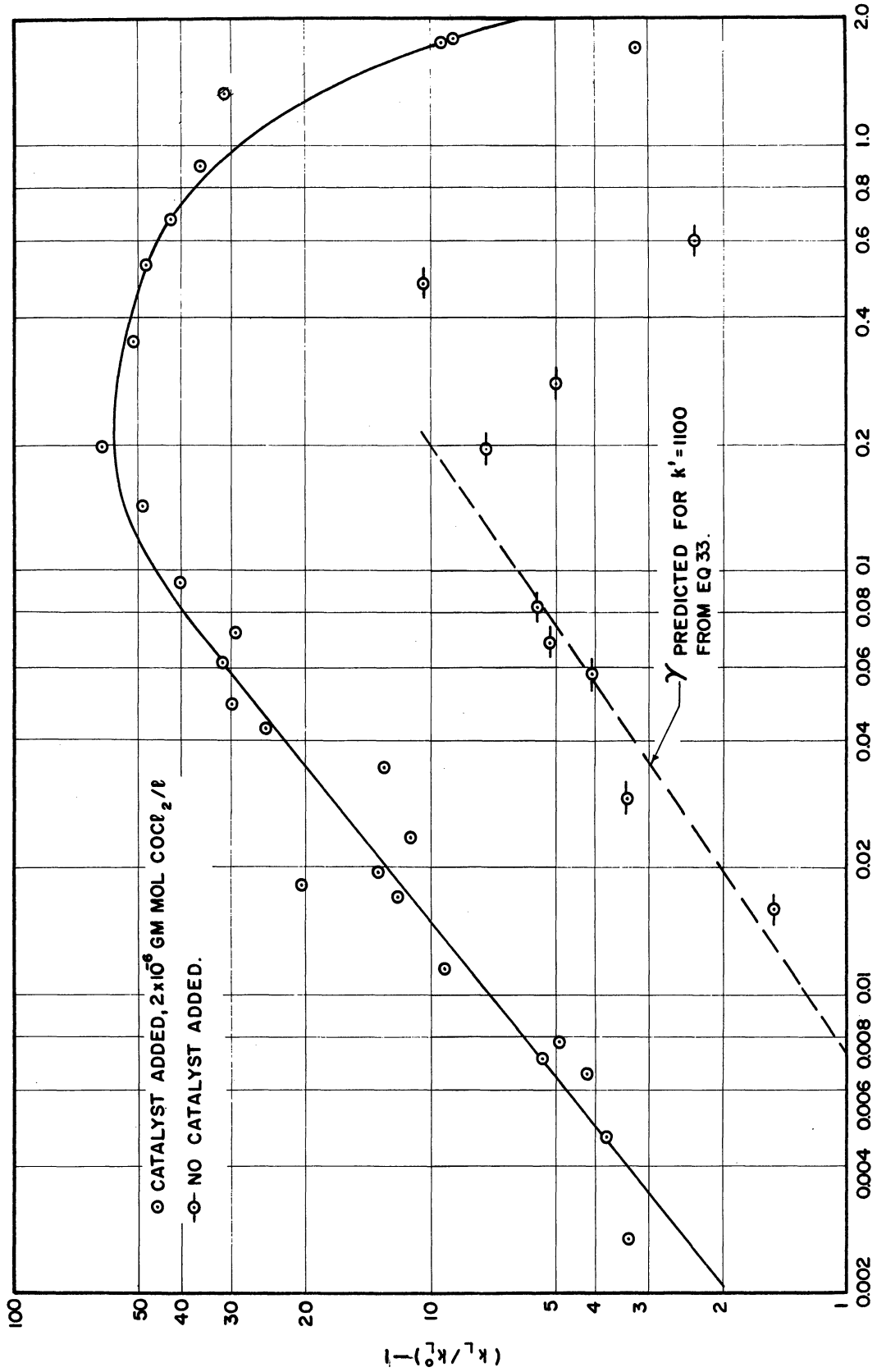

Figure 8. Effect of C_{B_o} on k_L with and without catalyst.

reported by Seidel[37] was used after extrapolation, Figure 111, Appendix VII. Figure 8 is a plot of $(k_L/k_L^o - 1)$ versus C_{Bo} from data in Table 12, Appendix VII. It is seen that k_L displays a first order dependence on sulfite ion concentration up to about 0.14 gm equiv./l. Above this concentration the solubility of O_2 in aqueous sodium sulfate decreases rapidly and presumably also in sodium sulfite. The viscosity of the solutions also increases, Tables 6 and 7, Appendix III, with corresponding decrease in diffusivity of O_2 . As a result the rate of absorption decreases at higher concentration. Some of the data obtained in this section will be used in Section 3 for the evaluation of various models. Runs were also made without any catalyst with 0.02 - 0.485 gm equiv Na SO_3/l . In order to estimate values of the second order reaction rate constant, k' , and compare them with those obtained without catalyst. The data, Table 12-b, Appendix VII, is plotted in Figure 8.

3. COMPARISON OF MODELS WITH DATA

It will be shown in Section II that the kinetic data presented by Fuller and Crist[13] are not true reaction rate constants but volumetric liquid phase mass transfer coefficients. The rate of sodium sulfite oxidation reaction is so rapid that the mass transfer resistance predominates and true kinetic coefficients cannot be measured. Such being the case, the comparison of k_L from various models will be made for the limiting case of instantaneous irreversible reaction obtained with high positive catalyst concentrations.

The film models of Hatta and of Sherwood and Wei, and penetration models of Higbie and of Danckwerts and the Kishinevskii model will be examined. The expressions for γ from each model are given in Table 1 and the calculations in Appendix VIII.

As suggested by Reid and Sherwood[33] the diffusivity of Na_2SO_3 was obtained from

$$D_B = \frac{(1/n_+ + 1/n_-)\ RT}{(1/\lambda_+ + 1/\lambda_-)\ F^2} \qquad (17)$$

In the penetration models the factor β , defined by

$$(C_{Ai}/\sqrt{D_B}) \cdot e^{\beta^2/D_B} - (C_{Ai}/\sqrt{D_B}) \cdot \mathrm{erf}(\beta/\sqrt{D_B}) \cdot e^{\beta^2/D_B}$$

$$- (C_{Bo}/\sqrt{D_A}) \cdot e^{\beta^2/D_A} \cdot \mathrm{erf}(\beta/\sqrt{D_A}) = 0 \qquad (18)$$

is determined by trial and error. When C_{Bo} is large compared to C_{Ai} , as in the present work, β is extremely small. For C_{Ai} less than 10.54×10^{-4} gm equiv./l the second term in Equation 18 can be neglected. Equation 18 then reduces to

$$(C_{Ai}/\sqrt{D_B}) - (C_{Bo}/\sqrt{D_A}) \cdot \mathrm{erf}(\beta/\sqrt{D_A}) = 0 \qquad (19)$$

or

$$\mathrm{erf}(\beta/\sqrt{D_A}) = \left[\sqrt{D_A/D_B} \cdot C_{Ai}/C_{Bo} \right] \qquad (20)$$

The experimental values of γ for rapid reaction were obtained from the runs with $CoCl_2$ concentrations between 5×10^{-7} and 2×10^{-6} gm mol/l , runs 33-49, Appendix VII and 87-92, Appendix IV. The data, Table 2, are plotted as $(k_L/k_L^o - 1)$ vs $[(D_B/D_A)\ (C_{Bo}/C_{Ai})]$ in Figure 9 for comparison with lines predicted from various models, Tables 14 and 15, Appendix VIII. It appears that at low $[D_B/D_A\ C_{Bo}/C_{Ai}]$ values the Danckwerts model fits the data and at high values the Higbie model is better.

TABLE 2

Data for $\gamma = (k_L/k_L^o) - 1$

Run #	Amt of Co Cl_2 gm mol/ℓ	C_{Bo} gm equiv./ℓ	$\frac{C_{Bo}}{C_{Ai}} \frac{D_B}{D_A}$ dimensionless	$\frac{k_L}{k_L^o} - 1$
33	2×10^{-6}	0.00270	1.40	3.35
34	2×10^{-6}	0.00470	2.43	3.78
35	2×10^{-6}	0.00656	3.40	4.13
36	2×10^{-6}	0.00714	3.69	4.34
37	2×10^{-6}	0.00764	3.95	4.86
38	2×10^{-6}	0.0116	6.05	9.20
39	2×10^{-6}	0.0172	9.02	11.85
40	2×10^{-6}	0.0182	9.40	20.00
41	2×10^{-6}	0.0196	10.30	13.20
42	2×10^{-6}	0.0238	13.00	11.10
43	2×10^{-6}	0.0344	19.20	12.70
44	2×10^{-6}	0.0426	23.80	24.80
45	2×10^{-6}	0.0490	27.90	29.00
46	2×10^{-6}	0.0616	35.90	32.00
47	2×10^{-6}	0.0716	41.60	29.10
48	2×10^{-6}	0.0926	56.40	39.90
49	2×10^{-6}	0.1426	88.60	48.40
87	5×10^{-7}	0.081	42.00	17.10
88	5×10^{-7}	0.120	61.97	28.07
89	7×10^{-7}	0.0772	36.14	32.28
90	1×10^{-6}	0.106	54.89	35.14
91	1×10^{-6}	0.081	41.85	34.09
92	2×10^{-6}	0.052	26.48	42.63

It is seen from Figure 9 that the data is not represented by any one of the theories but cross the various theoretical lines as the rate increases. At low absorption rates the data are best represented by those theories indicating greater rates while at high absorption rates the data follow those theories indicating lower rates. These theories assume that the hydrodynamics of this system remains unchanged. The lack of correlation between the theories and data may possibly be due to reaction induced turbulence at the interface of which the models do not take cognizance. Searle and Gordon[36] and Sherwood and Wei[42] observed such an effect in liquid-liquid systems. They report higher rates than those expected if the fluid dynamics of the system were not affected.

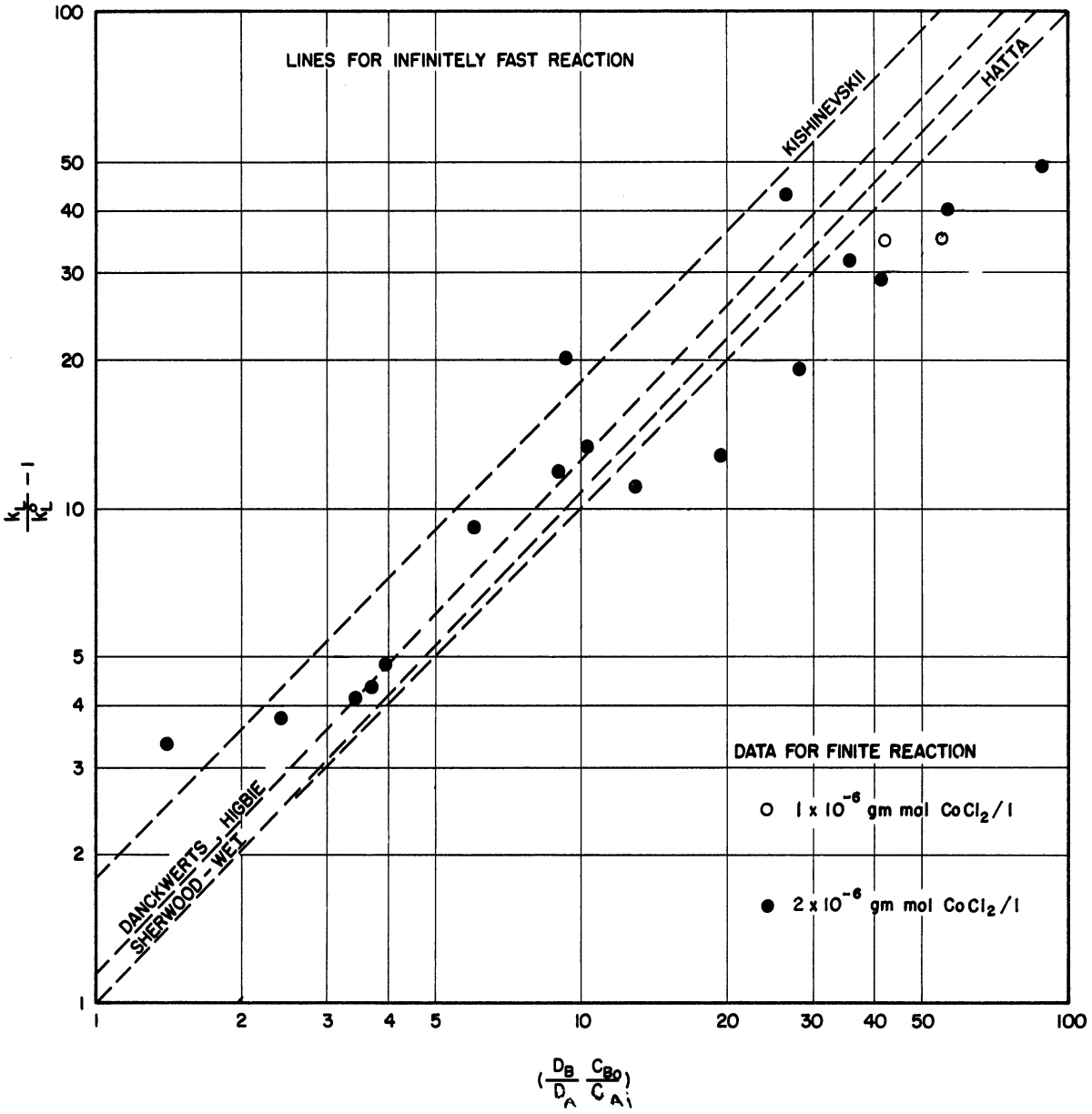

Figure 9. Comparison of models for infinitely fast reaction with data for reaction wiath high catalyst concentrations.

II. CHEMICAL KINETICS OF SODIUM SULFITE OXIDATION

To understand the effect of reaction on the absorption of oxygen by sodium sulfite solutions the chemical kinetic coefficients of the reaction should be known. The reaction rate was varied during absorption with Cu^{++} in $CuSO_4$ and Co^{++} in $CoCl_2$ as the positive and mannitol, benzyl alcohol and catechol as the negative catalysts.

Published kinetic coefficients are those of Fuller and Crist[13] for reaction without catalyst or with Cu^{++} and mannitol catalysts and Alyea and Bäckstrom[1] for reaction with benzyl alcohol. Those for reaction with Co^{++} catalyst could not be found in the literature. An attempt was made to determine the chemical kinetic coefficients with Co^{++} catalyst.

1. EXPERIMENTAL WORK

a. Modification of the apparatus

To reduce the diffusional resistance to oxygen a 20 mm diameter pyrex glass sparger of medium coarseness was attached to the air inlet tube submerged 2 in. below the normal liquid level. The stirrer was provided with an extra blade at right angles to and 1 in. above the first blade. The gas phase stirrer blade was removed. Four plexiglas baffles shaped like inverted truncated right angled triangles were provided along the periphery of the jar below the liquid level. They were 1/8 in. thick, 2 1/4 in. high with 1 in. base and 1/2 in. wide at the opposite end, kept in position by two plastic rings while the baffle assembly was held in the jar by two 1/2 in. polystyrene rods attached to the upper ring and reaching to the cover.

b. Procedure

Air was bubbled through the charge of 900 ml of double distilled water at 0.5 SCFM. When thermal equilibrium was reached a definite amount of the catalyst solution was

added. A known weight of sodium sulfite as crystals, or dissolved in 100 ml of double distilled water, was added. Two or three minutes later 10 ml samples were withdrawn at 1 min intervals and analysed iodimetrically for $SO_3^=$. To withdraw bubble free sample the stirrer was stopped for 4-6 sec. Runs without catalyst were also made in the same manner.

2. RESULTS

a. Uncatalysed reaction

Fuller and Crist[13] assumed that sodium sulfite oxidation was first order in $SO_3^=$ while oxygen concentration remained constant at saturation:

$$-\frac{d(SO_3^=)}{dt} = k_1(SO_3^=) \tag{21}$$

or

$$k_1 = -\frac{\Delta\, \ell n(SO_3^=)}{\Delta t} \tag{22}$$

The slope of $\log(SO_3^=)$ versus time should give the pseudo first order reaction rate coefficient, k_1. Figure 10 is such a plot for runs without catalyst, Table 16, Appendix IX. It is seen that the slope is not a constant but increases with decreasing $SO_3^=$ concentration showing that the data are not true first order. When plotted on an arithmetic plot, Figure 11 the rates appear constant for a given run yet decrease with decreasing sulfite concentration. Also, when the stirrer speed and the air rate are reduced, as in run J , Figure 11, the rate is considerably reduced. This indicates that the oxygen uptake is controlled by diffusion at high sulfite concentrations.

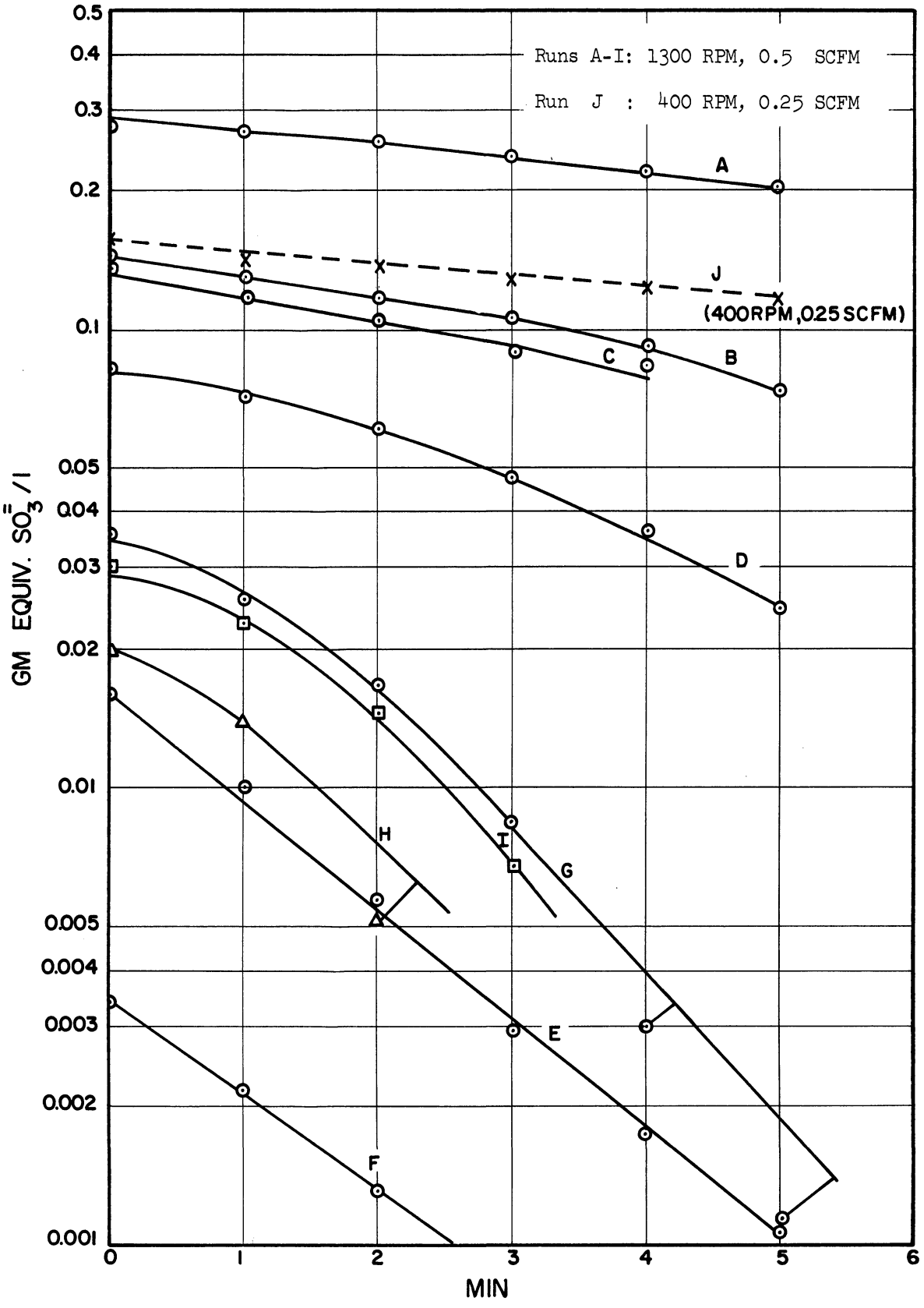

Figure 10. Reaction without catalyst, logarithmic plot.

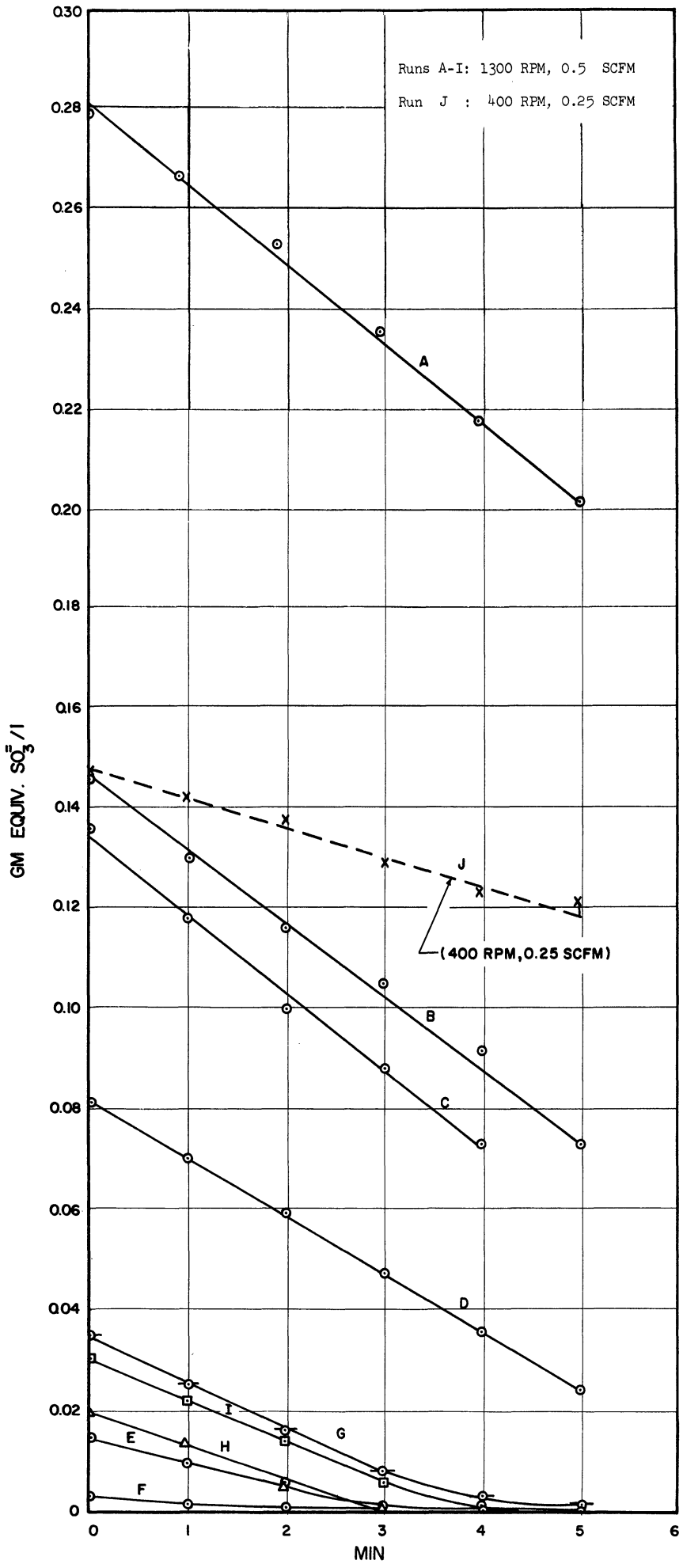

Figure 11. Reaction without catalyst, arithmetic plot.

b. Reaction catalysed with Co^{++} or Cu^{++}

Fuller and Crist[13] regarded the catalysed oxidation reaction to be first order in both Cu^{++} and $SO_3^{=}$ taking Cu^{++} as an additive factor in their equation

$$-\frac{d(SO_3^{=})}{dt} = \{(k_1 + k_{3(Cu^{++})} \cdot (Cu^{++})\} (SO_3^{=}) \qquad (23)$$

where k_1 has the same significance as before and $k_{3(Cu^{++})}$ was taken as a constant. Above about 10^{-9} gm mol $CuSO_4$/l when $Cu(OH)_2$ precipitates the Cu^{++} concentration is dependent on $SO_3^{=}$ concentration as the latter determines the OH^- concentration. The solubility product for $Cu(OH)_2$ is taken to be 1.6×10^{-19} (gm mol/l)^3 (25) and the secondary equilibrium constant for sulfurous acid 6.24×10^{-8} (gm mol/l), (25). Cu^{++} concentration is then

$$(Cu^{++}) = \frac{10^{-12}}{(SO_3^{=})} \qquad (24)$$

Substitution of Equation 24 in Equation 23 and integration gives

$$\log \frac{k_1(SO_3^{=})_1 + k_{3(Cu^{++})} \cdot 10^{-12}}{k_1(SO_3^{=})_2 + k_{3(Cu^{++})} \cdot 10^{-12}} = \frac{(t_2 - t_1)k_1}{2.303} \qquad (25)$$

Fuller and Crist used 1×10^{-19} (gm mol/l)^3 as the solubility

product of $Cu(OH)_2$ and 5×10^{-6} for the secondary equilibrium constant of sulfurous acid. The average value of $k_{3(Cu^{++})}$ they obtained was $2.5 \pm 0.33 \times 10^6$ liters/mol sec. The value of $k_{3(Cu^{++})}$ calculated from Equation 25 for the Fuller and Crist data varied from a negative value to 1.734×10^8, Table 17, Appendix IX. An average value of $k_{3(Cu^{++})}$ would be meaningless.

Similarly, if the Co^{++} catalysed reaction were assumed to be of first order in $SO_3^=$ and Co^{++} and the solubility product of $Co(OH)_2$ taken as 2.5×10^{-16} (25) then

$$(Co^{++}) = \frac{1.56 \times 10^{-9}}{(SO_3^=)} \qquad (26)$$

which on substitution in the rate equation and on integration gives

$$\log \frac{k_1(SO_3^=)_1 + 1.56 \times 10^{-9} k_{3(Co^{++})}}{k_1(SO_3^=)_2 + 1.56 \times 10^{-9} k_{3(Co^{++})}} = \frac{(t_2 - t_1)k_1}{2.303} \qquad (27)$$

Values of $k_{3(Co^{++})}$ calculated from Equation 27, Table 18, Appendix IX, vary from negative to 0.068×10^6 and an average value would be meaningless. As k_1 and k_3 are not constant Equation 25 and Equation 27 are invalid. Figure 12 is a plot of rate data with Cu^{++} catalyst, Table 19, Appendix IX, and Figure 13 for the Co^{++} data, Table 20, Appendix IX.

The rates in Figure 12, Runs I and II, and in Figure 13 for maximum stirrer speed, approximately 1300 rpm, and air rate of 0.5 SCFM are constant; for Runs III and IV, Figure 12, where low sulfite concentration was used the rate seems to fall exponentially with time as in a first order reaction. Lowering the stirrer speed and air flow rate reduces the rate of oxidation, Run V, Figure 12, showing that the mass transfer is important. One therefore concludes that the reaction is so fast that the diffusion is always controlling even for runs without catalyst and the published rate constants are not true rate constants but usually correspond to volumetric liquid phase mass transfer coefficients.

c. Determination of mass transfer resistance for kinetic study

It has been shown that the kinetic coefficients reported for sodium sulfite oxidation reaction are not true kinetic coefficients because the mass transfer resistance controls. In order to estimate the true second order reaction rate coefficient the mass transfer resistance is determined as follows.

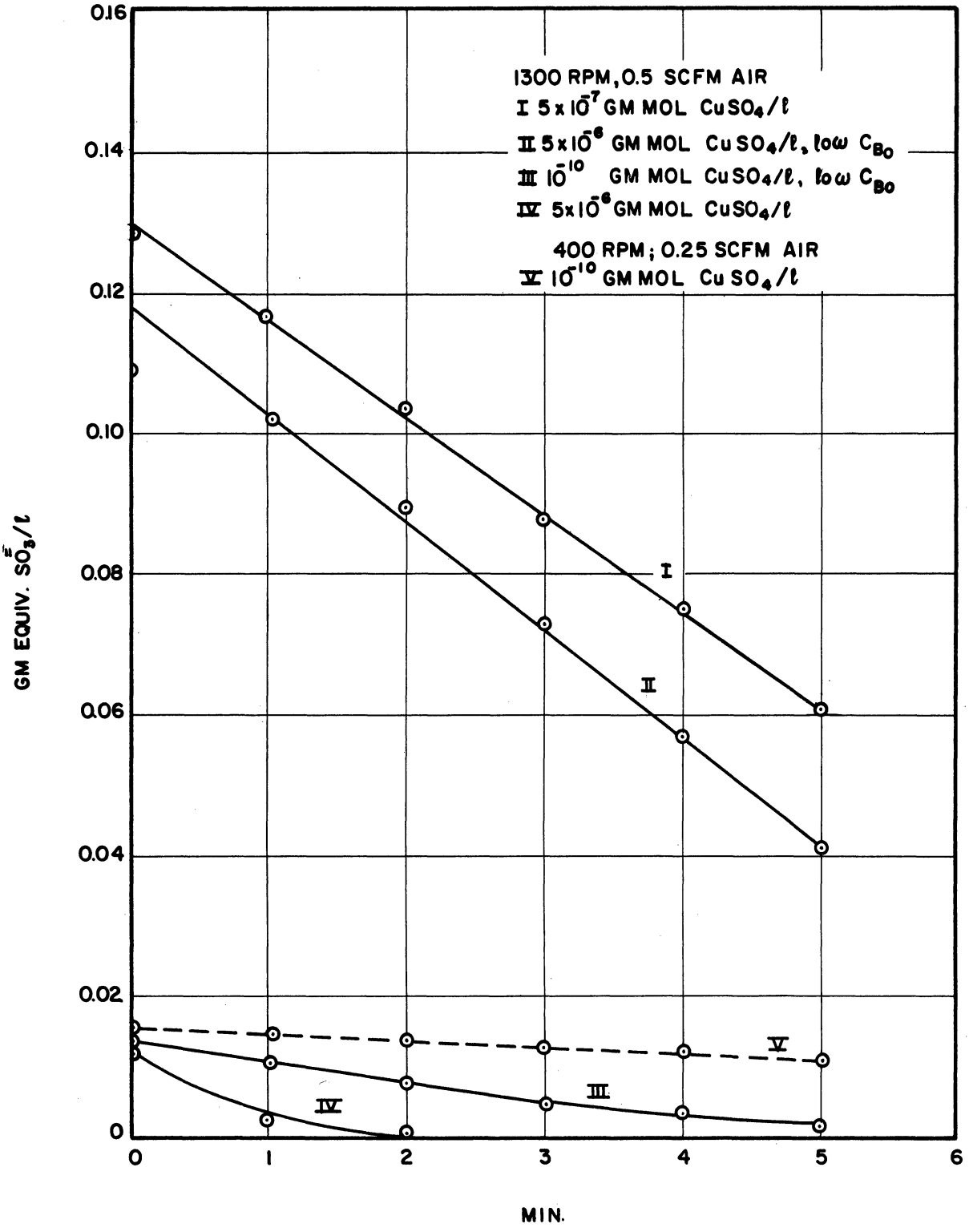

Figure 12. Reaction with Cu^{++} catalyst.

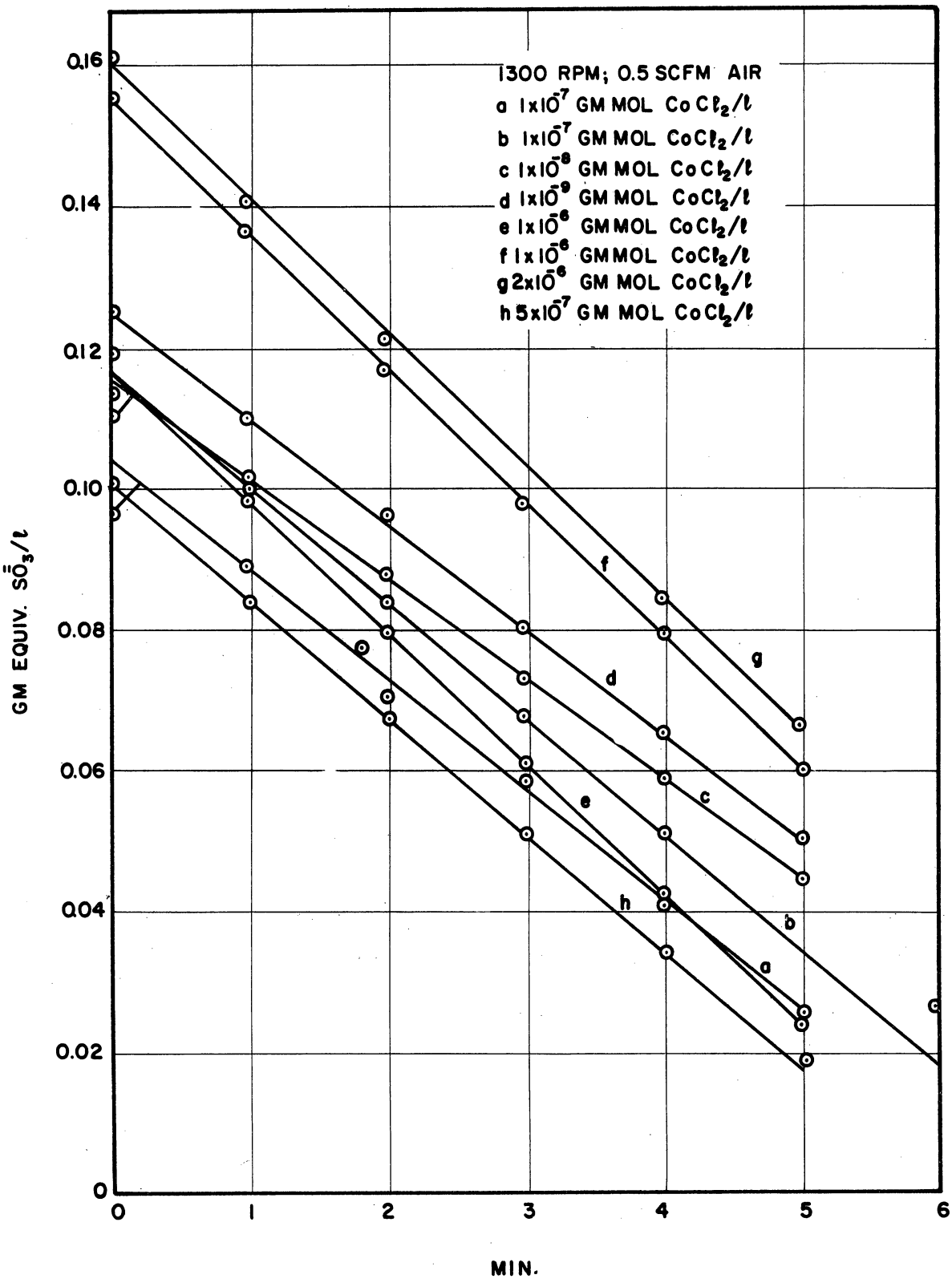

Figure 13. Reaction with Co^{++} catalyst.

In liquid phase the rate of oxygen uptake can be represented as

$$\frac{N_A}{V} = K_R\, a'(C_{Ai} - 0)$$

$$= k_L^o\, a'(C_{Ai} - C_{Ao})$$

$$= k' \cdot C_{Bo} \cdot C_{Ao} \qquad (28)$$

where K_R is the overall liquid phase transfer coefficient with reaction and $a' \equiv a/V$.

or

$$\frac{V}{N_A}[C_{Ai} - 0] = \frac{1}{K_R\, a'}$$

$$= \frac{V}{N_A}[(C_{Ai} - C_{Ao}) + (C_{Ao} - 0)]$$

$$= \frac{1}{k_L^o\, a'} + \frac{1}{k'\, C_{Bo}} \qquad (29)$$

For reaction without catalyst a plot of $\frac{1}{K_R\, a'}$ versus $\frac{1}{C_{Bo}}$ with intercept of $\frac{1}{k_L^o\, a'}$ would have a slope of $1/k'$.

The coefficient $k_L^o\, a'$ was determined in the same manner as k_L^o in Section I, B, b, except that the air was bubbled through the water and the stirrer speed was 1300 rpm with baffles provided as in the kinetic study. Slope of the

curve, in Figure 14 from the data in Table 21, Appendix IX, using the experimental value of C_{Ai} gave the value of $k_L^o a'$ as 12.2 min^{-1} .

The experimental value of C_{Ai} is about 10 per cent below that in the literature.(21) Despite great effort and careful checking of solutions this discrepancy could not be explained. If the error in all oxygen determination was of the same percentage magnitude then the value of $k_L^o a'$ will be unaffected for it is obtained as a function of the slope of a ratio on a semi-logarithmic plot. If the analysis of low concentration of oxygen is correct while the high saturated one is in error then the value of the slope obtained by using experimental C_{Ai} is about 20 per cent higher than the slope obtained by using the literature value. The corresponding value of $k_L^o a'$ is 20 per cent lower. It appears from Figure 15, which is a plot of $\frac{1}{K_R a'}$ versus $\frac{1}{C_{Bo}}$ with intercept of $\frac{1}{k_L^o a'}$, that any lower value of $\frac{1}{k_L^o a'}$ will not be consistent with the rest of the data on that plot. Therefore the value of $k_L^o a'$ obtained with experimental C_{Ai} is accepted.

The curve in Figure 15 is obtained from data in Table 22, Appendix IX for 5 runs and with intercept of $\left[\frac{1}{k_L^o a'}\right] = 0.0822$. The data for C_{Bo} is taken from the

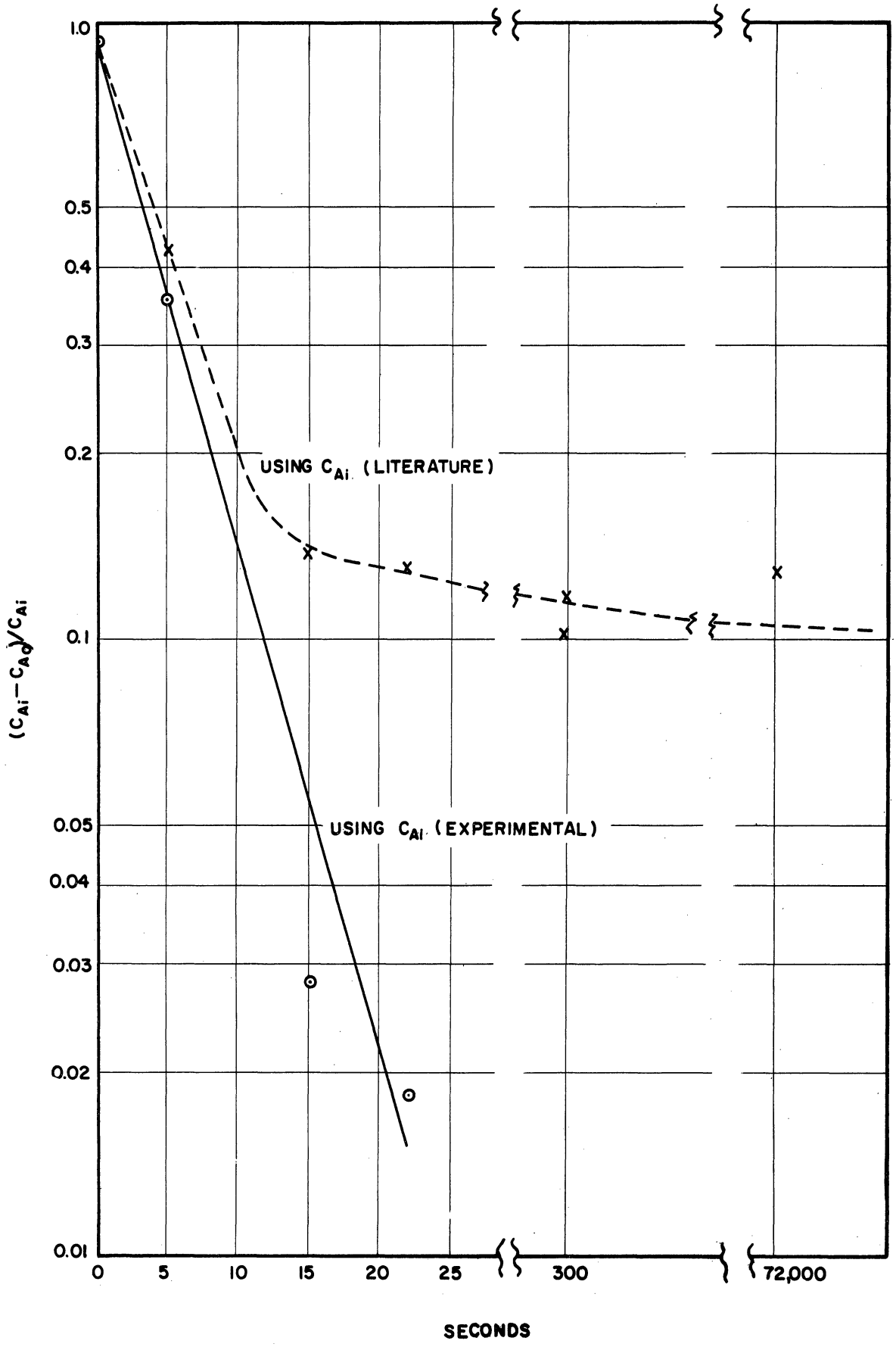

Figure 14. Determination of $k_L^o a'$.

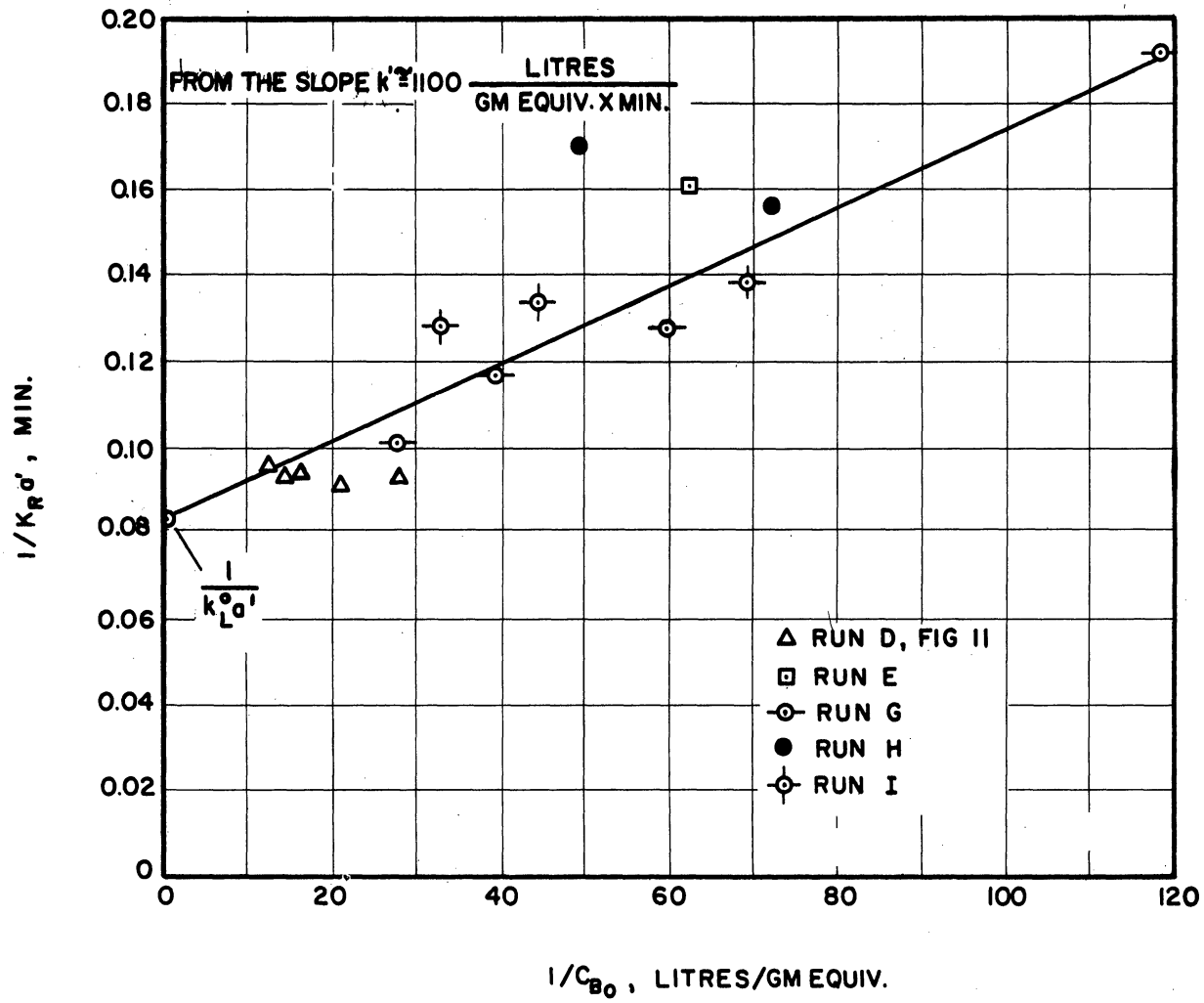

Figure 15. Determination of k' for reaction without catalyst.

lines in Figure 11 between the range of 0.01-0.1 gm equiv/l as the concentration below 0.01 gm equiv/l is subject to analytical error and at concentrations above 0.1 gm equiv/l the reaction is no longer first order in $SO_3^=$, Figure 8. The slope of the curve in Figure 15 gives $k' = 1100$ liters/gm equiv min.

d. Determination of chemical kinetic coefficient, k' from k_L

Brian, Hurley and Hasseltine[3] give a computer solution for second order reaction in mass transfer processes with penetration theory. They developed an approximate expression for γ:

$$\gamma + 1 = \frac{\sqrt{M} \cdot \sqrt{1 - (\gamma/\gamma_a)}}{\tanh \left[\sqrt{M} \cdot \sqrt{1 - (\gamma/\gamma_a)} \right]} \qquad (30)$$

Where

$$M \equiv \pi/4 \ (k' \ C_{Bo} \theta) \qquad (31)$$

$\gamma_a = (k_L/k_L^o) - 1$ is obtained by the Danckwerts equation for infinitely rapid reaction, Table 1.

When $\left[\sqrt{M} \cdot \sqrt{1 - (\gamma/\gamma_a)} \right]$ is greater than 5, as for the thesis data, the denominator in Equation 30 approaches unity and Equation 30 can be written as

$$\gamma + 1 = \sqrt{M} \cdot \sqrt{1 - (\gamma/\gamma_a)} \qquad (32)$$

or

$$M = \frac{\gamma_a \cdot (\gamma + 1)^2}{\gamma_a - \gamma} \qquad (33)$$

which will give the values of second order reaction rate coefficient k' .

According to Equation 33 the value of k' for reaction without catalyst is about 1200 liters/ gm equiv min , Table 24, Appendix IX. This value is based on the average of five runs at different sulfite concentrations which gave $k' = 1203$ liters/gm equiv min . It compares favorably with the value of k' obtained from Figure 15, 1100 liters/gm equiv min . Using the results of Figure 15 and those of Brian, et al., Equation 33, the dashed line in Figure 8 is predicted for reaction without catalyst. This line could be drawn before any rate data is taken for a smooth surface. The agreement between the data and the predicted line for reaction without catalyst, Table 23, Appendix IX, plotted in Figure 8 is excellent.

Values of k' estimated from Equation 33, Tables 25 and 26, Appendix IX, for reaction catalysed with Cu^{++} and Co^{++} are plotted as a function of catalyst ion concentration,

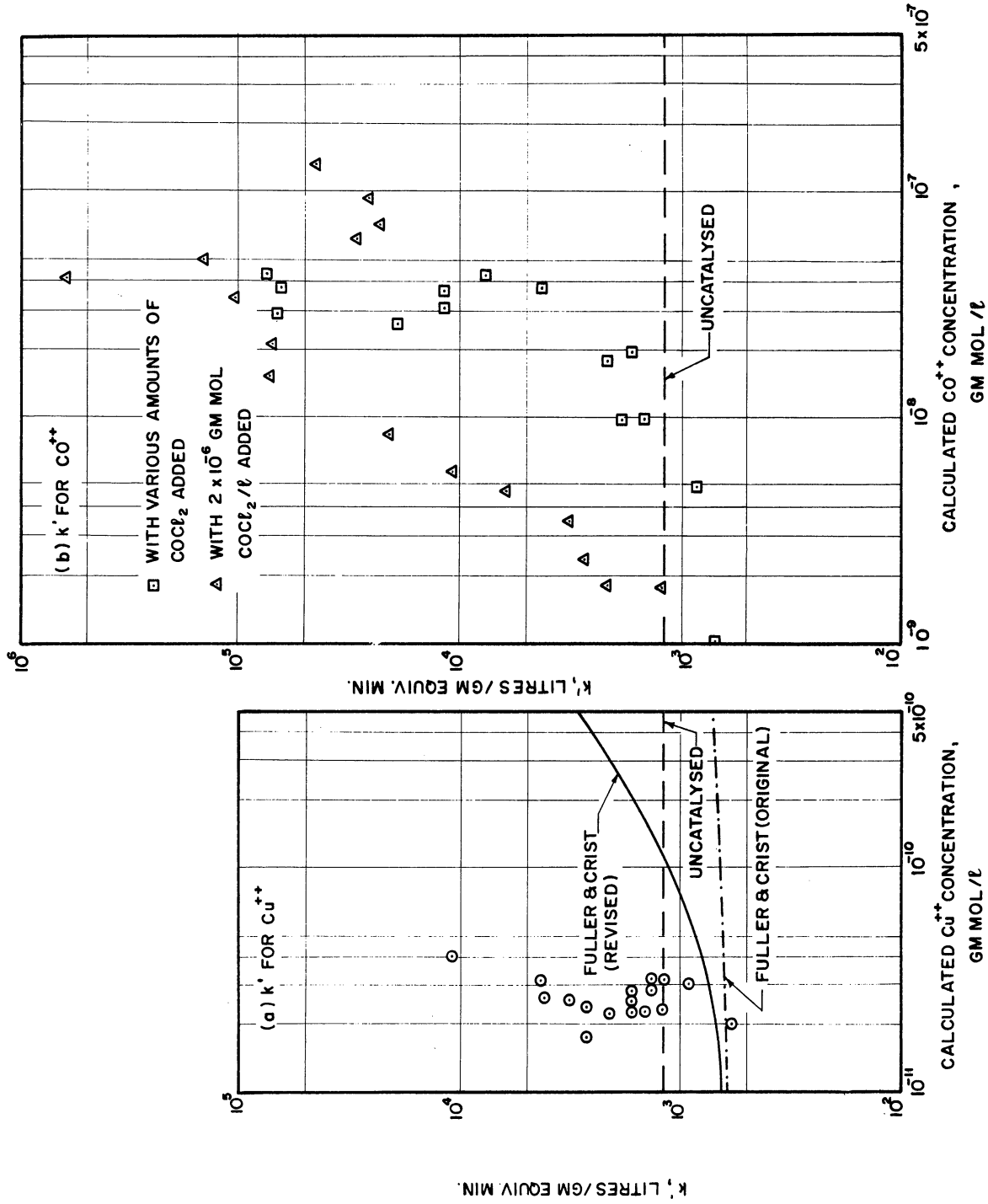

Figure 16. Second order kinetic coefficients from k_L versus calculated catalyst ion concentration.

Figure 16. For the sake of comparison k' for Cu^{++}-catalyst computed by using the constants k_1 and k_3 by Fuller and Crist and those corrected by using constants from Latimer,[25] Table 27, Appendix IX, are also plotted in Figure 16. It is seen that the values of k' obtained by Fuller and Crist are much lower than those calculated here as would be expected if their values were low because of mass transfer resistance.

Phillips and Johnson[29] report that oxygen absorption by sulfite solutions in unsparged vessel is not gas film or liquid film controlled because they observed no change in transfer rate due to agitation. To them it appeared that as the reaction took place in the bulk liquid and since the rate was dependent on the chemical reaction the major resistance to oxygen transfer must be in the liquid phase and that diffusion through a stagnant liquid film would not be the rate controlling step. It has already been shown in Section I, 2, c, that contrary to Phillips and Johnson, increased agitation in the liquid phase increases the rate of absorption. In Figure 10, Run J shows that the rate of absorption with stirrer speed of 400 rpm and air rate of 0.25 SCFM is lower than those with higher agitation and air rate, 1300 rpm and 0.5 SCFM. This indicates that the rate

of oxygen uptake is controlled by mass transfer resistance. This is further supported by the kinetic data where the absorption rate is zero order in sulfite concentration as required if mass transfer were controlling. The value of the second order reaction rate constant, k', obtained from Figure 15, which takes into account the mass transfer resistance according to Equation 29, compares favorably with the value of k' computed from k_L obtained in an unsparged reactor definitely establishing the effect of mass transfer resistance on the oxygen uptake.

e. Reaction inhibited by mannitol

For reaction inhibited by mannitol Fuller and Crist[13] report

$$-\frac{d(SO_3^{=})}{dt} = \left[\frac{1 \times 10^{-5} k_1}{1 \times 10^{-5} + (\text{mannitol})}\right](SO_3^{=}) \qquad (34)$$

Figure 17 is a plot of values of k' obtained from Equation 34 and from k_L as a function of mannitol concentration, Table 28, Appendix IX. As would be expected the values from k_L are larger than those from Equation 34 since the latter does not give true reaction rate coefficients.

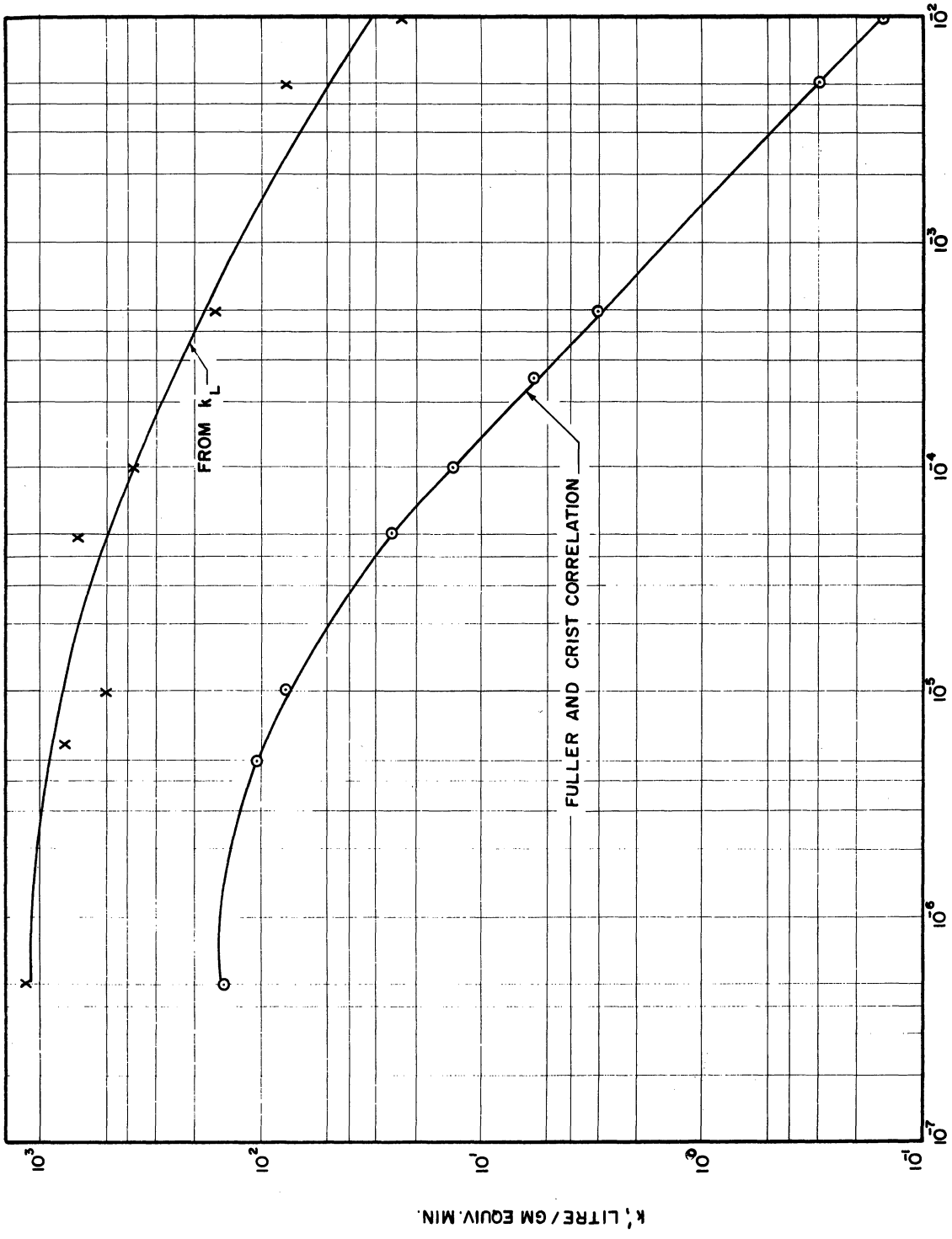

Figure 17. Second order kinetic coefficients versus mannitol concentration.

f. Reaction inhibited by benzyl alcohol

For reaction inhibited by benzyl alcohol in the presence of light Alyea and Bäckstrom[1] give for 0.6 molar sodium sulfite solutions

$$-\frac{d(SO_3^{=})}{dt} = k_{zero}$$

$$= \frac{0.000019}{0.0012 + (\text{benzyl alcohol})} \frac{\text{gm equiv}}{\ell \cdot \text{min}} \qquad (35)$$

The constant 0.000019 includes a constant equal to the ratio of rates in darkness and light. Unlike mannitol the rate here is considered to be independent of $SO_3^{=}$ concentration. For benzyl alcohol concentrations used in the present work, 5×10^{-7} to 5×10^{-5} gm mol/l , the rate predicted is practically constant as the denominator in Equation 35 is hardly affected. But the k_L data shows it to be a function of benzyl alcohol concentration in this range, Table 9, Appendix IV. The rate given by Equation 35 is pseudo-zero order

$$k_{zero} = k' \cdot C_{Ai} \cdot C_{Bo} \qquad (36)$$

or

$$k' = \frac{k_{zero}}{(C_{Ai} \cdot C_{Bo})} \qquad (37)$$

Figure 18 is a plot of k' obtained from Equation 37 and those from k_L as a function of benzyl alcohol concentration using Equation 33, Table 29, Appendix IX. The values of k' from k_L are higher than those of Alyea and Bäckstrom. This is in part due to their sulfite concentration being in region where the reaction is no longer first order in sulfite concentration whereas the thesis data was obtained at much lower sulfite concentration.

g. Reaction inhibited by catechol

Catechol is such an effective inhibitor that it completely kills the reaction.[27] Also, the plugging of the interface by the alcohol reduces the mass transfer. The data on absorption in presence of catechol, Figure 5-a or 5-b, supports this. The kinetic coefficients for reaction with catechol would be meaningless.

From the runs for chemical kinetic coefficients made here and elsewhere for the oxidation reaction with and without catalyst one can conclude that the coefficients previously reported are not true coefficients as mass transfer resistance is important. They are lower than those computed from mass transfer coefficients with reaction, k_L. This

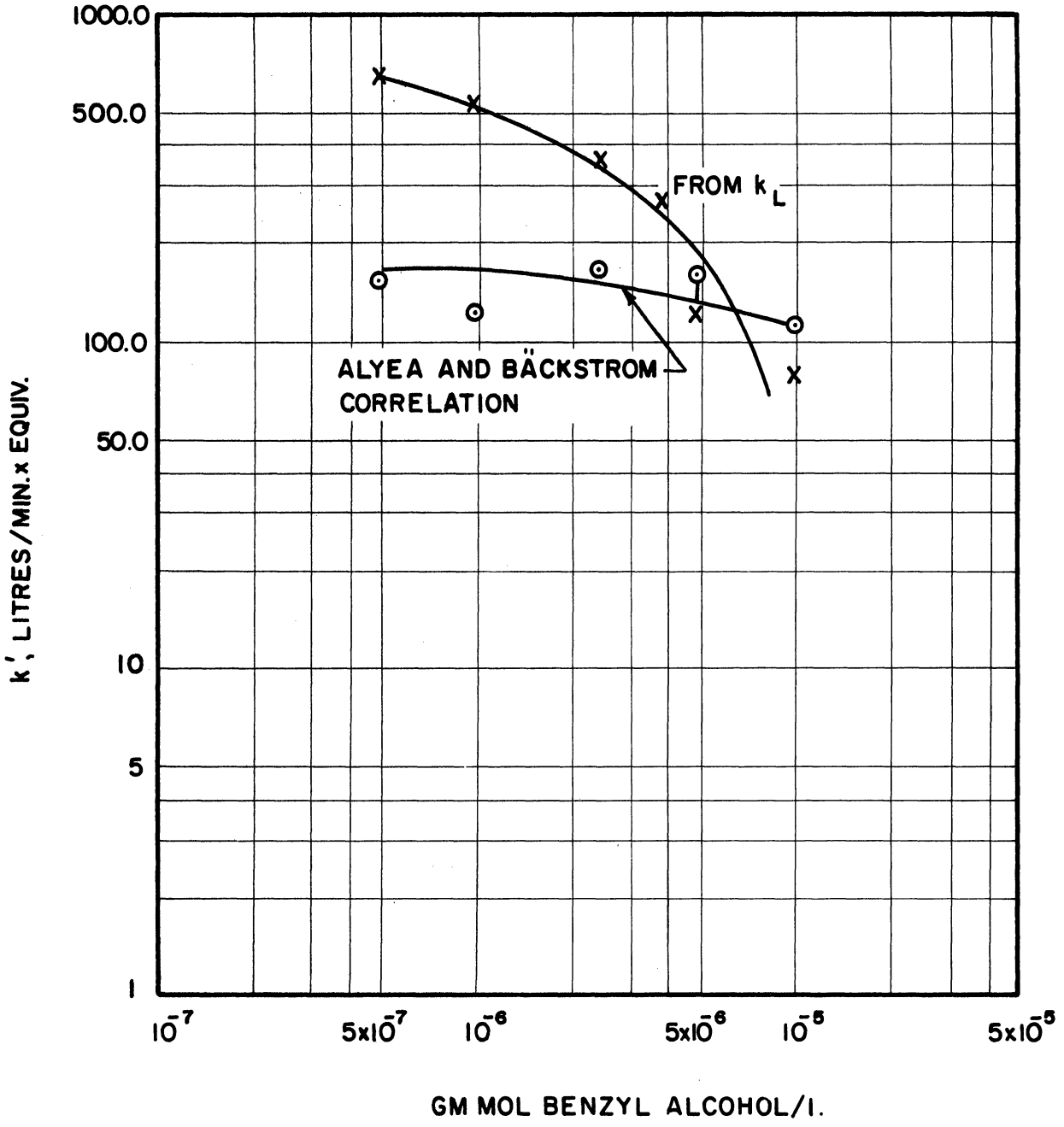

Figure 18. Second order kinetic coefficients versus benzyl alcohol concentrations.

is to be expected if mass transfer were important. The existence of mass transfer resistance in the kinetic process is established.

The chemical kinetic coefficients estimated from k_L with the numerical solutions of the diffusion equation published by Brian, et al.[3] are consistent with present knowledge. This is very easily seen when one compares the value of the second order kinetic coefficient $k' = 1100$ liters/gm equiv min for reaction without catalyst determined by taking into consideration the resistance due to mass transfer with that computed from k_L by the Brian solution, which is 1200 liters/gm equiv min .

III. CONCLUSIONS

Liquid phase mass transfer coefficients with and without chemical reaction for a gas-liquid system were determined using sodium sulfite oxidation reaction. From the absorption of oxygen into a turbulent solution of sodium sulfite with knwon interfacial area the following may be concluded.

1) Measured absorption rates 4-50 times those without reaction showed the increase as expected from the theories for infinitely fast reaction; namely those of Hatta, Sherwood and Wei, Danckwerts, Higbie and Kishinevskii. The data are not represented by any one of the theories but cross the various theoretical lines as the rate increases. At low absorption rates the data are best represented by those theories indicating greater rates while at high absorption rates the data follow those theories indicating lower rates.

2) As expected the runs with positive catalysts, Cu^{++} and Co^{++}, show increased absorption rates and those with negative catalysts, mannitol, benzyl alcohol and catechol, decreased rates. The rate of absorption with reaction increased with increased stirrer speed in the range 35-210 rpm. The study of the effect of varying the sulfite concentration showed that the rate was first order in sulfite concentration below 0.14 gm equiv $SO_3^=/l$. At higher concentrations the rate increased and then declined. Using 99.5 per cent oxygen in place of air gave slightly lower coefficients except at low catalyst concentrations (below 1×10^{-9} gm mol $CoCl_2/l$).

3) Previously reported chemical kinetic coefficients obtained by conventional techniques for the oxidation reaction with and without catalyst are not true coefficients but are lower because of mass transfer limitations. Kinetic coefficient for reaction without catalyst as determined by taking into consideration the mass transfer resistance is 11×10^2 liters/gm equiv min.

4) Chemical kinetic coefficients were determined from absorption of oxygen using the solution of diffusion

equation with reaction based on penetration model. The kinetic coefficient for reaction without catalyst was determined to be 12 x 10^2 liters/gm equiv min . This compares favorably with one obtained by another method referred to above.

NOMENCLATURE

A	Component A in gas phase
a	Area, sq cm
a'	Area per unit volume of the solution, a/V , cm^2/cc
b	Gm mol of B reacting with one gm mol of A
B	Component B in liquid phase
C_A	Concentration of A in bulk, gm equiv A/cc
C_{Ai}	Concentration of A at the interface, gm equiv A/cc
C_{Bo}	Concentration of B in bulk at the start, gm equiv B/cc
C_ℓ	Concentration of A at a distance ℓ from interface, gm equiv/cc
C_{I_2}	Concentration of I_2-catalyst, gm mol I_2/cc
C_+, C_-	Concentration of positive or negative ion, gm equiv ion/cc
ΔC	Difference in concentration (driving force)
D_A	Diffusivity of A in liquid phase, cm^2/min
D_B	Diffusivity of B in liquid phase, cm^2/min

D_{AB} Diffusivity of the product AB in liquid phase, cm^2/min

F Faraday or 96,500 coulombs/gm equiv

G_+, G_- Concentration gradient of ions, $\Delta c/\Delta x$, gm equiv/cc · cm

g_c Conversion factor between M-L-T and F-L-T systems, dimensionless

H Henry's law constant

k_{zero} Pseudo-zero order reaction rate coefficient, gm equiv/liter · min

k Pseudo-first order reaction rate coefficient, min^{-1}

k' Second order reaction rate coefficient, liters/gm equiv · min

k_1 Homogeneous reaction rate coefficient, min^{-1}

$k_{3(Cu^{++})}$ Catalytic coefficient for Cu^{++}

$k_{3(Co^{++})}$ Catalytic coefficient for Co^{++}

k_g Gas phase mass transfer coefficient, lb mol/atmos · ft^2 · hr

k_L Liquid phase mass transfer coefficient with reaction, cm/min or ft/hr

k_L^o Liquid phase mass transfer coefficient without reaction, cm/min or ft/hr

K $k' \cdot k_L^o \cdot \theta$

K_L Overall mass transfer coefficient based on k_L, cm/min or ft/hr

K_R Overall transfer coefficient in liquid phase, min^{-1}

ℓ Distance from the interface, cm

M Factor defined as $(k' C_{Bo} \theta)$

m Concentration of 1/2 $SO_4^=$, gm equiv 1/2 $SO_4^=$/cc

n Concentration of Na^+, gm equiv Na^+/cc

n_+, n_- Valence

N Stirrer speed, rpm

N_A Rate of absorption of A, gm equiv A/min

N'_A Rate of absorption of A per unit area, gm equiv A/cm^2 . min

N'_{AB} Rate of absorption of AB per unit area, gm equiv AB/cm^2 . min

N'_B Rate of absorption of B per unit area, gm equiv B/cm^2 . min

$N(\theta)$ Amount of gas absorbed in time θ per unit area, gm equiv/min . cm^2

N'_+, N'_- Rate of diffusion of ion, gm equiv ion/cm^2 . min

p_A Partial pressure of component A in gas phase, atmos

p_{Ai} Partial pressure of A at the interface, atmos

q	Concentration of $1/2\ SO_3^{=}$, gm equiv $1/2\ SO_3^{=}$/cc
R	Gas constant, 8.3144 joules/°K gm mol of electrolyte
s	Fractional rate of surface renewal, 1/time
t	Time, min
T	Temperature, °Absolute
u_+, u_-	Equivalent conductance of an ion, mhos . cc/cm . gm equiv ion
U'	Mobility of Cation, cm^2/sec . volt
V	Volume, cc
V'	Mobility of Anion, cm^2/sec . volt
x_1	Distance between the reaction zone and interface, cm
x_2	Thickness of the reaction zone in the liquid film, cm
x_L	Thickness of the liquid film, cm
y^+	Dimensionless distance from the interface or wall
y_R^+	Dimensionless distance from the wall to the reaction zone
β	A factor defined by the Equation 18
γ	$(k_L/k_L^o) - 1$
γ_a	γ according to Danckwerts model for rapid reaction

ϵ Eddy diffusivity, cm^2/min

$\varphi(t)$ Surface age distribution function

$\varphi(y^+, \sigma)$ The integral, $\int_0^{y^+} \frac{dy^+}{1/\sigma + \epsilon/\nu} = \left[\frac{\tau_w g_c}{\rho}\right]^{1/2} \left[\frac{C_{Ai} - C_{Ao}}{N_{Ai}}\right]$

μ A stoichiometric factor, number of moles of A reacting with one mole of B

η Viscosity, gm/cm . min

ν Kinetic viscosity, cm^2/min

ρ Density, gm/cc

σ Schmidt number, dimensionless, (ν/D_A)

θ Time

τ_w Shear stress at the wall, $dynes/cm^2$

ψ Electrostatic potential, volts

Subscripts

A relates to Component A

AB relates to product AB

B relates to component B

g relates to gas phase

i relates to interface

L relates to liquid phase

o relates to bulk

R relates to the reaction zone

+, - relates to cation and anion respectively

Superscripts

o indicates absence of reaction

' per unit area when it refers to the flux

REFERENCES

1. Alyea, H. N. and H. L. Bäckstrom, J.A.C.S., 51, 90, 1929.

2. Barth, K., Z. Phys. Chem., 9, 176, 1892.

3. Brian, P. L. T., J. F. Hurley and E. H. Hasseltine, A.I.Ch.E.J., 7, 226, 1961.

4. Carslaw, H. S. and J. C. Jaeger, Conduction of Heat in Solids, 2nd ed. Oxford University Press, 1947.

5. Chambré, P. L. and J. D. Young, Physics of Fluids, 1, 48, 1958.

6. Danckwerts, P. V., Ind. Eng. Chem., 43, 1460, 1951.

7. Danckwerts, P. V., A.I.Ch.E.J., 1, 456, 1955.

8. Danckwerts, P. V., Trans. Faraday Soc., 46, 300, 1950.

9. Danckwerts, P. V., Trans. Faraday Soc., 46, 701, 1950.

10. Danckwerts, P. V., App. Sci. Res., 3A, 385, 1953.

11. Danckwerts, P. V. and A. M. Kennedy, Trans. Inst. Chem. Eng., 32, S49, 1954.

12. Friedlander, S. K. and M. Litt, Chem. Eng. Sci., 7, 229, 1958.

13. Fuller, E. C. and R. H. Crist, J.A.C.S., 63, 1644, 1941.

14. Gaden, E. E. and J. E. Schultz, Ind. Eng. Chem., 48, 2209, 1956.

15. Grant, J., Sutton's Systematic Handbook of Volumetric Analysis, 13th ed., Butterworth Scientific Publications, London, 1955.

16. Hanratty, T. J., A.I.Ch.E.J., 2, 359, 1956.

17. Haskell, R., Physical Review, 27, 145, 1908.

18. Hatta, S., Technol. Reports, Tohoku Imperial Univ., 8, 1, 1928.

19. Higbie, R., Trans. Amer. Inst. Chem. Eng., 31, 365, 1935.

20. Hyman, D. and J. M. Van Den Boaerde, Ind. Eng. Chem., 52, 751, 1960.

21. International Critical Tables, McGraw-Hill Publishing Company, New York.

22. Kishinevskii, M. Kh., Zh. Prikladnoi Khimii, 24, 542, 1951.

23. Kishinevskii, M. Kh., Zh. Prikladnoi Khimii, 27, 382, 1954.

24. Kishinevskii, M. Kh. and A. B. Pamfulov, Zh. Prikladnoi Khimii, 22, 1173, 1949.

25. Latimer, W. M., Oxidation Potentials, 2nd ed., Prentice Hall, 1952.

26. Lynn, S., J. R. Straatemeier and H. Kramers, Chem. Eng. Sci., 4, 2, 49, 1955.

27. Mellor, J. W., A Comprehensive Treatise on Inorganic and Theoretical Chemistry, Vol X, Longmans Green, New York, 1956.

28. Peaceman, D. W., Thesis, M.I.T., 1951.

29. Phillips, D. H. and M. J. Johnson, Ind. Eng. Chem., 51, 83, 1959.

30. Potter, O. D., Trans. Inst. Chem. Eng., 36, 415, 1958.

31. Pozin, M. E., J. Applied Chem., U.S.S.R., 19, 1201, 1956. (English summary, Ind. Eng. Chem., Vol 41, 12, 1949)

32. Pozin, M. E. and A. M. Opykhtina, J. Applied Chem., U.S.S.R., 20, 523, 1947.

33. Reid, R. C. and T. K. Sherwood, Properties of Liquids and Gases, McGraw-Hill Publishing Company

34. Roper, G. H., Chem. Eng. Sci., 2, 18, 1953.

35. Scriven, L. E. and R. L. Pigford, A.I.Ch.E.J., 4, 429, 1958.

36. Searle, R. and K. F. Gordon, A.I.Ch.E.J., 3, 490, 1957.

37. Seidel, A., Solubilities of Inorganic and Metal-organic Compounds, Vol I, 3rd ed., D. Van Nostrand Company, 1940.

38. Sherwood, T. K. and F. A. L. Holloway, Trans. A.I.Ch.E., 36, 39, 1940.

39. Sherwood, T. K. and R. L. Pigford, Absorption and Extraction, 2nd ed., McGraw-Hill Publishing Company, 1952.

40. Sherwood, T. K. and C. E. Reed, Applied Mathematics in Chemical Engineering, McGraw-Hill Publishing Company, 1939.

41. Sherwood, T. K. and J. M. Ryan, Chem. Eng. Sci., 11, 2187, 1959.

42. Sherwood, T. K. and J. C. Wei, Ind. Eng. Chem., 49, 1030, 1957.

43. Sherwood, T. K. and J. C. Wei, A.I.Ch.E.J., 1, 522, 1955.

44. Stephens, E. J. and G. A. Morris, C.E.P., 47, 5, 232, 1951.

45. Toor, H. L. and J. M. Marchello, A.I.Ch.E.J., 4, 97, 1958.

46. Udani, L. H. and K. F. Gordon, A.I.Ch.E.J., 5, 510, 1959.

47. VanKrevelen, D. W. and P. J. Hoftijzer, C.E.P., 44, 529, 1948.

48. Vinograd, J. R. and J. W. McBain, J.A.C.S., 63, 2008, 1941.

49. Voznesewskii, S. K. and L. A. Klucharev, J. Gen. Chem., U.S.S.R., 2, 506, 1932.

50. Whitman, W. G., Chem. Met. Eng., 24, 146, 1923.

51. Yoshida, F., A. Ikeda, S. Imakawa and Y. Miura, Ind. Eng. Chem., 52, 438, 1960.

APPENDIX I

THE DERIVATION OF k_L VIA VARIOUS MODELS

APPENDIX I

DERIVATION OF k_L VIA VARIOUS MODELS

The effect of chemical reaction on mass transfer is measured by the ratio of liquid phase mass transfer coefficients with and without chemical reaction, k_L and k_L^o respectively. To derive this ratio consider a rapid irreversible reaction,

$$A_{(gas)} + B_{(aq)} = AB_{(aq)} \qquad (38)$$

A. The Film Models

i. Hatta model: Figure 19 shows the reaction of Equation 38.[18,39]

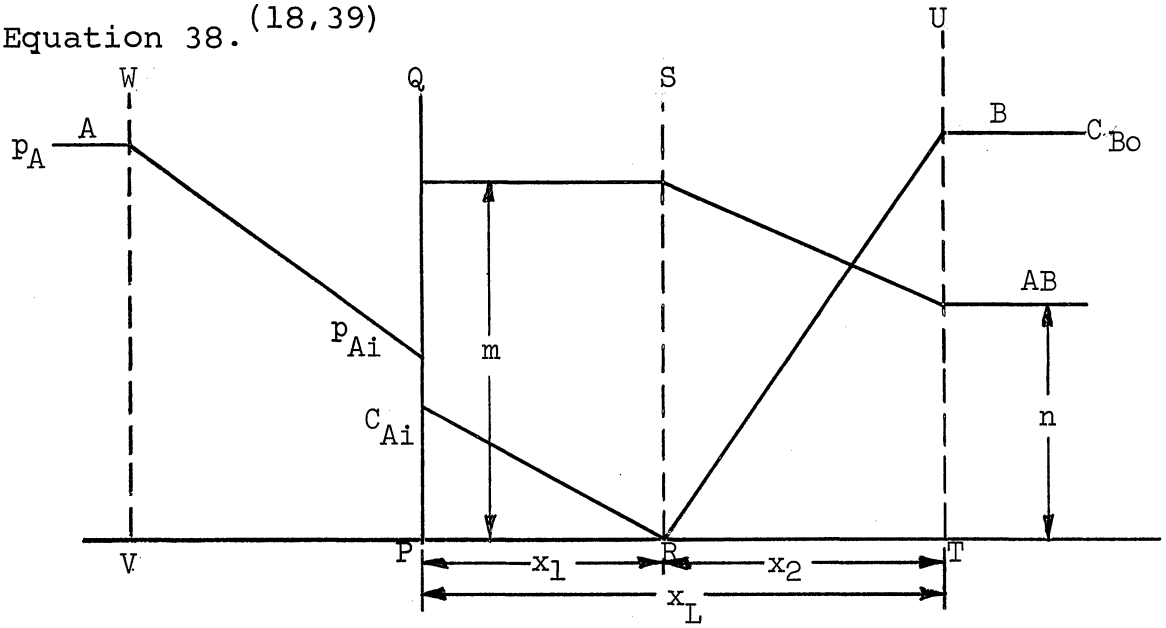

Figure 19. Hatta Model

The component A in the gas phase on contact with liquid at the interface PQ establishes an instantaneous equilibrium with the liquid phase. Scriven and Pigford[35] have demonstrated that such an equilibrium exists in the gas-liquid system during absorption. At the interface A dissolves physically in the liquid. The component B in the bulk is transported towards the interface. During this movement A and B react with each other in a reaction zone RS parallel to the interface and the product of the reaction, AB , is transported out of the reaction zone.

For the gas film the rate of absorption per unit area is given by

$$N'_A = k_g(p_A - p_{Ai}) \tag{39}$$

When the solvent concentration is large compared to those of the components A , B or AB we can write the rate equation for the QS section of the liquid film as

$$N'_A = \frac{D_A}{x_1}(C_{Ai} - 0) \tag{40}$$

For the SU section similar rate equation is

$$-N'_B = \frac{D_B}{x_2}(C_{Bo} - 0) = N'_A \tag{41}$$

and

$$N'_{AB} = \frac{D_{AB}}{x_2}(m - n + C_{Bo}) = N'_A \qquad (42)$$

Now if the gas-liquid interfacial equilibrium is assumed to follow the Henry's law we have

$$p_{Ai} = H\, C_{Ai} \qquad (43)$$

Equation 39 to 43 give on elimination of p_{Ai}, C_{Ai}, n, m, x_1, and x_2

$$N'_A = \frac{(p_A/H) + (D_B/D_A)\, C_{Bo}}{(x_L/D_A) + (1/H\, k_g)} \qquad (44)$$

or

$$N'_A = \frac{C_{Ai} + (D_B/D_A)\, C_{Bo}}{x_L/D_A} \qquad (45)$$

The liquid film coefficient with reaction, k_L, defined by the Equation 1

$$N'_A = k_L(C_{Ai} - 0) \qquad (1)$$

is obtained from Equation 45 as

$$k_L = \frac{D_A}{x_L}\left[1 + \frac{D_B}{D_A} \cdot \frac{C_{Bo}}{C_{Ai}}\right] \qquad (46)$$

The rate equation for mass transfer without reaction can be written as

$$N'_A = \frac{D_A}{x_L}(C_{Ai} - C_{Ao}) \qquad (47)$$

From Equations 2 and 47 we have

$$k_L^o = D_A/x_L \tag{48}$$

From Equations 46 and 48 we then have

$$\gamma = \frac{k_L}{k_L^o} - 1 = \left[\frac{D_B}{D_A} \cdot \frac{C_{Bo}}{C_{Ai}}\right] \tag{49}$$

ii. Sherwood and Wei model: Vinograd and McBain[48] write diffusion equations for each ion imposing electrical neutrality for the ion mixture.

For cation,

$$N'_+ = -\frac{RT}{F^2}\frac{u_+}{n_+}\left[G_+ - n_+C_+\frac{\Sigma u_+G_+/n_+ - \Sigma u_-G_-/n_-}{\Sigma u_+C_+ + \Sigma u_-C_-}\right] \tag{50}$$

For anion,

$$N'_- = -\frac{RT}{F^2}\frac{u_-}{n_-}\left[G_- + n_-C_-\frac{\Sigma u_+G_+/n_+ - \Sigma u_-G_-/n_-}{\Sigma u_+C_+ + \Sigma u_-C_-}\right] \tag{51}$$

The derivation of these equations from first principles, ignoring the activity coefficients, the collision effects and the effects of ion pairs or ionic complexes, is given in Appendix II. It may be noted that the factor $\frac{RT}{F^2} \cdot \frac{u}{n}$ in these equations is the diffusion coefficient of the ion in its free state and the factor in the parenthesis is the concentration gradient of that ion corrected for the presence of the other ions.

The reaction

$$Na_2SO_{3(aq)} + 1/2\ O_{2(gas)} \rightarrow Na_2SO_{4(aq)} \qquad (52)$$

or following the electrochemical convention

$$1/2\ Na_2SO_{3(aq)} + 1/4\ O_{2(gas)} \rightarrow 1/2\ Na_2SO_{4(aq)} \qquad (53)$$

is shown in Figure 20 according to the Hatta theory.

Tables 3 and 4 give data required in Equations 50 and 51.

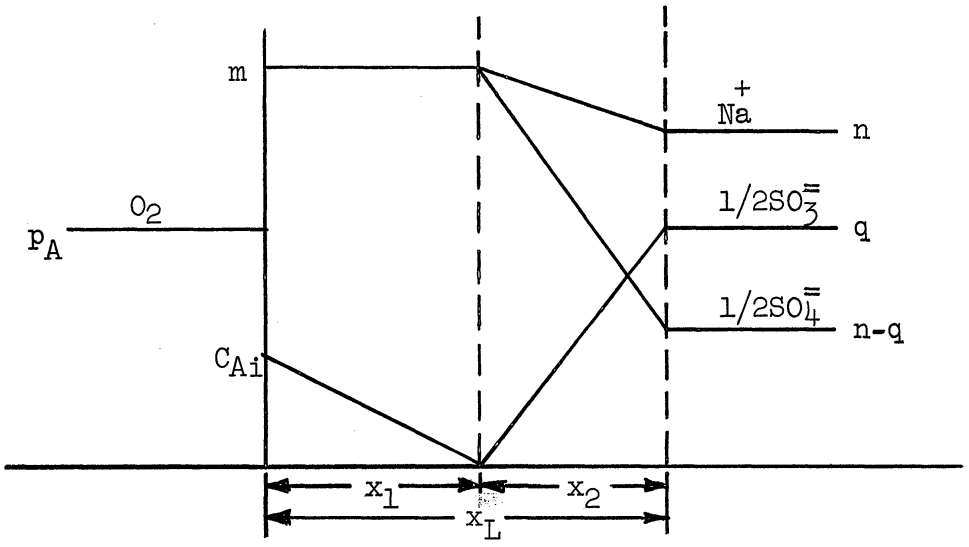

Figure 20. Sherwood and Wei model

For Na^+ - ion in x_2 - layer, the rate of diffusion is obtained from Equations 50 and 51, using data in Tables 3 and 4, as

$$N_{Na^+} = \frac{-7.97 \times 10^{-4}}{x_2}\left[\frac{9600(n^2 - m^2) - 2712\ n\ q}{7800(n + m) - 1356\ q}\right]; \quad \frac{\text{gm equiv.}}{\text{cm}^2 \times \text{min}} \qquad (54)$$

Similarly for $1/2\ SO_3^=$ - ion

TABLE 3

Ion	Valence	u, $\frac{cm^2}{sec \cdot volt}$	$G = \frac{\Delta C}{\Delta x}$, $\frac{gm\ equiv}{cc \cdot cm}$	C, $\frac{gm\ equiv}{cc}$	$\frac{RT}{F}\frac{u}{n}$, $\frac{cm^2}{min}$
Na^+	1	50/F (48)	$\frac{n - m}{x_2}$	$\frac{n + m}{2}$	7.97×10^{-4}
$\frac{1}{2}\ SO_3^=$	1	57.4/F (2)	$\frac{q - 0}{x_2}$	$\frac{q - 0}{2}$	9.15×10^{-4}
$\frac{1}{2}\ SO_4^=$	1	80/F (48)	$\frac{n - q - m}{x_2}$	$\frac{n + m - q}{2}$	12.75×10^{-4}

TABLE 4

Ion	$\frac{u \cdot G}{n}$; $\frac{\text{gm equiv}}{\text{min . volt . cm}^2}$	uC ; $\frac{\text{gm equiv}}{\text{min . volt . cm}}$
Na^+	$\frac{3000(n - m)}{F \circ x_2}$	$\frac{3000(n + m)}{2F}$
$\frac{1}{2}\ SO_4^=$	$\frac{3444\ q}{F\ x_2}$	$\frac{3444\ q}{2F}$
$\frac{1}{2}\ SO_4^=$	$\frac{4800(n - q - m)}{F\ x_2}$	$\frac{4800(m + n - q)}{2F}$

$$\Sigma \frac{u_+ G_+}{n_+} = \frac{3000(n - m)}{F\ x_2} \; ; \quad \Sigma \frac{u_- G_-}{n_-} = \frac{4800(n - m) - 1356\ q}{F\ x_2}$$

$$\Sigma\ u_+ C_+ = \frac{3000(n + m)}{2F} \; ; \quad \Sigma\ u_- C_- = \frac{4800(n + m) - 1356\ q}{2F}$$

$$N_{1/2\ SO_3^{=}} = \frac{-9.15 \times 10^{-4}}{x_2} \cdot q \left[\frac{6000\ n + 9600\ m}{7800(n + m) - 1356\ q}\right];$$

$$\frac{\text{gm equiv.}}{\text{cm}^2 \times \text{min}} \tag{55}$$

In the case of Na^+ - ion

$$N_{Na^+} = 0 \tag{56}$$

Equations 54 and 55, then yield

$$m = \pm\sqrt{n^2 - 0.281\ n\ q} \tag{57}$$

Positive values of m will be used to eliminate m in Equation 55. Now, the rate of absorption of oxygen with reaction is given by Equation 1:

$$N_A' = k_L(C_{Ai} - 0) \tag{1}$$

or

$$k_L = \frac{N_A'}{C_{Ai}} \tag{58}$$

In x_1 - layer

$$N_A' = \frac{D_A}{x_1}(C_{Ai} - 0) \tag{59}$$

For the entire x_L - layer,

$$N_A' x_1 = N_A' \cdot x_L = \frac{N_{(1/2\ SO_3^{=})}}{4} \cdot x_2 \tag{60}$$

But

$$k_L x_L = \frac{N_A'}{C_{Ai}} \cdot x_L = \frac{N_A' \cdot x_1}{C_{Ai}} + \frac{N_A' \cdot x_2}{C_{Ai}} \tag{61}$$

Therefore Equations 55, 59 and 60 yield

$$k_L x_L = D_A + \frac{9.16 \times 10^{-4}}{C_{Ai}} \cdot q \left[\frac{6000\ n + 9600\ m}{7800(n + m) - 1356\ q}\right] \frac{cm^2}{min} \tag{62}$$

Dividing Equation 62 by D_A and using Equation 48 we get

$$\frac{k_L}{k_L^o} - 1 = \frac{9.16 \times 10^{-4}}{D_A \cdot C_{Ai}} \cdot q \left[\frac{6000\ n + 9600\ m}{7800(n + m) - 1356\ q}\right] \tag{63}$$

iii. Boundary layer model: For the turbulent boundary layer model Sherwood and Ryan[41] obtain

$$\frac{k_L}{k_L^o} = \frac{\varphi(y_o^+, \sigma_A)}{\varphi(y_R^+, \sigma_B)} = \frac{C_{Bo}}{C_{Ai}} \cdot \frac{\varphi(y_o^+, \sigma_A)}{[\varphi(y_o^+, \sigma_B) - \varphi(y_R^+, \sigma_B)]} \tag{64}$$

where

$$\varphi(y, \sigma_A) = \int_o^{y^+} \frac{dy^+}{1/\sigma + \epsilon/\nu} = \frac{C_{Ai} - C_{Ao}}{N_{Ai}} \cdot \sqrt{\tau_w g_c/\rho}$$

The integral in Equation 65 represents the mass transfer resistance from the wall or the interface to y^+. It is interesting to note that for $\sigma_A = \sigma_B$ Equation 64 gives

$$\frac{k_L}{k_L^o} - 1 = \frac{C_{Bo}}{C_{Ai}} \quad \text{for} \quad D_A = D_B \tag{66}$$

Equation 66 is similar to the Equation 49. The same result is obtained when the ratio k_L/k_L^o approaches unity as y_R^+

becomes very large and the value of σ is not important. Thus, this theory leads to relations similar to Hatta's with the difference that the resistance per unit length varies with distance from the wall.

B. The Penetration Models

The difference between the Higbie and the Danckwerts models is in the definition of the surface age distribution function, $\varphi(t)$. To find the average absorption rate per unit area, the product of the fraction of surface which has age t and the stagnant liquid absorption rate for an exposure time t is integrated over all surface ages. Thus, the expression for average rate is

$$N'_A = \int_0^\infty N(\theta) \cdot \varphi(\theta) \cdot d\theta \tag{67}$$

where $N(\theta)$ is the amount of gas absorbed by unit area of stagnant surface in time θ . It is now necessary to determine the surface age distribution function $\varphi(t)$ for both the models. For the Higbie model[7] the distribution function $\varphi(t)$ for the exposure time θ is

$$\varphi(t) = \frac{1}{\theta} \qquad \text{for} \quad t < \theta \tag{68}$$

and

$$\varphi(t) = 0 \qquad \text{for} \quad t > \theta \tag{69}$$

For Danckwerts model[6] $\varphi(t)$ is given by

$$\varphi(t) = s \cdot e^{-s\theta} \tag{70}$$

where s is the fractional rate of renewal of the surface. By substituting Equations 68 and 69 in Equation 67 we get the rate equation for the Higbie model, as

$$N'_A = \int_0^{\theta} \frac{N(\theta)}{\theta} \cdot d\theta \tag{71}$$

Danckwerts[6] has published the derivation of expressions for $N(\theta)$ for different cases. For the case of purely physical absorption the partial differential equation and the related boundary conditions are as follows:

$$\frac{\partial C}{\partial \theta} = D_A \frac{\partial^2 C}{\partial x^2}$$

$$\text{i.} \quad C = C_{Ao}, \quad x > 0, \quad \theta = 0$$

$$\text{ii.} \quad C = C_{Ai}, \quad x = 0, \quad \theta > 0$$

$$\text{iii.} \quad C = C_{Ao}, \quad x = \infty, \quad \theta > 0 \tag{72}$$

Solution for Equation 72 as given by Carslaw and Jaeger[4] is

$$C = C_{Ao} + (C_{Ai} - C_{Ao}) \operatorname{erfc} [x/2\sqrt{\theta D_A}] \tag{73}$$

Hence,

$$N(\theta) = - D_A \left[\frac{\partial C}{\partial x}\right]_{x=o} = (C_{Ai} - C_{Ao})\sqrt{D_A/\pi\theta} \tag{74}$$

Equations 71 and 74 yield

$$N'_A = 2\sqrt{D_A/\pi\theta} \cdot (C_{Ai} - C_{Ao}) \tag{75}$$

On comparing Equations 2 and 75 we get, for the Higbie model

$$k^o_L = 2\sqrt{D_A/\pi\theta} \tag{76}$$

For the Danckwerts model, the rate equation can be written as

$$N'_A = \int_o^\infty N(\theta)\ s \cdot e^{-s\theta}\ d\theta \tag{77}$$

Equations 74 and 77 give

$$N'_A = \sqrt{D_A \cdot s}\ (C_{Ai} - C_{Ao}) \tag{78}$$

Therefore, for Danckwerts model we have,

$$k^o_L = \sqrt{D_A \cdot s} \tag{79}$$

Danckwerts[9] has shown that for instantaneous reaction between the absorbed gas and the reagent in solution, both the gas and the reagent obey the normal diffusion equations, but the boundary conditions are complicated. As Danckwerts has shown, for this case the flux, given by

$$N(\theta) = \frac{C_{Ai}}{\mathrm{erf}(\beta/\sqrt{D_A})} \cdot \sqrt{D_A/\pi\theta} \tag{80}$$

where β is given by Equation 18.

The expression for absorption rate with reaction for the Higbie model is obtained from Equations 71 and 80 as

$$N'_A = \frac{2 C_{Ai}}{\mathrm{erf}(\beta/\sqrt{D_A})} \cdot \sqrt{D_A/\pi\theta} \tag{81}$$

From Equations 1 and 81 k_L for Higbie model is,

$$k_L = \frac{2}{\mathrm{erf}(\beta/\sqrt{D_A})} \cdot \sqrt{D_A/\pi\theta} \tag{82}$$

Equations 76 and 82 give

$$\frac{k_L}{k_L^o} = \frac{1}{[\mathrm{erf}(\beta/\sqrt{D_A})]} \tag{83}$$

and

$$\gamma = \frac{k_L}{k_L^o} - 1 = \frac{1}{[\mathrm{erf}(\beta/\sqrt{D_A})]} - 1 \tag{84}$$

Similarly, the rate of absorption for the Danckwerts model is obtained from Equations 77 and 80 as

$$N'_A = \frac{C_{Ai}\sqrt{D_A \cdot s}}{\mathrm{erf}(\beta/\sqrt{D_A})} \tag{85}$$

Equations 1 and 85 give k_L for Danckwerts model as

$$k_L = \frac{\sqrt{D_A \cdot s}}{\mathrm{erf}(\beta/\sqrt{D_A})} \tag{86}$$

Equations 79 and 86 give

$$\frac{k_L}{k_L^o} = \frac{1}{\text{erf}(\beta/\sqrt{D_A})} \tag{87}$$

and

$$\gamma = \frac{k_L}{k_L^o} - 1 = \frac{1}{\text{erf}(\beta/\sqrt{D_A})} - 1 \tag{88}$$

C. Kishinevskii Model

Kishinevskii and others[24] assumed that during the period of surface renewal the passage of gas molecules from the surface element to the bulk takes place by turbulent or convective mass flow and derived an expression for k_L as follows:

For pure physical absorption the rate is given by

$$N_A' = - D_A \cdot \text{grad } C_A \tag{89}$$

For unidirectional diffusion normal to the interface

$$N_A' = k_L^o(C_{Ai} - C_{Ao}) \tag{2}$$

Also, for the case of absorption with reaction the rate is given by

$$N_A' = k_g(p_A - p_{Ai}) \tag{39}$$

The amount of A diffusing in the direction normal to the

interface where chemical reaction is present is given by

$$\frac{dN_A}{dA} \cdot dA = k_L^o(C_{ABi} + C_{Ai} - C_{ABo} - C_{Ao})\, dA \qquad (90)$$

Letting $\Delta C_{AB} = C_{ABi} - C_{ABo}$ and taking $C_{Ao} = 0$

Equation 90 gives

$$\frac{dN_A}{dA} \cdot dA = k_L^o(\Delta C_{AB} + C_{Ai}) \qquad (91)$$

Also,

$$-\frac{dC_{AB}}{d\theta} = f(C_{Bo}, C_{Ai}) \qquad (92)$$

Therefore,

$$\Delta C_{AB} = \int_o^\theta f(C_{Bo}, C_{Ai})\, d\theta \;;$$

$$\theta = \text{Time of contact of surface element.} \qquad (93)$$

Substitution of Equation 93 in Equation 91 gives

$$\frac{dN_A}{dA} \cdot dA = k_L^o \left[\int_o^\theta f(C_{Bo}, C_{Ai})\, d\theta + C_{Ai}\right] dA \qquad (94)$$

On integration, Equation 94 gives

$$N_A = \int_o^A k_L^o \left[\int_o^\theta f(C_{Bo}, C_{Ai})\, d\theta + C_{Ai}\right] dA \qquad (95)$$

or

$$N_A = k_L^o \left[\int_o^\theta f(C_{Bo}, C_{Ai})\, d\theta + C_{Ai} \right] A \tag{96}$$

or

$$N_A' = k_L^o \left[\int_o^\theta f(C_{Bo}, C_{Ai})\, d\theta + C_{Ai} \right] \tag{97}$$

For homogeneous reaction, the function $f(C_{Bo}, C_{Ai}) \equiv k' \cdot C_{Bo} \cdot C_{Ai}$ for there is no reaction in the bulk where $C_{Ao} = 0$. Therefore,

$$N_A' = k_L^o \left[\int_o^\theta k' \cdot C_{Bo} \cdot C_{Ai}\, d\theta + C_{Ai} \right] \tag{98}$$

When the reaction is slow, k', C_{Bo} and C_{Ai} can be considered constant so that

$$\int_o^\theta k' \cdot C_{Bo} \cdot C_{Ai}\, d\theta = k' \cdot C_{Bo} \cdot C_{Ai}\, \theta \tag{99}$$

and

$$N_A' = k_L^o \left[k' C_{Bo} C_{Ai} \theta + C_{Ai} \right] \tag{100}$$

$$= K C_{Bo} C_{Ai} + k_L^o C_{Ai} \tag{101}$$

where $K = k' k_L^o \theta$.

Equations 39, 43 and 101 give

$$N_A' = k_g p_A \left[\frac{K C_{Bo} + k_L^o}{K C_{Bo} + k_L^o + k_g/H} \right] \tag{102}$$

For the case when unreacted gas molecules are present in the bulk, Equation 101 can be written as

$$N'_A = K\, C_{Bo}\, C_{Ai} + k^o_L (C_{Ai} - C_{Ao}) \qquad (103)$$

Equations 39, 43 and 103 then give

$$N'_A = k_g \frac{K\, C_{Bo} \cdot k_g + k^o_L \cdot p_A - k^o_L \cdot C_{Ao}/H}{K\, C_{Bo} + k^o_L + k_g/H} \qquad (104)$$

For the case of rapid reaction Equations 102 and 104 are found to be inadequate and inaccurate. In this case

$$\int_o^\theta k'\, C_{Bo} \cdot C_{Ai}\, d\theta \neq k'\, C_{Bo}\, C_{Ai}\, \theta \qquad (105)$$

For rapid reaction case let

$$\int_o^\theta k'\, C_{Bo} \cdot C_{Ai}\, d\theta \equiv \mu \cdot C_{Bo} \qquad (106)$$

where μ is the stoichiometric factor. This is an element from the bulk with concentration C_{Bo} which reacts completely using $\mu\, C_{Bo}$ moles of absorbed gas per unit volume of the liquid. When concentrations are expressed in gram equivalents per unit volume μ becomes unity.

Substition of Equation 106 in Equation 98 gives

$$N'_A = k^o_L [C_{Bo} + C_{Ai}] \quad \text{for } \mu \text{ equal } 1 . \qquad (107)$$

Equations 39, 43 and 107 give

$$p_{Ai} = \frac{k_g p_A - k_L C_{Bo}}{k_L^o H + k_g} \tag{108}$$

From Equations 39, 43 and 108 the rate is obtained as

$$N'_A = \frac{C_{Bo} + H p_A}{1/k_L^o + H/k_g} \tag{109}$$

Equations 102 and 109 show the effect of chemical reaction on the rate of absorption for different degrees of turbulence. Equations 1 and 102 give for low turbulence

$$\frac{k_L}{k_L^o} = \frac{k_g p_A}{C_{Ai}} \frac{(k' \theta + 1)}{k_L^o(k' \theta + 1) + k_g/H} \tag{110}$$

and Equation 109 gives for high turbulence

$$\frac{k_L}{k_L^o} - 1 = \frac{C_{Bo}}{C_{Ai}} \tag{111}$$

Comparing Equations 49 and 111 we see that they differ in the factor $\mu = 1$ replacing the ratio of diffusivities.

D. The Film Penetration Model

To the partial differential equation for physical absorption,

$$\frac{\partial C_A}{\partial \theta} = - D_A \frac{\partial^2 C_A}{\partial x^2} \qquad (112)$$

Toor and Marchello[45] impose the following boundary conditions

$$\text{i.} \quad \theta = 0 \quad C_A = C_{A\ell} \,,$$

$$\text{ii.} \quad x = 0 \quad C_A = C_{Ai} \,,$$

$$\text{iii.} \quad x = \ell \quad C_A = C_{A\ell} \,.$$

and obtain a solution similar to the one by Carslow and Jaeger[4] as follows:

Short times

$$N'_A = (C_{Ai} - C_{A\ell}) \sqrt{D_A/\pi\theta} \left[1 + 2 \sum_{n=1}^{\infty} \exp(n^2\ell^2/D_A\theta) \right] \qquad (113)$$

Long times

$$N'_A = (C_{Ai} - C_{A\ell}) \cdot \frac{D_A}{\ell} \left[1 + 2 \sum_{n=1}^{\infty} (- n^2\pi^2 D_A\theta/\ell^2) \right] \qquad (114)$$

The difference between this model and the penetration models is the boundary condition iii . It is assumed here that at some distance ℓ below the surface the concentration remains constant at $C_{A\ell}$ and that a freshly formed surface has this concentration. Equations 113 and 114 show that for short times the penetration theory is approached and

$$N'_A = \sqrt{D_A/\pi\theta} \cdot (C_{Ai} - C_{A\ell}) \qquad (115)$$

For long times the film theory is approached and

$$N'_A = \frac{D_A}{\ell} (C_{Ai} - C_{A\ell}) \qquad (116)$$

However, when the absorption with infinitely rapid reaction is considered the boundary condition iii for Equation 112 can no longer hold as $C_{A\ell} = 0$. The solution to Equation 112 is then the same as Equation 80 for the case of instantaneous reaction.

APPENDIX II

THE ION FLUX EQUATION

APPENDIX II

ION FLUX EQUATION

Consider a diffusion cylinder, Figure 21, of cross section a sq cm containing a dissociated electrolyte of concentration C gm equiv./cc . In the diffusion process let C - dC gm equiv./cc be the concentration at a distance, dx , from the solution of concentration C .

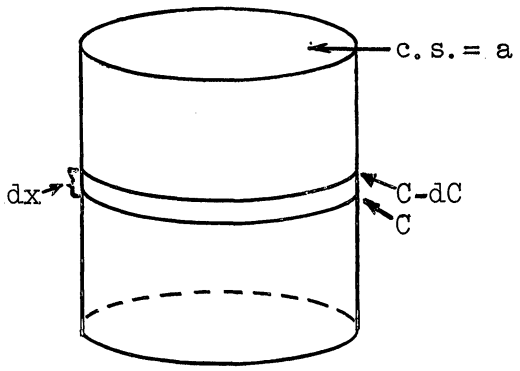

Figure 21. Ion concentration gradient.

Let U' and V' be the mobilities of cation and anion respectively. The amounts of the ions migrating per unit time through the cross section of the diffusion cylinder for the two ions of valence n_+ and n_- respectively are

$$\frac{d\,C_+}{dt} = N_+ = -\frac{U' \cdot a}{n_+} \cdot \frac{d\,C_+}{dx} \cdot \frac{RT}{F} \qquad (117)$$

and

$$\frac{dC_-}{dt} = N_- = - \frac{V' \cdot a}{n_-} \cdot \frac{dC_-}{dx} \cdot \frac{RT}{F} \qquad (118)$$

The electrostatic forces that come into play as a result of such a gradient will be $- \frac{d\psi}{dx}$ and $+ \frac{d\psi}{dx}$ volts per cm respectively. The rate of migration of ions through the cross section as a result of these forces of attraction and repulsion are

$$N_+ = - U' \, a \, C_+ \, \frac{d\psi}{dx} \qquad (119)$$

and

$$N_- = V' \, a \, C_- \, \frac{d\psi}{dx} \qquad (120)$$

When the rates of diffusion for the two ions under the combined influence of the concentration and the electrostatic potentials are equal it follows that for cation,

$$N_+ = - \frac{U' \, a}{n_+} \left[\frac{RT}{F} \cdot \frac{dC_+}{dx} + n_+ \frac{d\psi}{dx} \cdot C_+ \right] \qquad (121)$$

and for anion,

$$N_- = - \frac{V' \, a}{n_-} \left[\frac{RT}{F} \cdot \frac{dC_-}{dx} + n_- \frac{d\psi}{dx} \cdot C_- \right] \qquad (122)$$

$N' \equiv N/a$, gm equiv./cm^2 . min $\quad U' \equiv u_+/F \quad$ and $\quad V' \equiv u_-/F$.

Substitution for cation gives,

$$N'_+ = -\frac{u_+}{F}\left[\frac{RT}{F}\cdot\frac{1}{n_+}\cdot\frac{dC_+}{dx} + n_+\frac{C_+}{n_+}\cdot\frac{d\psi}{dx}\right]$$

or

$$= -\frac{u_+}{F^2}\cdot\frac{C_+}{n_+}\left[RT\frac{d\ \log\ C_+}{dx} + F\ n_+\frac{d\psi}{dx}\right] \qquad (123)$$

and for anion,

$$N'_- = -\frac{u_-}{F}\left[\frac{RT}{F}\cdot\frac{1}{n_-}\cdot\frac{dC_-}{dx} - n_-\frac{C_-}{n_-}\cdot\frac{d\psi}{dx}\right]$$

or

$$= -\frac{u_-}{F^2}\cdot\frac{C_-}{n_-}\left[RT\frac{d\ \log\ C_-}{dx} - F\ n_-\frac{d\psi}{dx}\right] \qquad (124)$$

$\frac{d\psi}{dx}$ is eliminated from the above by subtracting the sum of Equation 124 for all anions from the corresponding sum of Equation 123 for all cations and by the condition of electrical neutrality, i.e.

$$\Sigma\ n_+ = \Sigma\ n_-$$

or

$$\Sigma\ dN_+ = \Sigma\ dN_-$$

or

$$\Sigma\ dN_+ - \Sigma\ dN_- = 0 \qquad (125)$$

Thus an expression explicit in $\frac{d\psi}{dx}$ follows,

$$0 = -\frac{u_+C_+}{F^2n_+}\left[RT\frac{d\ \log\ C_+}{dx} + F\ n_+\frac{d\psi}{dx}\right]$$

$$+\frac{u_+C_+}{F^2n_-}\left[RT\frac{d\ \log\ C_-}{dx} - F\ n_-\frac{d\psi}{dx}\right]$$

$$= - RT \left[\frac{u_+ \ dC_+}{n_+ \ dx} - \frac{u_- \ dC_-}{n_- \ dx} \right] - F \frac{d\psi}{dx} [u_+C_+ + u_-C_-] \qquad (126)$$

Therefore,

$$F \frac{d\psi}{dx} = \frac{- RT \ [u_+/n_+ \cdot \ dC_+/dx - u_-/n_- \cdot \ dC_-/dx]}{[u_+C_+ + u_-C_-]} \qquad (127)$$

$$F \cdot \frac{d\psi}{dx} = - RT \frac{(\Sigma \ u_+G_+/n_+ - \Sigma \ u_-G_-/n_-)}{(\Sigma \ u_+C_+ + \Sigma \ u_-C_-)} \qquad (128)$$

where $G_+ = \frac{dC_+}{dx}$ and $G_- = \frac{dC_-}{dx}$.

Substitution of Equation 128 in Equations 123 and 124 gives

$$N'_+ = - \frac{RT}{F^2} \frac{u_+}{n_+} \left[G_+ - n_+C_+ \frac{\Sigma \ u_+G_+/n_+ - \Sigma \ u_-G_-/n_-}{\Sigma \ u_+C_+ + \Sigma \ u_-C_-} \right] \qquad (50)$$

and

$$N'_- = - \frac{RT}{F^2} \frac{u_-}{n_-} \left[G_- + n_-C_- \frac{\Sigma \ u_+G_+/n_+ - \Sigma \ u_-G_-/n_-}{\Sigma \ u_+C_+ + \Sigma \ u_-C_-} \right] \qquad (51)$$

APPENDIX III

THE DATA AND CALCULATIONS OF k_L^o AND THE VISCOSITY DATA

TABLE 5

Data and Calculations of k_L^o

No.	Duration of run min	C_{Ao} gm equiv/ℓ	$C_{Ai} - C_{Ao}$ gm equiv/ℓ	$\log(C_{Ai} - C_{Ao})$	$\Delta \log(C_{Ai} - C_{Ao})$	$\frac{\Delta \log(C_{Ai} - C_{Ao})}{\Delta t}$ min^{-1}	k_L^o cm/min
1	0	0.42×10^{-4}	10.14×10^{-4}	-2.9940	0.0000		
2	20	2.50×10^{-4}	8.06×10^{-4}	-3.0912	0.09717	0.004858	0.0670
3	20	2.46×10^{-4}	8.10×10^{-4}	-3.0937	0.09953	0.004976	0.0685
4	60	4.81×10^{-4}	5.75×10^{-4}	-3.2427	0.2485	0.004124	0.0568
5	60	5.22×10^{-4}	5.34×10^{-4}	-3.2725	0.2783	0.004639	0.0638
6	120	6.92×10^{-4}	3.64×10^{-4}	-3.4388	0.4448	0.003706	0.0510
7	180	8.58×10^{-4}	1.98×10^{-4}	-3.7033	0.7092	0.003940	0.0543
8	240	9.00×10^{-4}	1.56×10^{-4}	-3.8125	0.8183	0.003410	0.0469
9	240	9.02×10^{-4}	1.54×10^{-4}	-3.8068	0.8127	0.003386	0.0465

$\Sigma \delta^2 = 5.32 \times 10^{-4}$

$\sigma = \sqrt{\delta^2/n} = 8.3 \times 10^{-3}$

'3σ' test shows all data within 3σ limit

Average value of k_L^o = 0.0568 cm/min or 0.118 ft/hr

TABLE 6

Viscosity of Na_2SO_4(aq.) at 25°C (21)

η_{water} = 1 C.P.

Concentration gm mol Na_2SO_4/ℓ	$\eta_{25°}$
0.1	1.040
0.25	1.160
0.50	1.227
0.75	1.340
1.00	- -

TABLE 7

Viscosity of Na_2SO_3(aq.) at 25°C with Cannon 100 Viscometer

η_{water} = 1 C.P.

(Density was measured with NBS hydrometers)

$$\eta_{Na_2SO_3} = \frac{\eta_{water}\ t_{H_2O}\rho_{H_2O}}{t_{SO_3}\rho_{SO_3}}$$

Concentration $\frac{\text{gm mol } Na_2SO_3}{\ell}$	Sp . gr gm/cc	Cannon Visometer Time Min	$\eta_{Na_2SO_3}$
1.00	1.1146	1.655	1.562
0.50	1.0556	1.365	1.185
0.25	1.0263	1.300	1.102
0.125	1.0122	1.225	1.023
0.00 (pure water)	1.000	1.212	1.000

APPENDIX IV

DATA AND CALCULATIONS OF k_L WITH VARIOUS CATALYSTS

Figure 22. Sample Data Sheet

Date: 10-30-60 Run # 64 Amt of Catalyst 1.5×10^{-7} gm mol $CuSO_4/\ell$

System: SO_3-Air Other Conditions:

No.	Time hr	Titration ml			Temperatures °C				Florator	
		0.05 N I_2 added	0.05 N Titer	0.05 N $(SO_3^{=})$	Water	W.B.	D.B.	Air	F.R.	Δ P cm , Hg
1	1715	20.10	2.90	17.20	24.8	24.6	24.8	25	50	32
2	1730	20.10	3.25	16.85	24.9	24.8	25.0	25	50	32
3	1745	20.10	3.68	16.42	24.9	24.8	25.0	25	50	32
4	1800	20.10	4.00	16.10						
5	1815	20.10	4.36	15.74						
6	1830	20.10	4.72	15.38						
7	1845	20.10	5.12	14.98	24.9	24.8	25.0	25	50	32
8	1900	20.10	5.43	14.67						
9	1915	20.10	5.87	14.23						
10	1930	20.10	6.23	13.87	24.9	24.8	25.0	25	50	32
11	1945	20.10	6.60	13.50						
12	2000	20.10	6.89	13.21						
13	2015	20.10	7.24	12.86	24.9	24.8	25.0	25	50	32

Calculation Sheet Run # 64 Date 10-30-60

Time, hr	gm equiv $SO_3^{=}/\ell$	1% correction	Actual gm equiv $SO_3^{=}/\ell$	gm equiv Na^{+}/ℓ	1% correction	Actual gm equiv Na^{+}/ℓ	gm equiv O_2/ℓ	Cummulative gm equiv O_2/ℓ
1715	0.08600	0.00086	0.08514	0.08514	0.00085	0.08429	0.0	0.0
1730	0.08425	0.00084	0.08341	0.08429	0.00084	0.08345	0.00089	0.00089
1745	0.08210	0.00082	0.08128	0.08345	0.00083	0.08262	0.00131	0.00220
1800	0.08050	0.00080	0.07970	0.08262	0.00083	0.08179	0.00078	0.00298
1815	0.07870	0.00079	0.07791	0.08179	0.00082	0.08097	0.00100	0.00398
1830	0.07690	0.00077	0.07613	0.08097	0.00081	0.08016	0.00101	0.00499
1845	0.07490	0.00075	0.07415	0.08016	0.00080	0.07936	0.00123	0.00622
1900	0.07335	0.00073	0.07262	0.07936	0.00079	0.07857	0.00080	0.00702
1915	0.07115	0.00071	0.07044	0.07857	0.00078	0.07779	0.00147	0.00849
1930	0.06935	0.00069	0.06866	0.07779	0.00078	0.07701	0.00109	0.00958
1945	0.06750	0.00068	0.06682	0.07701	0.00077	0.07624	0.00116	0.01074
2000	0.06605	0.00066	0.06539	0.07624	0.00076	0.07548	0.00077	0.01151
2015	0.06430	0.00064	0.06366	0.07548	0.00075	0.07473	0.00109	0.01260

Figure 23. Sample Calculation Sheet.

TABLE 8

i. Determination of $k_{g(O_2)}$

$$D_{g(H_2O)} = 0.853 \text{ ft}^2/\text{hr} \quad (21)$$

$$D_{g(O_2)} = 0.69 \text{ ft}^2/\text{hr} \quad (21)$$

Using Equation 110 from Sherwood and Pigford[39]

$$k_{g(O_2)} = k_{g(H_2O)} \left[\frac{D_{g(O_2)}}{D_{g(H_2O)}}\right]^{0.56}$$

and

$$k_{g(H_2O)} \cong 0.31 \frac{\text{lb mol}}{\text{hr . ft}^2 \text{ . atmos}}, \quad (46)$$

We have

$$k_{g(O_2)} \cong 0.31 \left[\frac{0.69}{0.853}\right]^{0.56}$$

$$\cong 0.2755 \frac{\text{lb mol}}{\text{hr . ft}^2 \text{ . atmos}}$$

$$\cong 2.25 \times 10^{-3} \frac{\text{gm mol}}{(\text{min . cm}^2 \text{ . atm})}$$

ii. Determination of % resistance due to gas phase:

For $k_L = 1.104$ cm/min

$$\frac{1}{K_L} = \frac{1}{k_g} + \frac{H}{k_L}$$

$$H = 7.884 \times 10^{-5} \frac{\text{atmos . cc}}{\text{gm mol}}, \quad \text{Perry, 3rd Ed.}$$

TABLE 8 (Continued)

$$\frac{1}{K_L} = \frac{1}{2.25 \times 10^{-3}} + \frac{7.884 \times 10^5}{1.104}$$

$$= 4.445 \times 10^2 + 7.14 \times 10^5$$

$$\% \text{ Resistance due to gas phase} = \frac{4.445 \times 10^2}{7.14 \times 10^5} \times 100 = 0.062\%$$

Although the estimated value of $k_{g(O_2)}$ is not exact, it is clear that the gas phase resistance is negligible.

$$\therefore K_L = k_L .$$

iii. Sample calculations for C_{Ai} and k_L :

Run # 64

From Figure 26

$$N'_A = 4.18 \times 10^{-7} \frac{\text{gm equiv } O_2}{\text{cm}^2 \cdot \text{min}}$$

$$= 5.16 \times 10^{-5} \frac{\text{lb mol } O_2}{\text{ft}^2 \cdot \text{hr}}$$

Equation 39 gives

$$N'_A = k_g (p_A - p_{Ai})$$

$$p_{Ai} = p_A - N'_A / k_g$$

$$p_A = 0.2085 \text{ Atm}$$

$$k_g = 0.2755 \frac{\text{lb mol}}{\text{hr} \cdot \text{ft}^2 \cdot \text{atm}} \quad \text{Table 8, i}$$

TABLE 8 (Continued)

$$\therefore \quad p_{Ai} = 0.2085 - \frac{5.16 \times 10^{-5}}{0.2755}$$

$$= 0.2085 \text{ atm}$$

$$C_{Ai} = \frac{p_{Ai}}{H}$$

$$H = \frac{4.38 \times 10^{7}}{4 \times 55.55} \quad \text{Perry, 3rd Ed.}$$

$$C_{Ai} = \frac{0.2085 \times 4.00 \times 55.55}{4.38 \times 10^{7}}$$

$$= 10.54 \times 10^{-7} \frac{\text{gm equiv.}}{\text{cc}}$$

From Equation 1

$$k_L = \frac{N'_A}{C_{Ai}} = \frac{4.18 \times 10^{-7}}{10.56 \times 10^{-7}} = 0.397 \frac{\text{cm}}{\text{min}} \quad \text{or} \quad 0.783 \text{ ft/hr}$$

TABLE 9

Calculations of k_L for Various Catalysts with Data from Figures 24-78

Run #	Catalyst	Amount of catalyst added gm mol/ℓ	C_{Bo} gm equiv/ℓ	N'_A gm equiv / cm² x min	k_L' ft/hr	Run #	Catalyst	Amount of catalyst added gm mol/ℓ	C_{Bo} gm equiv/ℓ	N'_A gm equiv / cm² x min	k_L' ft/hr
59	$CuSO_4$	4×10^{-9}	0.097	3.22×10^{-7}	0.602	87		5×10^{-7}	0.081	11.28×10^{-7}	2.100
60		4×10^{-9}	0.070	4.44×10^{-7}	0.756	88		5×10^{-7}	0.120	16.88×10^{-7}	3.155
61		4×10^{-8}	0.090	2.99×10^{-7}	0.891	89		7×10^{-7}	0.077	19.48×10^{-7}	3.620
62		4×10^{-8}	0.066	3.22×10^{-7}	0.600	90		1×10^{-6}	0.106	22.04×10^{-7}	4.120
63		4×10^{-8}	0.062	3.74×10^{-7}	0.697	91		1×10^{-6}	0.082	21.28×10^{-7}	3.940
64		1.5×10^{-7}	0.086	4.18×10^{-7}	0.783	92		2×10^{-6}	0.052	25.60×10^{-7}	4.790
65		4×10^{-7}	0.080	4.8×10^{-7}	0.891			-			
66		4×10^{-7}	0.072	4.44×10^{-7}	0.826	93	Mannitol	5×10^{-7}	0.086	4.16×10^{-7}	0.776
67		1×10^{-6}	0.063	6.09×10^{-7}	1.137	94		5×10^{-6}	0.097	3.68×10^{-7}	0.685
68		1×10^{-6}	0.062	5.68×10^{-7}	0.657	95		1×10^{-5}	0.130	3.46×10^{-7}	0.646
69		1×10^{-6}	0.086	4.92×10^{-7}	0.917	96		5×10^{-5}	0.090	3.28×10^{-7}	0.622
70		1×10^{-6}	0.088	5.48×10^{-7}	1.023	97		1×10^{-4}	0.116	2.88×10^{-7}	0.532
71		3×10^{-6}	0.084	6.06×10^{-7}	1.131	98		2.5×10^{-4}	0.092	2.40×10^{-7}	0.440
72		4×10^{-6}	0.077	6.28×10^{-7}	1.170	99		5×10^{-4}	0.048	1.22×10^{-7}	0.228
73		4×10^{-6}	0.112	7.11×10^{-7}	1.330	100		5×10^{-3}	0.068	1.00×10^{-7}	0.187
74		8×10^{-6}	0.074	7.36×10^{-7}	1.378	101		1×10^{-2}	0.156	0.84×10^{-7}	0.157
75		1×10^{-5}	0.048	8.0×10^{-7}	1.496						
						102	Benzyl	5×10^{-7}	0.100	3.4×10^{-7}	0.629
76	$CoCl_2$	1×10^{-11}	0.096	4.16×10^{-7}	0.775	103	Alcohol	1×10^{-6}	0.124	3.44×10^{-7}	0.642
77		1×10^{-10}	0.122	4.24×10^{-7}	0.793	104		2.5×10^{-6}	0.092	3.16×10^{-7}	0.590
78		1×10^{-9}	0.158	4.48×10^{-7}	0.836	105		5×10^{-6}	0.096	1.50×10^{-7}	0.275
79		5×10^{-9}	0.168	5.04×10^{-7}	0.944	106		1×10^{-5}	0.136	1.42×10^{-7}	0.266
80		1×10^{-8}	0.158	7.2×10^{-7}	1.340	107		5×10^{-5}	0.124	0.34×10^{-7}	0.065
81		1×10^{-8}	0.150	6.96×10^{-7}	1.200	108		1×10^{-4}	0.152	0.62×10^{-7}	0.114
82		2×10^{-8}	0.106	5.52×10^{-7}	1.030	109		1×10^{-2}	0.146	1.39×10^{-8}	0.026
83		5×10^{-8}	0.082	7.44×10^{-7}	1.385						
84		1×10^{-7}	0.170	8.0×10^{-7}	1.490	110	Catechol	1×10^{-4}	0.092	3.68×10^{-8}	0.069
85		2×10^{-7}	0.070	8.72×10^{-7}	1.627	111		1×10^{-3}	0.098	8.40×10^{-8}	0.157
86		3×10^{-7}	0.100	12.91×10^{-7}	2.400						
						112	None		0.0812	3.54×10^{-7}	0.76
						113			0.4780	3.68×10^{-7}	1.01

FIGURES 24 THROUGH 78 REPRESENT THE

RATE DATA FOR VARIOUS CATALYSTS

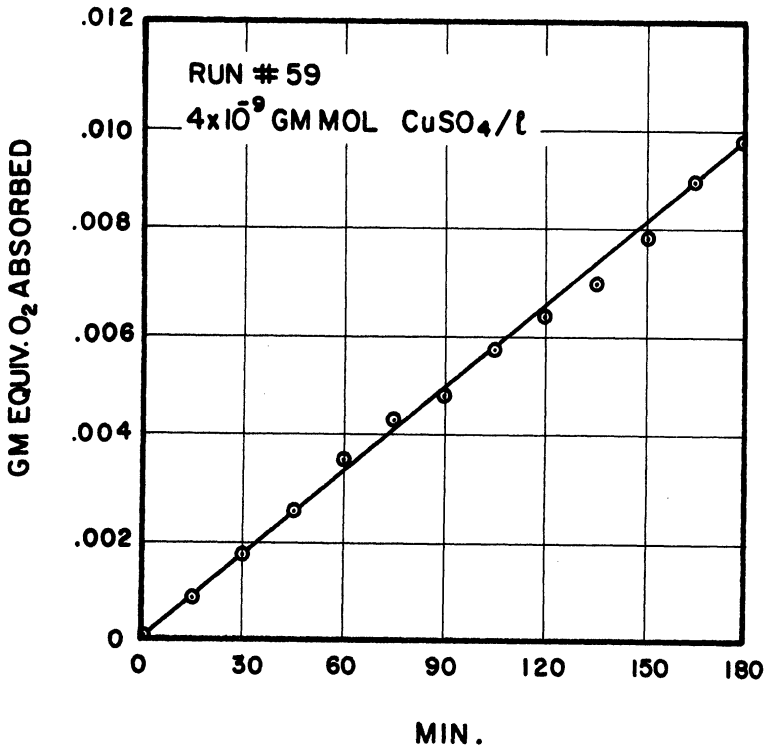

Figure 24.

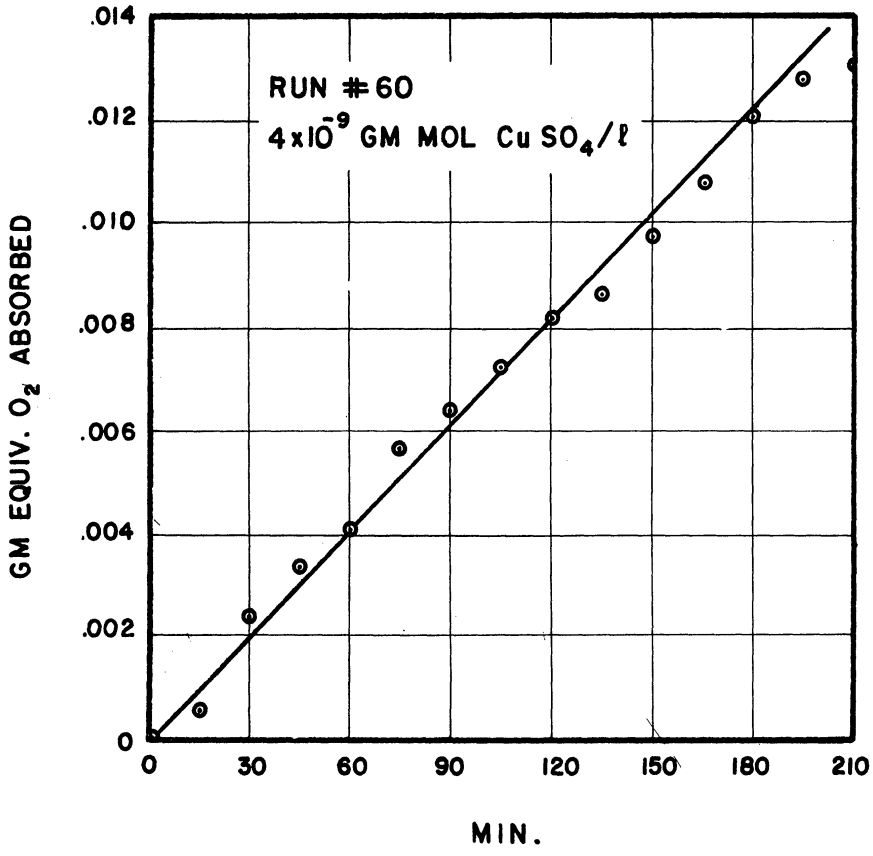

Figure 25.

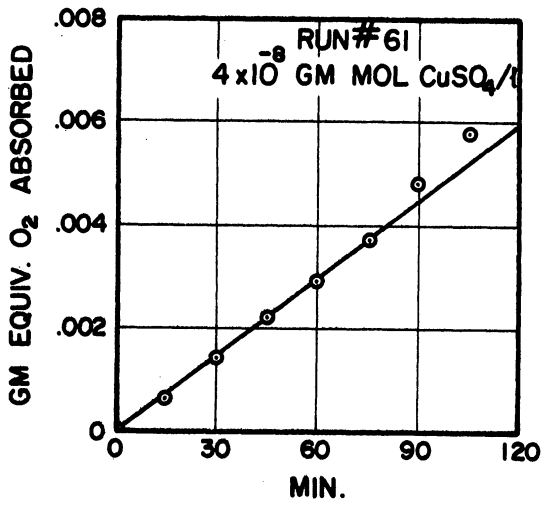

Figure 26.

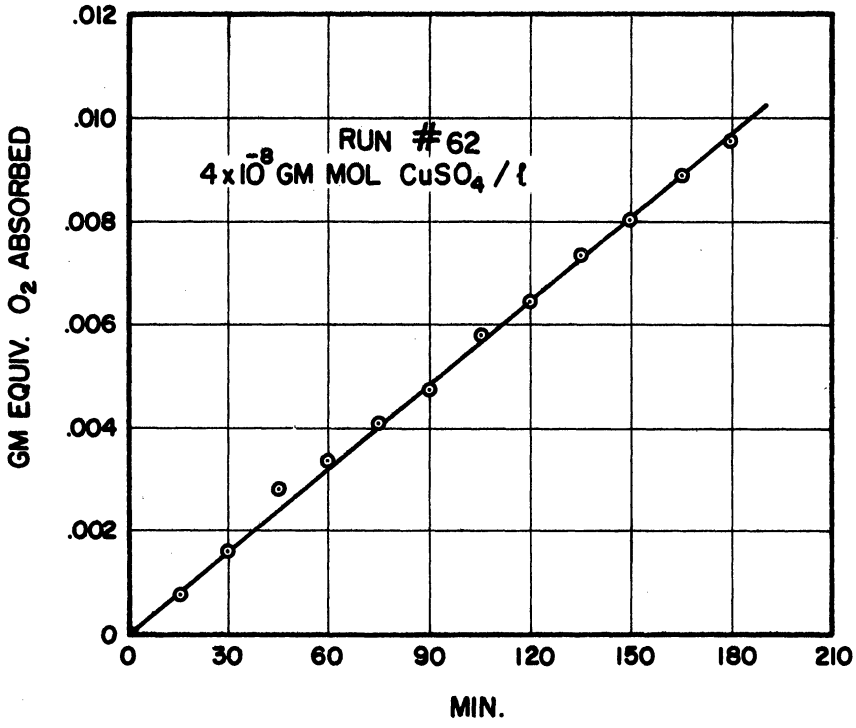

Figure 27.

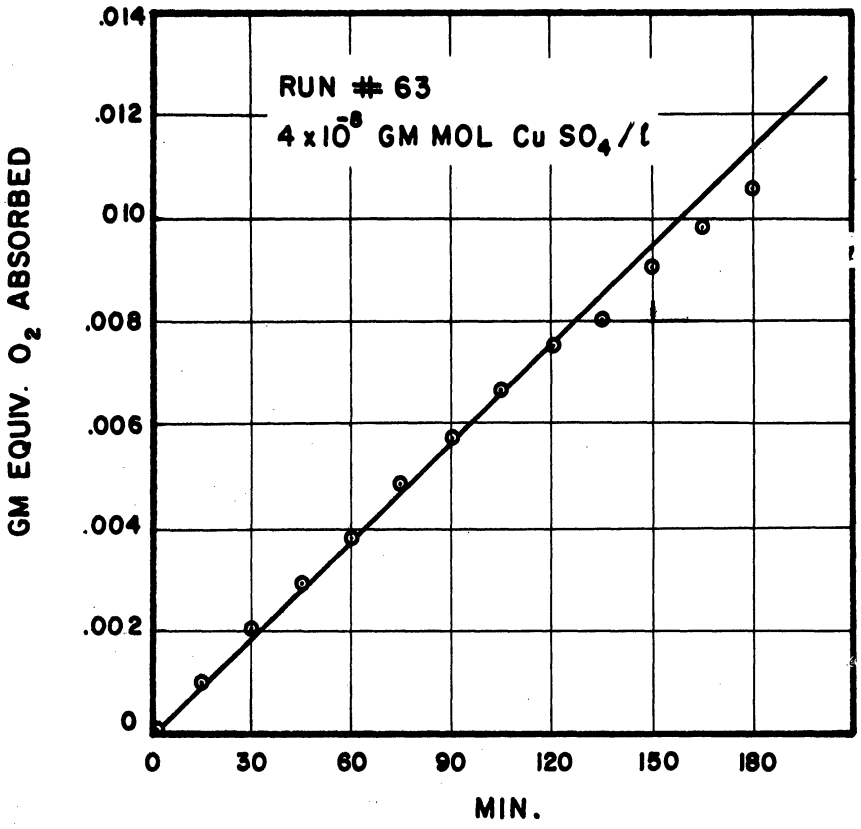

Figure 28.

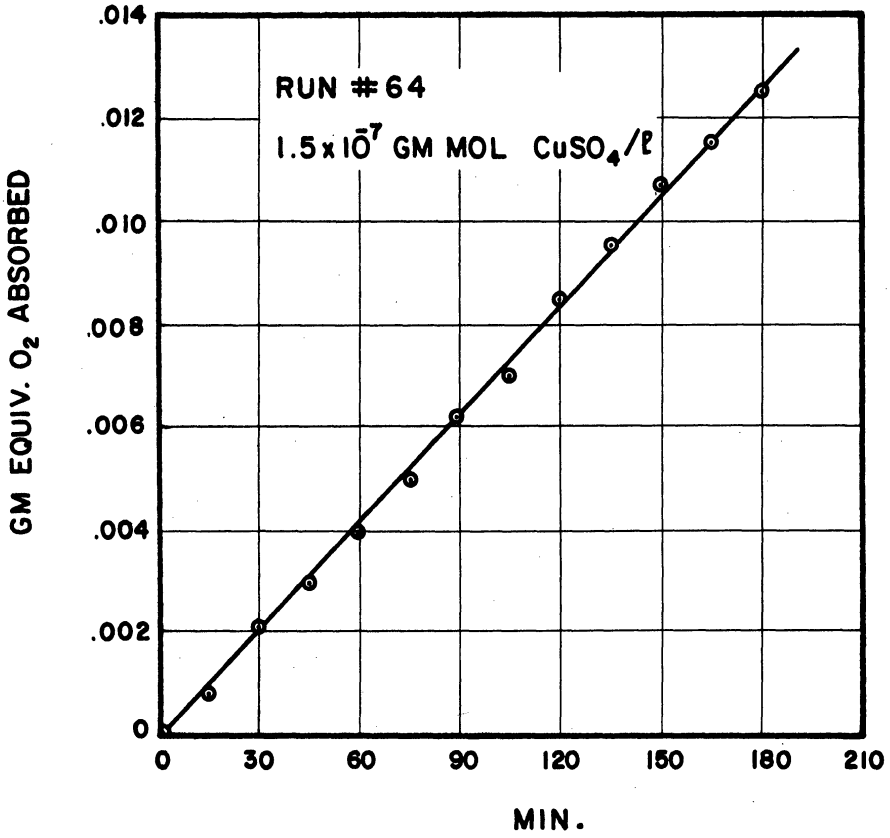

Figure 29.

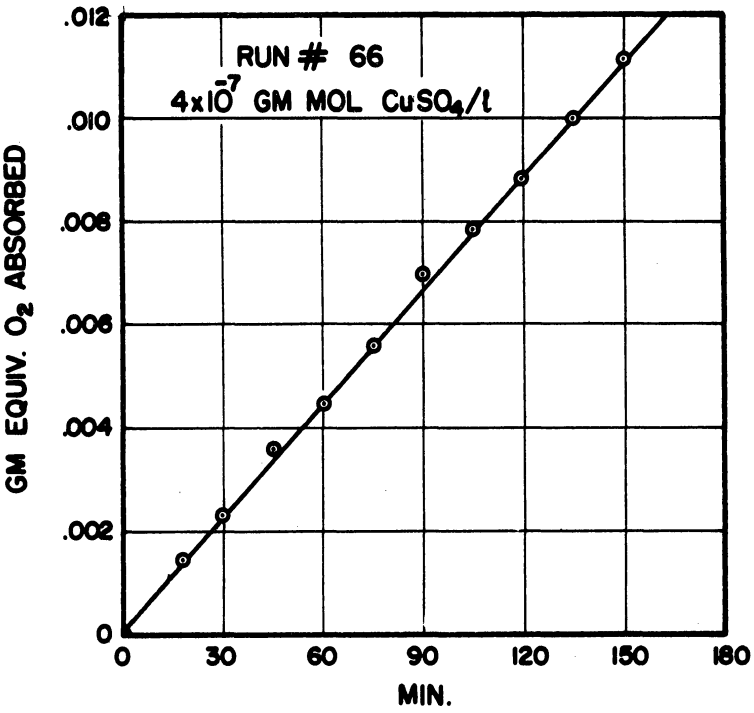

Figure 30.

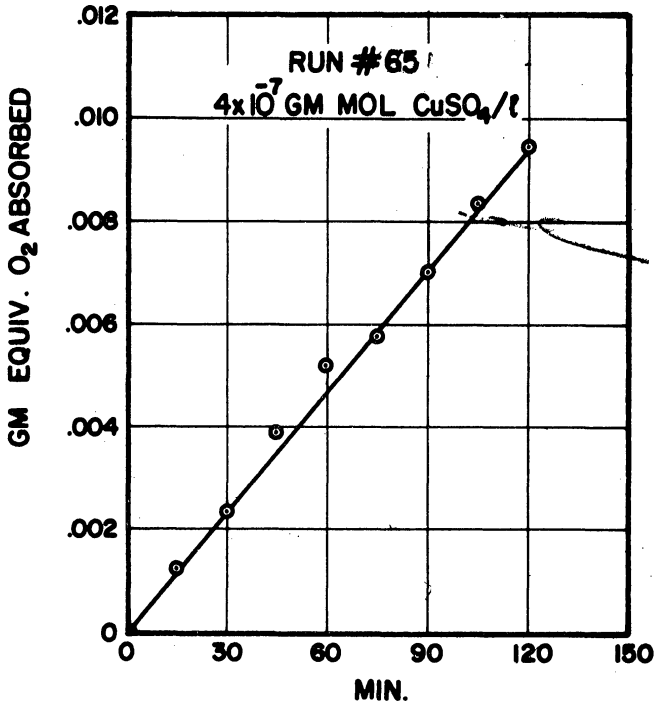

Figure 31.

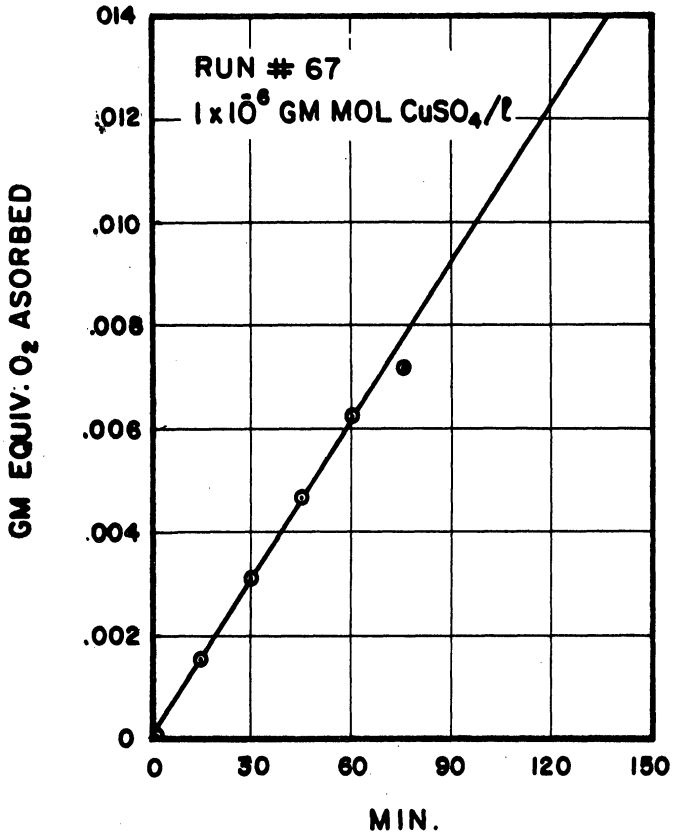

Figure 32.

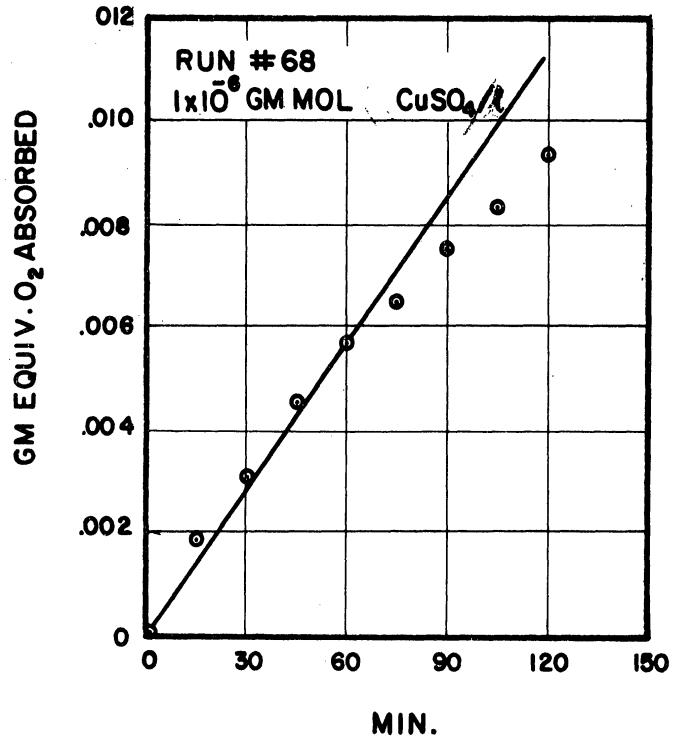

Figure 33.

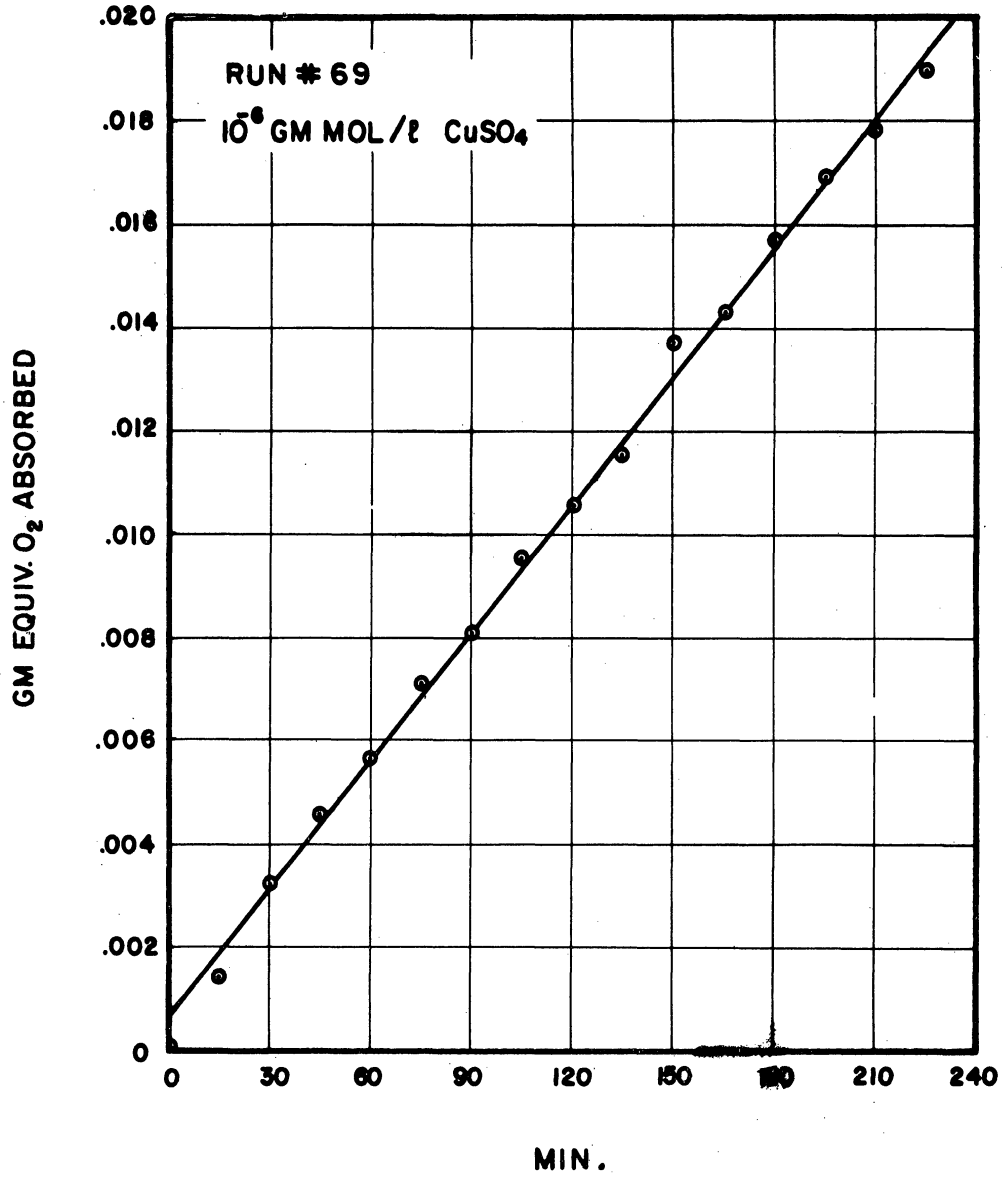
RUN # 69
10^{-6} GM MOL/ℓ $CuSO_4$
GM EQUIV. O_2 ABSORBED
.020
.018
.016
.014
.012
.010
.008
.006
.004
.002
0
0
30
60
90
120
150
180
210
240
MIN.

Figure 34.

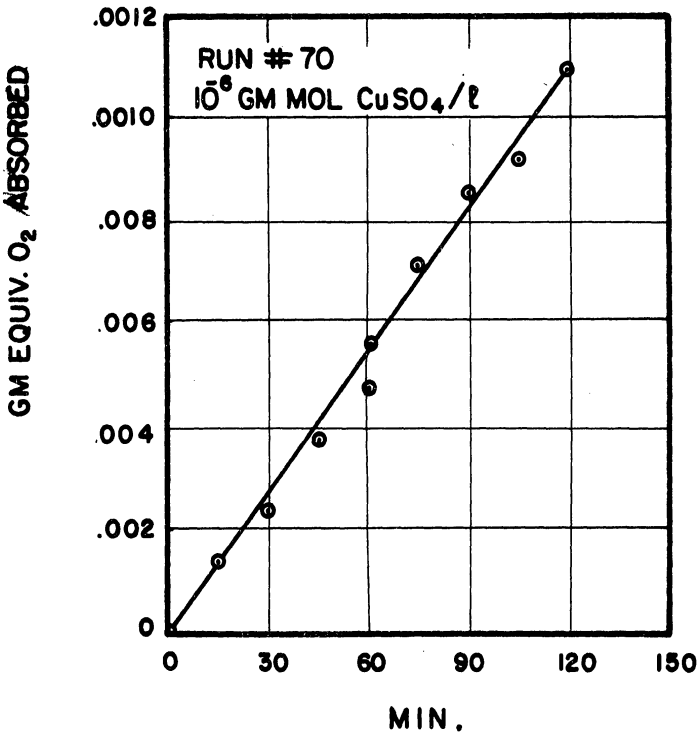

Figure 35.

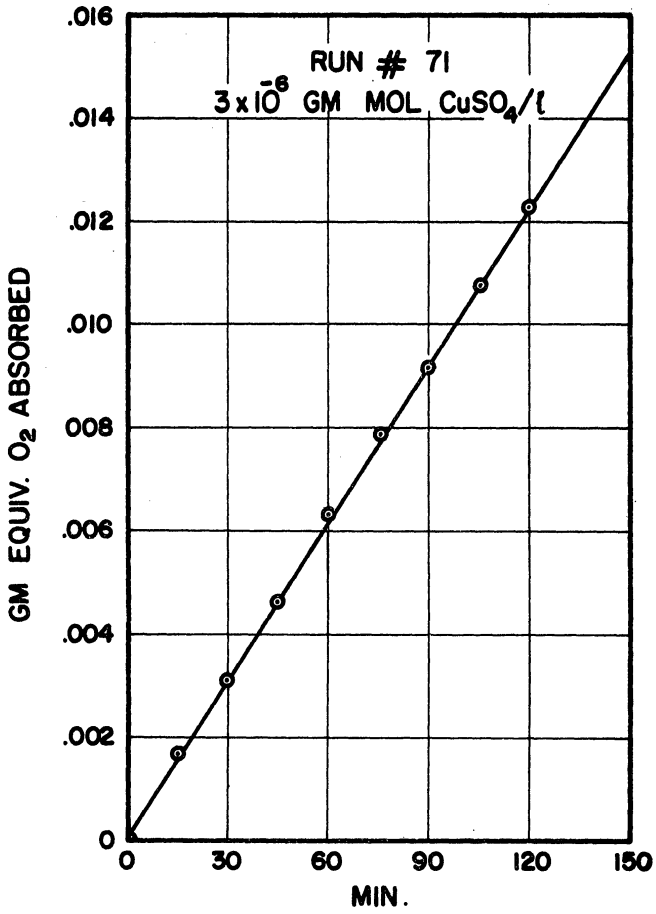

Figure 36.

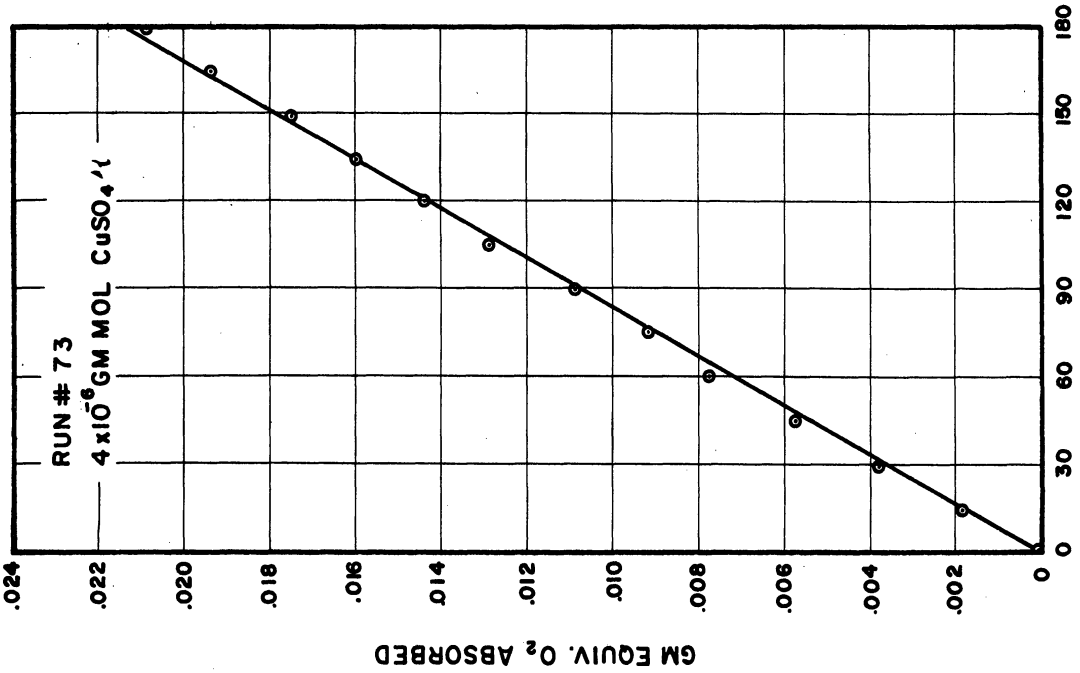

Figure 38.

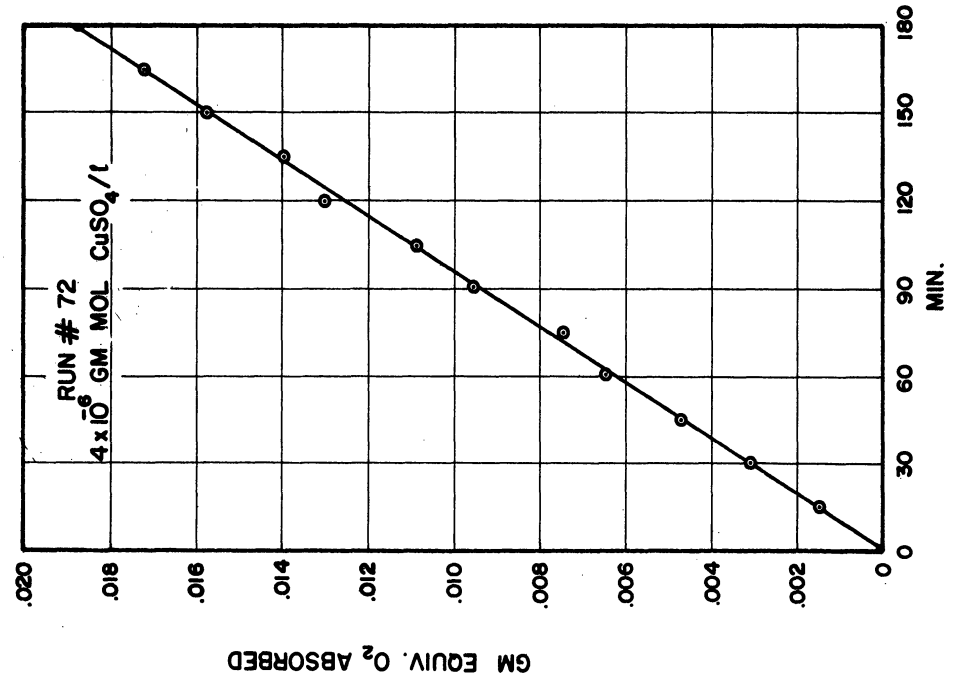

Figure 37.

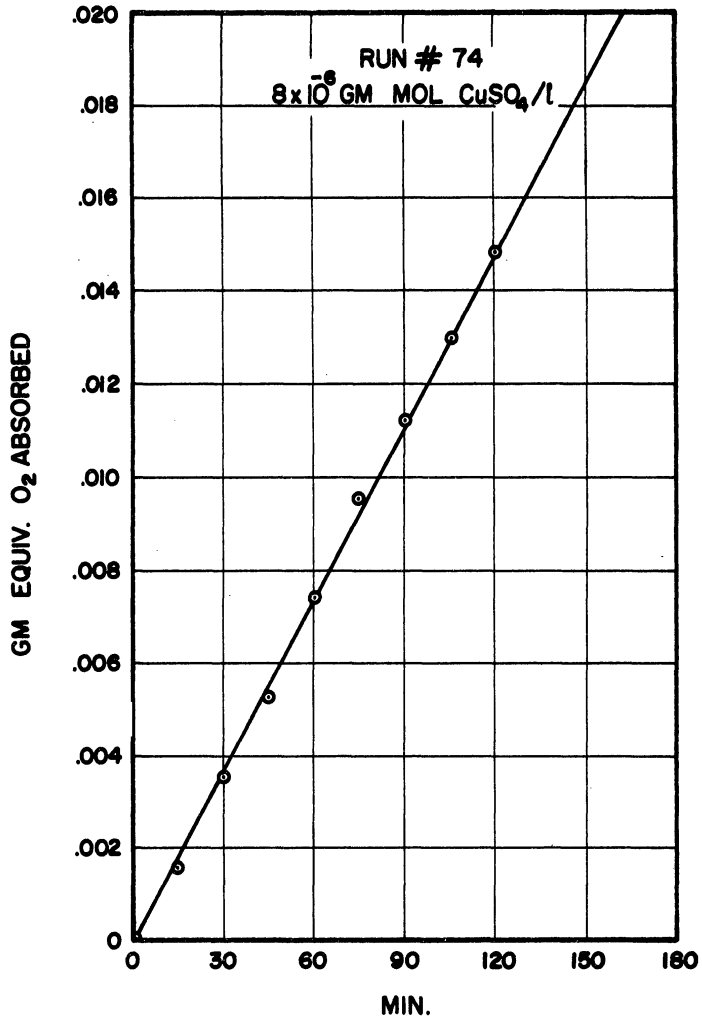

Figure 39.

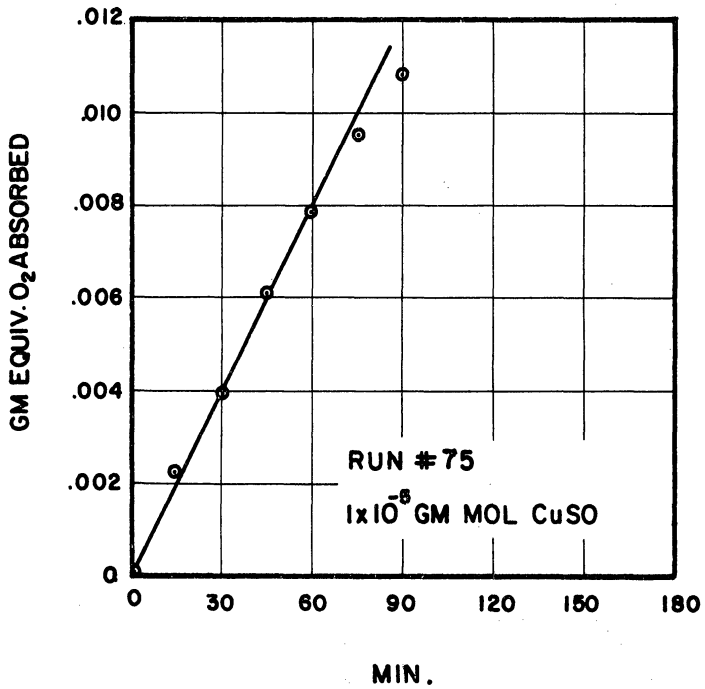

Figure 40.

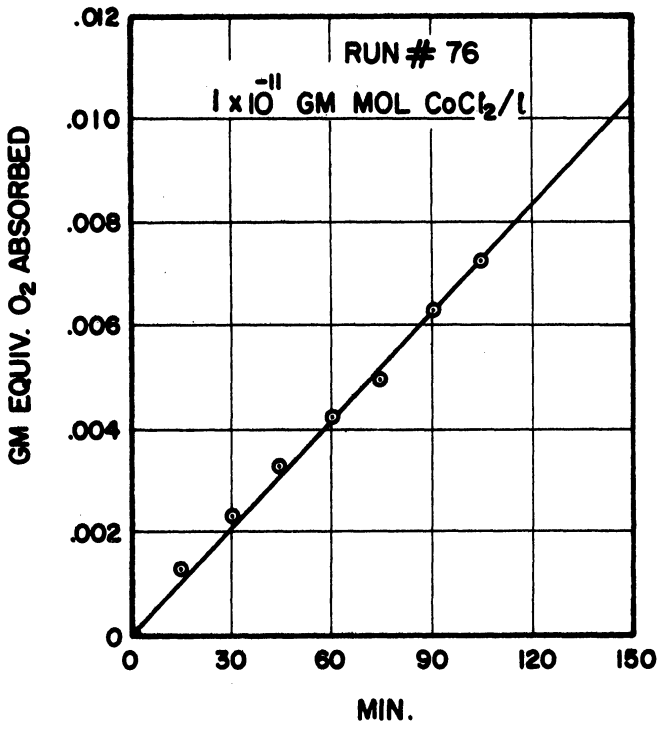

Figure 41.

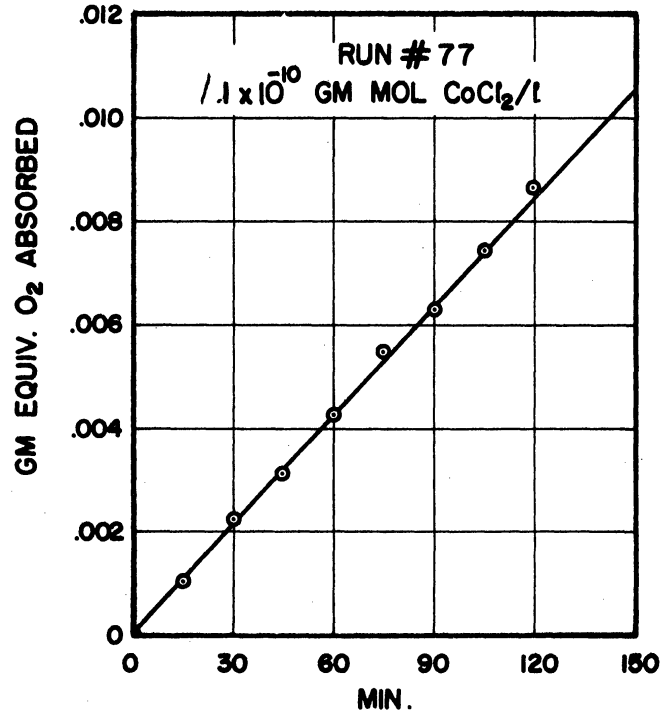

Figure 42.

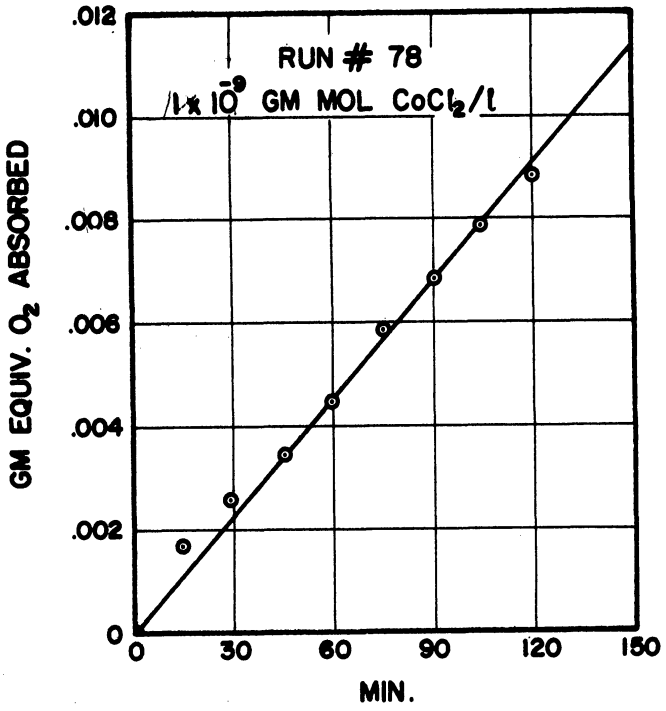

Figure 43.

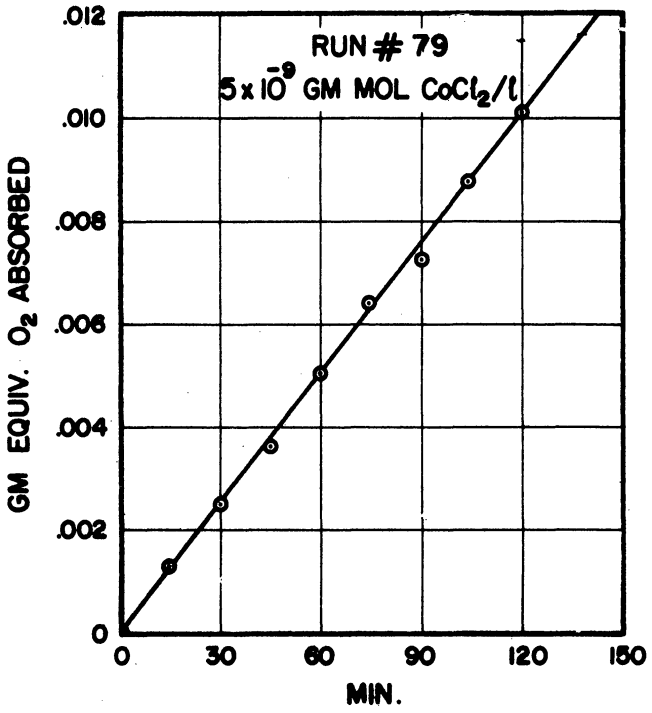

Figure 44.

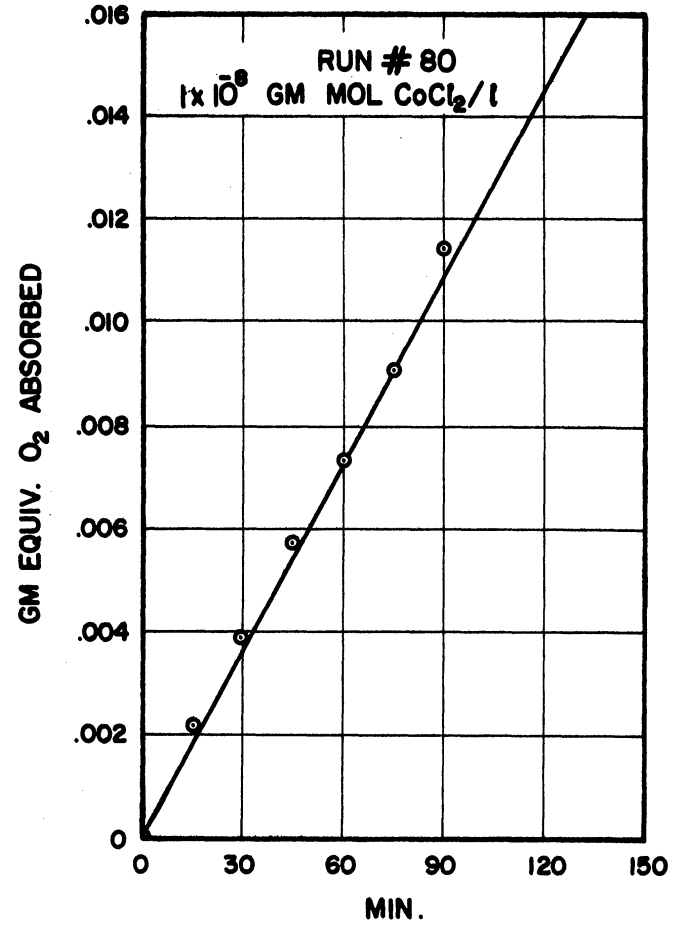

Figure 45.

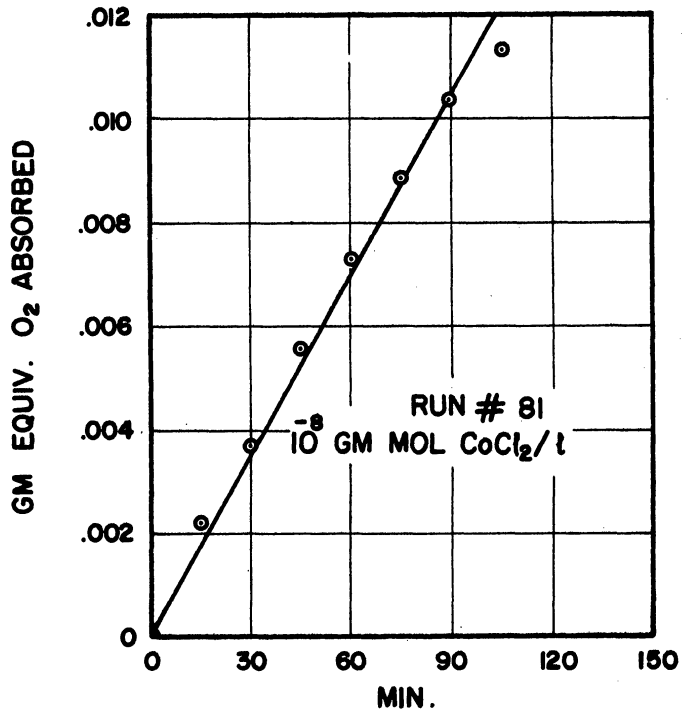

Figure 46.

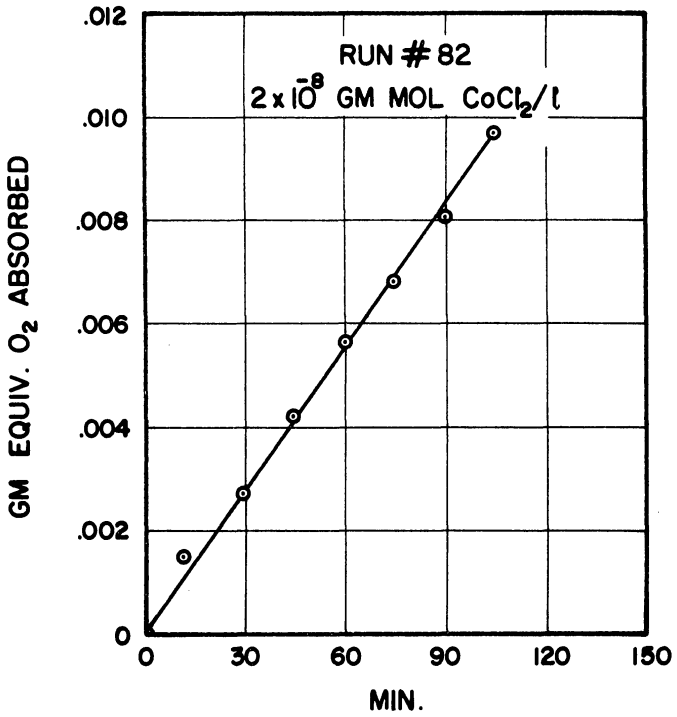

Figure 47.

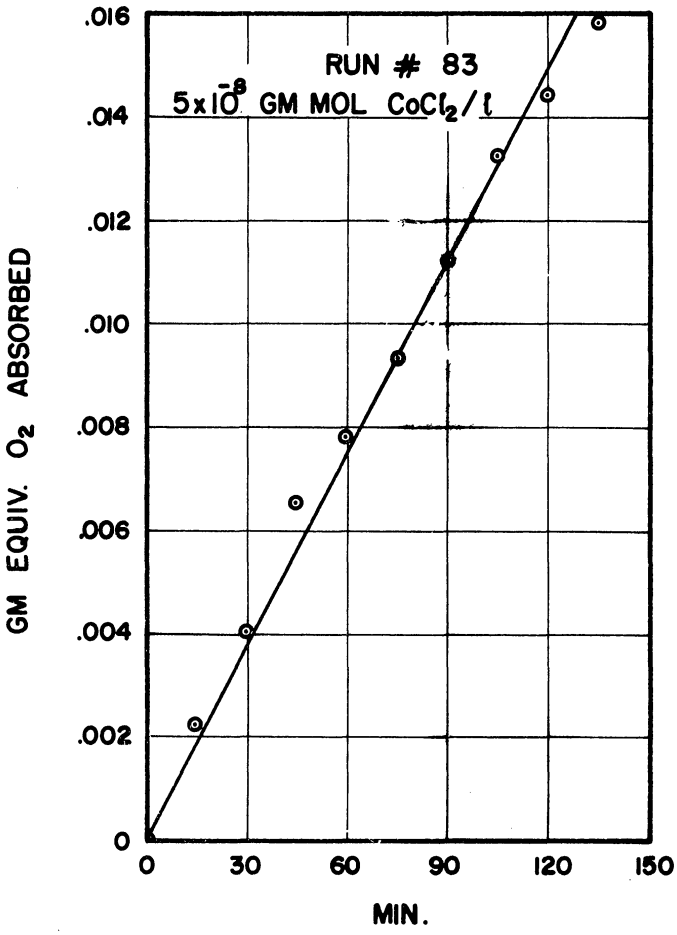

Figure 48.

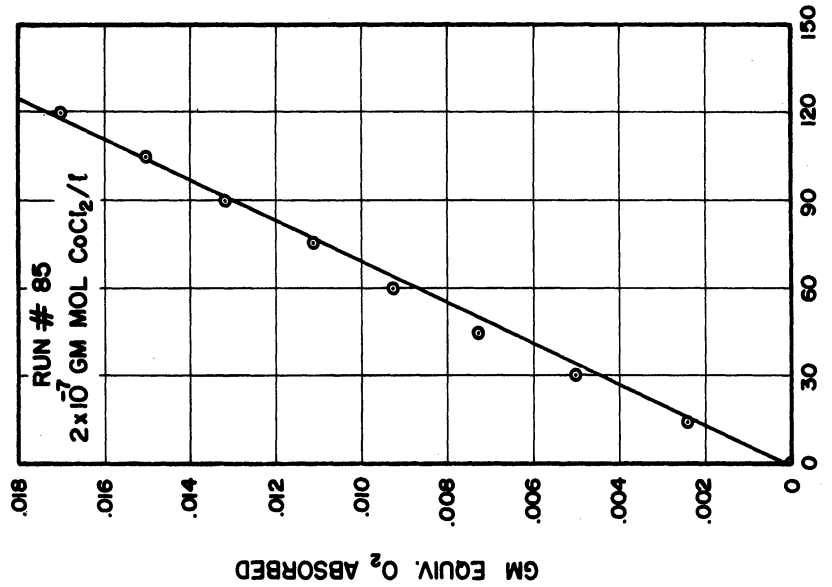
RUN # 85
2x10⁻⁷ GM MOL CoCl₂/l
GM EQUIV. O₂ ABSORBED
MIN.
0
.002
.004
.006
.008
.010
.012
.014
.016
.018
0
30
60
90
120
150

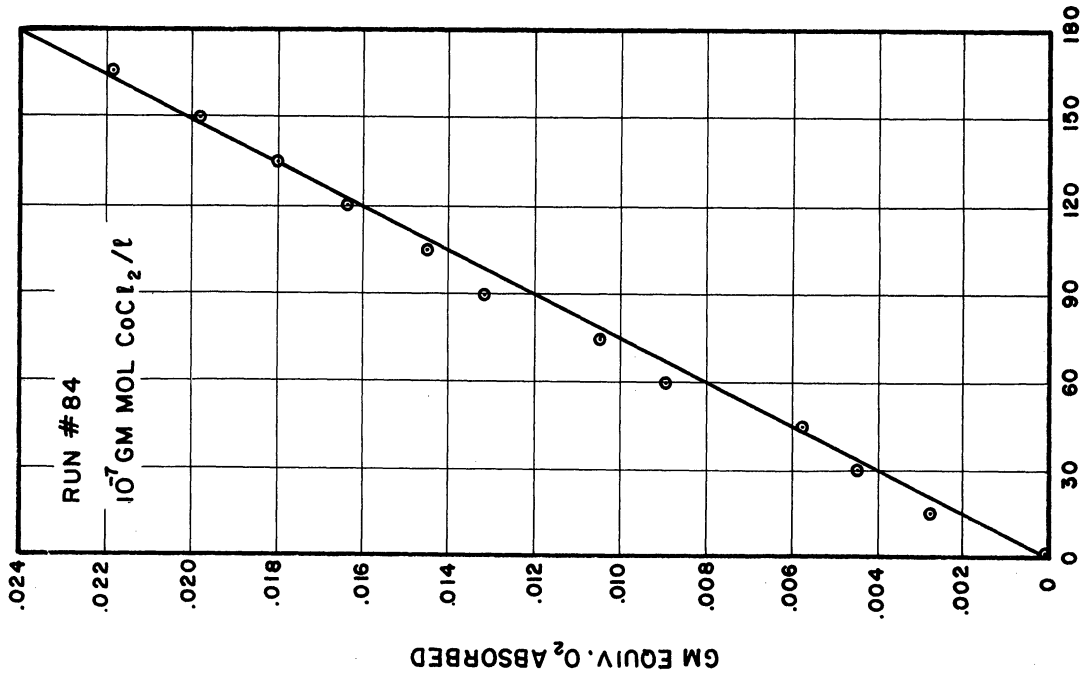
RUN #84
10⁻⁷GM MOL CoCl₂/l
GM EQUIV. O₂ ABSORBED
0
.002
.004
.006
.008
.010
.012
.014
.016
.018
.020
.022
.024
0
30
60
90
120
150
180

Figure 50.

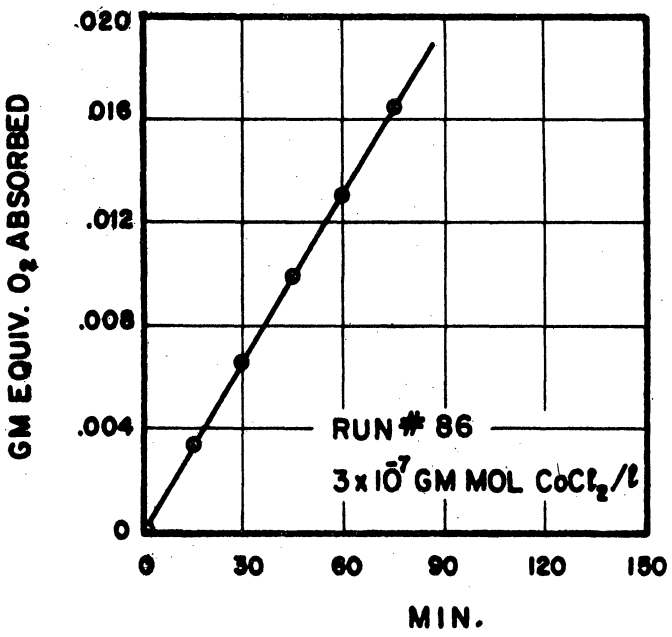

Figure 51.

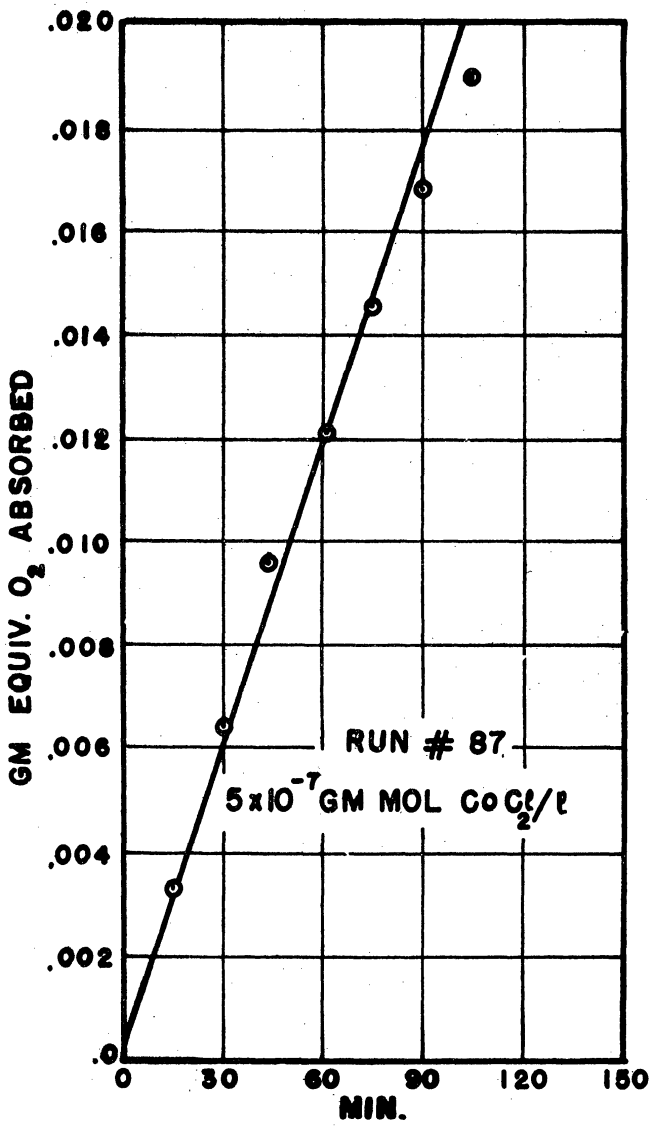

Figure 52.

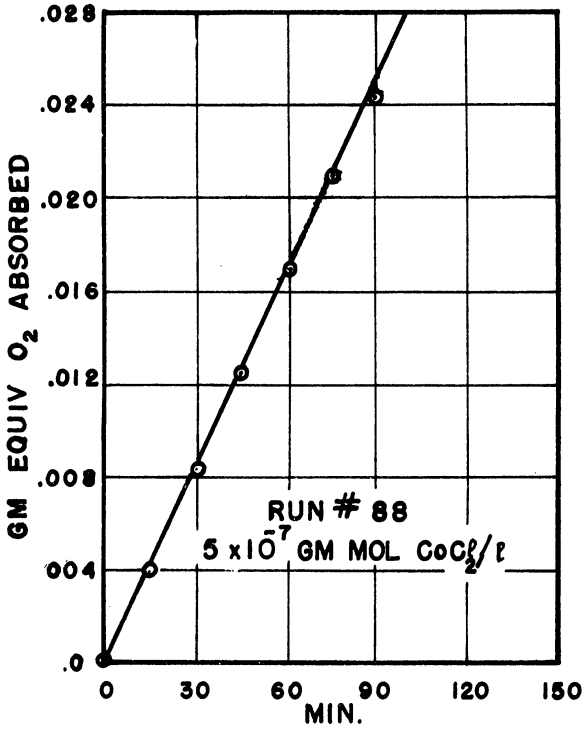

Figure 53.

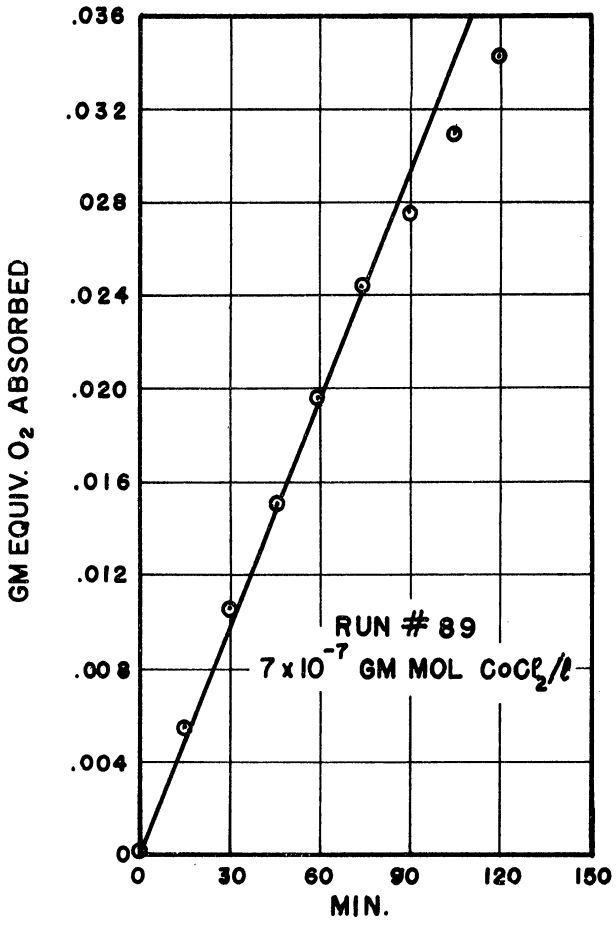

Figure 54.

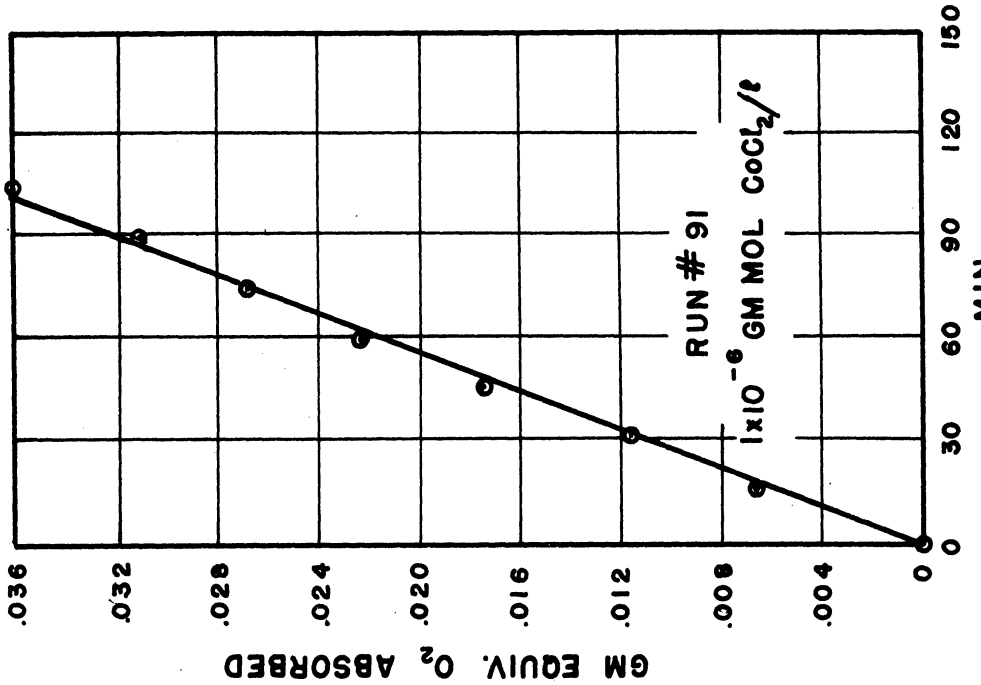

Figure 56.

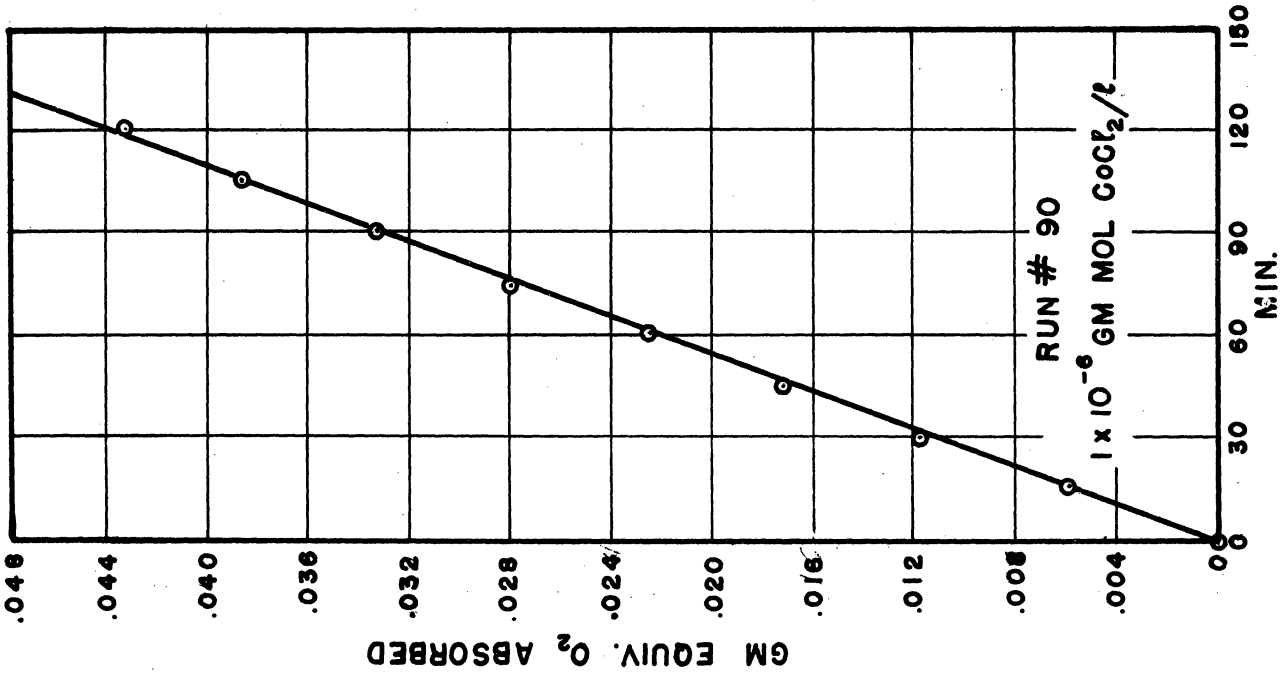

Figure 55.

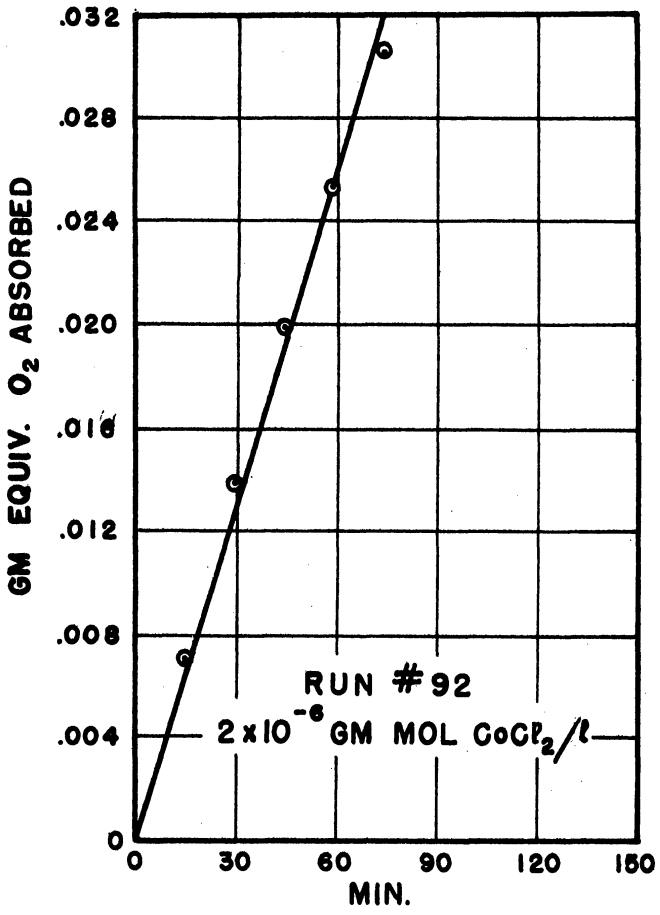

Figure 57.

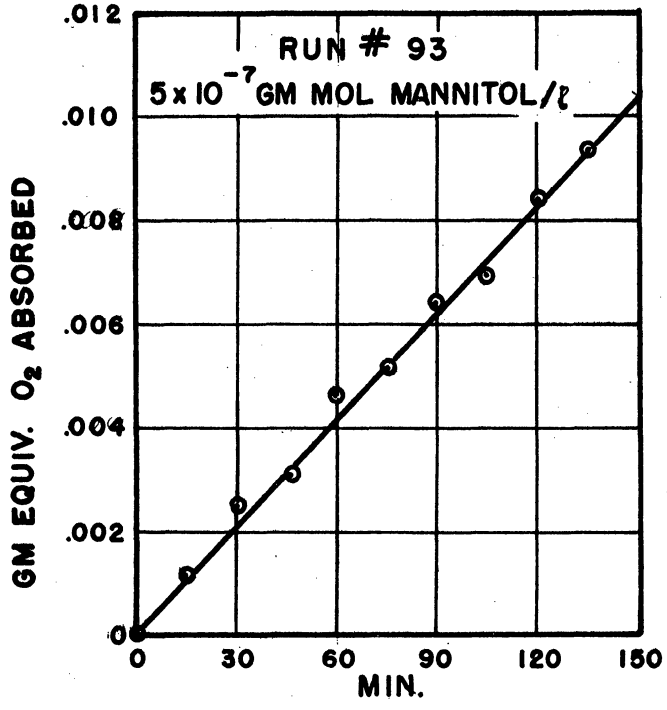

Figure 58.

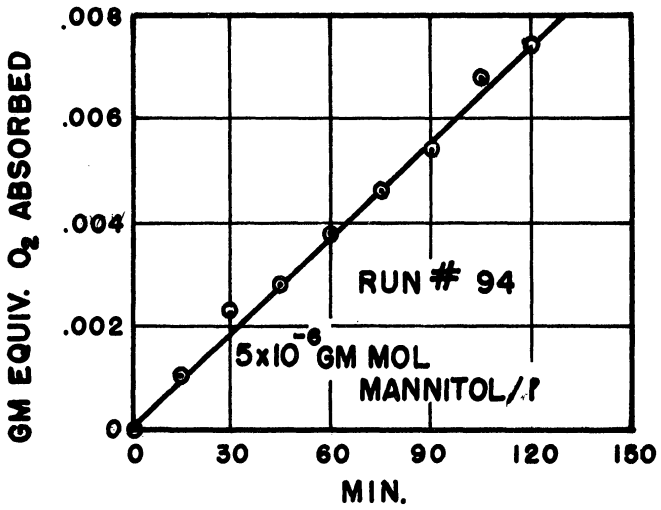

Figure 59.

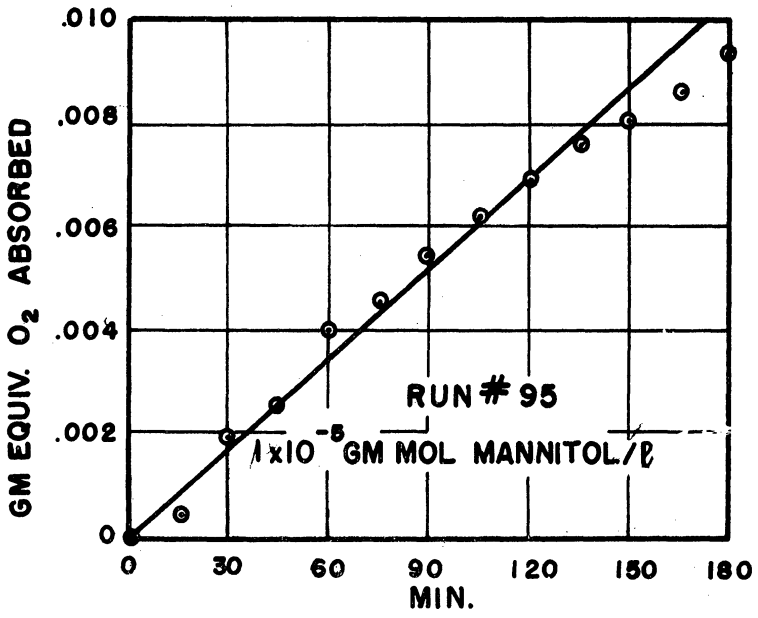

Figure 60.

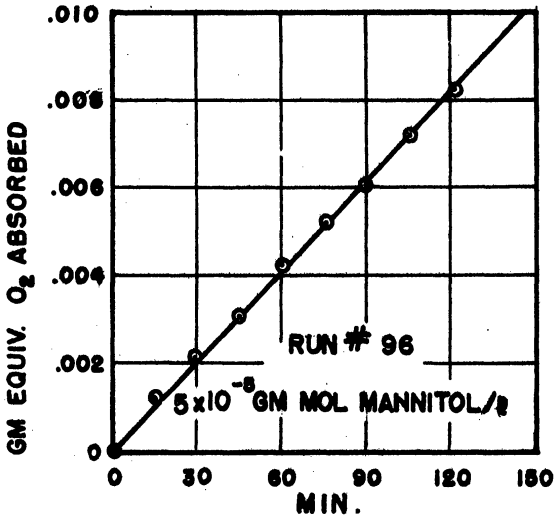

Figure 61.

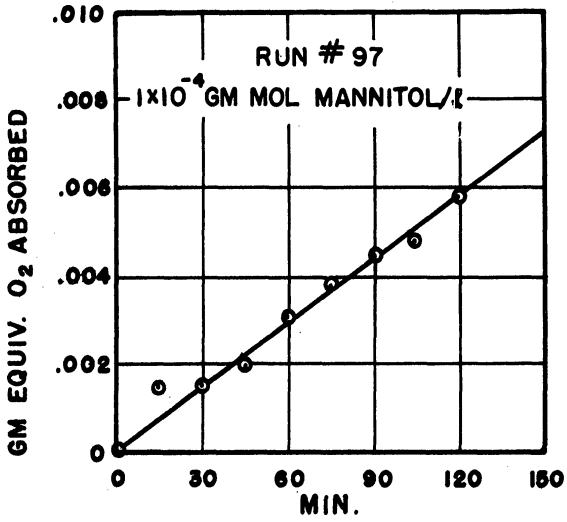

Figure 62.

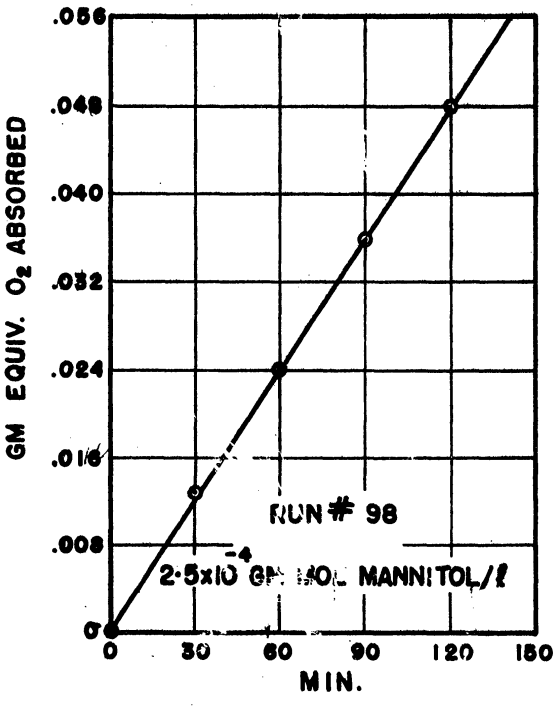

Figure 63.

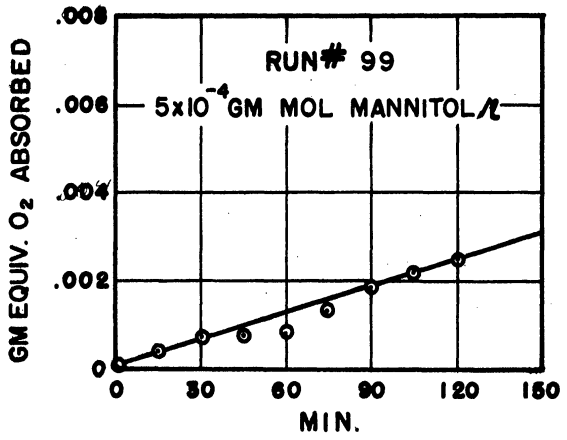

Figure 64.

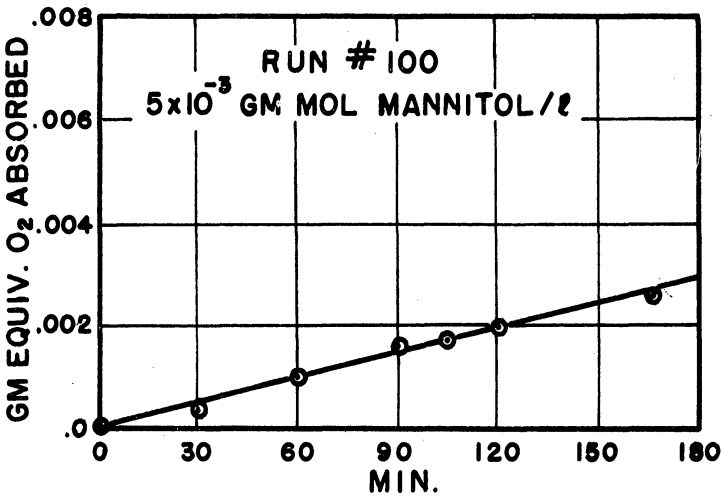

Figure 65.

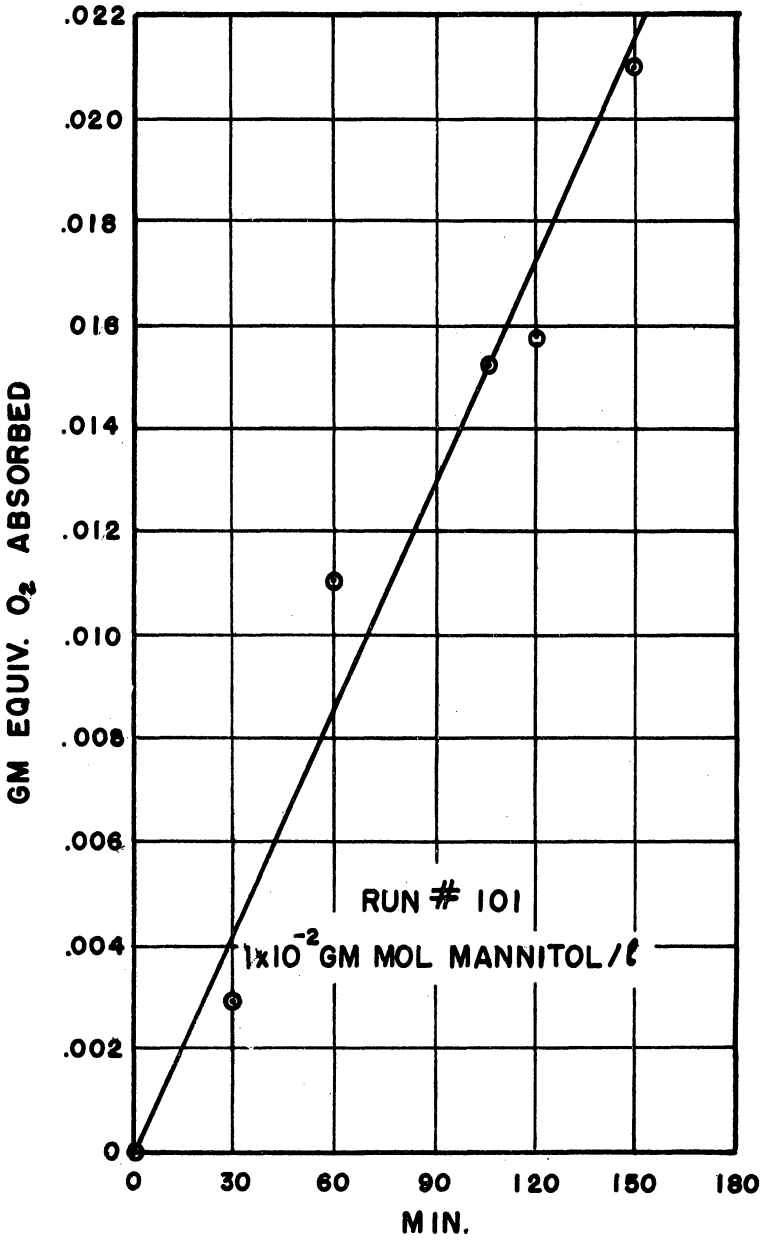

Figure 66.

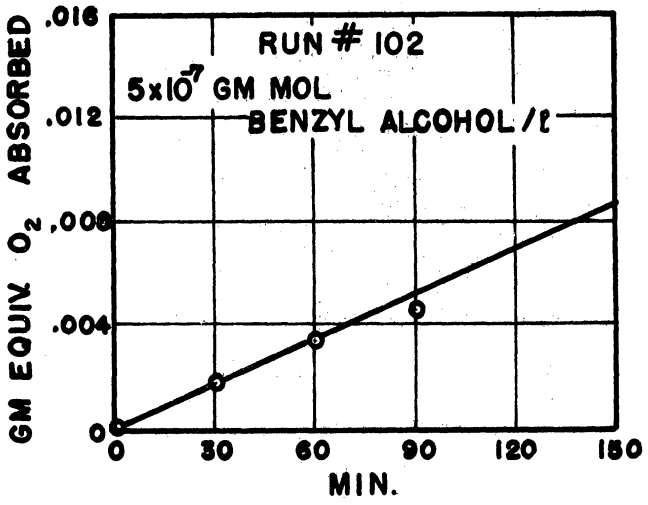

Figure 67.

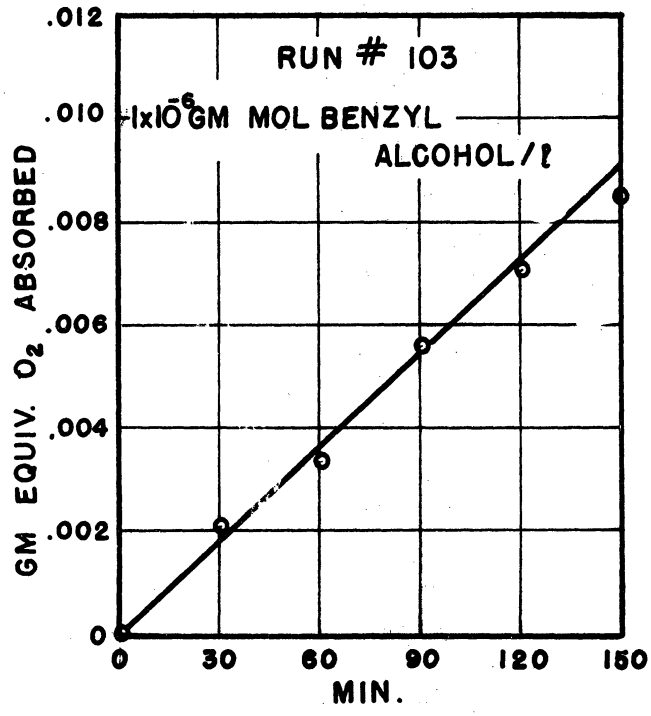

Figure 68.

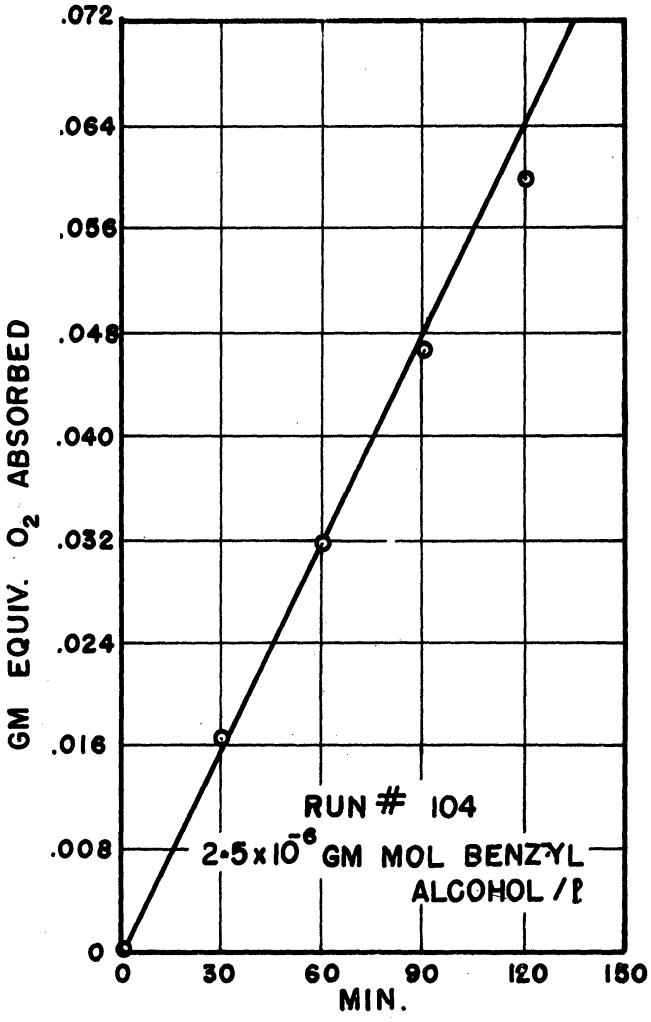

Figure 69.

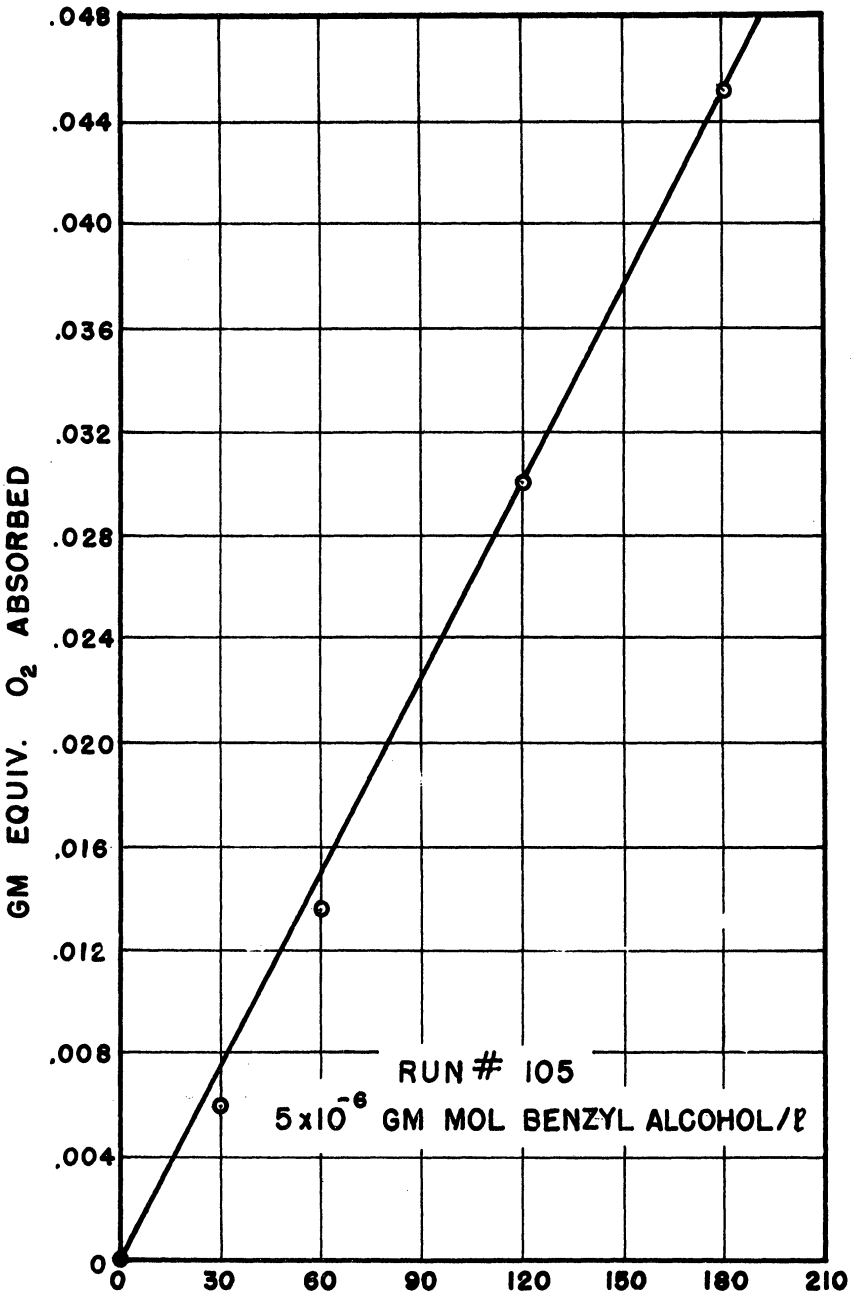
.048
.044
.040
.036
.032
.028
.024
.020
.016
.012
.008
.004
0
GM EQUIV. O_2 ABSORBED
0
30
60
90
120
150
180
210
RUN # 105
5×10^{-6} GM MOL BENZYL ALCOHOL/ℓ

Figure 70.

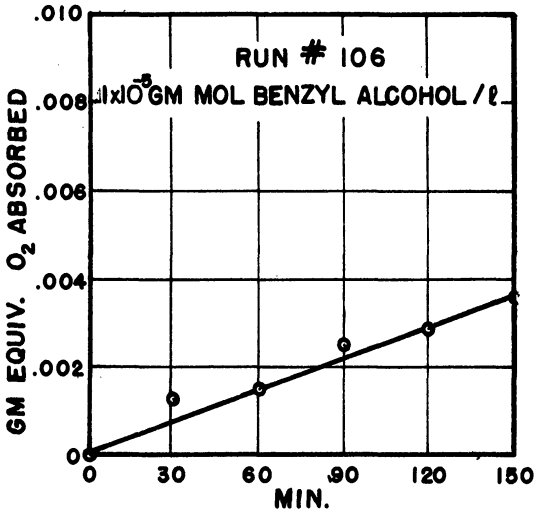

Figure 71.

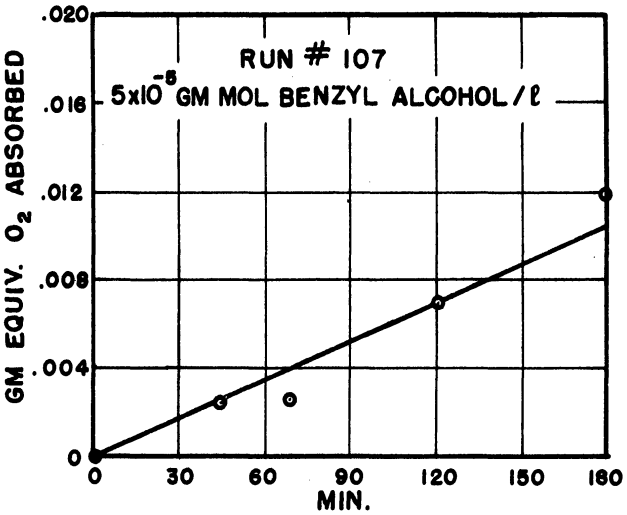

Figure 72.

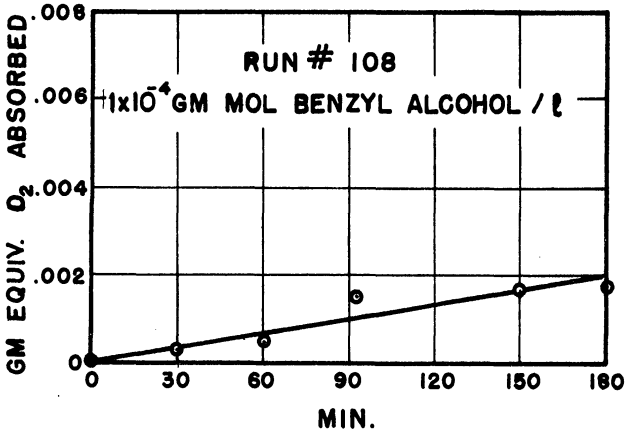

Figure 73.

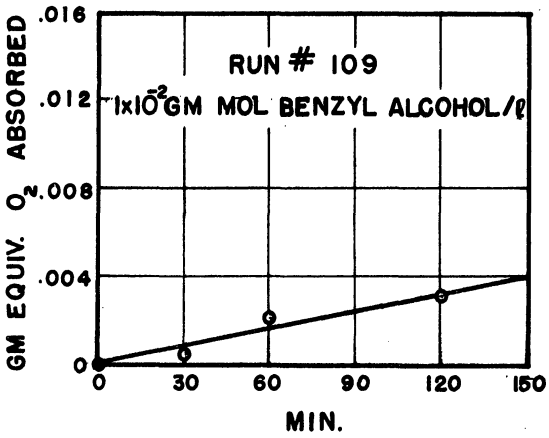

Figure 74.

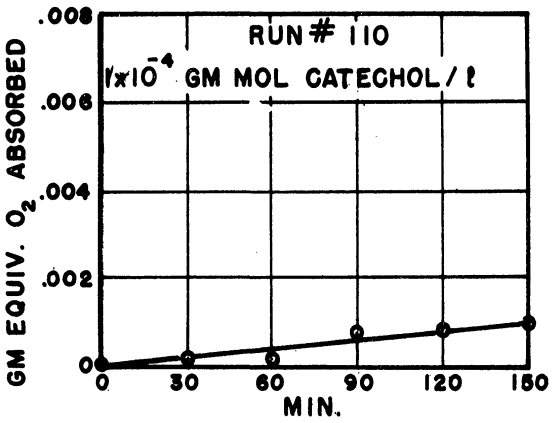

Figure 75.

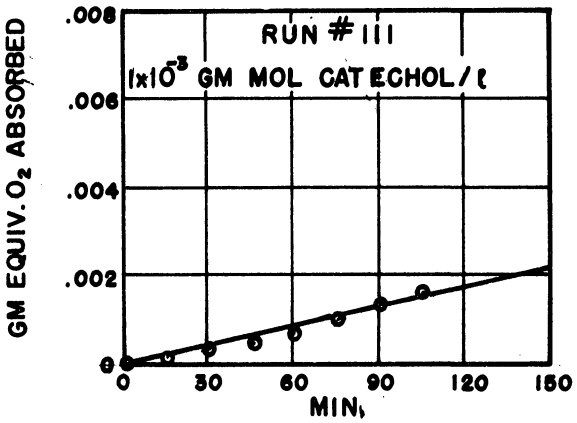

Figure 76.

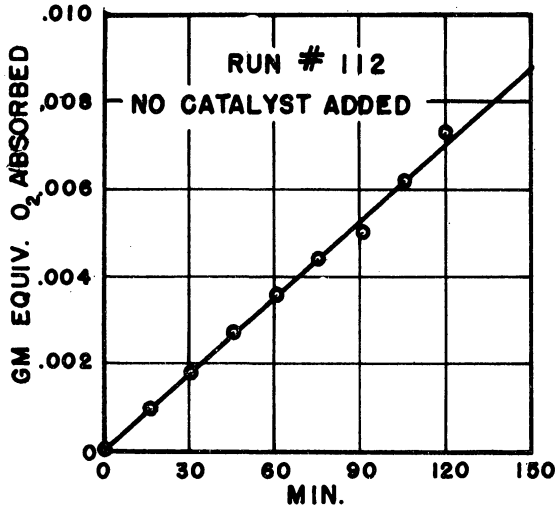

Figure 77.

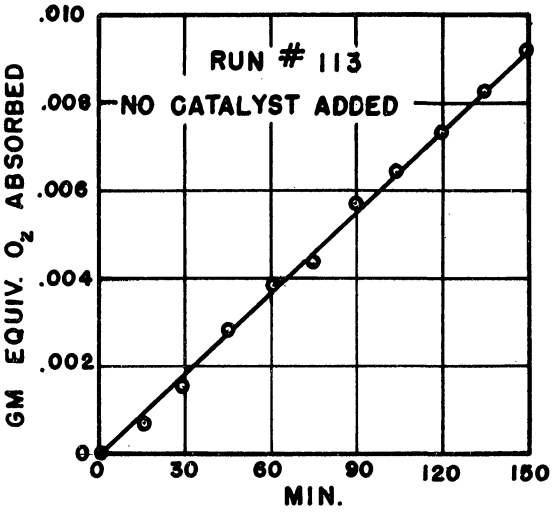

Figure 78.

APPENDIX V

DATA AND CALCULATIONS OF k_L WITH DIFFERENT STIRRER SPEEDS

TABLE 10

Calculations of k_L from data in Figures 79-103

C_{Ai} = 10.54×10^{-4} gm equiv./ℓ ;

Catalyst concentration = 2×10^{-6} gm mol $CoCl_2$/l added

Run #	Stirrer speed RPM	C_{Bo} gm equiv. / l	N'_A gm equiv. / $cm^2 \times min$	k_L ft/hr
1	35	0.126	2.34×10^{-6}	4.37
2	40	0.216	2.64×10^{-6}	4.92
3	41	0.156	2.58×10^{-6}	4.80
4	45	0.200	2.46×10^{-6}	4.59
5	52	0.156	2.30×10^{-6}	4.29
6	60	0.276	2.70×10^{-6}	4.92
7	62	0.340	2.97×10^{-6}	5.55
8	76	0.244	2.91×10^{-6}	5.43
9	80	0.380	2.80×10^{-6}	5.22
10	80	0.276	2.96×10^{-6}	5.51
11	85	0.444	3.93×10^{-6}	7.34
12	85	0.352	3.76×10^{-6}	7.03
13	90	0.432	2.86×10^{-6}	5.34
14	100	0.344	3.70×10^{-6}	6.83
15	100	0.352	3.62×10^{-6}	6.75
16	120	0.424	2.92×10^{-6}	5.41
17	125	0.240	2.54×10^{-6}	6.22
18	140	0.460	3.91×10^{-6}	7.30
19	150	0.164	2.91×10^{-6}	5.51
20	165	0.520	3.29×10^{-6}	6.14
21	175	0.252	3.40×10^{-6}	6.34
22	180	0.288	3.70×10^{-6}	6.89
23	200	0.324	3.90×10^{-6}	7.27
24	200	0.406	3.33×10^{-6}	6.23
25	210	0.411	3.54×10^{-6}	6.64

FIGURES 79 THROUGH 103 REPRESENT THE

RATE DATA FOR VARIOUS STIRRER SPEEDS

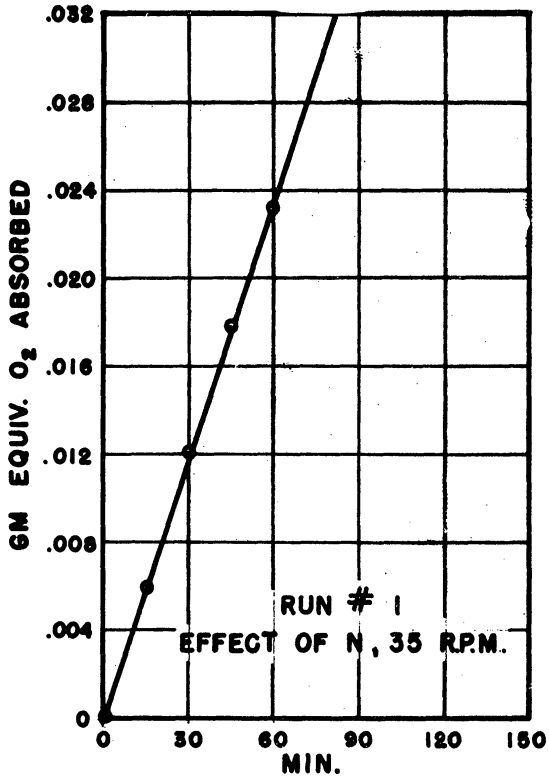

Figure 79.

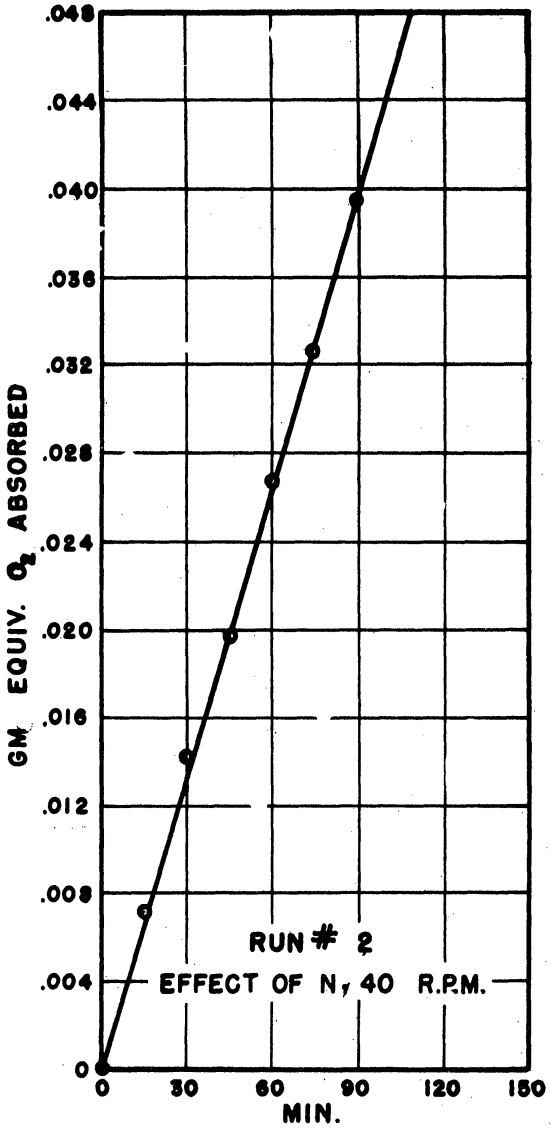

Figure 80.

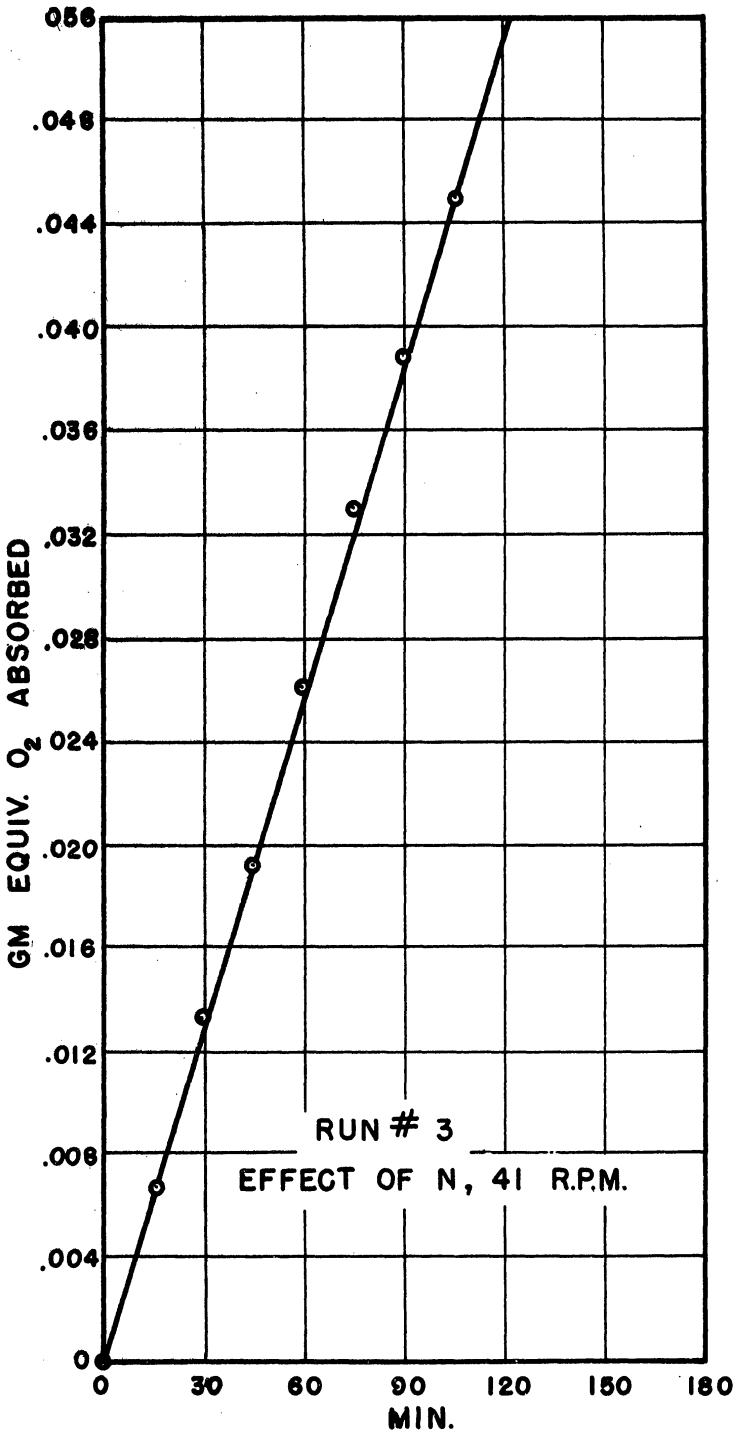
.048
.044
.040
.036
.032
.028
.024
.020
.016
.012
.008
.004
0
GM EQUIV. O_2 ABSORBED
RUN # 3
EFFECT OF N, 41 R.P.M.
0
30
60
90
120
150
180
MIN.

Figure 81.

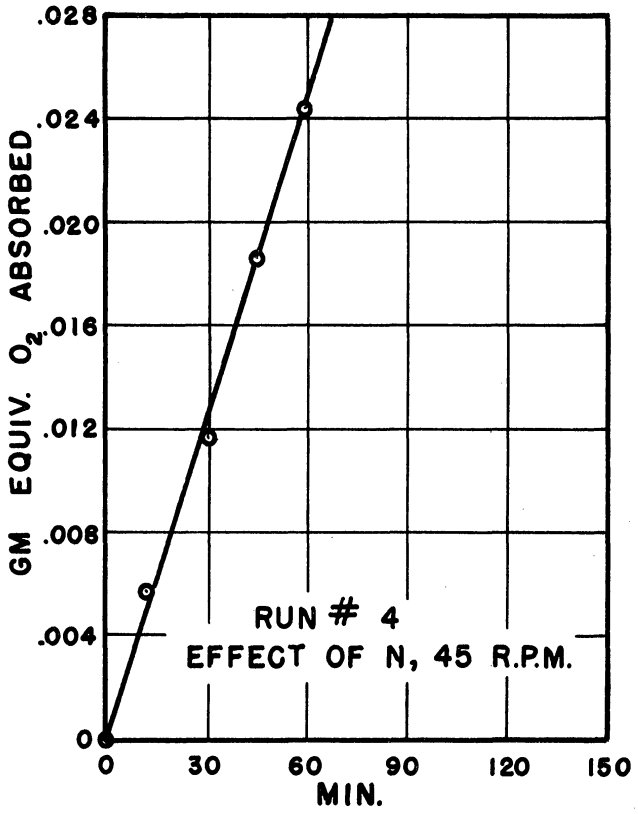

Figure 82.

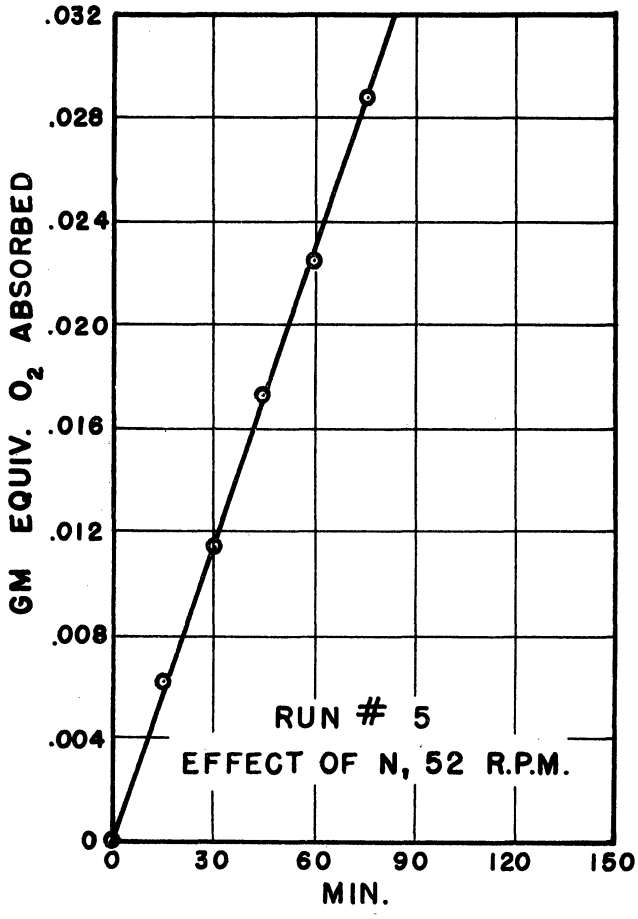

Figure 83.

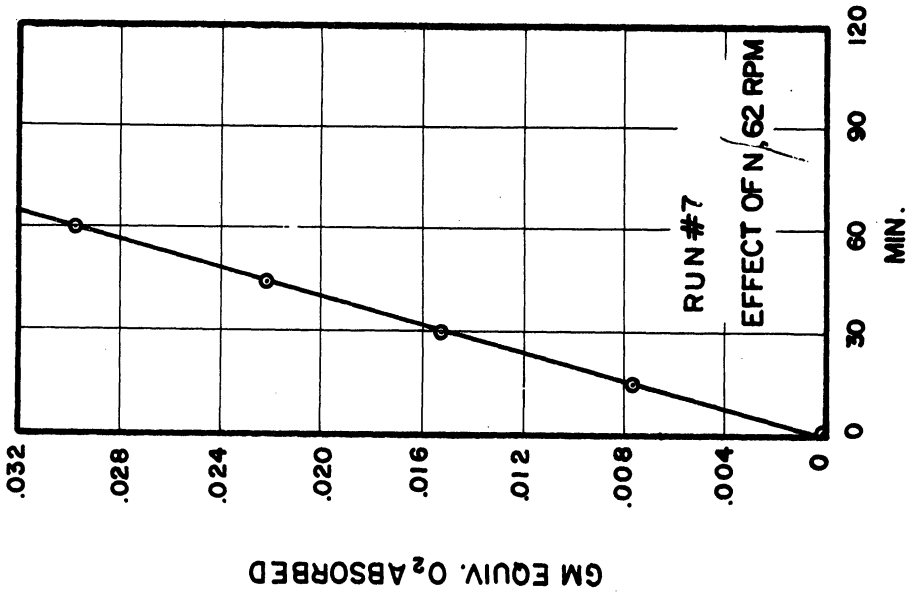

Figure 85.

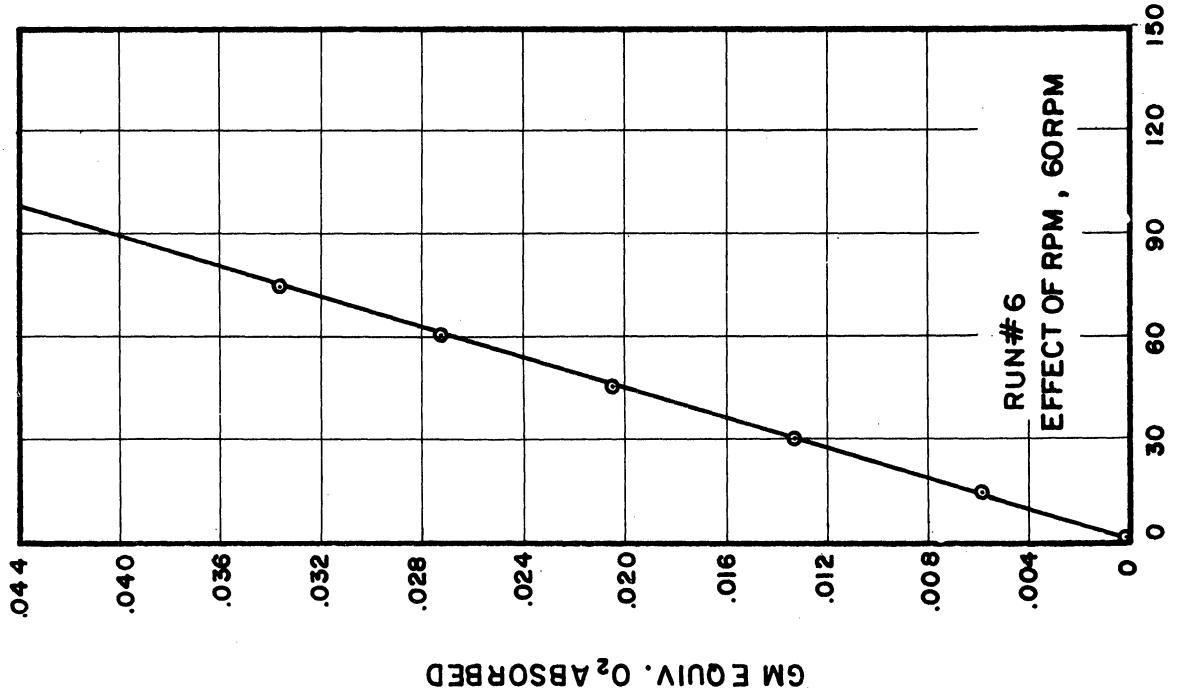

Figure 84.

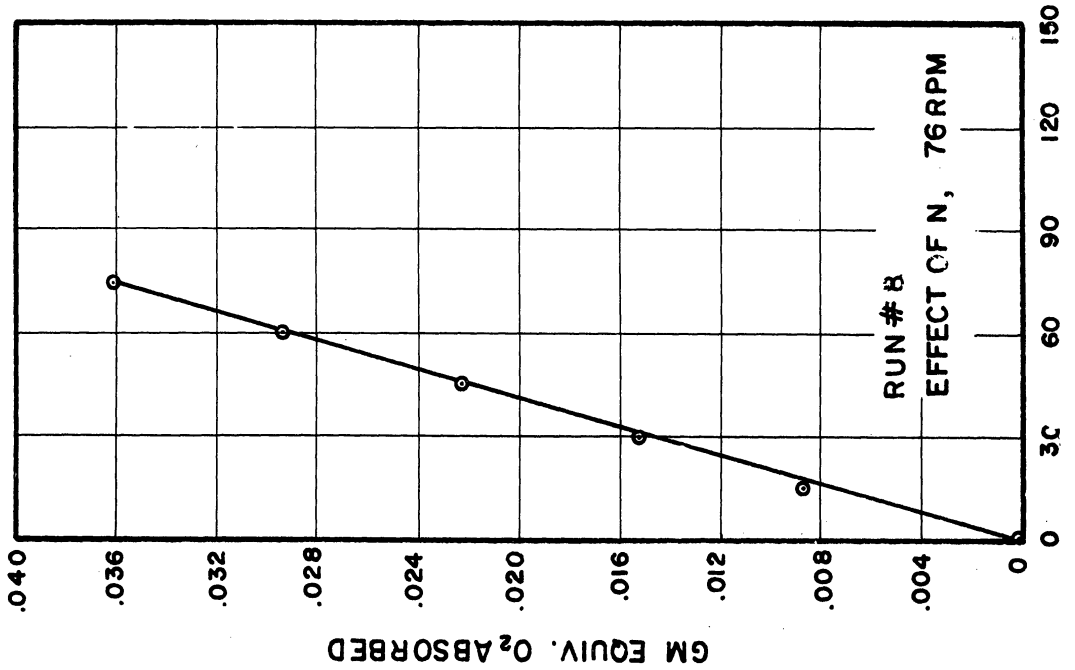

Figure 87.

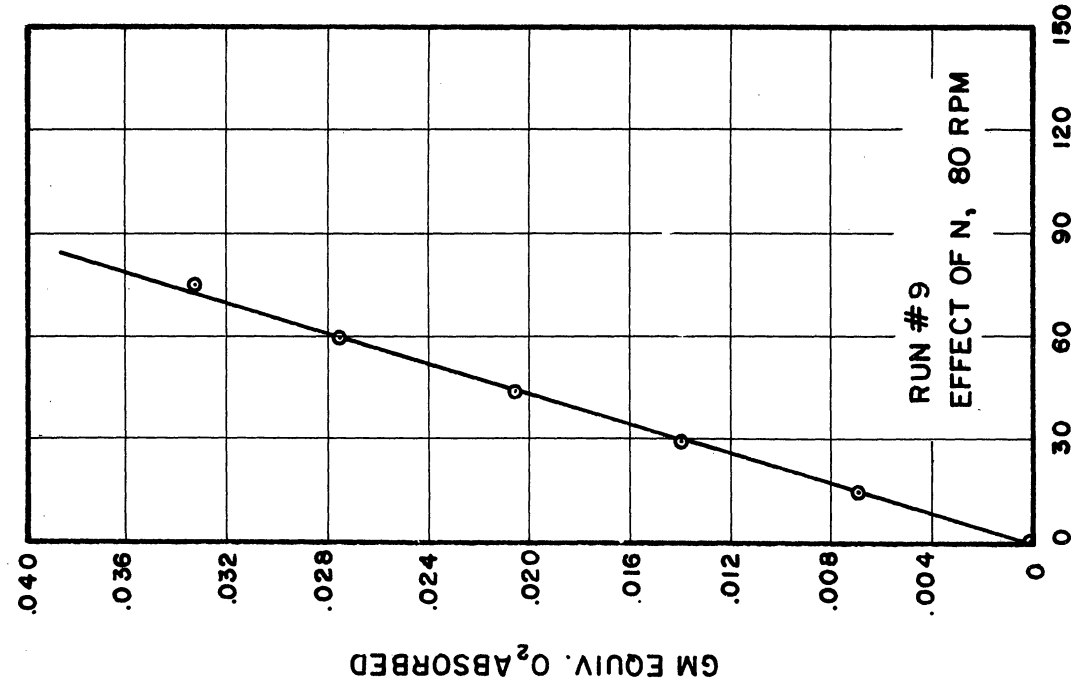

Figure 86.

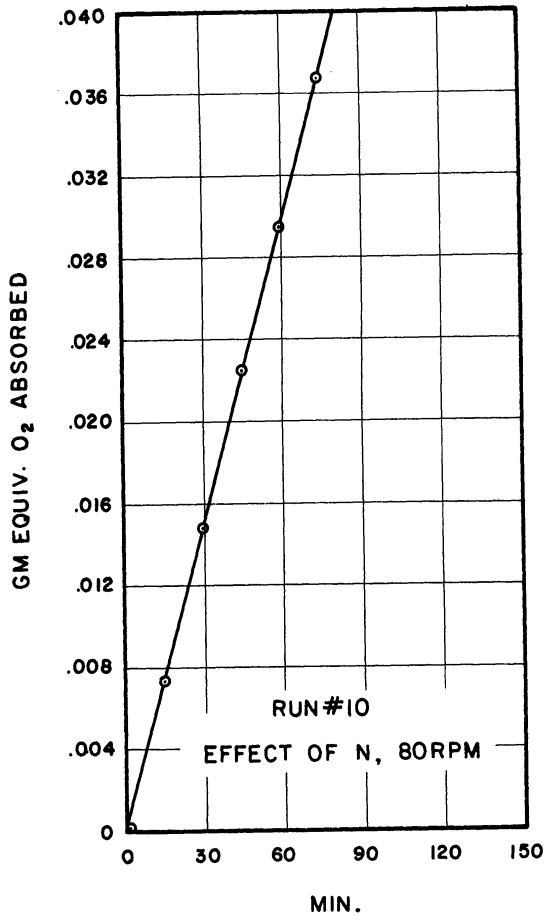

Figure 88.

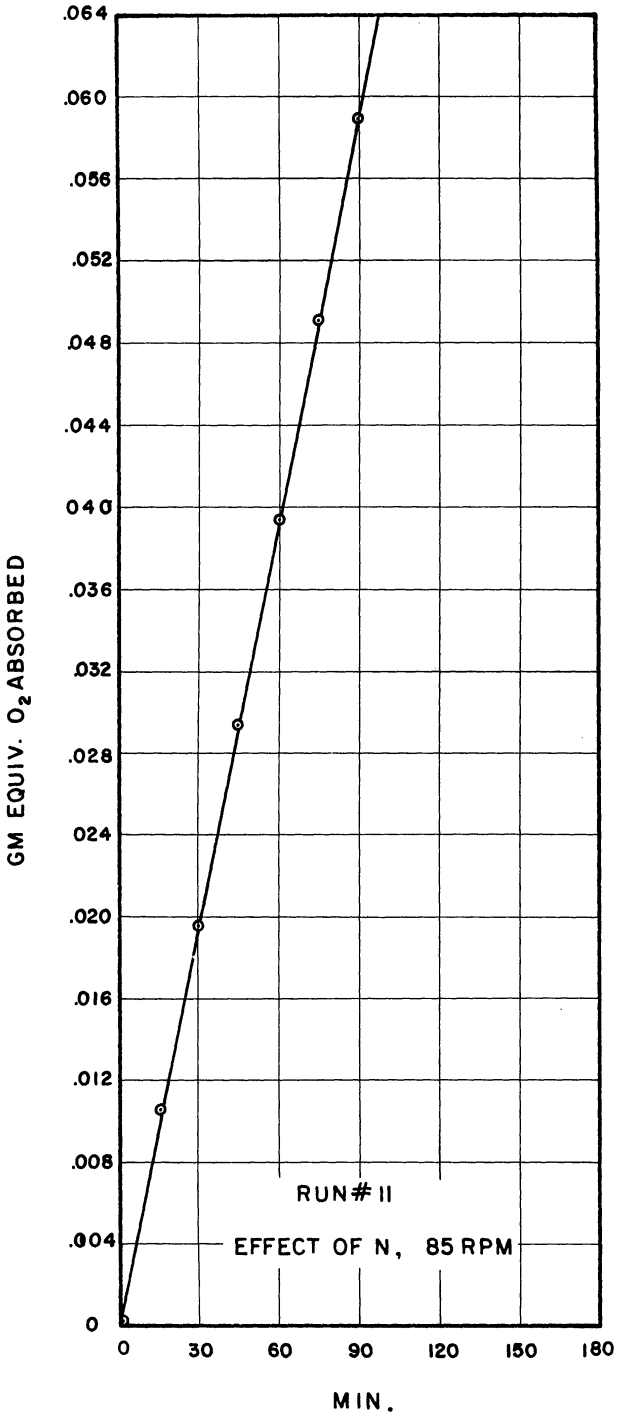

Figure 89.

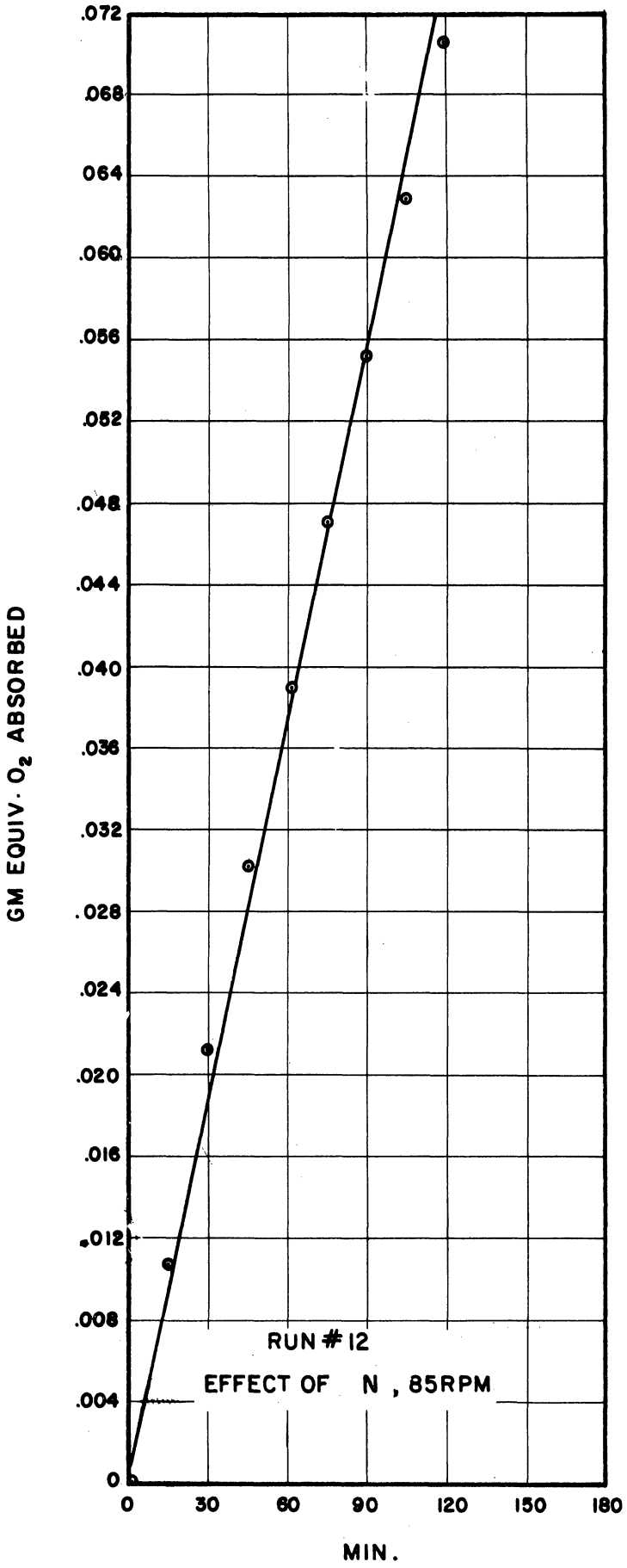
.072
.068
.064
.060
.056
.052
.048
.044
.040
.036
.032
.028
.024
.020
.016
.012
.008
.004
0
GM EQUIV. O_2 ABSORBED
RUN # 12
EFFECT OF N , 85RPM
0
30
60
90
120
150
180
MIN.

Figure 90.

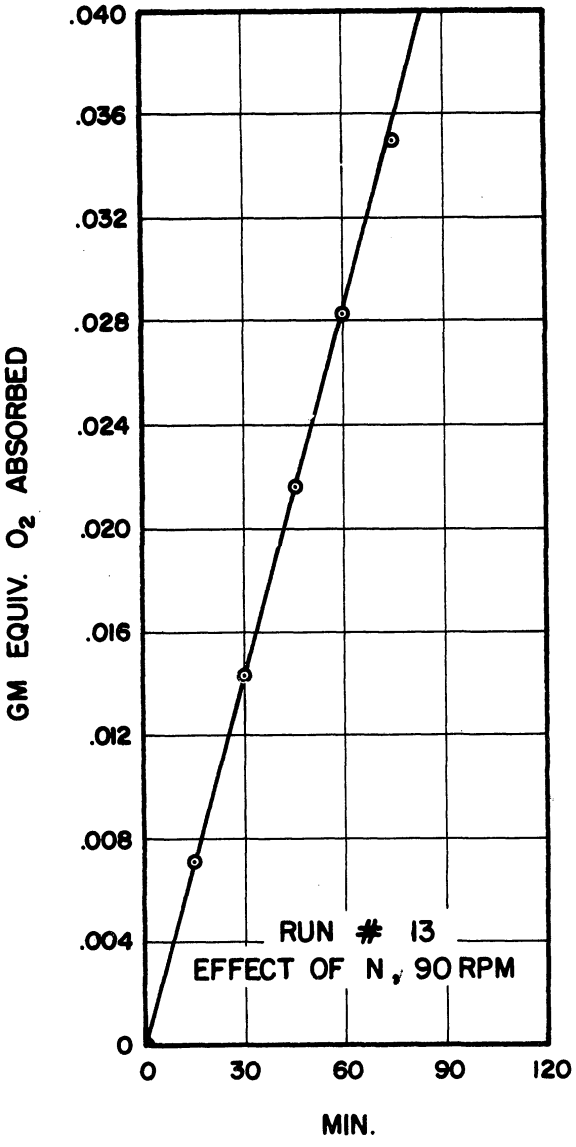

Figure 91.

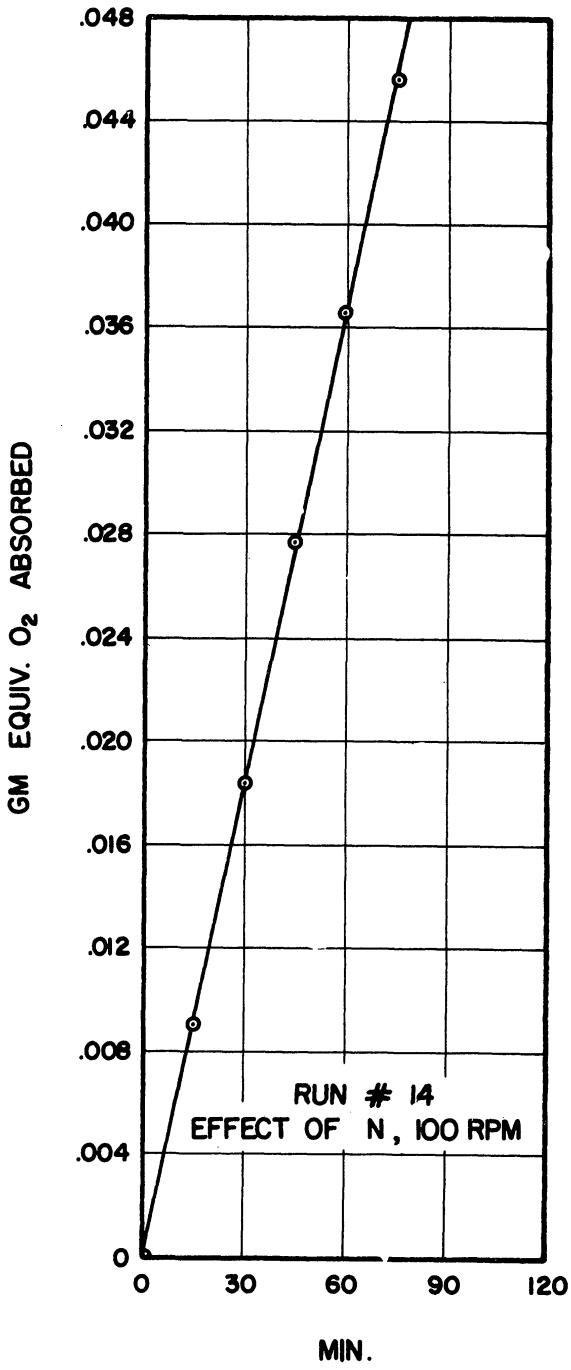

Figure 92.

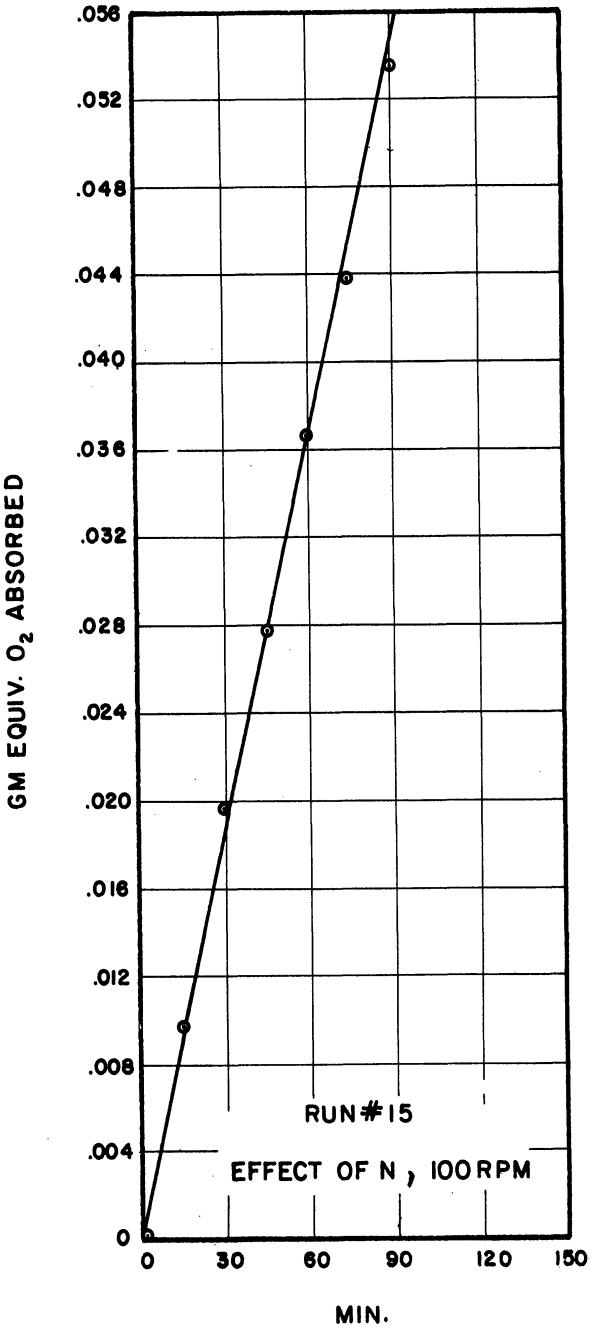

Figure 93.

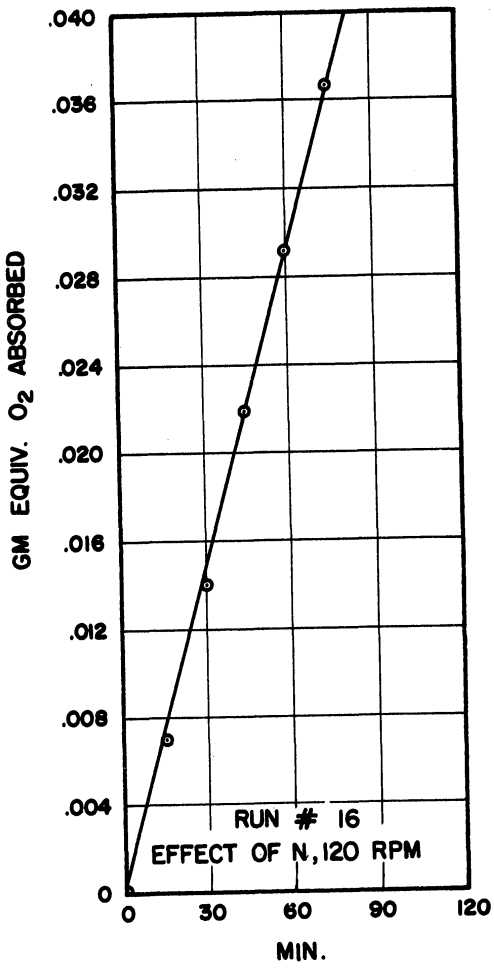

Figure 94.

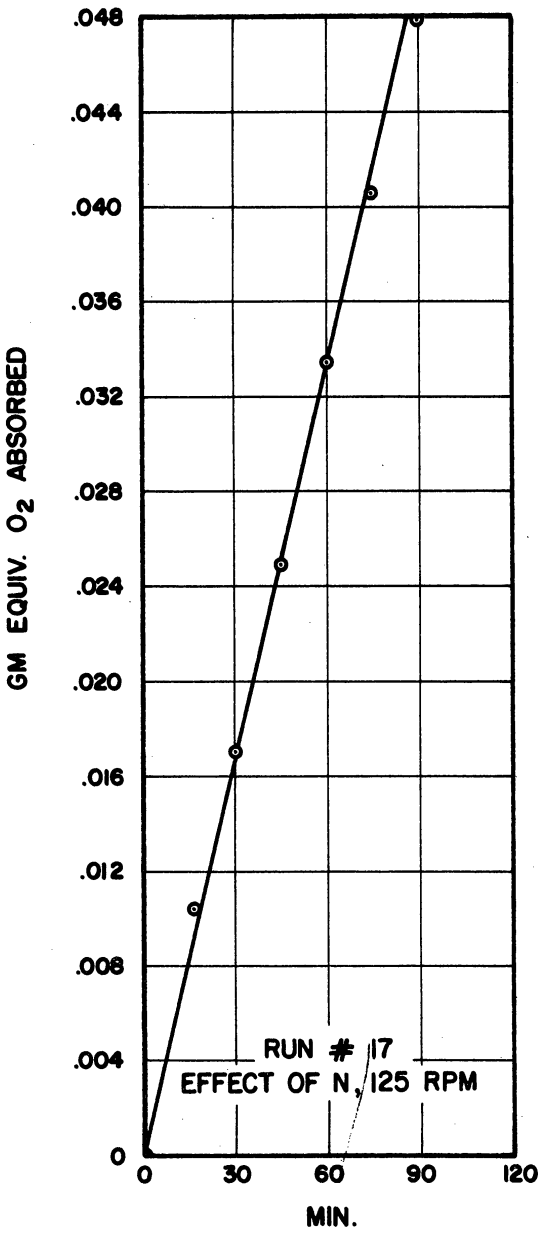

Figure 95.

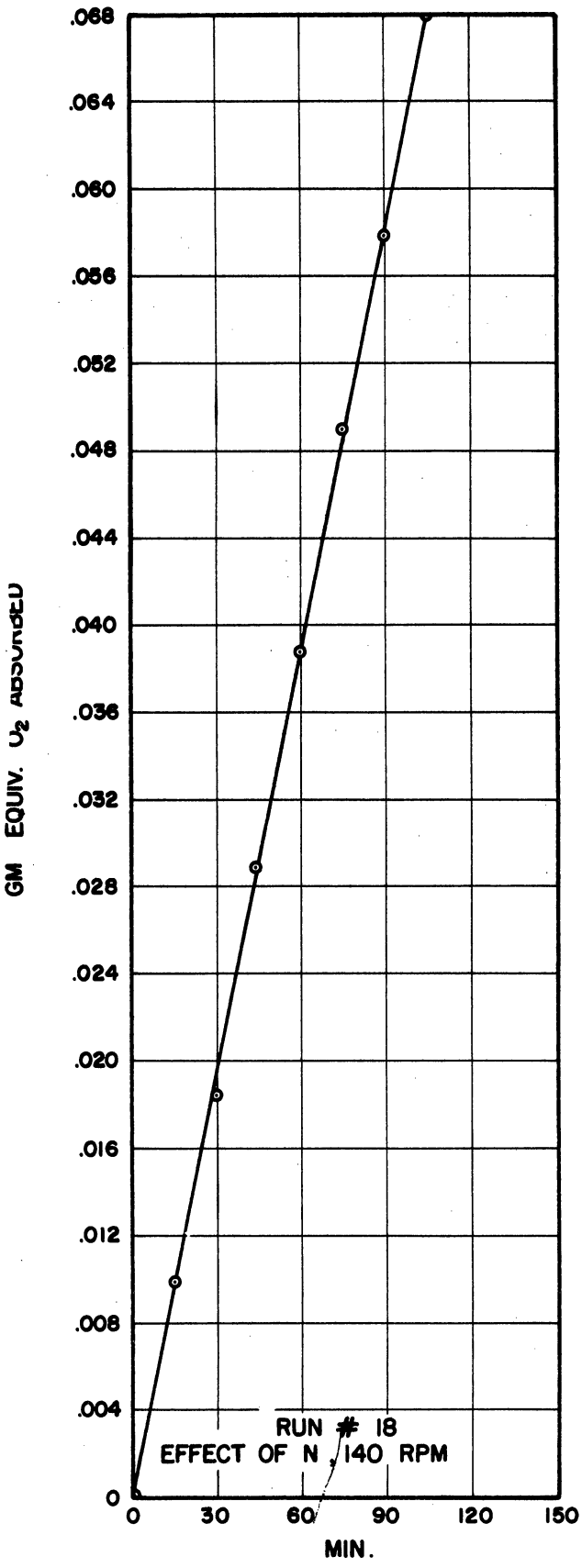

Figure 96.

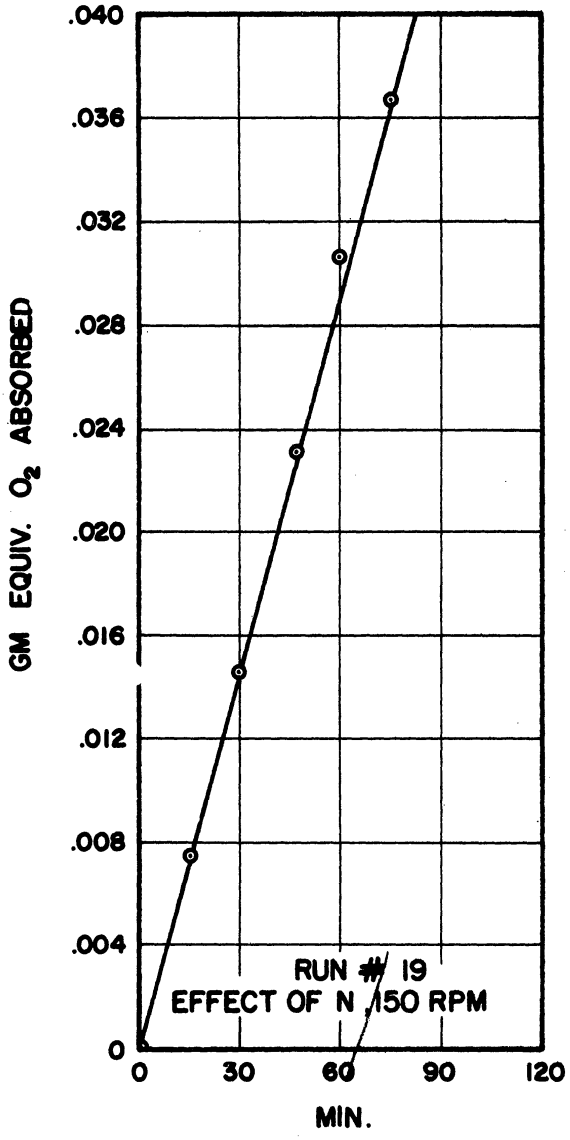

Figure 97.

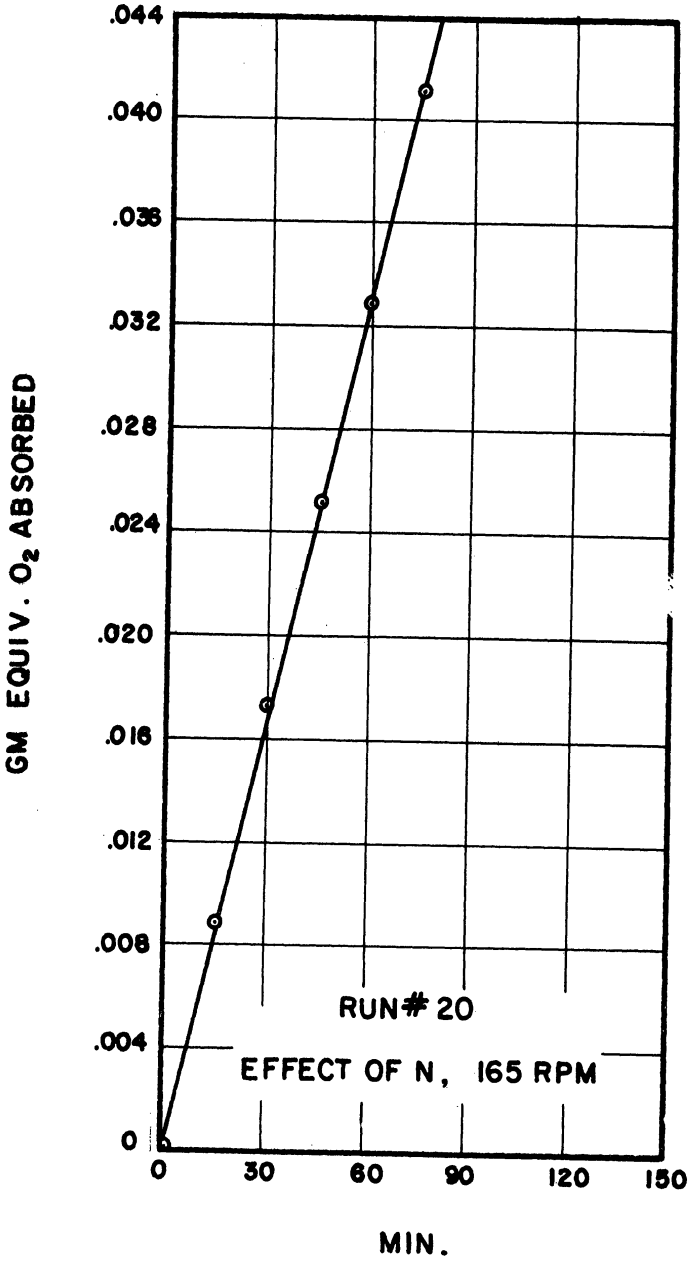

Figure 98.

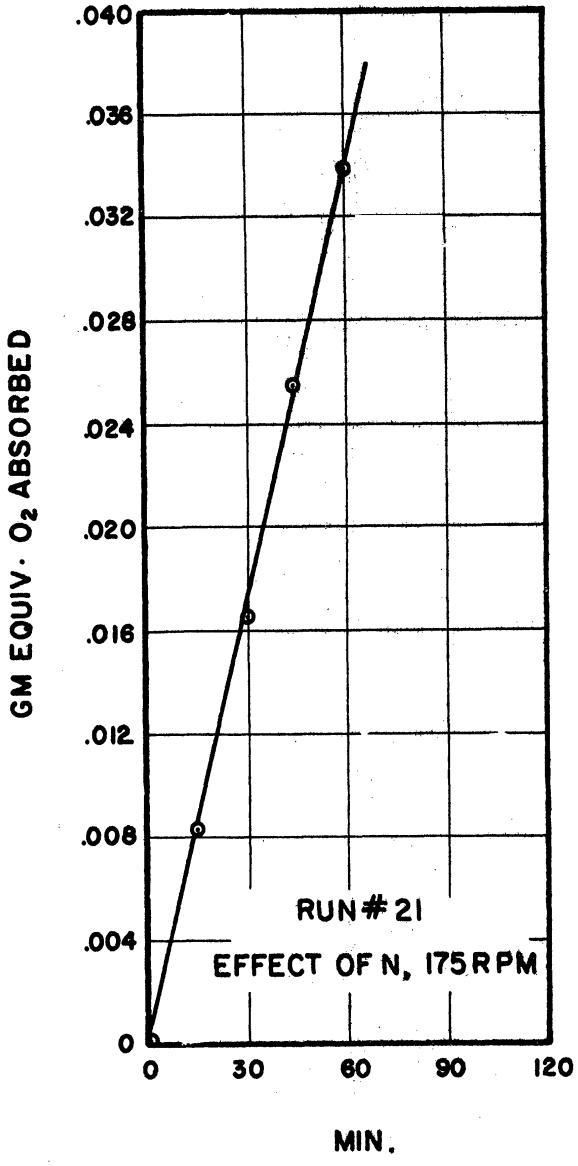

Figure 99.

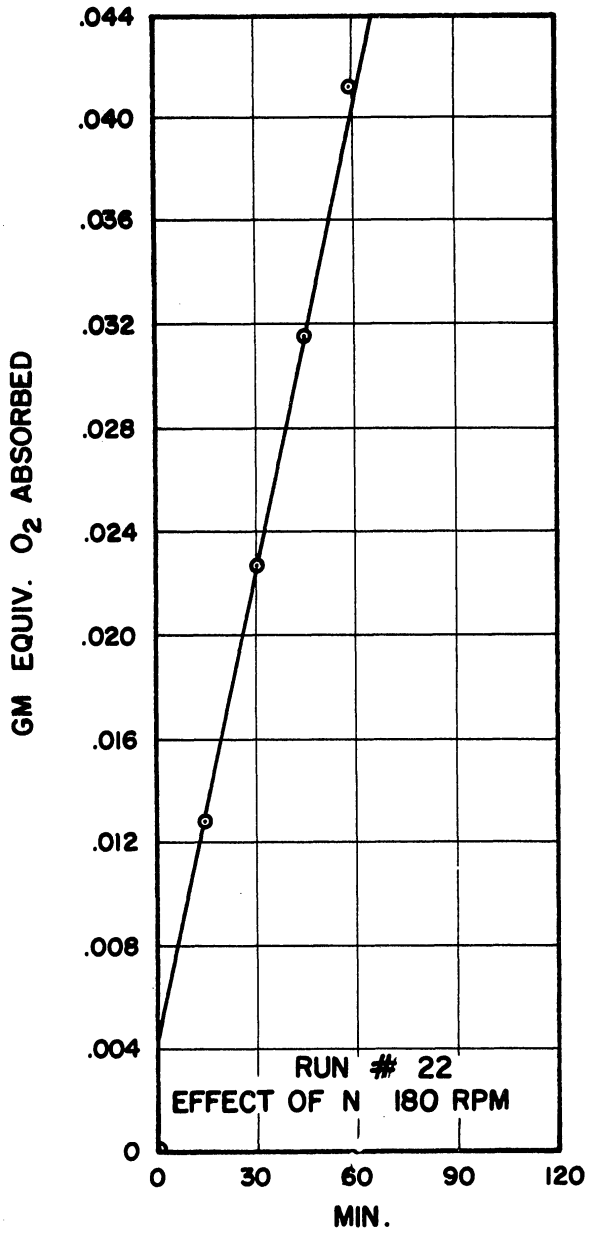

Figure 100.

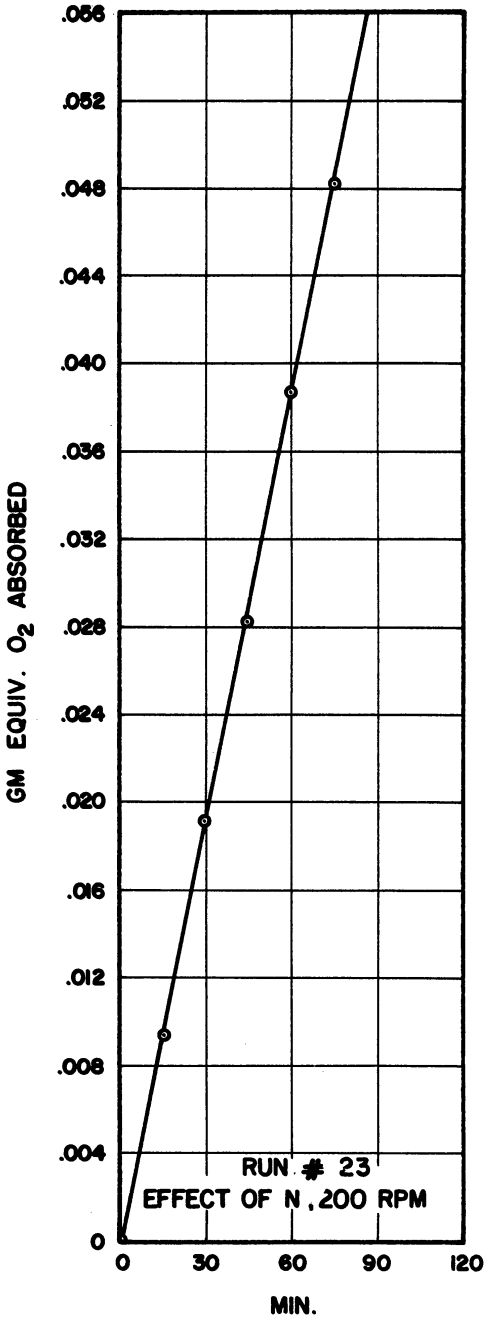

Figure 101.

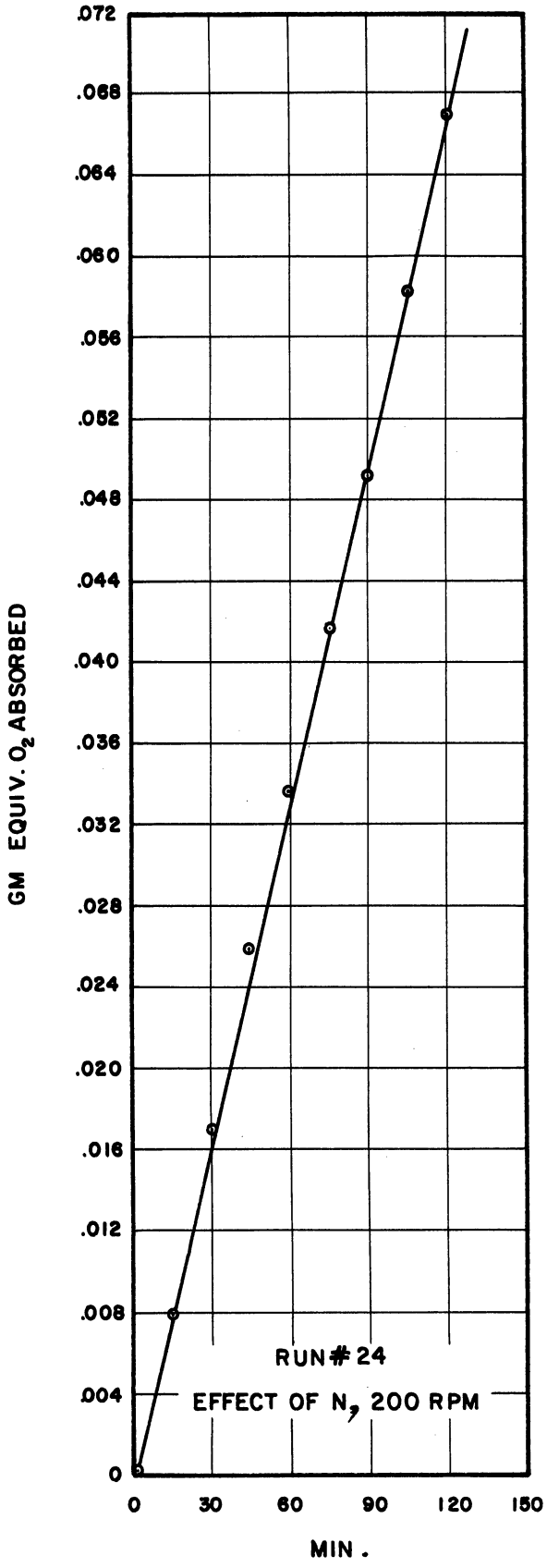

Figure 102.

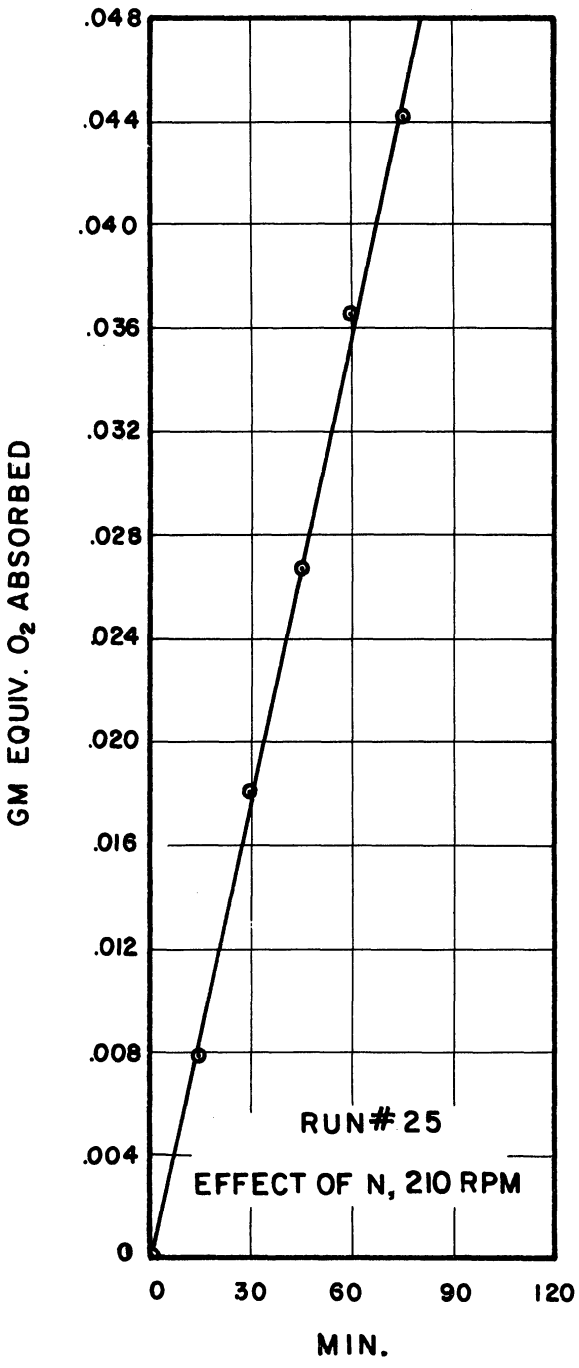
.048
.044
.040
.036
.032
.028
.024
.020
.016
.012
.008
.004
0
GM EQUIV. O_2 ABSORBED
RUN# 25
EFFECT OF N, 210 RPM
0
30
60
90
120
MIN.

Figure 103.

APPENDIX VI

DATA AND CALCULATIONS OF k_L

FOR THE EFFECT OF OXYGEN CONCENTRATION

TABLE 11

Calculations of k_L with 99.5% O_2 ,

Data from Figures 104-110

Run #	Catalyst used	Amount of catalyst added gm mol/ℓ	C_{Bo} gm equiv/ℓ	C_{Ai} gm equiv/ℓ	N'_A $\frac{\text{gm equiv}}{\text{cm}^2 \times \text{min}}$	k_L, ft/hr
26	$CO\ Cl_2$	1×10^{-10}	0.216	1.27×10^{-3}	2.28×10^{-6}	0.88
27	$CO\ Cl_2$	1×10^{-9}	0.225	1.27×10^{-3}	2.35×10^{-6}	0.91
28	$CO\ Cl_2$	1×10^{-8}	0.213	1.27×10^{-3}	2.24×10^{-6}	0.86
29	$CO\ Cl_2$	1×10^{-7}	0.220	1.27×10^{-3}	3.66×10^{-6}	1.41
30	$CO\ Cl_2$	1×10^{-6}	0.198	1.27×10^{-3}	6.4×10^{-6}	2.47
31	$CO\ Cl_2$	2×10^{-6}	0.248	1.27×10^{-3}	8.39×10^{-6}	3.24
32	$CO\ Cl_2$	2×10^{-6}	0.170	1.27×10^{-3}	8.24×10^{-6}	3.18

FIGURES 104 THROUGH 110 REPRESENT THE

RATE DATA WITH 99.5 PER CENT O_2

FOR VARIOUS Co^{++} CONCENTRATIONS

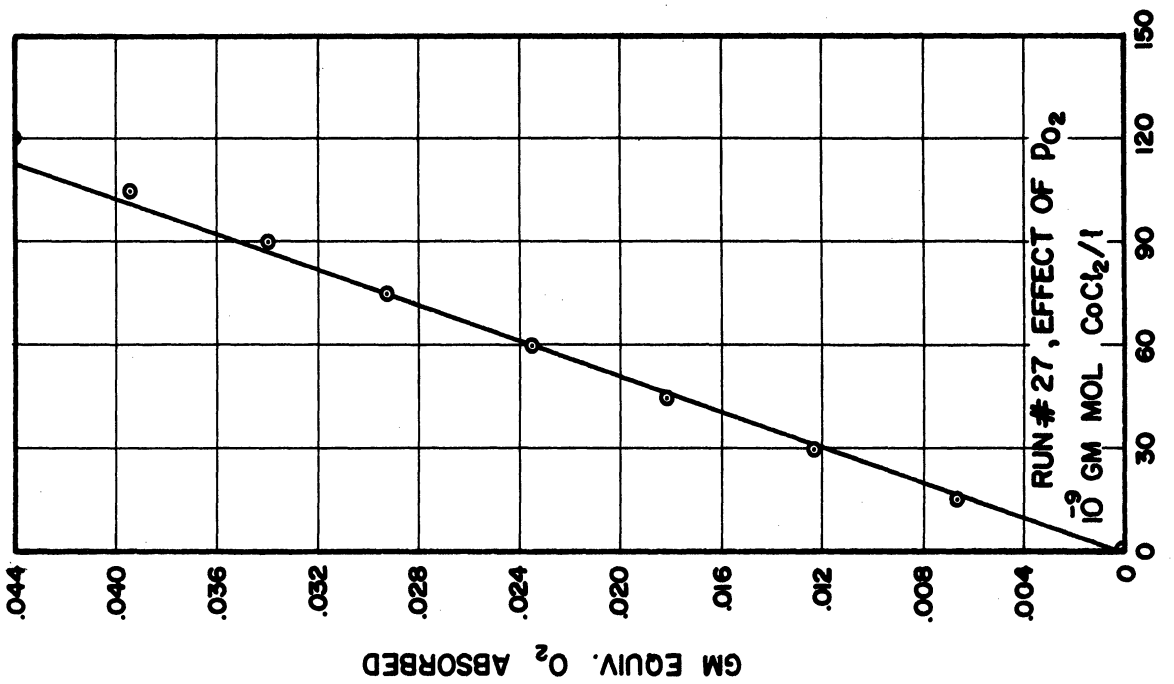

Figure 105.

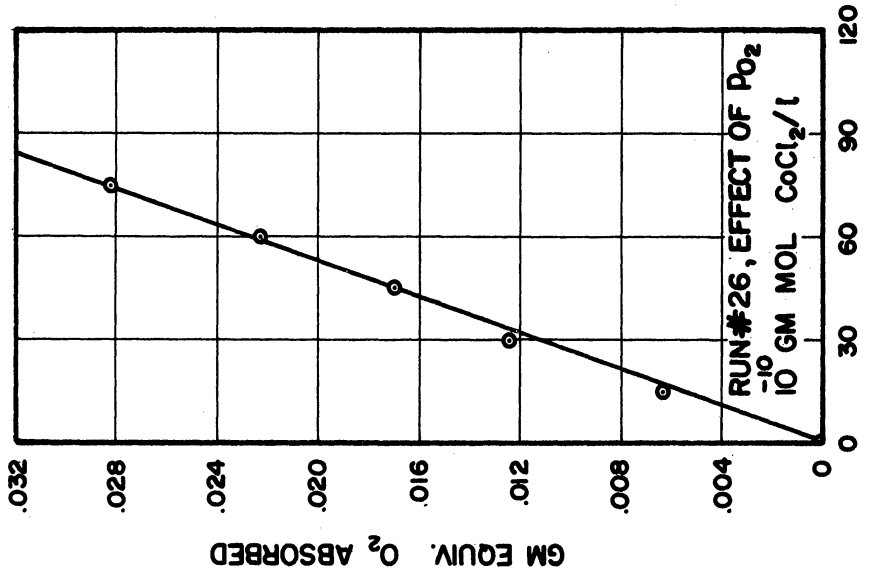

Figure 104.

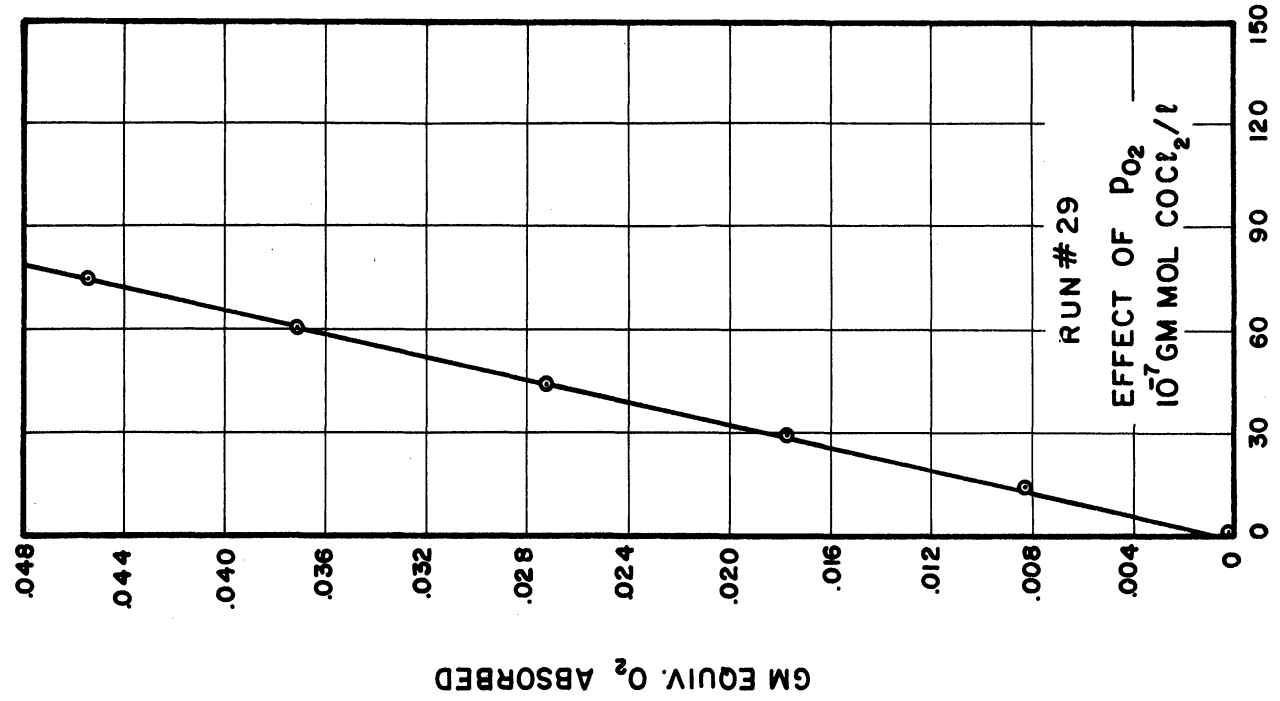

Figure 107.

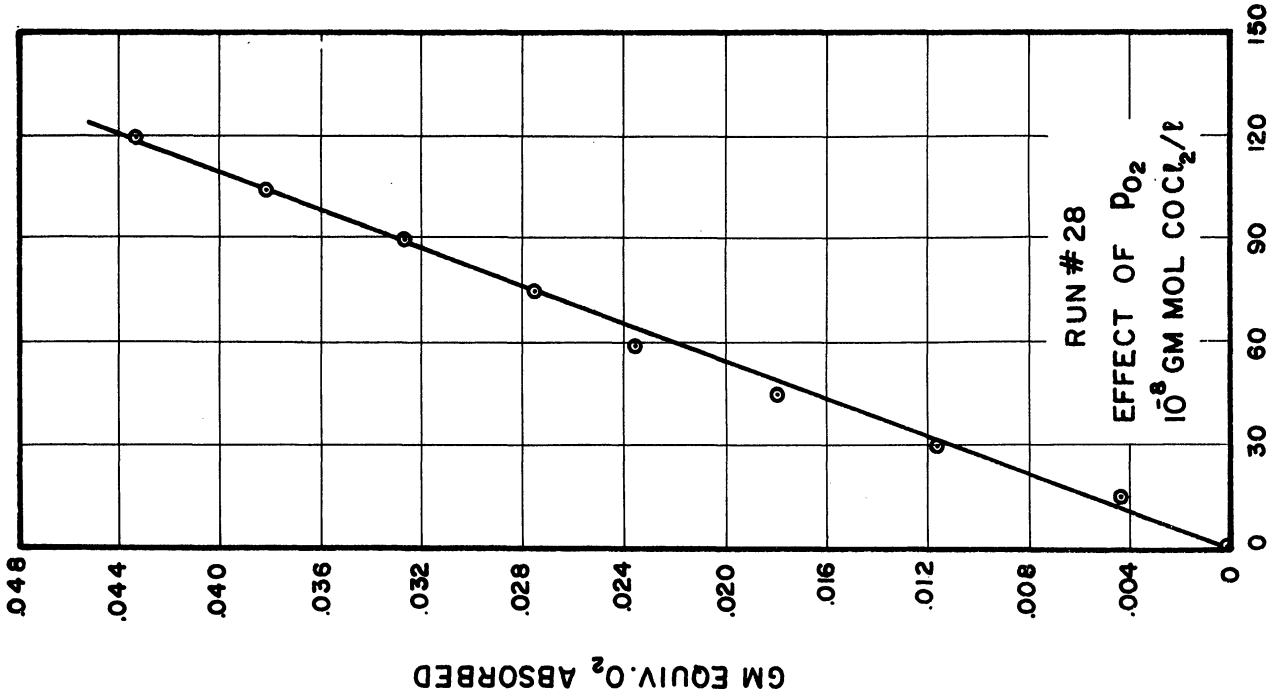

Figure 106.

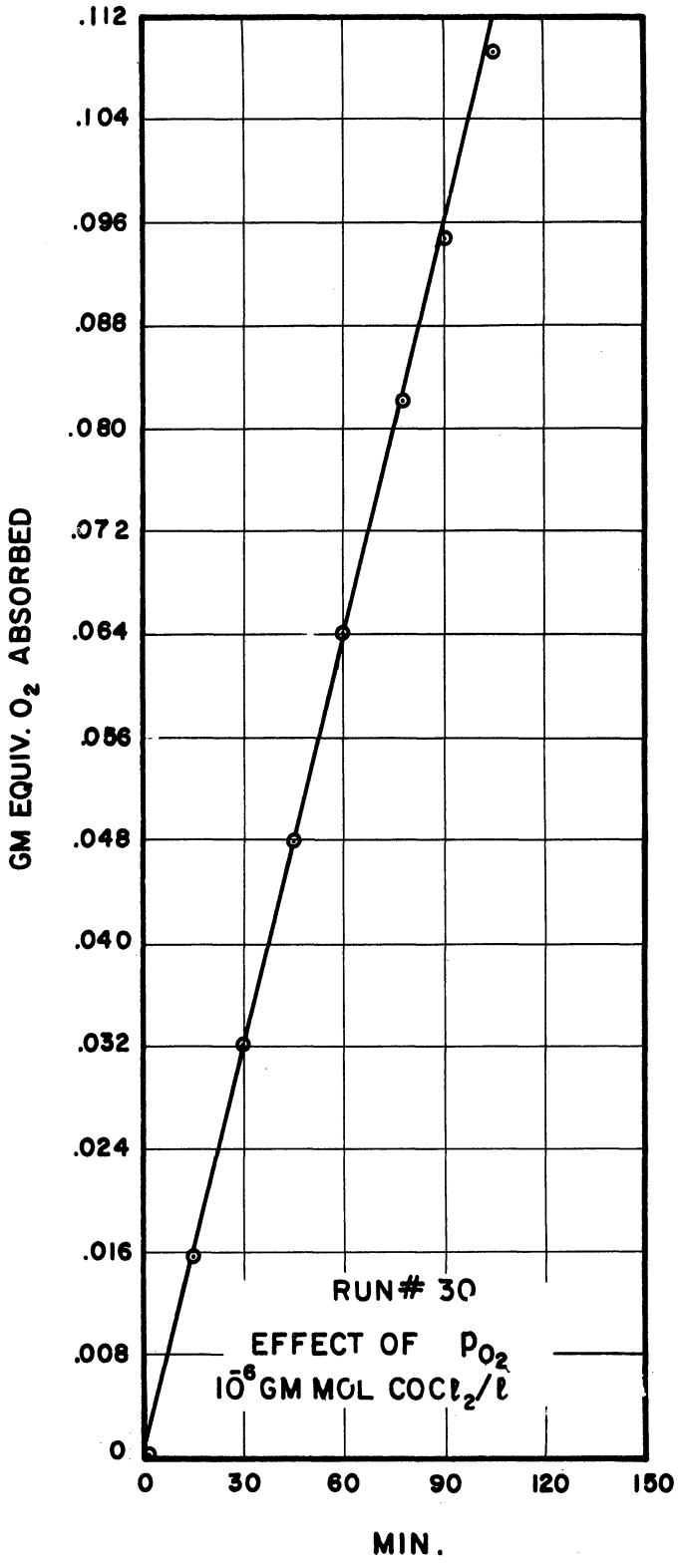
.112
.104
.096
.088
.080
.072
.064
.056
.048
.040
.032
.024
.016
.008
0
GM EQUIV. O_2 ABSORBED
RUN# 30
EFFECT OF P_{O_2}
10^{-6} GM MOL $COCl_2/l$
0
30
60
90
120
150
MIN.

Figure 108.

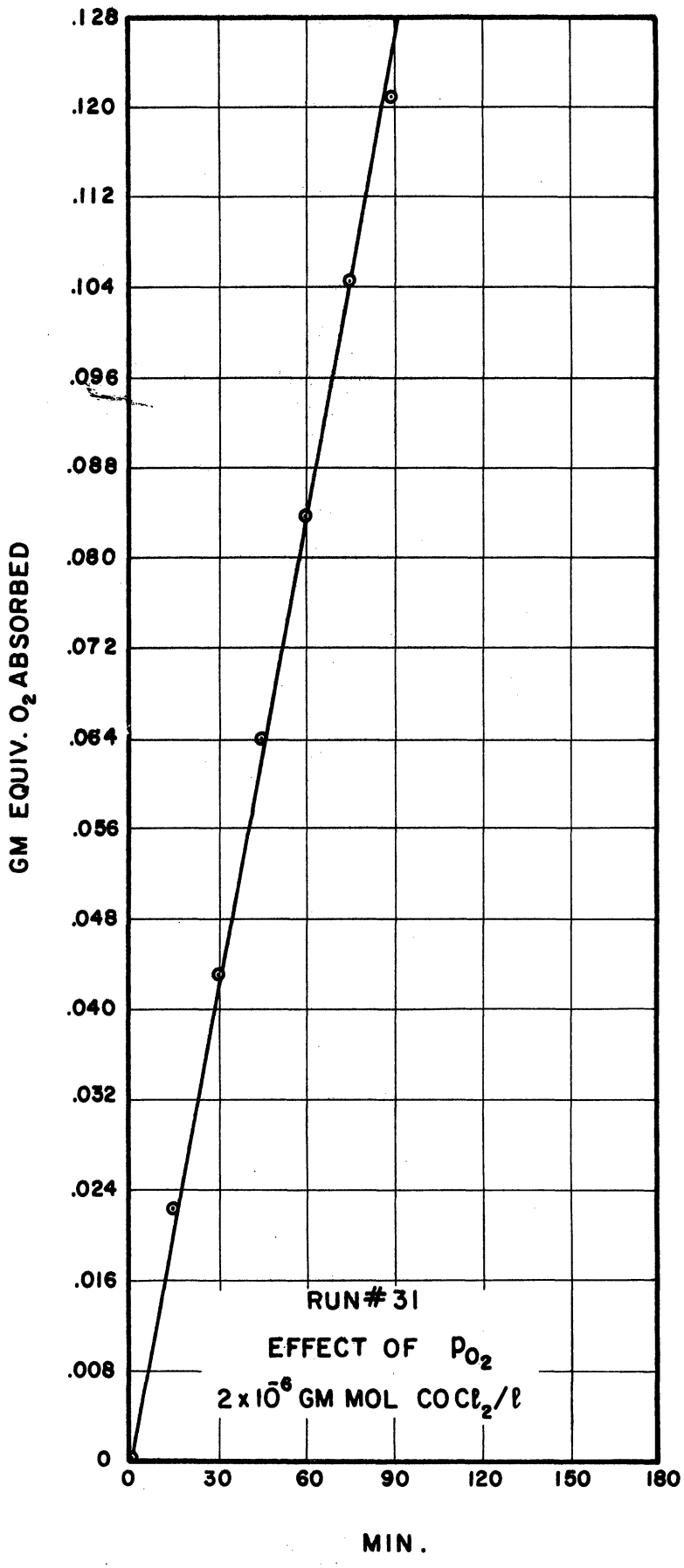
.128
.120
.112
.104
.096
.088
.080
.072
.064
.056
.048
.040
.032
.024
.016
.008
0
GM EQUIV. O_2 ABSORBED
RUN# 31
EFFECT OF P_{O_2}
2×10^{-6} GM MOL $COCl_2/l$
0
30
60
90
120
150
180
MIN.

Figure 109.

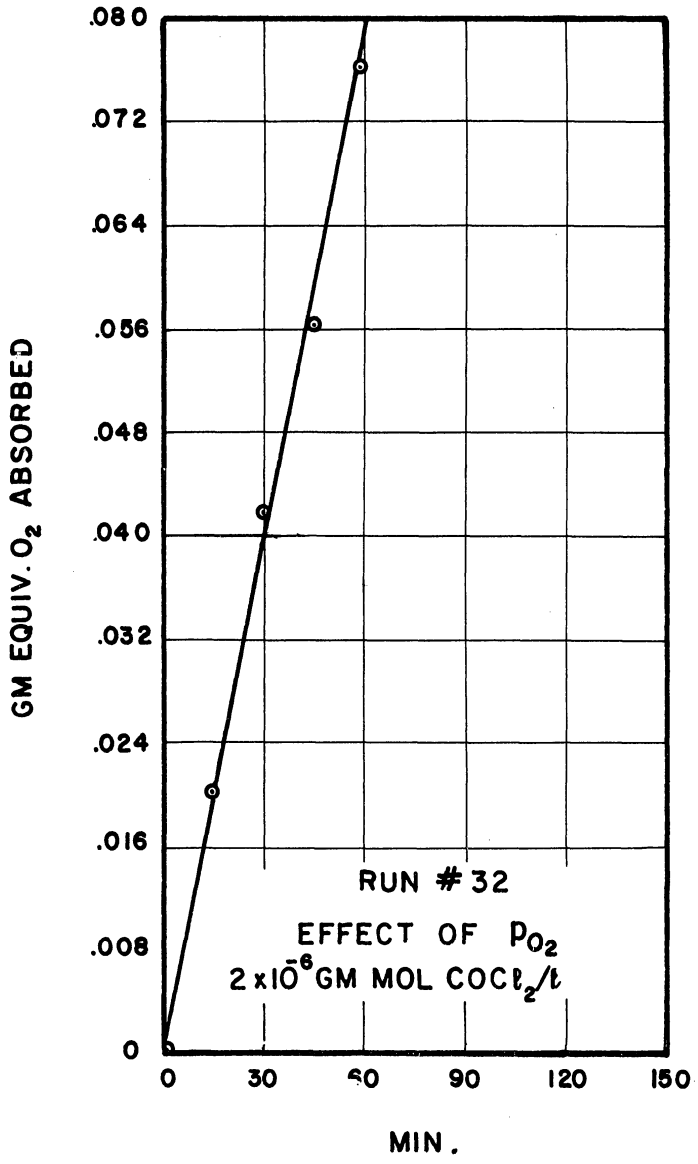
.080
.072
.064
.056
.048
.040
.032
.024
.016
.008
0
GM EQUIV. O_2 ABSORBED
RUN #32
EFFECT OF P_{O_2}
2×10^{-6} GM MOL $COCl_2/l$
0
30
60
90
120
150
MIN.

Figure 110.

APPENDIX VII

DATA AND CALCULATIONS OF k_L

WITH VARIOUS SODIUM SULFITE CONCENTRATIONS

WITH AND WITHOUT CATALYST

TABLE 12

(a) Calculations of k_L and γ with Data from Figures 112-136 and C_{Ai} from Figure 111

k_L^o = 0.118 ft/hr (Appendix III) D_B/D_A = 0.546 (Appendix VIII)

Catalyst Concentration: 2×10^{-6} gm mol $CoCl_2/\ell$

Run #	C_{Bo} gm equiv/ℓ	C_{Ai} gm equiv/ℓ	N_A' $\frac{\text{gm equiv}}{\text{cm}^2 \times \text{min}}$	k_L' ft/hr	$\frac{C_{Bo}}{C_{Ai}}$	$\frac{D_B}{D_A} \cdot \frac{C_{Bo}}{C_{Ai}}$	$\gamma = \frac{k_L}{k_L^o} - 1$
33	0.00270	10.54×10^{-4}	2.76×10^{-7}	0.513	2.56	1.40	3.35
34	0.00470	10.54×10^{-4}	3.04×10^{-7}	0.565	4.45	2.43	3.78
35	0.00656	10.54×10^{-4}	3.32×10^{-7}	0.613	6.21	3.40	4.13
36	0.00714	10.54×10^{-4}	3.40×10^{-7}	0.630	6.75	3.69	4.34
37	0.00764	10.54×10^{-4}	3.72×10^{-7}	0.692	7.22	3.95	4.86
38	0.01160	10.40×10^{-4}	6.40×10^{-7}	1.210	11.15	6.09	9.20
39	0.0172	10.40×10^{-4}	8.0×10^{-7}	1.515	16.50	9.02	11.85
40	0.0182	10.40×10^{-4}	13.32×10^{-7}	2.48	17.20	9.40	20.00
41	0.0196	10.40×10^{-4}	8.88×10^{-7}	1.68	18.85	10.30	13.20
42	0.0238	10.00×10^{-4}	5.2×10^{-7}	1.02	23.80	13.00	11.10
43	0.0344	9.8×10^{-4}	8.08×10^{-7}	1.62	35.20	19.20	12.70
44	0.0426	9.8×10^{-4}	15.2×10^{-7}	3.05	43.5	23.80	24.80
45	0.0490	9.6×10^{-4}	17.28×10^{-7}	3.54	51.0	27.9	29.00
46	0.0616	9.4×10^{-4}	18.60×10^{-7}	3.89	65.6	35.9	32.00
47	0.0716	9.4×10^{-4}	17.0×10^{-7}	3.55	76.2	41.6	29.10
48	0.0926	9.0×10^{-4}	22.1×10^{-7}	4.83	103.0	56.4	39.9
49	0.143	8.8×10^{-4}	30.24×10^{-7}	5.84	162.0	88.6	48.4
50	0.197	8.4×10^{-4}	30.8×10^{-7}	7.22	234.0	128.0	60.2
51	0.348	7.6×10^{-4}	24.0×10^{-7}	6.21	458.0	251.0	51.6
52	0.530	6.8×10^{-4}	19.3×10^{-7}	5.78	780.0	426.0	48.0
53	0.664	6.0×10^{-4}	16.0×10^{-7}	5.04	1106.0	602.0	41.6
54	0.914	5.44×10^{-4}	12.0×10^{-7}	4.32	1675.0	913.0	35.6
55	1.350	5.12×10^{-4}	10.0×10^{-7}	3.84	2640.0	1440.0	31.5
56	1.720	5.00×10^{-4}	1.25×10^{-7}	0.495	3420.0	1870.0	3.18
57	1.782	5.00×10^{-4}	3.08×10^{-7}	1.210	3564.0	1945.0	9.25
58	1.788	5.00×10^{-4}	2.88×10^{-7}	1.130	3576.0	1955.0	8.57

(b) Calculations of k_L and γ for Reaction without Catalyst

(Data from Figures 137-143)

114	0.0685	9.4×10^{-4}	3.44×10^{-7}	0.729			5.16
115	0.0577	9.5×10^{-4}	2.85×10^{-7}	0.594			4.03
116	0.0295	10.0×10^{-4}	2.60×10^{-7}	0.515			3.36
117	0.0162	10.4×10^{-4}	1.55×10^{-7}	0.295			1.50
118	0.1966	8.4×10^{-4}	4.11×10^{-7}	0.97			7.2
119	0.6011	6.4×10^{-4}	1.26×10^{-7}	0.39			2.3
120	0.280	8.0×10^{-4}	2.81×10^{-7}	0.639			4.85

FIGURES 111 THROUGH 143 REPRESENT THE SOLUBILITY OF O_2 IN AQUEOUS Na_2SO_4 [SEIDEL (36)] AND THE RATE DATA FOR VARYING SODIUM SULFITE CONCENTRATIONS

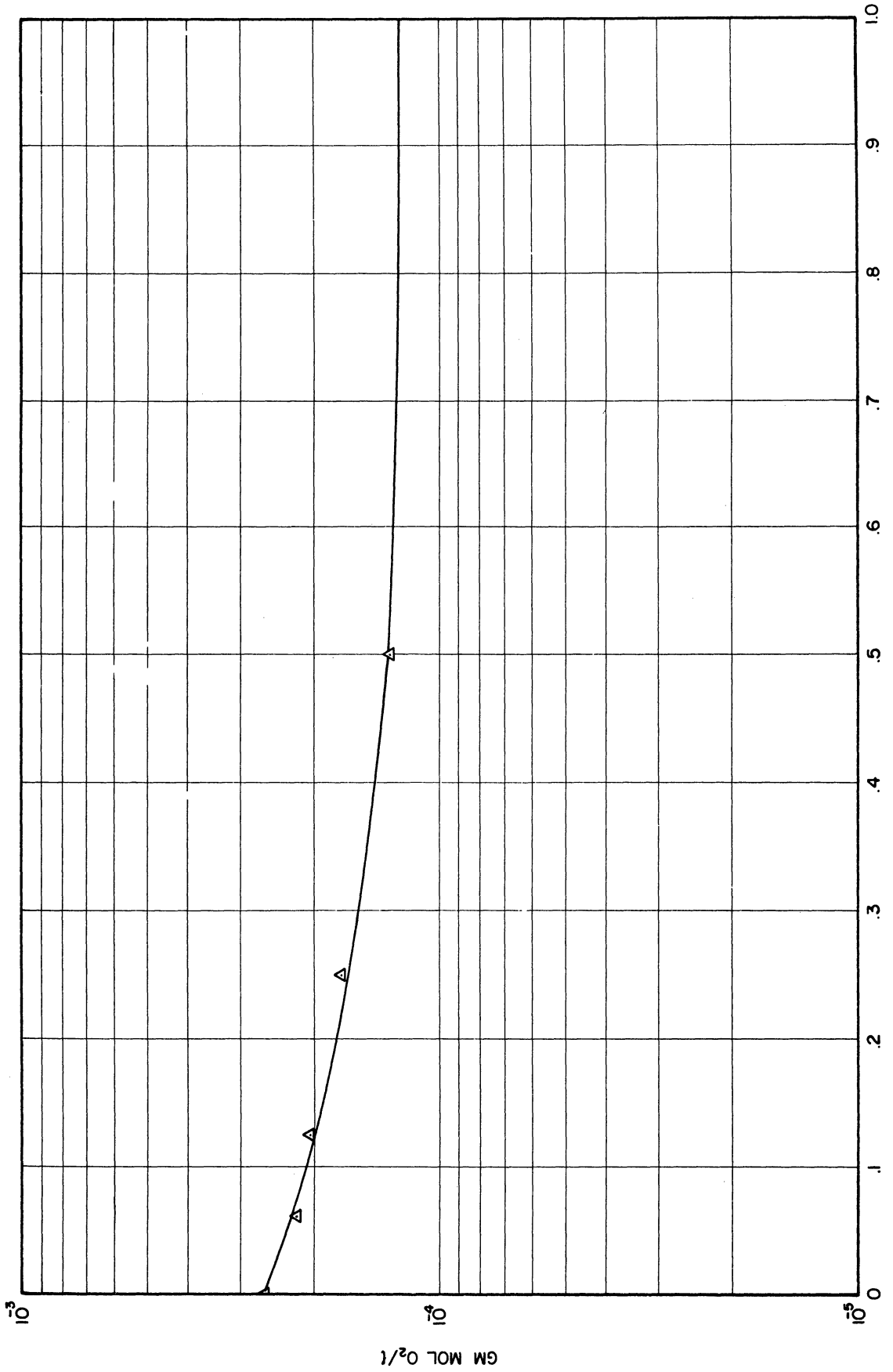

Figure 111. Solubility of O_2 in aqueous Na_2SO_4, Seidel.(37)

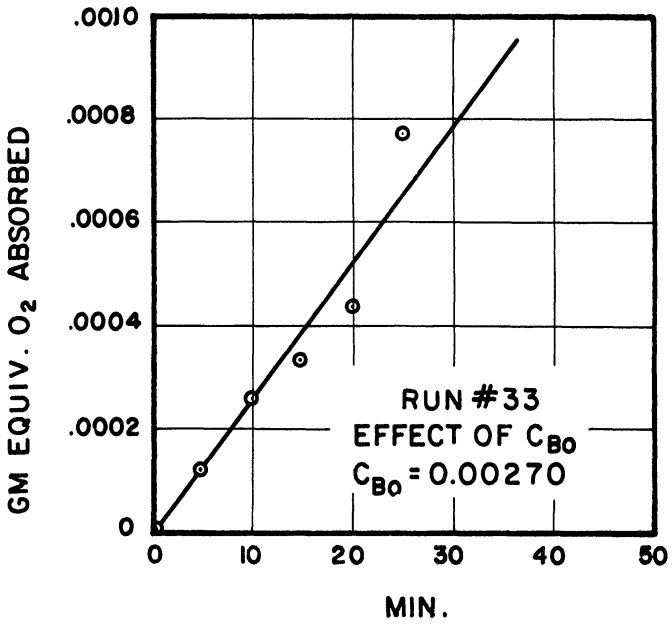

Figure 112.

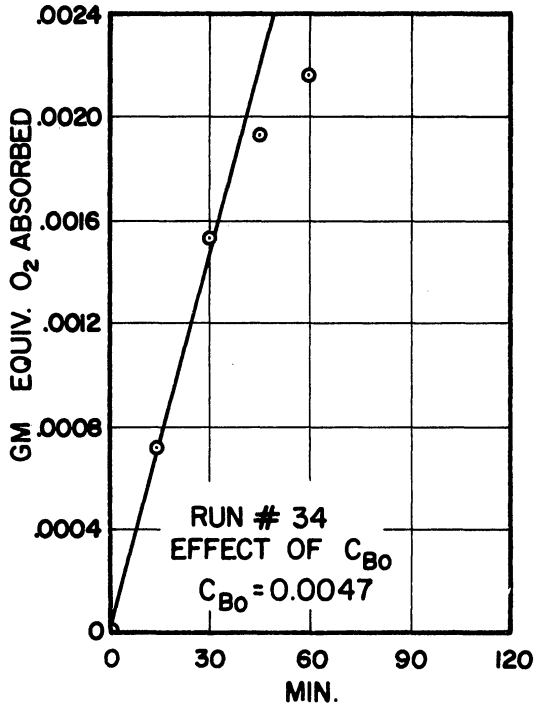

Figure 113.

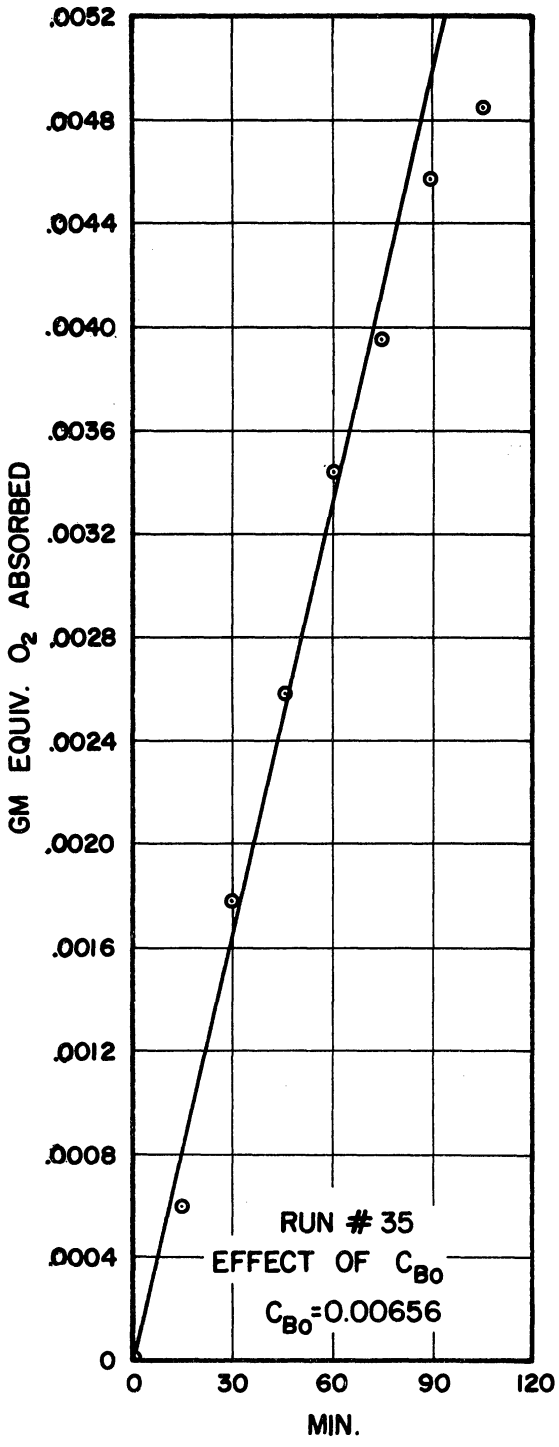

Figure 114.

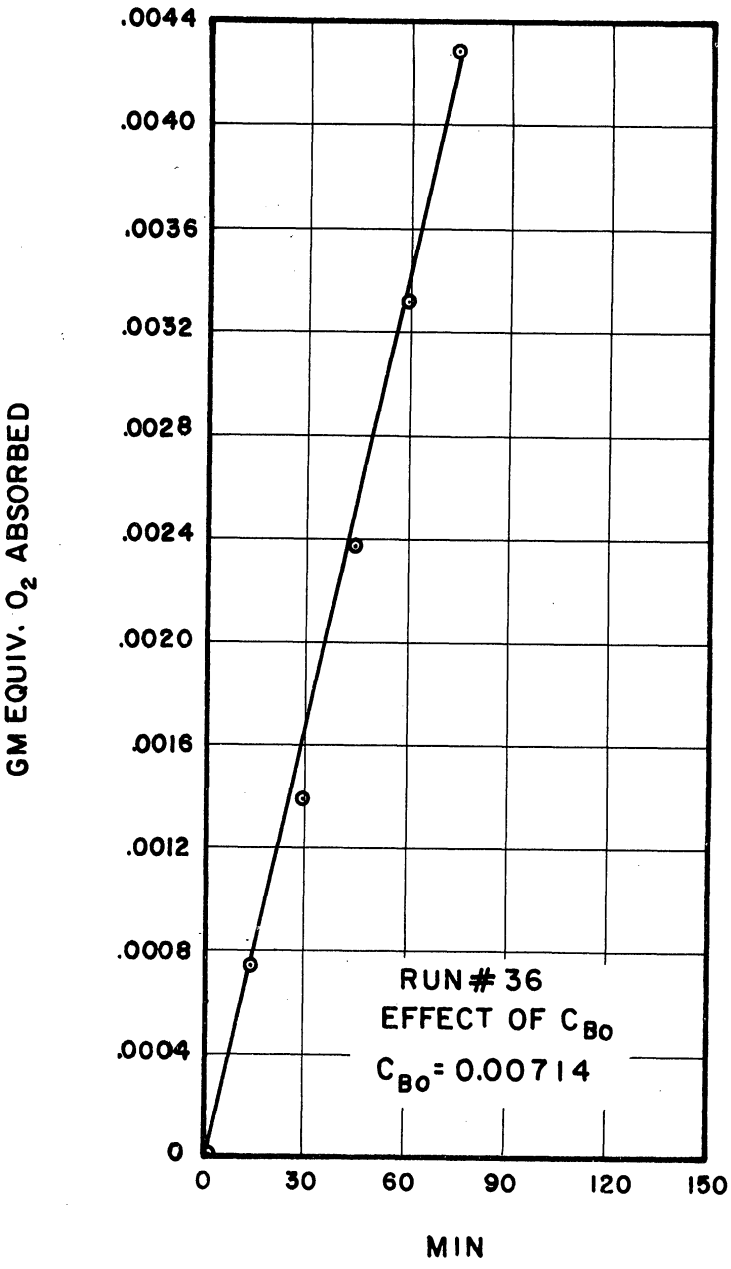

Figure 115.

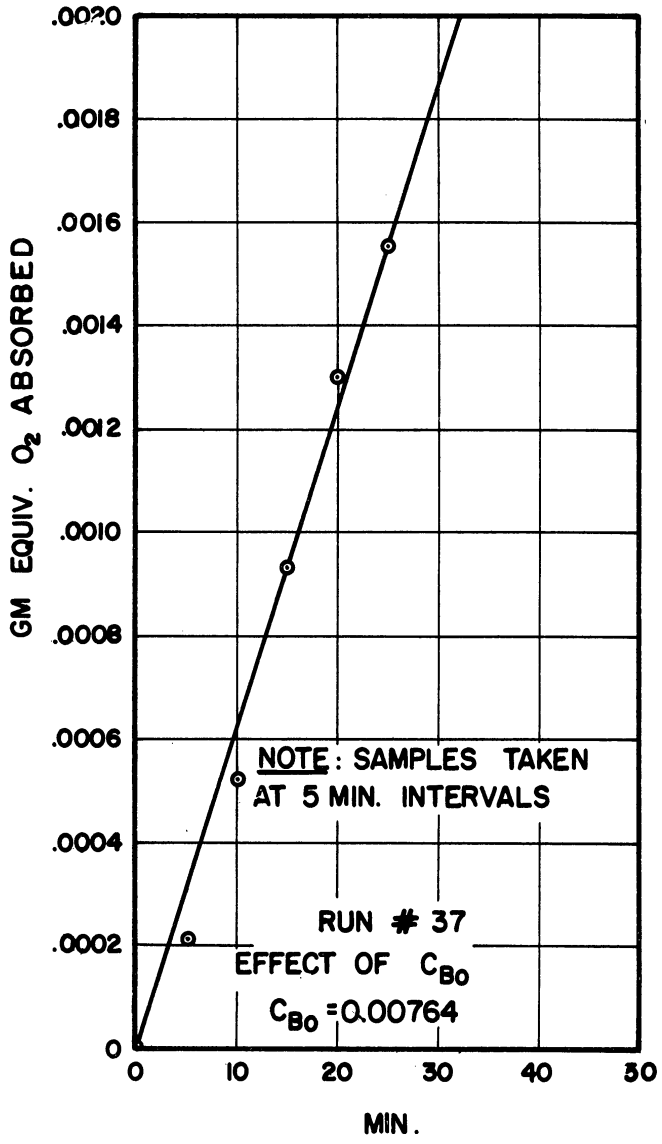

Figure 116.

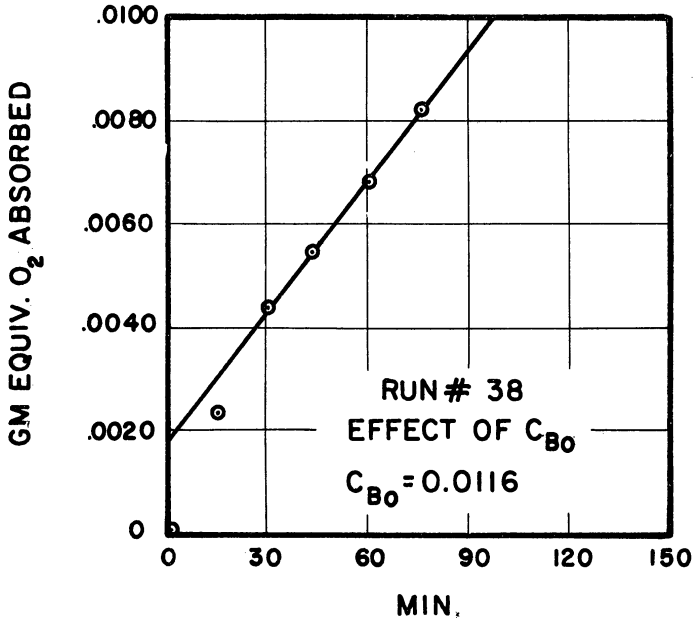

Figure 117.

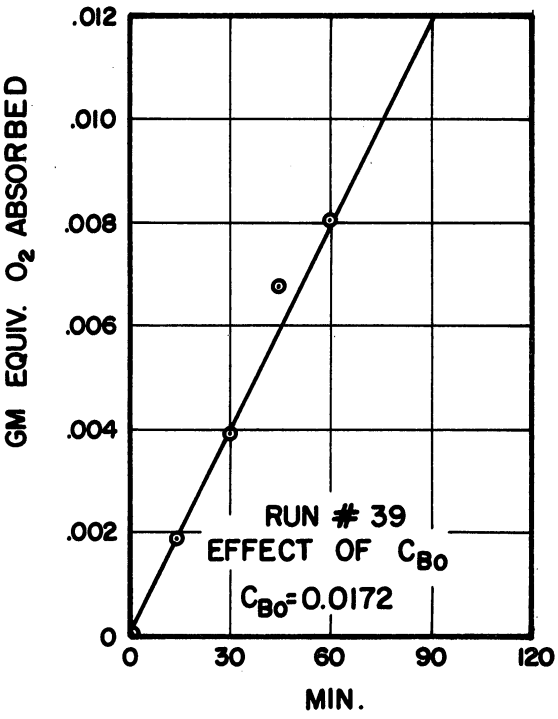

Figure 118.

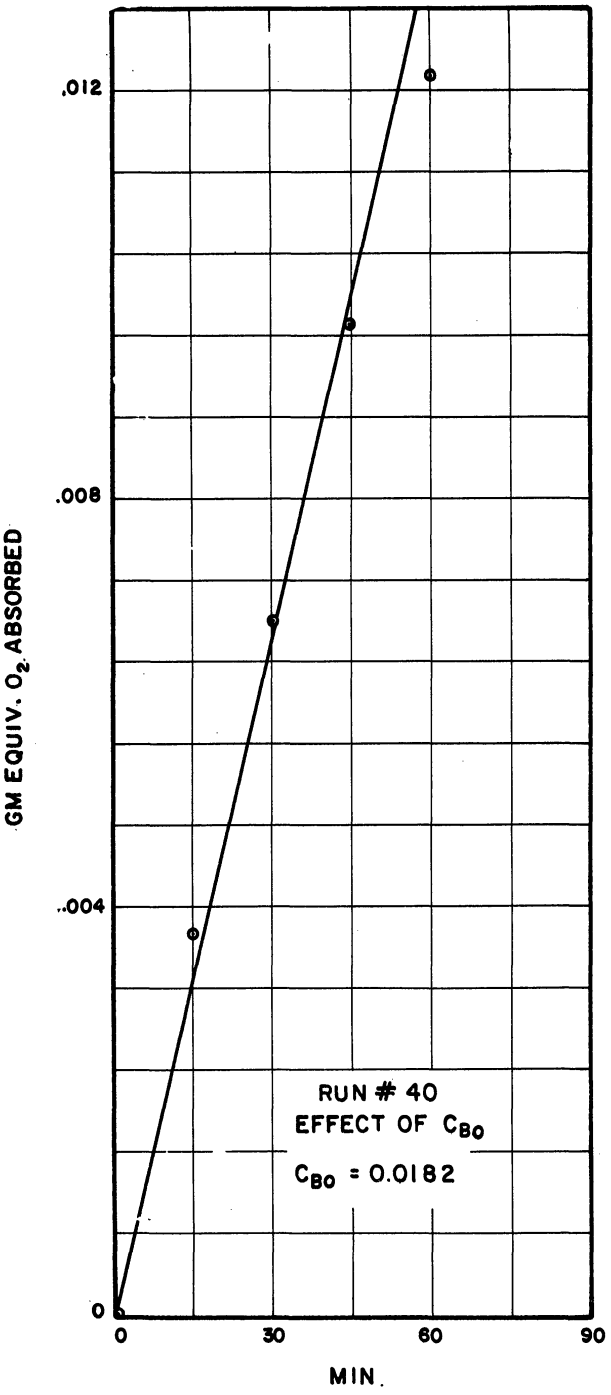

Figure 119.

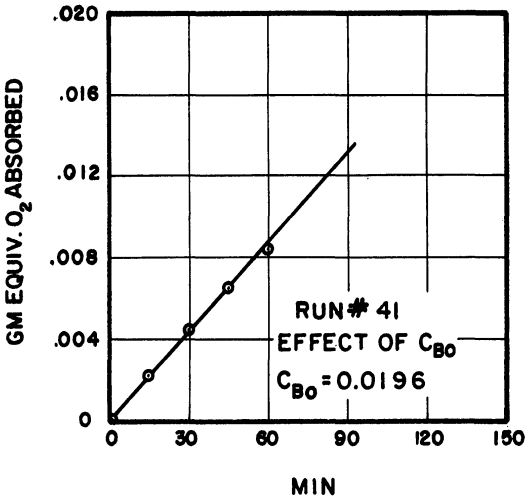

Figure 120.

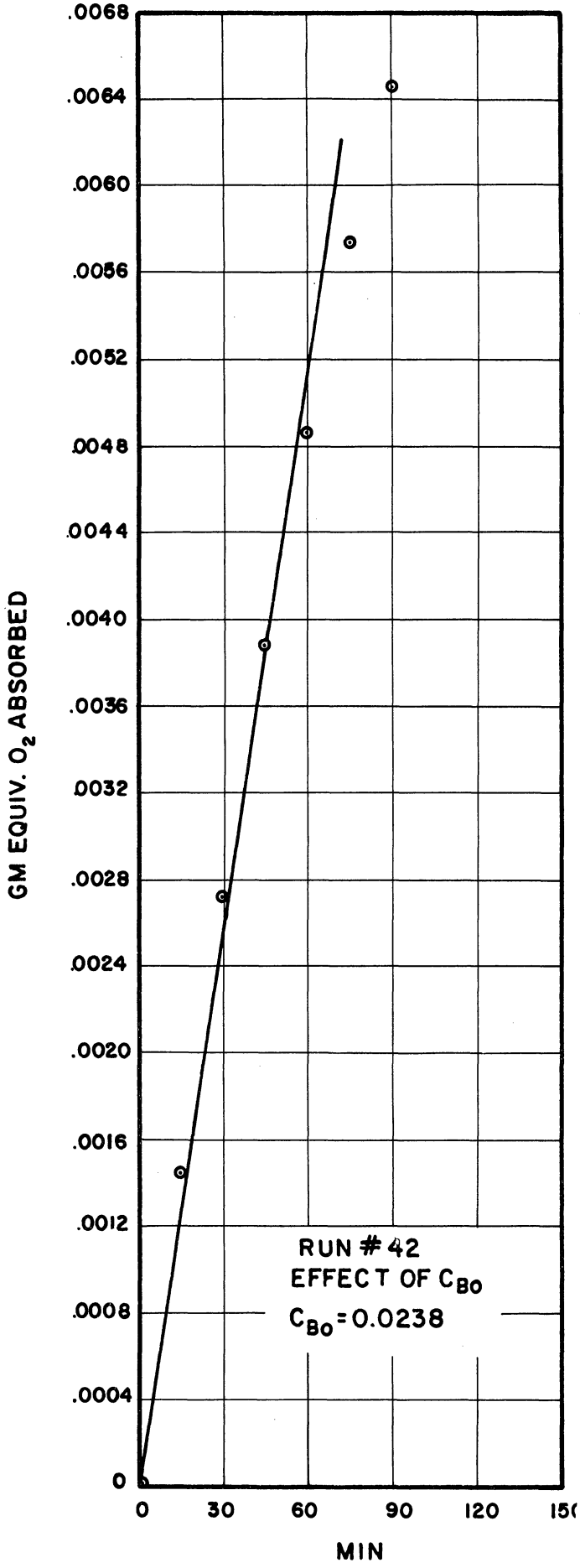

Figure 121.

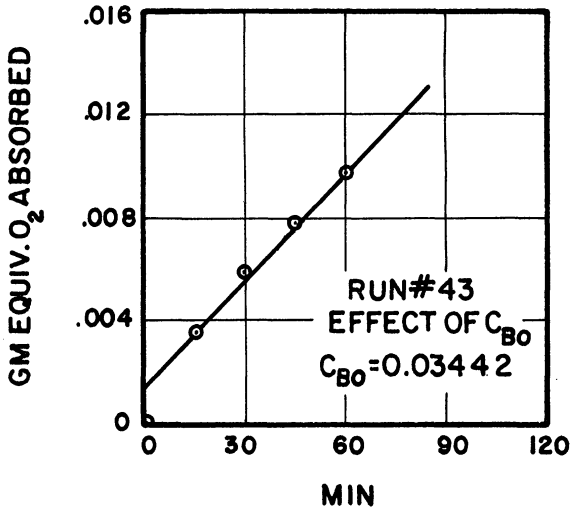

Figure 122.

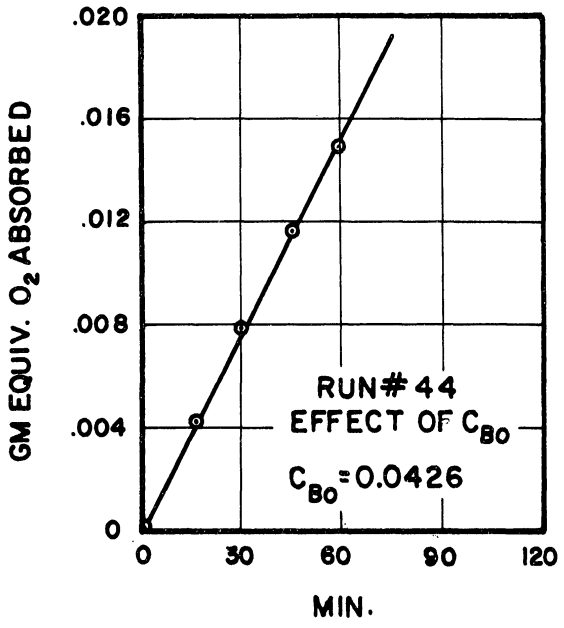

Figure 123.

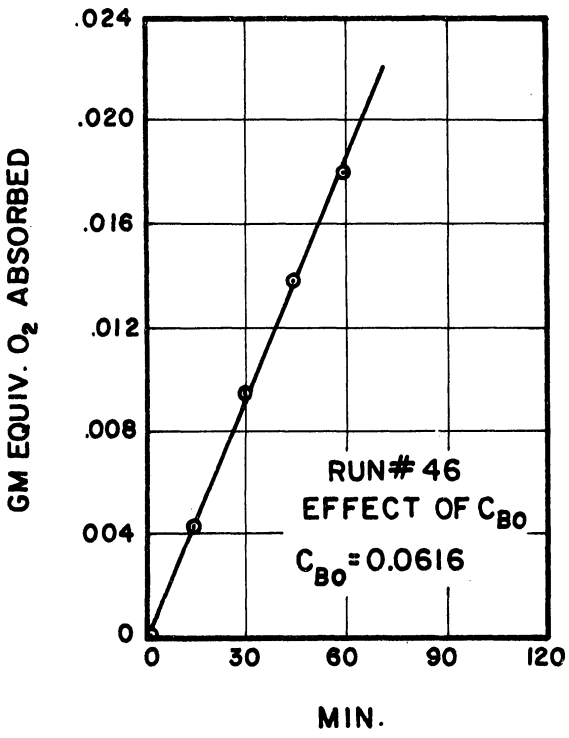

Figure 125.

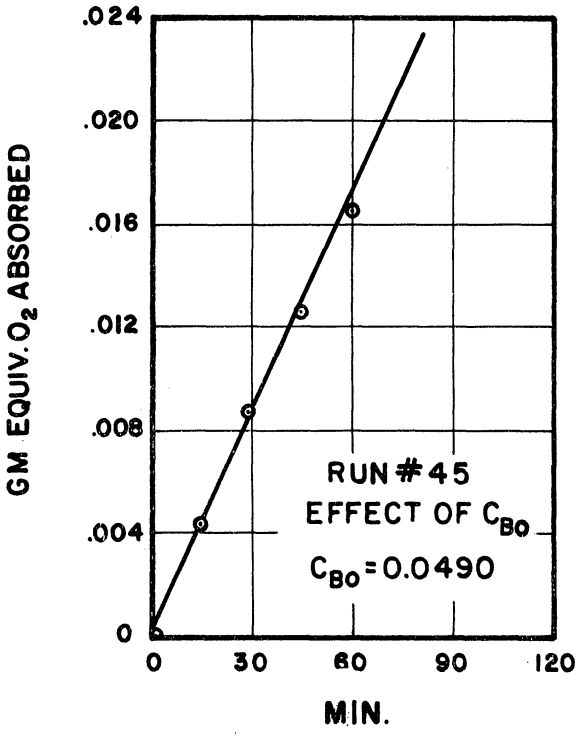

Figure 124.

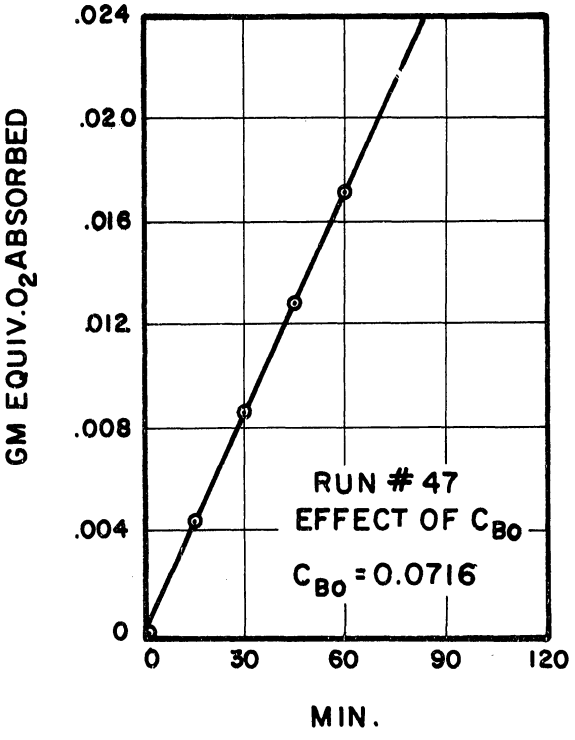

Figure 126.

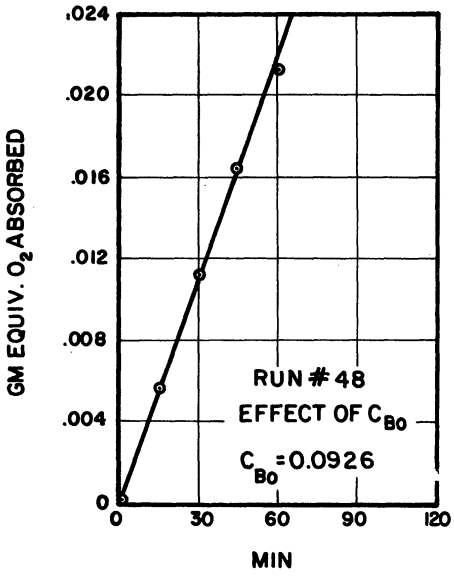

Figure 127.

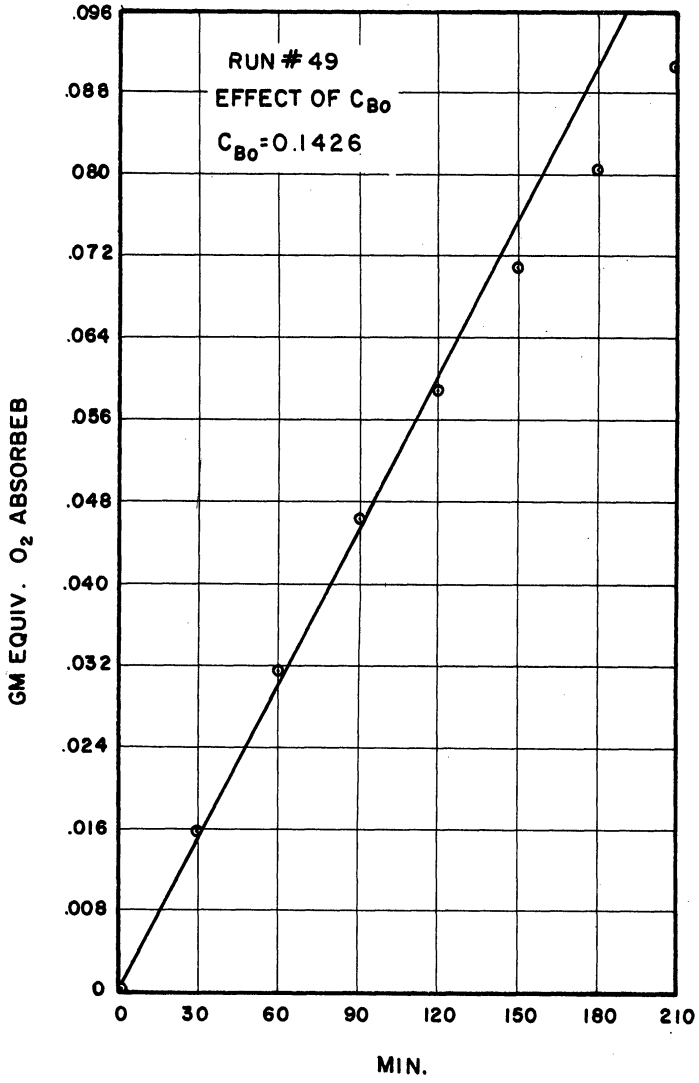

Figure 128

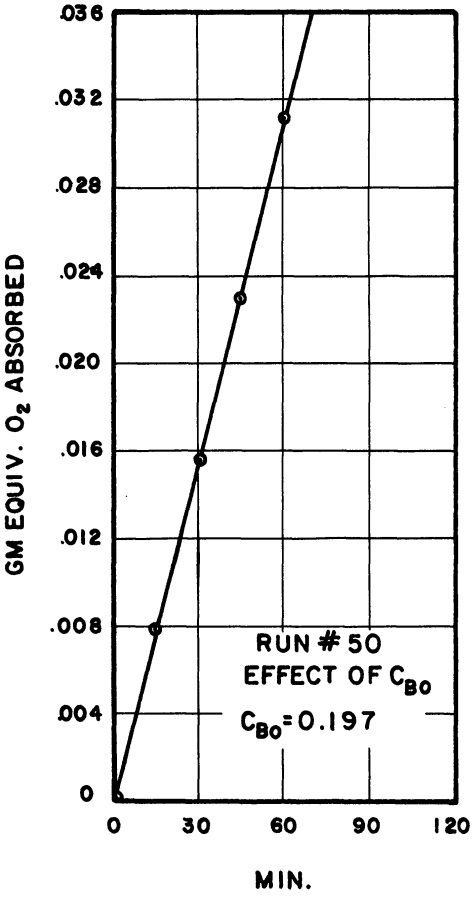

Figure 129.

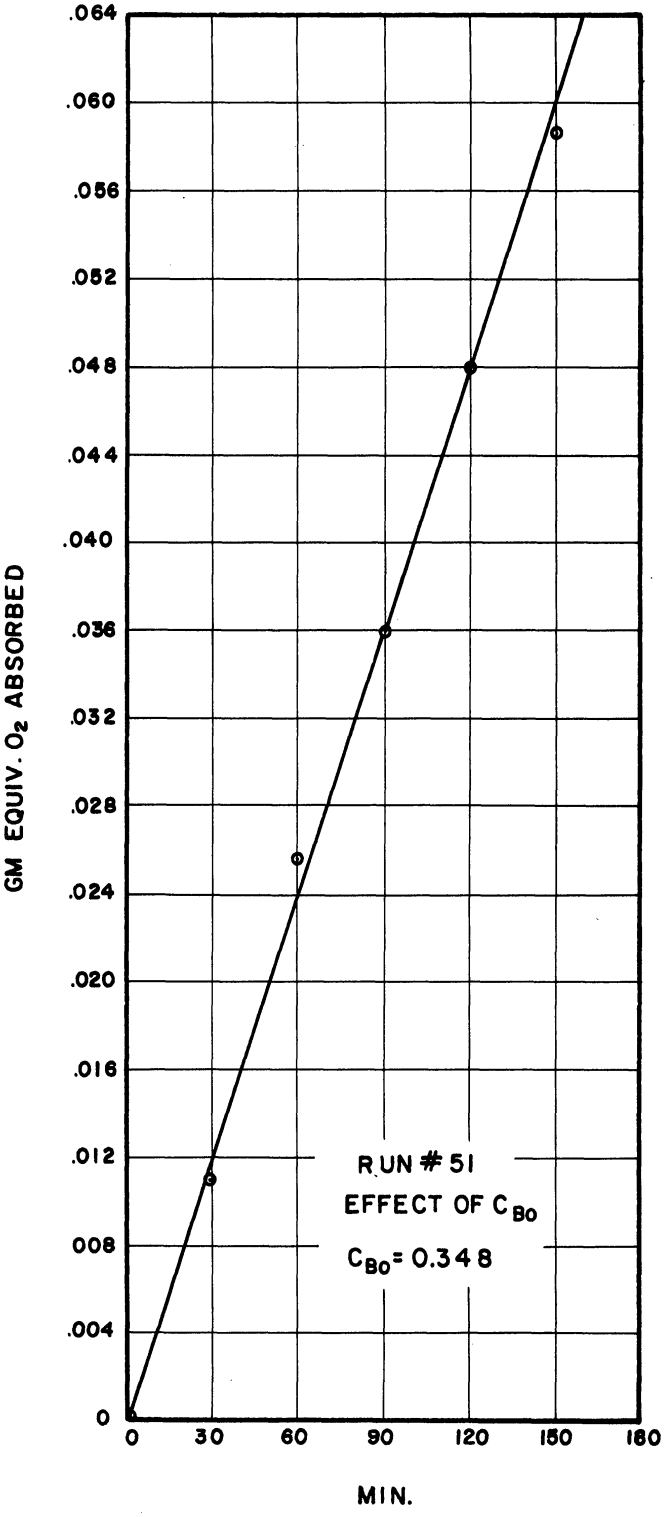

Figure 130.

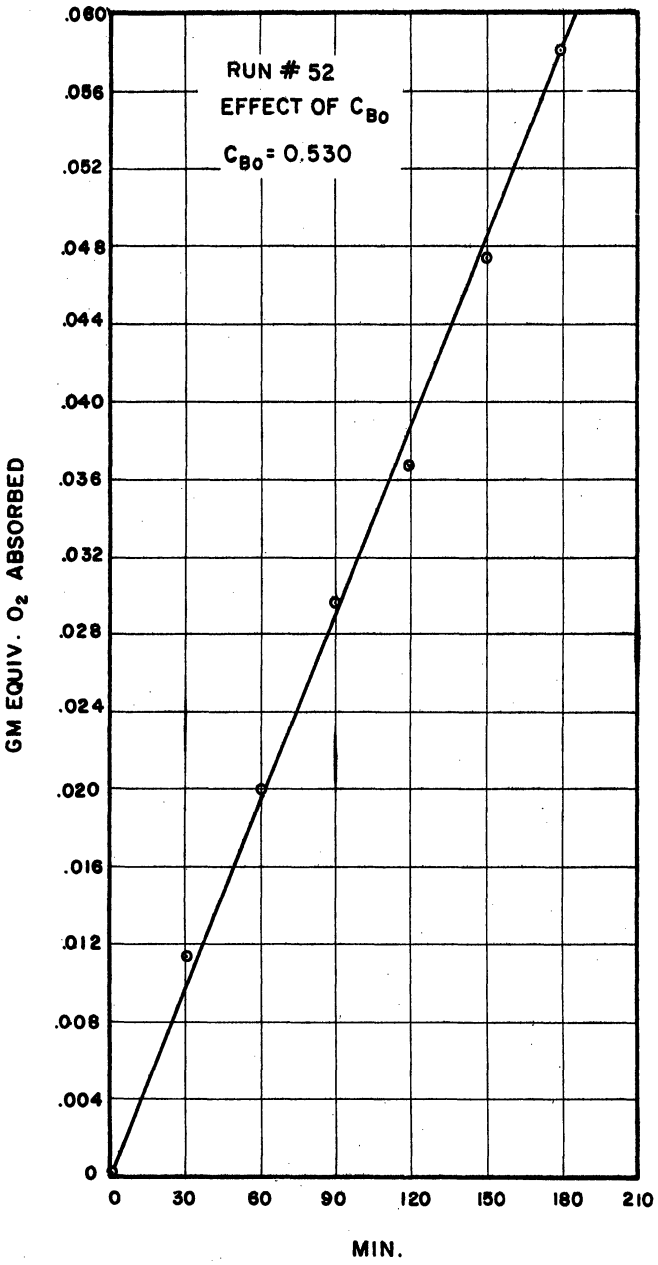

Figure 131.

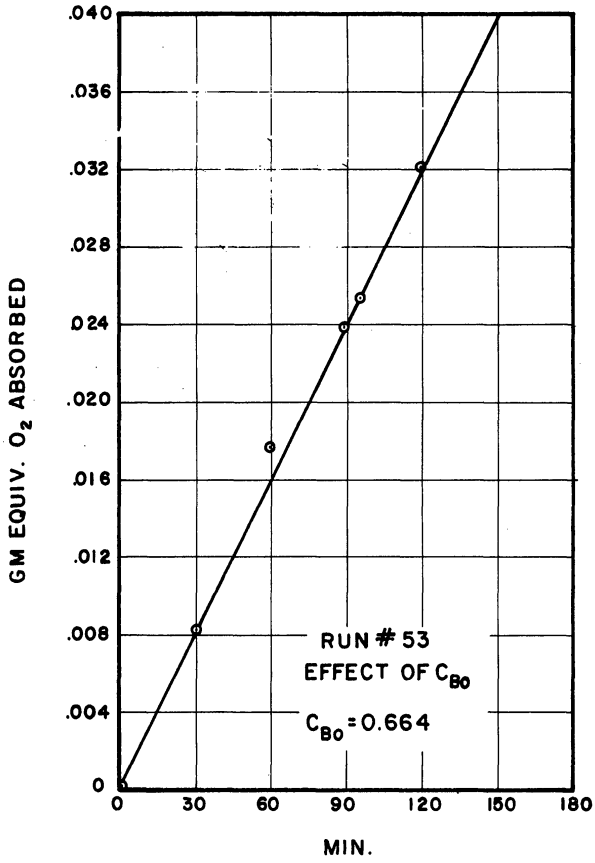

Figure 132.

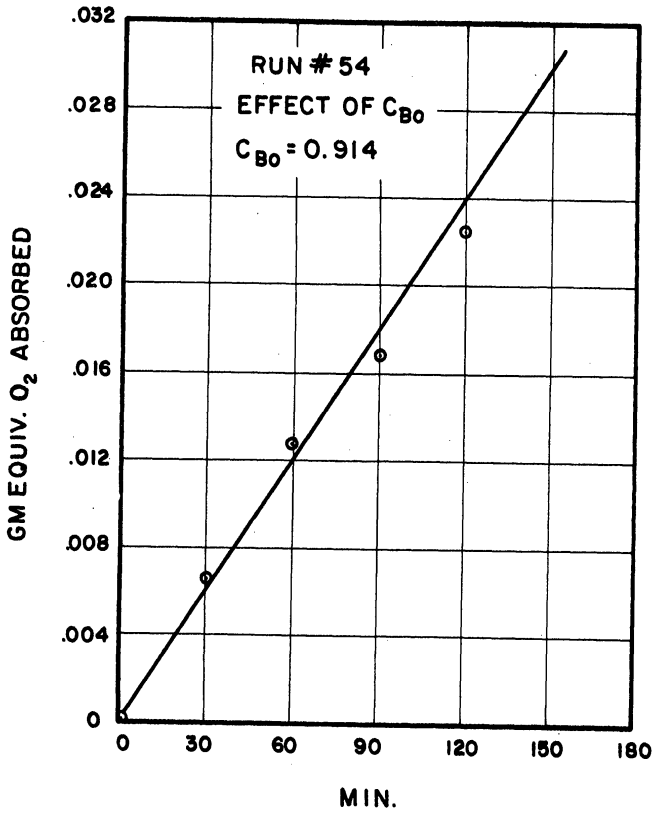

Figure 133.

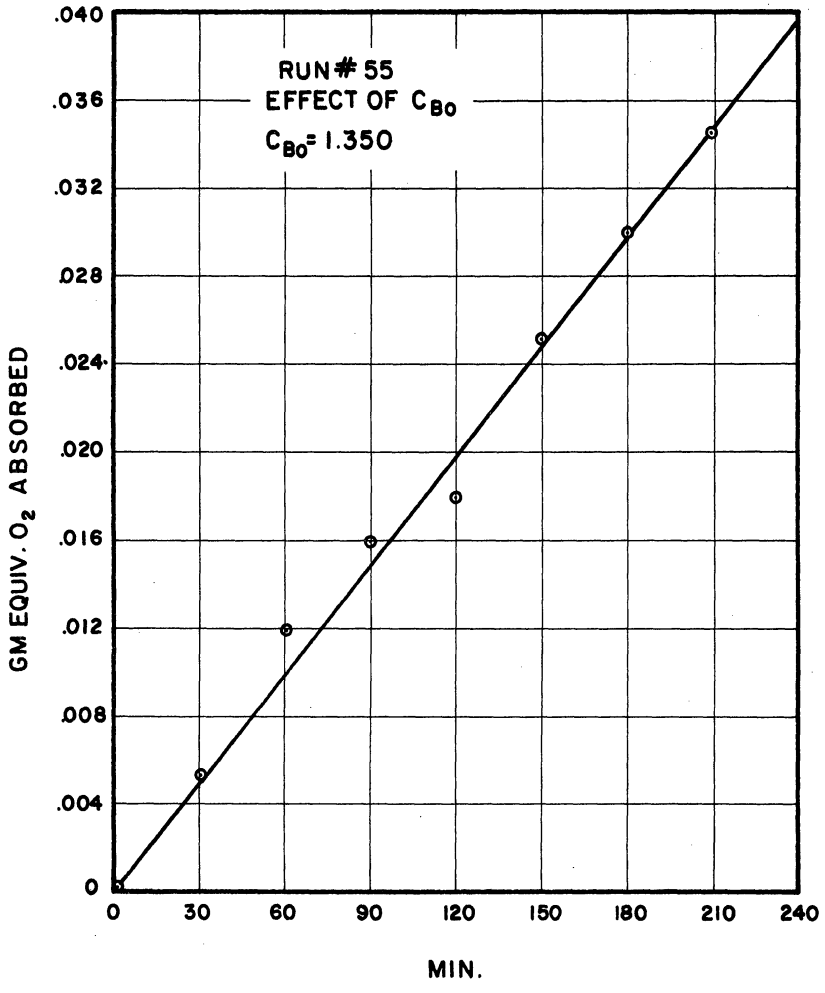

Figure 134.

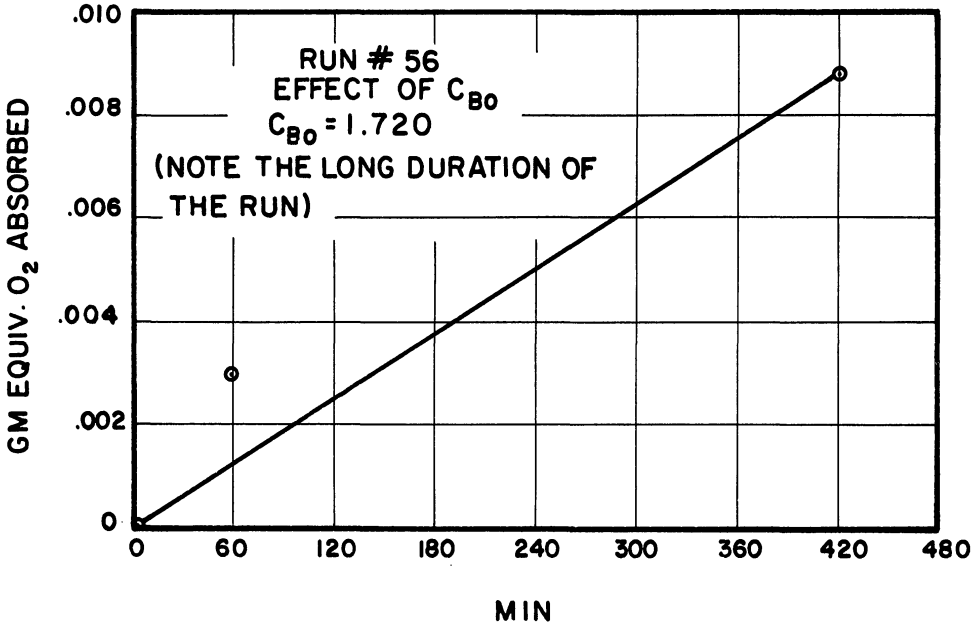
RUN # 56
EFFECT OF C_{Bo}
C_{Bo} = 1.720
(NOTE THE LONG DURATION OF THE RUN)
GM EQUIV. O_2 ABSORBED
.010
.008
.006
.004
.002
0
0
60
120
180
240
300
360
420
480
MIN

Figure 135.

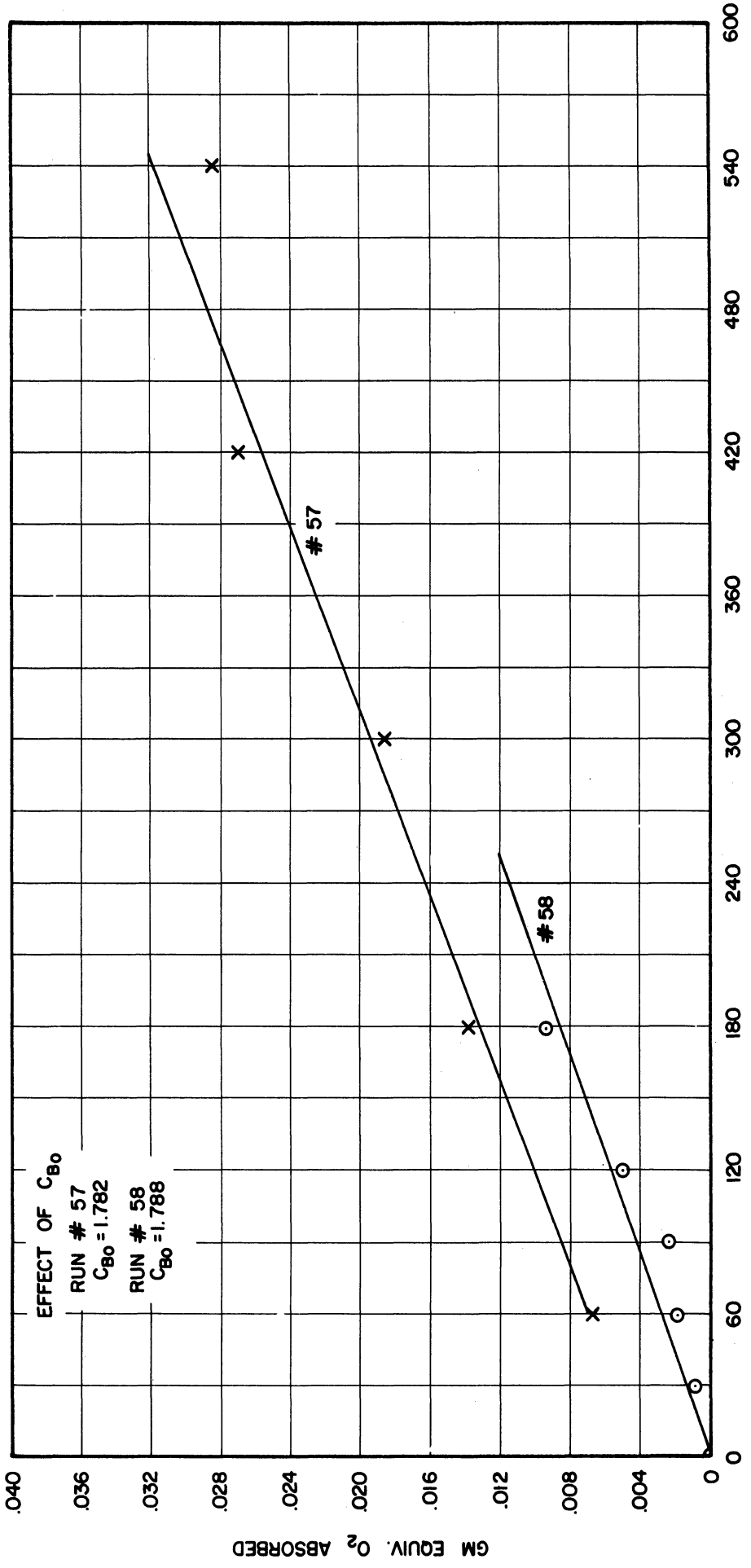
EFFECT OF C_{Bo}
RUN # 57
C_{Bo} = 1.782
RUN # 58
C_{Bo} = 1.788
#57
#58
GM EQUIV. O_2 ABSORBED
MIN.
0
.004
.008
.012
.016
.020
.024
.028
.032
.036
.040
60
120
180
240
300
360
420
480
540
600

Figure 136.

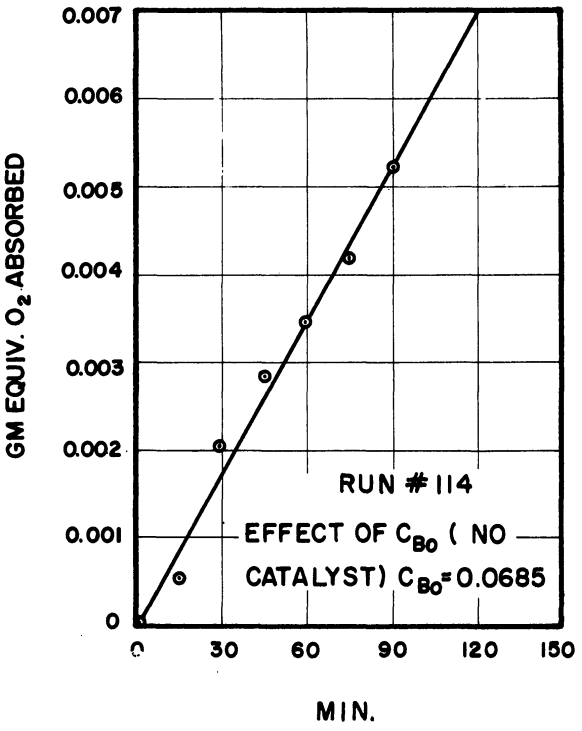

Figure 137.

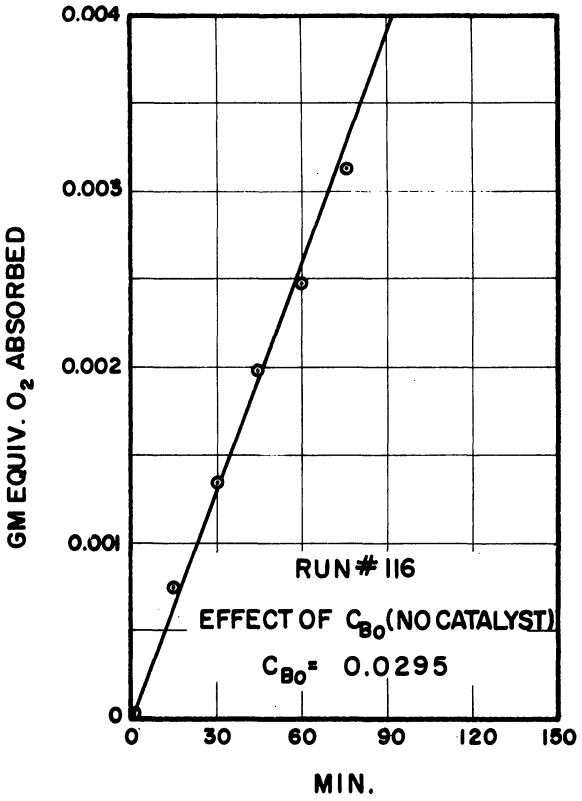

Figure 139.

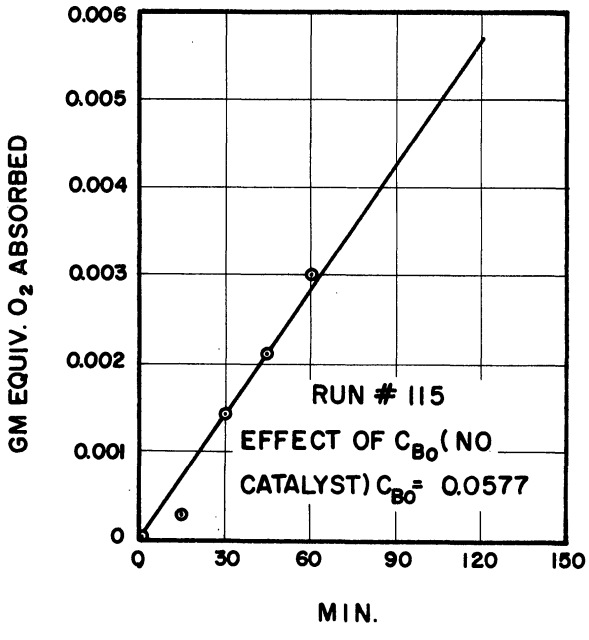

Figure 138.

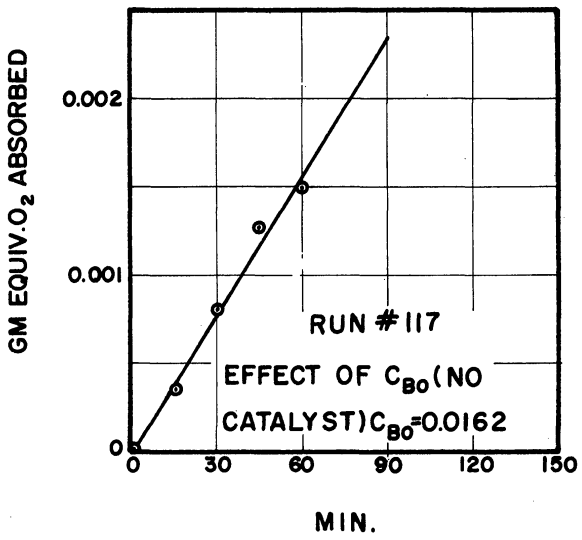

Figure 140.

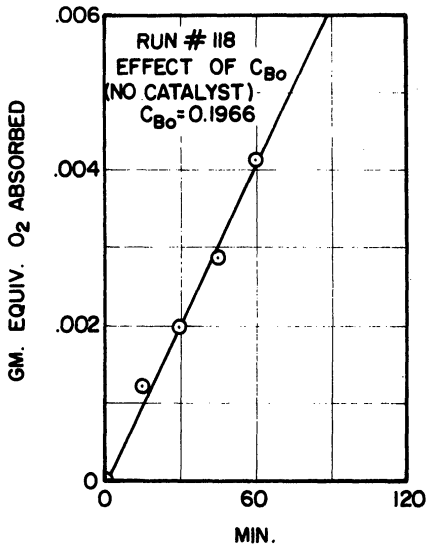

Figure 141.

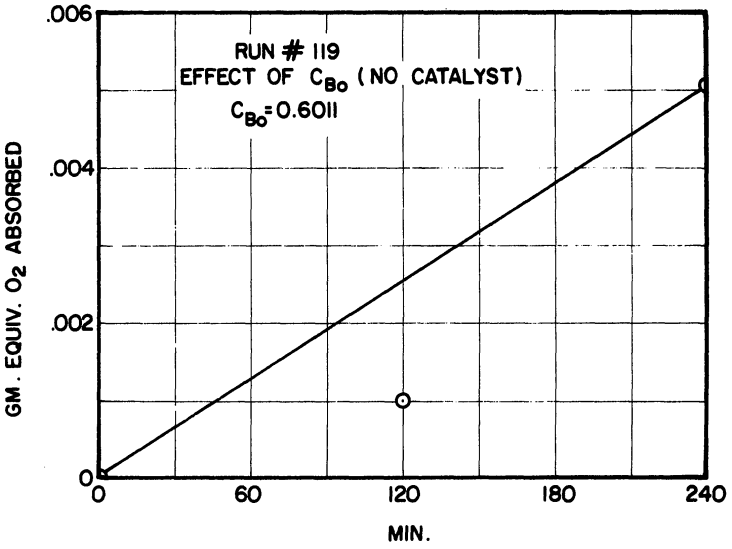

Figure 142.

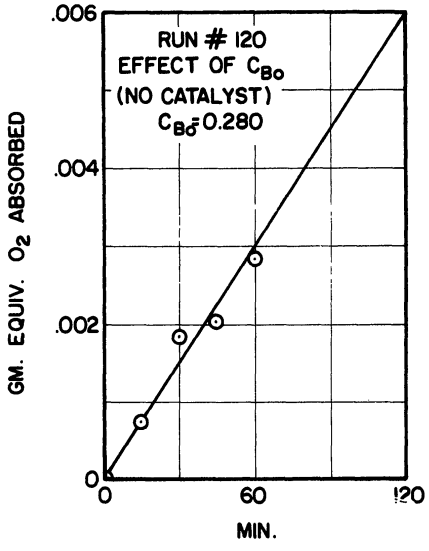

Figure 143.

APPENDIX VIII

CALCULATIONS OF γ FROM VARIOUS MODELS

$D_A = 1.56 \times 10^{-3}$ cm^2/min, Sherwood and Reid

$C_{Ai} = 10.54 \times 10^4$ gm equiv O_2/ℓ .

TABLE 13

Calculation of the Diffusivity of Na_2SO_3 at 25°C

$$D_B = \frac{(1/n_+ + 1/n_-)\ RT}{(1/\lambda_+ + 1/\lambda_-)\ F^2} \qquad (17)$$

Using the conductivity convention

$\lambda_{Na^+} = 50$ Table 3

$\lambda_{\frac{1}{2}SO_3^=} = 57.4$ Table 3

$n_+ = n_- = 1$

$$D_B = \frac{2 \times 8.318 \times 298}{(1/50.1 + 1/57.4)\,(96{,}500)^2}$$

$= 1.422 \times 10^{-5}$ cm^2/sec

$= 8.532 \times 10^{-4}$ cm^2/min

TABLE 14

Calculation of γ for Hatta, Kishinevskii, Danckwerts and Higbie Models According to Table 1

Run #	Amount of catalyst gm mols $CoCl_2/\ell$	C_{Bo} gm equiv/ℓ	$\gamma_{Kishinevskii}$	γ_{Hatta}	$\left[\frac{D_B}{D_A}\right]^{\frac{1}{2}} \cdot \frac{C_{Bo}}{C_{Ai}}$	γ_{Higbie} and $\gamma_{Danckwerts}$
90	1×10^{-6}	0.10598	100.55	54.89	74.40	73.40
		0.09930	94.21	51.44	69.72	68.72
		0.09232	87.59	47.83	64.82	63.82
		0.08598	81.58	44.54	60.36	59.36
		0.07989	75.80	41.39	56.10	55.10
		0.07351	69.74	38.08	51.60	50.60
91	1×10^{-6}	0.08078	76.64	41.85	56.72	55.72
		0.07346	69.69	38.05	51.57	50.57
		0.06787	64.40	35.16	47.65	46.65
		0.06143	56.27	31.82	43.12	42.12
		0.05504	52.22	28.51	38.64	37.64
		0.05009	47.53	25.95	35.17	34.17
89	7×10^{-7}	0.06975	66.18	36.14	48.97	47.97
		0.06371	60.46	33.01	44.74	43.74
		0.05801	55.00	30.03	40.70	39.70
		0.05297	50.25	27.44	37.18	36.18
		0.04802	45.59	24.89	33.73	32.73
		0.04272	40.80	22.28	30.20	29.20
88	5×10^{-7}	0.11964	113.50	61.97	83.99	82.99
		0.11444	108.57	59.28	80.35	79.35
		0.10885	103.28	56.39	76.43	75.43
		0.10370	98.35	53.69	72.77	71.77
		0.09826	93.22	50.89	68.98	67.98
		0.09331	88.51	48.33	65.50	64.50
92	2×10^{-6}	0.05173	48.50	26.46	35.89	34.89
		0.04435	43.56	23.79	32.24	31.24
		0.03703	35.12	19.18	25.99	24.99
		0.03079	29.20	16.00	21.60	20.60
		0.02500	23.72	12.95	17.55	16.55
		0.01980	18.79	10.25	13.90	12.90

TABLE 15

Calculations of $\gamma = (k_L/k_L^o - 1)$ for Sherwood and Wei Model

using Equations 63 and 57, Appendix I, ii.

$D_A = 1.56 \times 10^{-3} \frac{cm^2}{min}$; $C_{Ai} = 10.54 \times 10^{-4} \frac{gm\ equiv\ O_2}{\ell}$

Run #	q $\frac{gm\ equiv\ SO_3^=}{\ell}$	n $\frac{gm\ equiv\ Na^+}{\ell}$	n^2	nq	0.281 nq	m = $(n^2 - 0.281\ nq)^{1/2}$	n + m	6000 x n	9600 x m	7800(n + m)	1356 q	6000n + 9600m	7800(n + m) - 1356 q	$\frac{6000n + 9600m}{7800(n + m) - 1356\ q}$	$\frac{9.16 \times 10^{-4}}{D_A \times C_{Ai}} \times q$	$k_L/k_L^o - 1$
90	0.10598	0.10492	0.01101	0.01112	0.00312	0.08882	0.19374	629.5	852.7	1511.2	143.0	1482	1368	1.082	58.1	62.7
	0.09930	0.10387	0.01079	0.01031	0.00290	0.08301	0.18688	623.2	796.9	1457.7	134.5	1419	1323	1.070	55.4	58.4
	0.09232	0.10284	0.01058	0.00949	0.00266	0.08898	0.19182	617.0	854.2	1496.2	125.2	1471	1371	1.070	51.5	55.2
	0.08598	0.10181	0.01036	0.00875	0.00246	0.08888	0.19069	610.5	853.3	1487.4	116.5	1463	1371	1.065	48.0	51.2
	0.07989	0.10079	0.01015	0.00805	0.00226	0.08882	0.18961	604.8	852.7	1478.9	108.5	1457	1370	1.070	44.6	47.8
	0.07351	0.09978	0.00995	0.00734	0.00206	0.08884	0.18862	598.7	852.9	1471.2	100.0	1450	1371	1.054	41.0	43.3
91	0.08078	0.07998	0.00639	0.00646	0.00182	0.06759	0.14757	479.8	648.8	1151.0	109.5	1129	1042	1.082	45.1	48.6
	0.07346	0.07917	0.00627	0.00581	0.00164	0.06805	0.14723	475.0	653.3	1148.4	99.5	1128	1049	1.074	41.0	44.0
	0.06787	0.07839	0.00614	0.00532	0.00149	0.06819	0.14658	470.0	654.6	1143.3	92.0	1124	1051	1.070	37.9	39.8
	0.06143	0.07760	0.00602	0.00477	0.00134	0.06841	0.14601	465.6	656.7	1138.9	83.3	1121	1055	1.062	34.3	36.4
	0.05504	0.07682	0.00590	0.00423	0.00119	0.06863	0.14545	460.9	658.8	1134.5	74.6	1118	1060	1.052	30.7	32.4
	0.05009	0.07606	0.00588	0.00361	0.00107	0.06934	0.14540	456.4	665.7	1134.1	69.0	1121	1065	1.051	29.9	31.5
89	0.06975	0.06906	0.00477	0.00481	0.00135	0.05848	0.12754	414.4	561.4	994.8	94.5	975	900	1.080	38.9	42.0
	0.06371	0.06836	0.00467	0.00436	0.00122	0.05872	0.12708	410.2	563.7	991.2	85.5	973	906	1.075	35.6	38.2
	0.05801	0.06766	0.00458	0.00392	0.00110	0.05900	0.12666	406.1	566.4	987.9	78.7	972	909	1.072	32.4	34.8
	0.05297	0.06700	0.00449	0.00354	0.00099	0.05916	0.12616	402.0	567.9	984.0	72.0	969	912	1.050	29.5	31.0
	0.04802	0.06634	0.00440	0.00318	0.00089	0.05923	0.12557	398.0	568.6	979.4	65.2	966	914	1.060	26.8	28.4
	0.04272	0.06567	0.00431	0.00280	0.00078	0.05943	0.12510	394.0	570.5	975.8	58.0	964	917	1.050	23.8	25.0
88	0.11964	0.11844	0.01403	0.01417	0.00398	0.10006	0.21850	710.6	960.6	1705.0	162.2	1671	1543	1.080	66.7	72.0
	0.11444	0.11726	0.01375	0.01342	0.00377	0.09988	0.21714	703.6	958.8	1700.0	155.2	1661	1545	1.072	64.0	68.6
	0.10885	0.11609	0.01348	0.01263	0.00355	0.09965	0.21574	696.6	956.6	1682.0	147.5	1652	1535	1.072	60.8	65.2
	0.10370	0.11493	0.01321	0.01192	0.00335	0.09922	0.21415	689.6	952.5	1672.0	141.0	1641	1531	1.072	58.0	62.2
	0.09826	0.11378	0.01295	0.01118	0.00314	0.09904	0.21282	682.7	950.8	1660.0	133.2	1632	1527	1.070	54.8	58.6
	0.09331	0.11264	0.01269	0.01051	0.00295	0.09872	0.21136	675.8	947.7	1620.0	126.5	1623	1524	1.065	52.0	55.4
92	0.05173	0.05173	0.00267	0.00267	0.00075	0.04383	0.09556	310.3	420.8	746.0	70.1	731	676	1.035	28.8	29.8
	0.04435	0.05122	0.00262	0.00227	0.00063	0.04462	0.09584	307.3	428.3	748.0	60.1	735	688	1.028	24.8	25.5
	0.03703	0.05070	0.00257	0.00188	0.00053	0.04516	0.09586	304.2	433.5	750.0	50.2	737	700	1.021	20.6	21.0
	0.03079	0.05020	0.00252	0.00154	0.00043	0.04571	0.09591	301.2	438.8	750.0	41.7	739	708	1.018	17.2	17.5
	0.02500	0.04970	0.00249	0.00124	0.00035	0.04647	0.09617	298.2	446.1	752.0	33.9	744	718	1.015	13.9	14.1
	0.01980	0.04920	0.00242	0.00098	0.00027	0.04636	0.09556	295.2	445.0	745.0	26.8	740	719	1.012	11.1	11.2

TABLE 16

Reaction Rates Without Catalyst

Runs # A-I with 1300 RPM; 0.5 SCFM Air

Run # J with 400 RPM; 0.25 SCFM Air

Run #	Time, min	gm equiv/ℓ $SO_3^=$	$\frac{\Delta(SO_3^=)}{\Delta t}$ gm equiv / ℓ . min	Run #	Time, min	gm equiv/ℓ $SO_3^=$	$\frac{\Delta(SO_3^=)}{\Delta t}$ gm equiv / ℓ . min
A	0	0.2810	0.0158	F	0	0.00335	0.0007
	1	0.2664			1	0.00215	
	2	0.2520			2	0.00130	
	3	0.2343			3	0.00070	
	4	0.2166			4	0.00037	
	5	0.2009			5	0.00024	
B	0	0.1460	0.0146	G	0	0.03565	0.01
	1	0.1305			1	0.0256	
	2	0.1166			2	0.0166	
	3	0.1053			3	0.00835	
	4	0.0920			4	0.00300	
	5	0.0732			5	0.00115	
C	0	0.1365	0.0157	H	0	0.0195	0.0057
	1	0.1183			1	0.0138	
	2	0.1030			2	0.0051	
	3	0.0885			3	0.00066	
	4	0.0734			4	0.00016	
D	0	0.0814	0.0113	I	0	0.0306	0.0083
	1	0.0704			1	0.0223	
	2	0.0597			2	0.0144	
	3	0.0476			3	0.0066	
	4	0.0359			4	0.00037	
	5	0.0242					
E	0	0.01551	0.0050	J	0	0.148	0.0064
	1	0.00989			1	0.1425	
	2	0.00565			2	0.1374	
	3	0.00291			3	0.1290	
	4	0.00175			4	0.1236	
	5	0.00106			5	0.1161	

APPENDIX IX

DATA AND CALCULATIONS FOR CHEMICAL KINETIC COEFFICIENTS

TABLE 17

Recalculation of $k_{s(Cu^{++})}$ from Fuller-Crist Data from Equation 25 using Constants from Latimer

Cu^{++} added gm mol/ℓ	Time, sec	Conc. of $SO_3^{=}$ gm mol/ℓ	Calculated Cu^{++} conc. gm mol/ℓ	$k_{s(Cu^{++})}$ $\frac{\ell}{min \times mol}$
1×10^{-4}	0	0.0143	0.0699×10^{-9}	1.378×10^{8}
	20	0.0086	0.1163×10^{-9}	1.438×10^{8}
	40	0.0041	0.2430×10^{-9}	1.341×10^{8}
	60	0.0008	1.250×10^{-9}	
1×10^{-5}	0	0.0125	0.0800×10^{-9}	1.376×10^{8}
	20	0.0072	0.1389×10^{-9}	1.734×10^{8}
	40	0.0025	0.4000×10^{-9}	0.981×10^{8}
	60	0.0002	5.00×10^{-9}	
1×10^{-6}	0	0.0131	0.0763×10^{-9}	1.081×10^{8}
	20	0.0082	0.1219×10^{-9}	1.377×10^{8}
	40	0.0039	0.2564×10^{-9}	1.254×10^{8}
	60	0.0008	1.250×10^{-9}	
1×10^{-7}	0	0.0135	0.0740×10^{-9}	0.915×10^{8}
	20	0.0088	0.1136×10^{-9}	1.299×10^{8}
	40	0.0045	0.222×10^{-9}	1.176×10^{8}
	60	0.0014	0.714×10^{-9}	
1×10^{-8}	0	0.0127	0.0787×10^{-9}	1.039×10^{8}
	20	0.0080	0.1250×10^{-9}	1.290×10^{8}
	40	0.0039	0.2564×10^{-9}	0.800×10^{8}
	60	0.0016	0.625×10^{-9}	
1×10^{-9}	0	0.0150	0.0665×10^{-9}	negative
	20	0.0122	0.082×10^{-9}	0.00
	40	0.0094	0.1062×10^{-9}	0.04×10^{8}
	60	0.0072	0.139×10^{-9}	

TABLE 18

Calculations of $k_{s(Co^{++})}$ from Equation 27

Run #	Co^{++} added gm mol/ℓ	Time, min	Conc. of $SO_s^{=}$ gm mol/ℓ	Calculated Co^{++} conc. gm mol/ℓ	$k_{s(Co^{++})}$, $\frac{\ell}{\text{mol x min}}$
a	1×10^{-7}	0	0.0483	3.23×10^{-8}	
		1	0.0443	3.52×10^{-8}	negative
		2	0.0352	4.44×10^{-8}	0.034×10^{6}
		3	0.0292	5.35×10^{-8}	0.012×10^{6}
		4	0.0210	7.42×10^{-8}	0.050×10^{6}
		5	0.0127	10.0×10^{-8}	0.062×10^{6}
b	1×10^{-7}	0	0.0566	2.75×10^{-8}	
		1	0.0498	3.13×10^{-8}	negative
		2	0.0417	3.74×10^{-8}	0.016×10^{6}
		3	0.0336	4.65×10^{-8}	0.026×10^{6}
		4	0.0251	6.21×10^{-8}	0.043×10^{6}
		5	- -	- -	0.012×10^{6}
		6	0.0161	9.80×10^{-8}	
c	1×10^{-8}	0	0.0550	1×10^{-8}	
		1	0.0508	1×10^{-8}	negative
		2	0.0436	1×10^{-8}	0.0
		3	0.0364	1×10^{-8}	0.013×10^{6}
		4	0.0292	1×10^{-8}	0.024×10^{6}
		5	0.0223	1×10^{-8}	0.032×10^{6}
d	1×10^{-9}	0	0.0625	1×10^{-9}	
		1	0.0548	1×10^{-9}	negative
		2	0.0470	1×10^{-9}	0.002×10^{6}
		3	0.0399	1×10^{-9}	0.006×10^{6}
		4	0.0325	1×10^{-9}	0.021×10^{6}
		5	0.0248	1×10^{-9}	0.036×10^{6}
e	1×10^{-6}	0	0.0593	2.63×10^{-8}	
		1	0.0495	3.15×10^{-8}	0.018×10^{6}
		2	0.0396	3.93×10^{-8}	0.034×10^{6}
		3	0.0303	5.14×10^{-8}	0.043×10^{6}
		4	0.0208	7.48×10^{-8}	0.060×10^{6}
		5	0.0120	12.95×10^{-8}	0.068×10^{6}
f	1×10^{-6}	0	0.0777	2.0×10^{-8}	
		1	0.0681	2.29×10^{-8}	negative
		2	0.0582	2.68×10^{-8}	0.004×10^{6}
		3	0.0489	3.19×10^{-8}	0.013×10^{6}
		4	0.0393	3.96×10^{-8}	0.031×10^{6}
		5	0.0297	5.25×10^{-8}	0.047×10^{6}
g	2×10^{-6}	0	0.0806	1.93×10^{-8}	
		1	0.0704	2.22×10^{-8}	negative
		2	0.0605	2.58×10^{-8}	negative
		3	- -		0.012×10^{6}
		4	0.0418	3.72×10^{-8}	0.033×10^{6}
		5	0.0331	4.70×10^{-8}	
h	5×10^{-7}	0	0.0502	3.10×10^{-8}	
		1	0.0416	3.74×10^{-8}	0.019×10^{6}
		2	0.0334	4.66×10^{-8}	0.027×10^{6}
		3	0.0252	6.18×10^{-8}	0.040×10^{6}
		4	0.0168	9.25×10^{-8}	0.056×10^{6}
		5	0.0092	16.95×10^{-8}	0.060×10^{6}

TABLE 19

Reaction Rates with Cu^{++} Catalyst

Runs # I-IV with 1300 RPM; 0.5 SCFM Air

Run # V with 400 RPM; 0.25 SCFM Air

Run #	Amt of catalyst gm mol/ℓ	Time, min	gm equiv/ℓ $SO_3^=$	$\frac{\Delta(SO_3^=)}{\Delta t}$ gm equiv / ℓ · min	Run #	Amt of catalyst gm mol/ℓ	Time, min	gm equiv/ℓ $SO_3^=$	$\frac{\Delta(SO_3^=)}{\Delta t}$ gm equiv / ℓ · min
I	5×10^{-7}	0	0.1286	0.0136	III	1×10^{-10}	0	0.01330	0.0045
		1	0.1163				1	0.01020	
		2	0.1033				2	0.00784	
		3	0.0887				3	0.00478	
		4	0.0752				4	0.00326	
		5	0.0608				5	0.00144	
II	5×10^{-6}	0	0.1170	0.0156	IV	5×10^{-6}	1	0.01200	0.0094
		1	0.1039				2	0.00264	
		2	0.0886				3	0.00000	
		3	0.0728						
		4	0.0568		V	1×10^{-10}	0'-00"	0.0154	0.0013
		5	0.0041				0'-20"	0.01455	
							0'-40"	0.01381	
							1'-00"	0.01279	
							1'-25"	0.01212	
							1'-45"	0.01098	

TABLE 20

Reaction Rates with Co^{++} Catalyst

Data from Table 18

1300 RPM; 0.5 SCFM Air

Run #	Amt of catalyst gm mol/ℓ	Time, min	gm equiv/ℓ $SO_3^=$	$\frac{\Delta(SO_3^=)}{\Delta t}$ gm equiv / ℓ . min	Run #	Amt of catalyst gm mol/ℓ	Time, min	gm equiv/ℓ $SO_3^=$	$\frac{\Delta(SO_3^=)}{\Delta t}$ gm equiv / ℓ . min
a	1×10^{-7}	0	0.0966	0.0164	e	1×10^{-6}	0	0.1186	0.0187
		1	0.0886				1	0.0990	
		2	0.0703				2	0.0792	
		3	0.0583				3	0.0606	
		4	0.0420				4	0.0417	
		5	0.0254				5	0.0240	
b	1×10^{-7}	0	0.1132	0.0164	f	1×10^{-6}	0	0.1550	0.0190
		1	0.0997				1	0.1362	
		2	0.0834				2	0.1164	
		3	0.06770				3	0.0978	
		4	0.0503				4	0.0785	
		5	- - -				5	0.0594	
		6	0.0322						
c	1×10^{-8}	0	0.1100	0.0141	g	2×10^{-6}	0	0.1612	0.0194
		1	0.1017				1	0.1408	
		2	0.0873				2	0.1210	
		3	0.0728				3	- - -	
		4	0.0583				4	0.0835	
		5	0.0447				5	0.0661	
d	1×10^{-9}	0	0.1250	0.0150	h	5×10^{-7}	0	0.1005	0.0166
		1	0.1095				1	0.0833	
		2	0.0940				2	0.0669	
		3	0.0798				3	0.0504	
		4	0.0649				4	0.0337	
		5	0.0497				5	0.0184	

TABLE 21

Data for the Determination of $k_{T.}^{o}$ a'

$C_{Ai(Literature)}$ = 10.54 x 10^{-4} gm equiv O_2/ℓ

No.	Duration of a run sec	mls of N/200 Thiosulfate for 100 ml sample	ppm O_2	C_{Ao} gm equiv/ℓ	$C_{Ai} - C_{Ao}$ gm equiv/ℓ	$\frac{C_{Ai} - C_{Ao}}{C_{Ai}}$	$C_{Ai(Lit.)} - C_{Ao}$	$\frac{C_{Ai(Lit.)} - C_{Ao}}{C_{Ai(Lit.)}}$
1	0	1.21	0.484	0.605 x 10^{-4}	8.735 x 10^{-4}	0.936	9.94 x 10^{-4}	0.94
2	5	12.24	4.896	6.12 x 10^{-4}	3.22 x 10^{-4}	0.345	4.42 x 10^{-4}	0.419
3	15	18.16	7.264	9.08 x 10^{-4}	0.26 x 10^{-4}	0.028	1.46 x 10^{-4}	0.138
4	22	18.34	7.336	9.17 x 10^{-4}	0.17 x 10^{-4}	0.0182	1.37 x 10^{-4}	0.130
5	300	18.95	7.580	9.47 x 10^{-4}			1.07 x 10^{-4}	0.101
6	300	18.67	7.468	9.33 x 10^{-4}			1.21 x 10^{-4}	0.115
7	720,000	18.39	7.356	9.19 x 10^{-4}			1.35 x 10^{-4}	0.128
	Average of # 5-7	18.67	7.468	9.34 x 10^{-4} ($\equiv C_{Ai}$)	0	0		

Slope of the curve, Figure 14 = 5.28 $\frac{1}{min}$ $\qquad$ k_{L}^{o} a' = 2.303 x 5.28 = 12.2 $\frac{1}{min}$

TABLE 22

Data Obtained from Figure 11 for the Determination of k' from $k_L^o \cdot a'$ and $K_R \cdot a'$ for Reaction without Catalyst

Run #	Time, min	C_{Bo} gm equiv / ℓ	$\frac{\Delta C_{Bo}}{\Delta t}$ gm equiv / ℓ · min	$\frac{1}{C_{Bo}}$ (average)	$\frac{1}{K_R} \cdot a' = \frac{C_{Ai}}{\Delta C_{Bo}/\Delta t}$
D	0	0.0815	0.0111	12.3	0.0950
	1	0.0704	0.0114	14.2	0.0925
	2	0.0590	0.0114	16.7	0.0925
	3	0.0476	0.0116	21.0	0.0905
	4	0.0369	0.0114	28.0	0.0925
	5	0.0246			
E	0	0.0160	0.0066	62.5	0.160
	1	0.0094	0.0040	106.5	0.264
	2	0.0054			
G	0	0.0356	0.0100	28.0	0.105
	1	0.0256	0.0090	39.5	0.117
	2	0.0166	0.0083	60.0	0.127
	3	0.0083	0.0053	119.0	0.191
	4	0.0030			
H	0	0.0200	0.0062	50.0	0.170
	1	0.0138	0.0068	72.5	0.155
	2	0.0070			
I	0	0.0306	0.0083	32.5	0.127
	1	0.0223	0.0079	44.8	0.133
	2	0.0144	0.0078	69.5	0.137
	3	0.0066			

TABLE 23

Calculation of γ from Equation 33 for $k' = 1100$

$\theta = 0.613$ min

C_{Bo} $\frac{gm\ equiv}{\ell}$	$M = \frac{\pi}{4} k' C_{Bo} \theta$	$\gamma_a = \left[\frac{D_B}{D_A}\right]^{1/2} \frac{C_{Bo}}{C_{Ai}} - 1$	$\frac{M}{\gamma_a}$	$\frac{M}{2\gamma_a}$	$\frac{M^2}{4\gamma_a^2}$	γ
0.02	10.63	14	0.757	0.378	0.142	2.01
0.03	15.95	21	0.757	0.378	0.142	2.74
0.04	21.25	28	0.757	0.378	0.142	3.32
0.06	31.90	42	0.757	0.378	0.142	4.37
0.08	42.50	56	0.757	0.378	0.142	5.20

TABLE 24

Estimation of k' from k_L for reaction without catalyst

Data from Figures 77 and 137-140

θ = 0.613 min

Run #	C_{Bo} gm equiv / ℓ	ft/hr	$\gamma + 1$	γ	$\gamma_a = \left[\frac{D_B}{D_A}\right]^{1/2} \frac{C_{Bo}}{C_{Ai}} - 1$	$(\gamma+1)^2$	$\gamma_a - \gamma$	M	k' liters / gm equiv · min
112	0.0812	0.76	6.45	5.45	56.0	41.5	50.5	46.0	1170
114	0.0685	0.729	6.16	5.16	47.0	38.0	42.0	42.5	1275
115	0.0577	0.594	5.03	4.03	39.5	25.4	35.5	28.3	1020
116	0.0295	0.515	4.36	3.36	19.7	19.0	16.3	23.0	1620
117	0.0162	0.295	2.50	1.50	10.35	6.25	8.9	7.28	930

Average value of k' = 1203 $\frac{\text{liters}}{\text{gm equiv min}}$

TABLE 25

Estimation of k' from k_L for reaction with Cu^{++} catalyst

θ = 0.613 min

Run #	gm mol $\frac{Cu\ SO_4}{\ell}$	C_{Bo} $\frac{gm\ equiv}{\ell}$	Calculated Cu^{++} $\frac{gm\ mol}{\ell}$	k_L, ft/hr	$\gamma + 1$ (k_L/k_L^o)	γ	$\gamma_a = \left[\frac{D_B}{D_A}\right]^{1/2} \frac{C_{Bo}}{C_{Ai}} - 1$	$(\gamma + 1)^2$	$\gamma_a - \gamma$	M	k' $\frac{liters}{gm\ equiv \cdot min}$
59	4×10^{-9}	0.097	2.06×10^{-11}	0.602	5.1	4.1	67.0	26.0	62.9	27.8	593
60	4×10^{-9}	0.070	2.86×10^{-11}	0.756	6.41	5.41	48.2	41.0	42.8	46.2	1,370
61	4×10^{-8}	0.090	2.22×10^{-11}	0.891	7.55	6.55	62.3	57.0	55.8	63.6	1,470
62	4×10^{-8}	0.066	3.03×10^{-11}	0.600	5.09	4.09	45.5	26.0	41.4	28.6	900
63	4×10^{-8}	0.062	3.22×10^{-11}	0.697	5.92	4.92	42.6	35.0	37.7	39.6	1,330
64	1.5×10^{-7}	0.086	2.32×10^{-11}	0.783	6.63	5.63	59.4	44.0	53.8	48.5	1,170
65	4×10^{-4}	0.080	2.50×10^{-11}	0.891	7.55	6.55	55.2	57.0	48.7	64.5	1,680
66	4×10^{-4}	0.072	2.78×10^{-11}	0.826	7.00	6.00	49.5	49.0	43.5	55.6	1,610
67	1×10^{-6}	0.063	3.17×10^{-11}	1.137	10.15	9.15	43.5	103.0	34.3	130.2	4,250
68	1×10^{-6}	0.062	3.22×10^{-11}	0.657	5.57	4.57	42.5	31.2	38.0	34.9	1,170
69	1×10^{-6}	0.086	2.32×10^{-11}	0.917	7.77	6.77	59.5	60.5	52.8	67.8	1,640
70	1×10^{-6}	0.088	2.27×10^{-11}	1.023	8.67	7.67	60.8	75.2	53.1	85.8	2,030
71	3×10^{-6}	0.084	2.38×10^{-11}	1.131	9.60	8.60	58.0	92.5	49.4	108.0	2,670
72	4×10^{-6}	0.077	2.59×10^{-11}	1.171	9.94	8.94	53.2	98.5	44.3	117.0	3,160
73	4×10^{-6}	0.112	1.78×10^{-11}	1.330	11.25	10.25	77.0	127.0	66.7	147.0	2,660
74	8×10^{-6}	0.074	2.70×10^{-11}	1.378	11.70	10.70	51.0	113.0	40.3	143.0	4,010
75	1×10^{-5}	0.048	4.16×10^{-11}	1.496	12.70	11.70	32.9	162.0	21.2	251.0	10,900

TABLE 26

Estimation of k' from k_L for reaction with Co^{++} catalyst

θ = 0.613 min

Run #	gm mol CO $C\ell_2$ / ℓ	C_{Bo} gm equiv / ℓ	Calculated Co^{++} gm mol / ℓ	k_L, ft/hr	$\gamma + 1$	γ	$\gamma_a = \left[\frac{D_B}{D_A}\right]^{1/2} \frac{C_{Bo}}{C_{Ai}} - 1$	$(\gamma + 1)^2$	$\gamma_a - \gamma$	M	k' liters / gm equiv . min
76	1×10^{-11}	0.096		0.775	6.55	5.55	66.5	43	61.0	47	1,010
77	1×10^{-10}	0.112		0.793	6.72	5.72	77.6	45	72.0	48	900
78	1×10^{-9}	0.158		0.836	7.08	6.08	110.0	50	104.0	53	700
79	5×10^{-9}	0.168		0.944	8.00	7.00	117.0	64	110.0	68	840
80	1×10^{-8}	0.158		1.340	11.38	10.38	110.0	129	99.6	142	1,870
81	1×10^{-8}	0.150		1.200	10.15	9.15	104.5	103	95.3	107	1,480
82	2×10^{-8}	0.106		1.030	8.70	7.70	73.5	75	66.8	83	1,620
83	5×10^{-8}	0.082	3.8×10^{-8}	1.385	11.75	10.75	56.5	138	45.7	171	4,320
84	1×10^{-7}	0.170	1.83×10^{-8}	1.490	12.62	11.62	118.0	159	106.4	176	2,150
85	2×10^{-7}	0.070	4.45×10^{-8}	1.627	13.80	12.80	48.2	190	35.4	259	7,660
86	3×10^{-7}	0.100	3.12×10^{-8}	2.400	20.35	19.35	69.2	413	49.9	573	11,900
87	5×10^{-7}	0.081	3.86×10^{-8}	2.100	17.80	16.80	55.8	316	39.0	453	11,650
88	5×10^{-7}	0.01196	2.6×10^{-8}	3.155	26.70	25.70	83.0	712	57.3	1030	17,900
89	7×10^{-7}	0.06975	4.46×10^{-8}	3.620	30.70	29.70	48.0	940	18.3	2460	73,000
90	1×10^{-6}	0.106	2.91×10^{-8}	4.120	39.9	38.9	73.5	1590	34.6	3380	66,000
91	1×10^{-6}	0.0808	3.86×10^{-8}	3.940	33.4	32.4	55.8	1056	23.4	2520	64,000
92	2×10^{-6}	0.052	6.00×10^{-8}	4.790	40.6	39.6	35.5	1600	negative		
33	2×10^{-6}	0.00270			4.35	3.35	0.8		negative		
34	2×10^{-6}	0.0047			4.78	3.78	2.3		negative		
35	2×10^{-6}	0.00656			5.13	4.13	3.6		negative		
36	2×10^{-6}	0.00714			5.34	4.34	4.02		negative		
37	2×10^{-6}	0.00764			5.86	4.86	4.35		negative		
38	2×10^{-6}	0.0116			10.20	9.2	8.05		negative		
39	2×10^{-6}	0.0172			12.85	11.85	11.1		negative		
40	2×10^{-6}	0.0182			21.0	20.0	11.7		negative		
41	2×10^{-6}	0.0196			14.2	13.2	12.8		negative		
42	2×10^{-6}	0.0238	13.2×10^{-8}		12.1	11.1	15.7	146	4.6	497	4.35×10^4
43	2×10^{-6}	0.0344	9.06×10^{-8}		13.7	12.7	23.2	188	10.5	415	2.51×10^4
44	2×10^{-6}	0.0426	7.3×10^{-8}		25.8	24.8	29.0	665	4.2	4580	2.24×10^5
45	2×10^{-6}	0.0490	6.35×10^{-8}		30.0	29.0	33.5	900	4.5	6700	2.84×10^5
46	2×10^{-6}	0.0616	5.06×10^{-8}		33.0	32.0	42.3	1043	10.3	4280	1.44×10^5
47	2×10^{-6}	0.0716	4.35×10^{-8}		30.1	29.1	49.5	905	20.4	2180	6.3×10^5
48	2×10^{-6}	0.0926	3.37×10^{-8}		40.9	39.9	64.0	1670	24.1	4430	1.0×10^5
49	2×10^{-6}	0.1426	2.19×10^{-8}		49.4	48.4	99.0	2440	50.6	4770	6.95×10^4
50	2×10^{-6}	0.197	1.57×10^{-8}		61.2	60.2	137.0	3730	77.0	6600	6.95×10^4
51	2×10^{-6}	0.348	8.8×10^{-9}		52.6	51.6	243.0	2760	192.0	3490	2.08×10^4
52	2×10^{-6}	0.530	5.9×10^{-9}		49.0	48.0	371.0	2400	323.0	2760	1.08×10^4
53	2×10^{-6}	0.664	4.7×10^{-9}		42.6	41.6	465.0	1820	424.0	1990	6,230
54	2×10^{-6}	0.914	3.42×10^{-9}		36.6	35.6	641.0	1340	606.0	1420	3,200
55	2×10^{-6}	1.315	2.37×10^{-9}		32.6	31.6	914.0	1060	883.0	1095	1,730
56	2×10^{-6}	1.72	1.82×10^{-9}		4.18	3.18	1210.0	1750	1207.0	1755	2,120
57	2×10^{-6}	1.782	1.75×10^{-9}		10.25	9.25	1250.0	1050	1241.0	1055	1,220

TABLE 27

Estimation of k' from Fuller and Crist Data

$k_1 = 0.78 \frac{1}{min}$ $C_{Ai} = 1.27 \times 10^{-3}$ gm equiv/ℓ

	gm mol $(Cu^{++})/\ell$	$k_3 \times (Cu^{++})$	$k = k_1 + k_3(Cu^{++})$ min^{-1}	$k' = \frac{k}{C_{Ai}}$ $\frac{liters}{gm\ equiv\ min}$
I $k_{3(original)} = 1.56 \times 10^8 \frac{liters}{mol \cdot min}$	1×10^{-11}	1.56×10^{-3}	0.165	614
	1×10^{-10}	1.56×10^{-2}	0.178	626
	1×10^{-9}	1.56×10^{-1}	0.318	736
	1×10^{-8}	1.56×10^{0}	1.723	1,845
	1×10^{-7}	1.56×10^{1}	15.763	12,880
II $k_{3(corrected)} = 7 \times 10^9 \frac{liters}{mol \cdot min}$	1×10^{-11}	7×10^{-2}	0.233	669
	1×10^{-10}	7×10^{-1}	0.863	1,168
	1×10^{-9}	7×10^{0}	7.163	6,120
	1×10^{-8}	7×10^{1}	70.163	55,600
	1×10^{-7}	7×10^{2}	700.163	551,000

TABLE 28

Calculation of k' for Mannitol from k_L and from Equation 34

Amount of Mannitol gm mol/ℓ	C_{Bo} gm equiv/ℓ	k_L ft/hr	$\gamma = \frac{k_L}{k_L^o} - 1$	$\gamma_a = \left[\frac{D_B}{D_A}\right]^{1/2} \cdot \frac{C_{Bo}}{C_{Ai}} - 1$	$(\gamma + 1)^2$	$\gamma_a - \gamma$	M	k' $\frac{\text{liters}}{\text{gm equiv x min}}$	k from Eq. 34 min^{-1}	$k' = \frac{k}{C_{Ai}}$ $\frac{\text{liter}}{\text{gm equiv x min}}$
5×10^{-7}	0.086	0.776	5.58	47.0	43.2	41.4	49.2	1160	0.155	147
5×10^{-6}	0.097	0.685	4.80	53.0	33.5	48.2	36.9	791	0.108	102
1×10^{-5}	0.130	0.646	4.47	71.0	30.0	66.5	32.1	512	0.081	76.7
5×10^{-5}	0.090	0.622	4.27	49.2	27.7	45.0	30.3	700	0.027	25.6
1×10^{-4}	0.116	0.532	3.50	63.2	20.2	59.7	21.4	383	0.0147	13.8
2.5×10^{-4}	0.092	0.440	2.73	50.2	13.9	47.5	14.7	333	0.0063	5.97
5×10^{-4}	0.048	0.228	0.93	26.2	3.72	25.1	3.88	168	0.0032	3.02
5×10^{-3}	0.068	0.187	0.585	37.1	2.50	36.5	2.54	77.5	0.00033	0.309
1×10^{-2}	0.156	0.157	0.330	85.0	1.77	84.7	1.78	23.8	0.000163	0.154

TABLE 29

Calculation of k' for Benzyl Alcohol from k_L and from Equation 35

Amount of Benzyl Alcohol gm mol/ℓ	C_{Bo} gm equiv/ℓ	k_L ft/hr	$\gamma = \frac{k_L}{k_L^o} - 1$	$\gamma_a = \left[\frac{D_B}{D_A}\right]^{1/2} \cdot \frac{C_{Bo}}{C_{Ai}} - 1$	$(\gamma + 1)^2$	$\gamma_a - \gamma$	M	k' $\frac{\text{liters}}{\text{gm equiv x min}}$	k_{zero} from Eq. 35	$k' = \frac{k_{zero}}{C_{Ai} \cdot C_{Bo}}$
5×10^{-7}	0.100	0.629	4.33	54.7	28.3	50.4	30.8	640	0.016	152
1×10^{-6}	0.124	0.642	4.44	63.9	29.5	59.5	31.7	532	0.016	122
2.5×10^{-6}	0.092	0.590	3.82	47.2	14.6	43.4	15.9	359	0.016	165
5×10^{-6}	0.096	0.275	1.33	49.2	5.4	47.9	5.55	120	0.016	158
1×10^{-5}	0.136	0.266	1.26	70.0	5.1	68.75	5.18	79.5	0.016	112
5×10^{-5}	0.124	0.098	--							
1×10^{-4}	0.152	0.114	--							
1×10^{-2}	0.146	0.0256	--							